

1956

Plastic design of multi-span rigid frames, Lehigh University, (1956) Ph. D.

R. L. Ketter

Follow this and additional works at: <http://preserve.lehigh.edu/engr-civil-environmental-fritz-lab-reports>

Recommended Citation

Ketter, R. L., "Plastic design of multi-span rigid frames, Lehigh University, (1956) Ph. D." (1956). *Fritz Laboratory Reports*. Paper 19. <http://preserve.lehigh.edu/engr-civil-environmental-fritz-lab-reports/19>

This Technical Report is brought to you for free and open access by the Civil and Environmental Engineering at Lehigh Preserve. It has been accepted for inclusion in Fritz Laboratory Reports by an authorized administrator of Lehigh Preserve. For more information, please contact preserve@lehigh.edu.

LEHIGH UNIVERSITY LIBRARIES



3 9151 00897477 2



Lehigh University

I N S T I T U T E O F R E S E A R C H

205.48

INTERIM REPORT No. 31

**PLASTIC DESIGN OF MULTI-SPAN
RIGID FRAMES**

by

ROBERT L. KETTER

MECH. ENGINEERING
LIBRARY

Welded Continuous Frames and Their Components

INTERIM REPORT No.31

PLASTIC DESIGN OF MULTI-SPAN RIGID FRAMES

by

Robert L. Ketter

(Not for Publication)

June 1956

**FRITZ ENGINEERING
LABORATORY LIBRARY**

Fritz Engineering Laboratory
Lehigh University
Bethlehem, Pennsylvania

Fritz Laboratory Report No. 205.48

ACKNOWLEDGEMENTS

The author wishes to express his appreciation for the helpful suggestions and criticisms made by a number of the research personnel at Fritz Engineering Laboratory while various parts of the development presented in this dissertation were in preparation. Dr. Bruno Thürlimann was particularly encouraging in his support. Thanks are also expressed to Mrs. Veronica Olanovich, who typed the manuscript, David Hait, who carried out many of the calculations and George Driscoll, who computed the plastic modulus constants tabulated in Appendix D.

The supervision, encouragement, and critical review of this work by Dr. Lynn S. Beedle, Professor in charge of the dissertation, are sincerely appreciated.

This study has been carried out as part of the research project on "Welded Continuous Frames and Their Components" being conducted under the general direction of Dr. Lynn S. Beedle. It is sponsored jointly by the Welding Research Council and the Navy Department with funds furnished by the following: American Institute of Steel Construction, American Iron and Steel Institute, Column Research Council (Advisory), Office of Naval Research (Contract No. 39303), Bureau of Ships and Bureau of Yards and Docks.

Work was done at Fritz Engineering Laboratory of which Professor William J. Eney is Director.

TABLE OF CONTENTS

	<u>Page</u>
SYNOPSIS	1
I. INTRODUCTION	
1. Historical Review	2
2. Behavior of Structures Above the Elastic Limit	5
3. Necessary and Sufficient Conditions for a Plastic Analysis Solution	12
4. Methods of Solution	13
5. The Mechanism Method	16
6. The Problem of Concentrated versus Distributed Loads	27
7. Modifying Factors	30
II. PLASTIC DESIGN OF SINGLE SPAN GABLE FRAMES	32
1. Pinned-Base Gable Frames	33
2. Fixed-Base Gable Frames	41
3. The Problem of Distributed Horizontal Loads	43
III. PLASTIC DESIGN OF MULTI-SPAN RIGID FRAMES	
1. Direct Procedure	48
2. Solution by Separation	53
3. Development of Design Charts	65
IV. DISCUSSION	
1. Factor of Safety	70
2. Economic Designs	72
3. Initial Choice of Members	76
V. DESIGN EXAMPLES	
1. Single-Span Gabled Frame	77
2. Two-Span, Unsymmetrical Rectangular Portal Frame	78
3. Three-Span Symmetrical Gabled Frame	80
4. Three-Span Unsymmetrical Gabled Frame	83
5. Mill-Building with Lean-To's	86
VI. SUMMARY	89
VII. NOMENCLATURE	90
VIII. REFERENCES	93

Table of Contents (cont'd.)

	<u>Page</u>
IX. APPENDIX	
A. Derivation of Equivalent Concentrated Loads to Replace Uniformly Distributed Loads	95
B. Implicit Differentiation of Function of Three Variables	99
C. Summary of Important Equations	101
D. Table of Plastic Modulus Values	110
X. DESIGN CHARTS	116

SYNOPSIS

Present day analysis and design of continuous structures as defined by specifications and design codes are based on an assumed elastic behavior of the structure. The criterion of the design in most cases is the attainment of an allowable extreme fiber stress. While a design that results from using such a procedure will be safe, the actual degree of safety is unknown and may vary between extreme limits.

During the past several years a different type of analysis based on the ultimate strength of a structure as a whole has been developed. This new procedure known as "plastic analysis" or "plastic design" gives a clearer insight into the actual strength behavior of structures and therefore promises a more economic usage of materials. It should also be noted that the procedure is rational and has proven to be extremely time saving.

After reviewing the basic assumptions of plastic analysis, this dissertation presents a method whereby extremely complex multiple span frames can be readily designed. Several examples are carried out. The problem of economy in main member is also discussed and procedures are presented whereby the design of a "least weight" structure can be approached.

I. INTRODUCTION

1. Historical Review

In 1917 in his inaugural address* at the University of Delft in Holland, Kist raised the question—should design be based on an arbitrary allowable stress value or should it rather be based on the actual ultimate carrying capacity of a structure. (1)** It was realized even then that structures possessed reserves in strengths beyond that predicted on the basis of initial yield of the most highly strained fibers within the structure. Kazinczy⁽²⁾ had in 1914 carried out a series of tests on indeterminate beams and had verified that such members possess a large reserve in strength beyond the elastic limit. Further, he had observed that at near ultimate loads what might be thought of as "yield-hinges" developed at sections of maximum moment within the girder. That is, the beam would rotate at these sections while maintaining a relatively constant value of high moment. It is with the realization of these two concepts that "Plastic Analysis" came into being.

The early developments of this method of structural analysis were due primarily to the efforts of Grüning,

* "Leidt een sterkteberekening, die uitgaat van de evenredigheid van kracht en vormverandering, tot een goede constructie van ijzeren bruggen en gebouwen?", Inaugural Dissertation of N.C. Kist, Polytechnic Institute, Delft (1917)

** These numbers correspond to references tabulated at the end of the report. They are listed in order of appearance.

Maier-Liebnitz, Girkmann and Bleich in Europe. It should be pointed out, however, that during this period few if any structures were designed using such an analysis. The concern over the problem of variable repeated loading and the lack of full scale confirmatory tests resulted in a feel of insecurity on the part of the designer when using such a procedure.

In 1936, however, the problem was revitalized. This was due almost entirely to the efforts of J.F. Baker in England who initiated a research investigation into the ultimate strength behavior of steel structures first at Bristol University and later (1943) at Cambridge University. This study, which is still underway⁽³⁾, has resulted in the formulation of a Plastic Design Specification (or as it is termed in England, the "Collapse Method of Design"⁽⁴⁾). Many structures have been designed using this procedure.

Several years after Baker's group started work in England Van den Broek published his paper on "Limit Design"⁽⁵⁾. This work again focused the attention of the profession on the question, what should be the basis for design. In 1946 a research investigation was started at Brown University by Prager and his colleagues. Their efforts were in general directed toward the establishment of the mathematical laws and proofs governing plastic analysis. This work has now advanced to the stage where it is felt that at least theoretically plastic analysis solutions to extremely complex problems can be obtained.

At the same time that this work at Brown was undertaken a study of the behavior of Welded Continuous Frames and Their Components was initiated at Lehigh University. A large part of this work has also been concerned with the general problem of plastic analysis and design. Many full size structures have been tested as part of this study.

2. Behavior of Structures Above the Elastic Limit

To understand the behavior of structures or structural components it is necessary that attention first of all be directed toward a consideration of the basic bending stiffness relationships of structural members. In the elastic range it is known that a linear correspondence exists between applied bending moments and resulting curvatures. The equation relating these quantities is

$$\phi = M/EI^* \dots\dots\dots(1)$$

where ϕ is the rotation per unit length (i.e. curvature), M is the bending moment at the section in question, E is Young's Modulus of Elasticity and I is the moment of inertia of the cross-section about an axis perpendicular to the plane of the applied bending moments.

In deriving the relationship between moment and curvature above the elastic limit, it is necessary that certain assumptions be made. These are as follows:

1. Plane sections remain plane; that is, bending strains are proportional to the distance from the neutral axis.

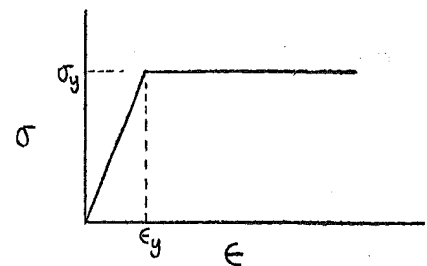


FIGURE 1

*See any standard text on Strength of Materials.

2. The stress-strain relationship is as shown in Figure (1). (It is further assumed that the behavior in tension is the same as that in compression).

3. Equilibrium exists between applied loads and moments and the resulting stress distribution pattern. That is,

$$\left. \begin{aligned} P &= \int_A \sigma dA \\ M &= \int_A \sigma y dA \end{aligned} \right\} \dots\dots\dots (2)$$

4. Deformations are small such that

$$\tan \phi = \phi$$

Based on these assumptions it can be shown^{(6),(7)} that the moment-curvature relationship for a wide flange type of cross-section is in general as shown in Figure 2b.

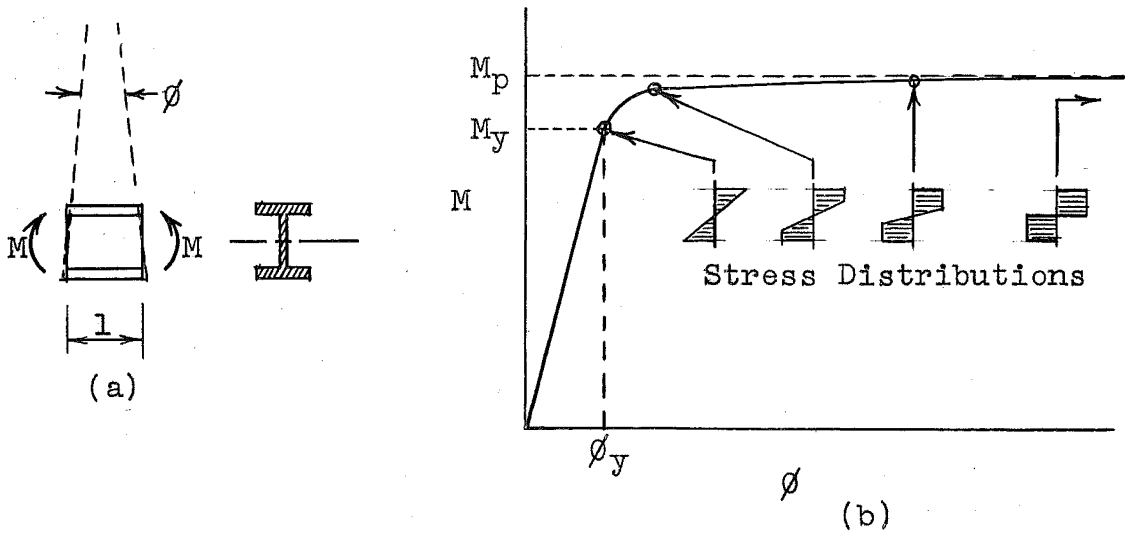


FIGURE 2

It should be noted that as the moment is increased beyond the initial yield moment, M_y , curvature increases at an ever increasing rate approaching M_p , the full plastic moment value, asymptotically. This value of moment is approached rapidly.

The magnitude of the full plastic moment is determined from an integration of the stress distribution pattern shown in Figure 3. Even though the value of curvature indicated by this diagram could never be realized, the error in moment value resulting from the assumption of this stress distribution versus a "more realistic" one is extremely small.

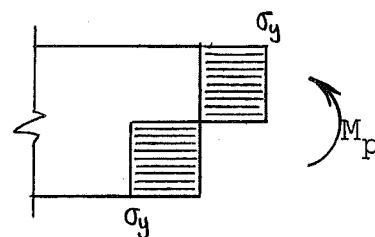


FIGURE 3

As in the elastic case where it is convenient to express the yield moment as $S\sigma_y$ (where S is the section modulus of the section in question), the full plastic moment value M_p can be expressed as

$$M_p = Z\sigma_y \dots\dots\dots(3)$$

where Z is the plastic modulus. Plastic modulus values for standard rolled shapes are tabulated in Appendix D of this paper according to descending values of Z . The most economical (i.e. least-weight) sections are at the head of each grouping.

Having this relationship between moment and curvature in mind, consider now the behavior of a simply supported beam loaded as shown in Figure 4a.

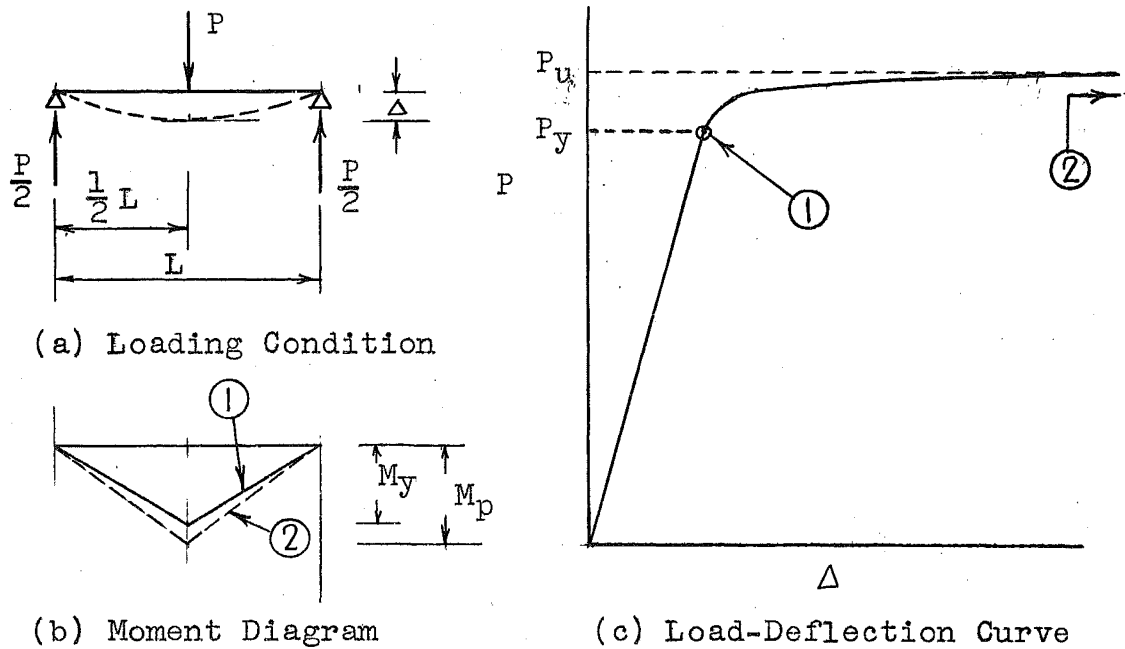


FIGURE 4

Moment diagrams corresponding to two values of the load P are given in Figure 4b. In Figure 4c is shown a load versus centerline deflection plot for the beam. As the load is increased from zero there is first observed a linear range of P versus Δ . This would correspond to the linear range of M versus ϕ of Figure 2(b). As moment at the centerline

section exceeds the value M_y , however, the relative stiffness (i.e. the increased moment associated with a unit increase in curvature) is markedly reduced. This results in a relatively weaker member for an increase in load and therefore the beam deflects at a greater rate. As the load P approaches its maximum value P_u (which corresponds to M_p at the centerline section) the beam reacts to increases in load as if a hinge ("plastic hinge") were located at its point of maximum moment (see Figure 5).

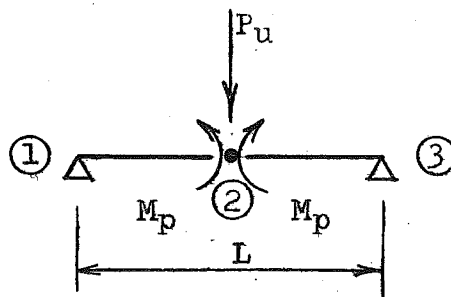


FIGURE 5

It is therefore seen that failure corresponds to the development of a kinematic mechanism, real hinges being located at sections ① and ③ and a plastic hinge at section ②.

The behavior of a redundant structure is quite different. Consider for example the same beam but with one end fixed (see Figure 6a).

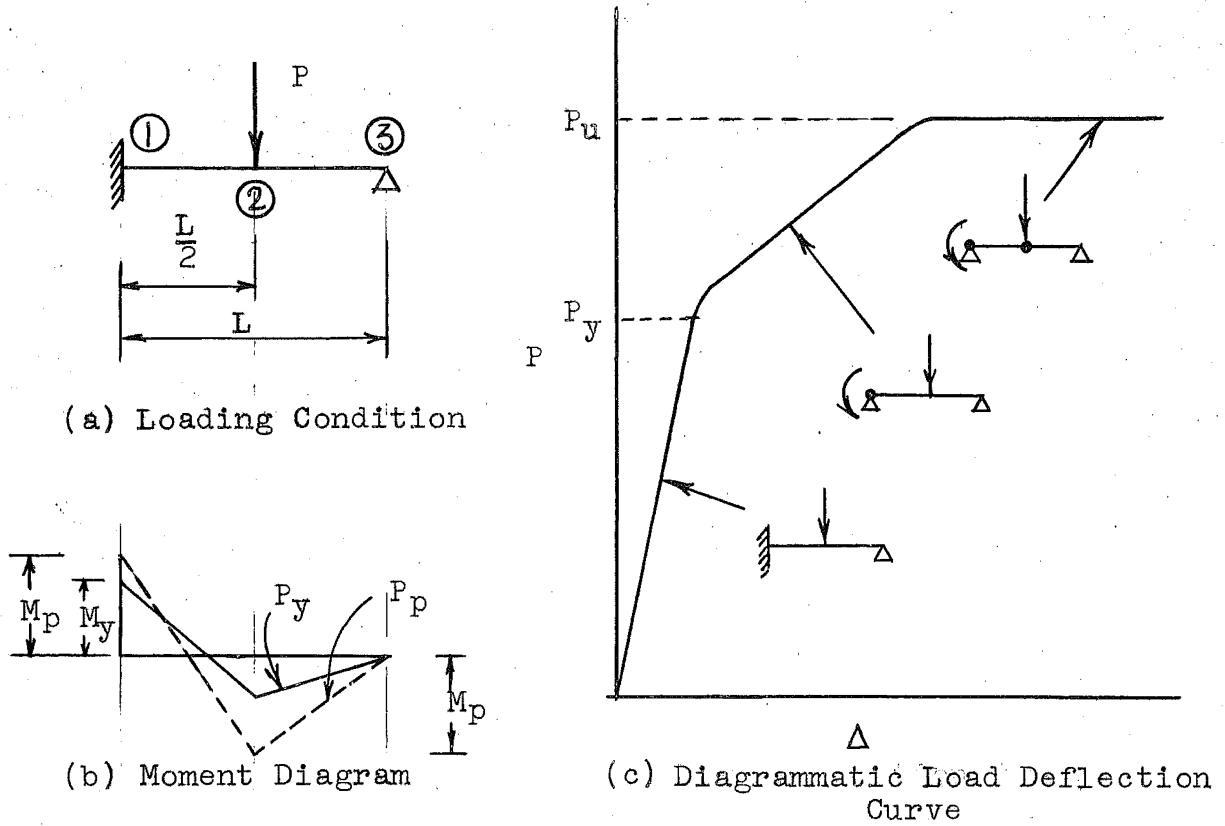


FIGURE 6

As the load is increased from zero there is first observed the linear range of P versus Δ the same as in the case of the simple beam. Also, as the load continues to increase yielding occurs at the fixed end. This, however, does not result in the failure of the beam. In this case, after M_p is reached at the fixed end, the beam responds to further increases in load as if it were a simple beam subjected to an end moment. In other words, a redistribution of moments

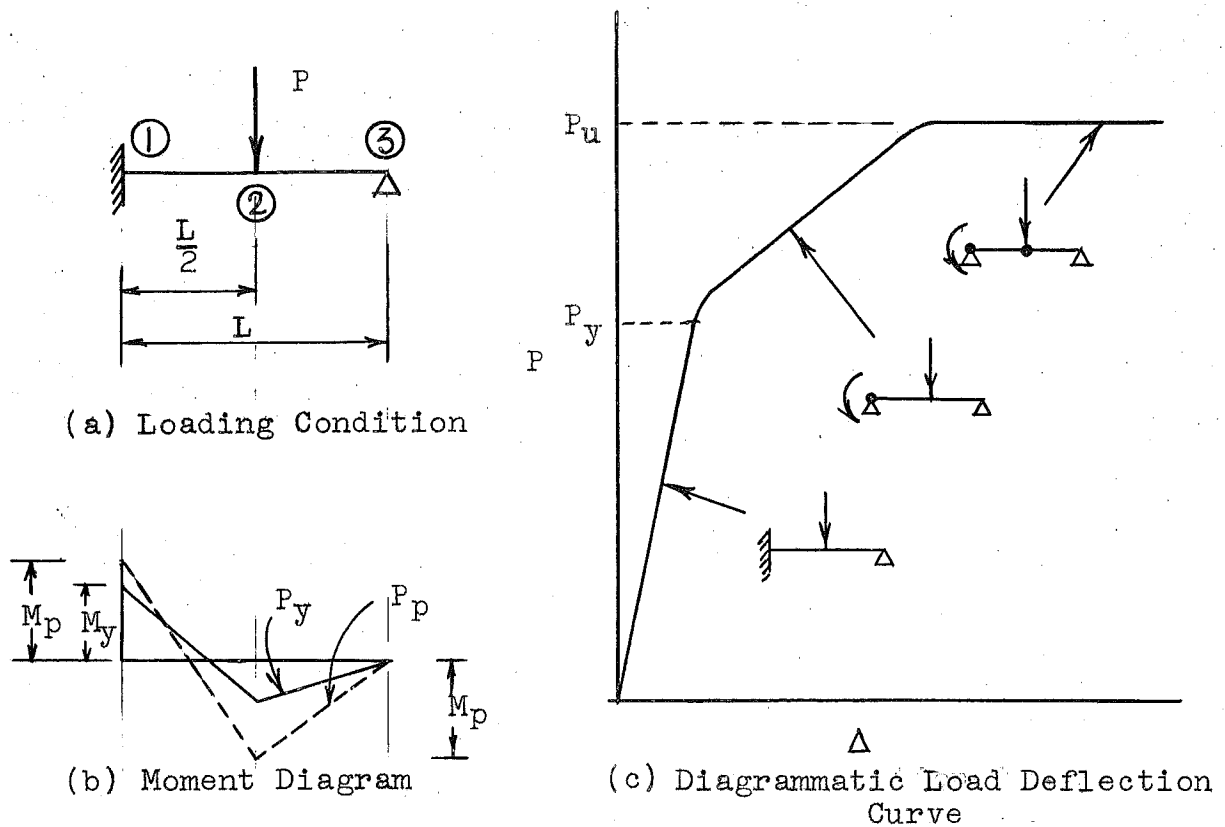


FIGURE 6

As the load is increased from zero there is first observed the linear range of P versus Δ the same as in the case of the simple beam. Also, as the load continues to increase yielding occurs at the fixed end. This, however, does not result in the failure of the beam. In this case, after M_p is reached at the fixed end, the beam responds to further increases in load as if it were a simple beam subjected to an end moment. In other words, a redistribution of moments

will be associated with an increased load. Continuing to increase the load still more initial yield occurs at the centerline section and the load deflection curve again changes slope. As M_p is developed at this section the load deflection curve becomes horizontal, or in other words the maximum load is realized. Here again the condition of failure is the development of a mechanism, a real hinge existing at section (3) and two plastic ones developing at sections (1) and (2).

Other similar examples could be cited. It is felt, however, that these are sufficient to illustrate the basic behavior.

For completeness, it should be pointed out that the following assumptions common to simple plastic theory types of solutions have been made:

1. No instability will occur prior to the attainment of the full plastic load.
2. The influence of normal and shearing forces on the plastic moment is neglected.
3. Deformations are small such that the equilibrium equations can be formulated for the undeformed structure.

Other assumptions necessary for a simple plastic theory solution that will be made in the remainder of this paper are:

4. Connections are continuous such that the plastic moment M_p can be transmitted.
5. The loading is proportional (i.e. the ratios between the various loads remains constant during loading).

3. Necessary and Sufficient Conditions for a Plastic Analysis Solution⁽³⁾

It is noted that in each case discussed in the preceding section failure corresponded to the development of a mechanism. That is, the structure could deform with a zero increase in applied loads. Also observed was the condition that the maximum moment to which a member can be subjected is its full plastic moment. Since a structure must at all times be in equilibrium with the loading to which it is subjected, this constitutes a third necessary condition for the analysis. The conditions that must be fulfilled then for the attainment of a plastic analysis solution are according to the simple plastic theory as follows⁽³⁾:

1. the structure must be in equilibrium with the applied loads,
2. a Mechanism must be formed, and
3. nowhere will the moment value exceed the full plastic moment of the section in question (i.e. $-M_p \leq M \leq M_p$).

For comparison, in an elastic analysis solution the conditions required are as follows:

1. the structure must be in equilibrium with the applied loads,
2. there must be continuity at the joints, and
3. nowhere will the stress exceed the initial yield stress. ($\sigma \leq \sigma_y$).

The correspondence between the necessary and sufficient conditions of an elastic analysis and a plastic one is therefore as shown in Table 1. (9)

TABLE 1

ELASTIC ANALYSIS	PLASTIC ANALYSIS
1. Equilibrium	1. Equilibrium
2. Continuity at Joints	2. Development of Mechanism
3. $-\sigma_y \leq \sigma \leq +\sigma_y$	3. $-M_p \leq M \leq +M_p$

4. Method of Solution

Several approaches or procedures could be used to arrive at a solution that will satisfy these conditions. The more noteworthy among these are (a) the "Equilibrium" Method, (b) the Mechanism Method, (c) the Method of Inequalities, and (d) the Moment Balancing Method,

(a) "Equilibrium Method" (4), (10)

For a continuous beam problem it is possible to visualize from the outset the general pattern that the

ultimate strength moment diagram must take. A plastic analysis solution could therefore be obtained by adjusting the magnitudes of the maximum moment values of this diagram always keeping $M \leq M_p$ until a sufficient number of plastic hinges had been developed to reduce the structure to a mechanism. This method is a simple and relatively fast means of solving continuous beam problems. It can also be effectively used in the solution of certain types of frame problems where only one or two redundants exist. The solution to more complex problems by this method, however, becomes extremely complicated.

(b) Mechanism Method^{(9), (11)}

The mechanism method approaches the problem from an entirely different point of view. Since the structure will fail at its first opportunity, a systematic investigation of each of the possible failure configurations and a determination of the corresponding critical loads will enable one to select the lowest of these and thereby the correct solution. Since a procedure of this type gives an upper bound to the carrying capacity of the structure⁽¹¹⁾, it is necessary to determine a lower bound in order that one be certain of the correctness of the assumed answer. This is accomplished by the establishment of the moment diagram (Plasticity check). If it nowhere exceeds M_p the assumed solution is the correct one, each of the three necessary conditions being fulfilled.

This type of procedure is very general and lends itself readily to the solution of extremely complicated problems. It will be used in the development of the solution to the multi-span problem to be discussed later.

(c) Method of Inequalities⁽¹²⁾

Since it is known that a member can sustain a moment equal to or less than its full plastic value, a set of linear inequalities could be written for each of the points of possible plastic hinge formation within the structure. By combining and eliminating these inequalities the correct solution can be obtained. While this type of procedure is elegant, a computer is recommended for the solution of the more complex problems.

(d) Moment Balancing^{(13), (14)}

As in the case of elastic design a successive relaxation of moment values could be carried out for plastic design taking into account the plasticity condition. For analysis or design by this method a much greater degree of freedom is allowed the designer than in the elastic case.

The mechanism method will be used in the development of the solution to the multi-span rigid frame problem. It will be discussed more in detail in the following section.

5. Mechanism Method of Solution

Since the mechanism method assumes a possible failure configuration from the outset, one of the three necessary conditions for a plastic analysis solution is automatically fulfilled. If in addition a virtual displacement type of procedure is used to relate the external loads to the internal stiffnesses of the various members, then equilibrium is also satisfied*. As was pointed out earlier the only remaining condition to be fulfilled is the plasticity one (i.e. $-M_p \leq M \leq M_p$).

For illustration of the method of solution consider the fixed base gable frame loaded as shown in Figure 7. As in all solutions based on the simple plastic theory loads are assumed to be proportional, the influence of shear and normal force are neglected, deformations are small such that equilibrium can be formulated in the undeformed position, the connections are such that full moment transfer can occur and the structure will not become unstable prior to the attainment of the full plastic load.

First of all, the locations of all points of possible plastic hinge formation must be ascertained. Since no loads

*It should be pointed out that such a procedure assumes that the structure and the applied loads are in equilibrium at the instant that a mechanism is formed. Therefore, the increase in internal work associated with the virtual displacement must equal the corresponding external work. Moreover, the increase in internal work will take place only at points of plastic hinge formation since only at these points will increased rotations occur.

are applied to the columns along their lengths, shear in these members will be constant. Therefore, maximum moments can occur only at the ends. This gives four possible points of plastic hinge formation. Under each of the vertical loads, P , shear can also be equal to zero. These then are also points of possible "hinge" development. Since the structure abruptly changes shape at the peak of the rafters this presents another possibility. The points of possible plastic hinge formation then are as numbered ① through ⑦ in Figure 7.

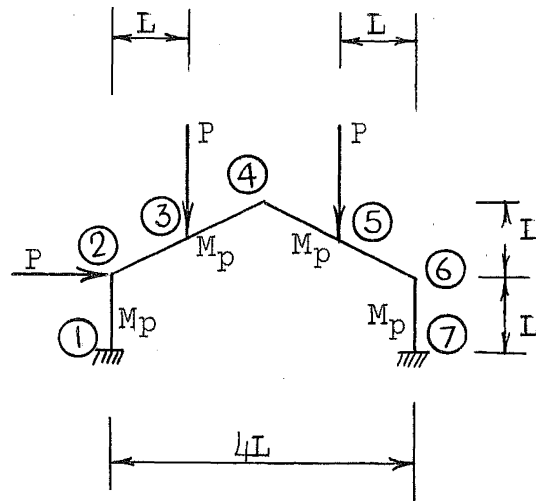


FIGURE 7

The next step is to define all of the possible combinations of these "hinges" that result in failure configurations (i.e. mechanisms). As an aid in determining these failure forms, a rule has been formulated (see Ref. 9 or 11) for the definition of the number of independent condition required to solve a given problem. These independent conditions correspond to the independent failure mechanism that must be sought. The rule states⁽¹¹⁾ that if N represents the number of possible plastic hinges and X the number of

redundancies of the structure, then $(N-X)$ independent mechanisms will be needed to solve the problem.

For the problem under consideration there are 7 points of possible plastic hinge formation and the structure is 3 times redundant. Therefore

7 = number of possible hinges

- 3 = redundancy

4 = number of independent mechanisms

Obviously, each of the rafters could fail as a beam as shown in Figures 8a and 8b. The roof part of the structure could remain rigid in itself and the whole could side sway as shown in Figure 8c. The fourth chosen independent type of failure occurs when the left hand column remains vertical and the rafters spread as shown in Figure 8d, (i.e. a gable mechanism).

Not only must these failure configurations be investigated but also all combinations of them. For example, beam mechanism (a) could be combined with gable mechanism (d) and result in a "new" mechanism having plastic hinges

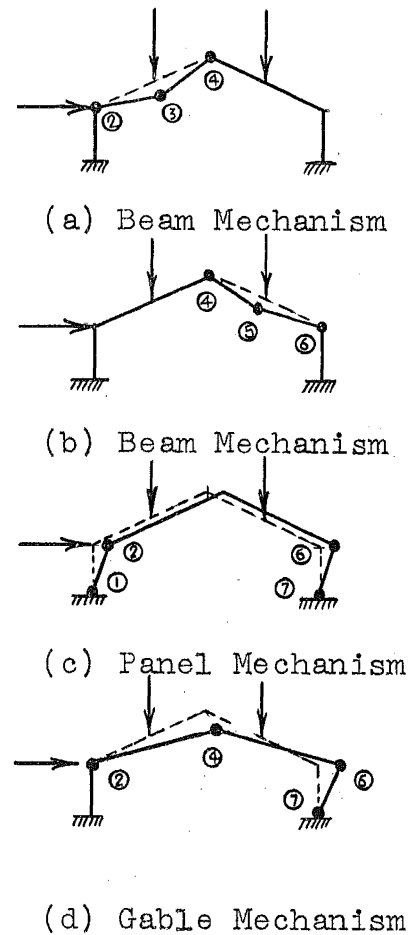


FIGURE 8

at locations ②, ③, ⑥ and ⑦.
 A majority of the possible combinations are shown in Figure 9.

The next step in the solution of the problem by the mechanism method is the determination, in terms of the given loads, of the critical M_p value corresponding to each mechanism.

Beam Mechanism (a)

As shown in Figure 10, if the link ②-③ of the rafter ②-④ is subjected to a virtual rotation of θ about point ②, then point ③ will move to the right and down

through a vertical distance θL . Since the horizontal projection of the link ③-④ is also L , the linkage ③-④ will also rotate through a virtual angle θ with respect to its original position. The total change in angle of the member at plastic hinge ③ is best determined from a consideration of Figure 10(b). As seen, the member rotates through an angle of θ on each side. Therefore, the total angle change equals 2θ . Equating the internal and external

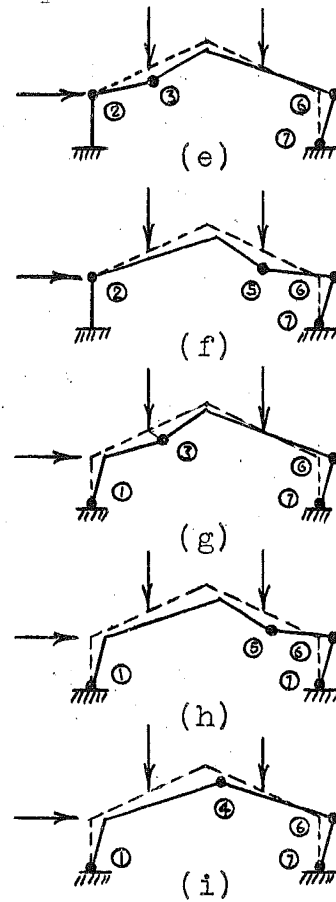


FIGURE 9

works associated with this virtual deformation condition gives

$$W_{int} = W_{ext}$$

$$M_p\theta + M_p(2\theta) + M_p\theta = P(\theta L)$$

$$\underbrace{}_{@2} + \underbrace{}_{@3} + \underbrace{}_{@4} = P(\theta L)$$

or

$$M_p = \frac{PL}{4} \dots\dots\dots (4)$$

Beam mechanism (b) of Figure 8 will result in the same value of M_p .

For the panel mechanism (see Figure 11) it has been assumed that a virtual rotation θ occurs in each of the columns. The corresponding angular relationships are as shown. Therefore,

$$W_{int} = W_{ext}$$

$$M_p\theta + M_p\theta + M_p\theta + M_p\theta = P(L\theta)$$

or

$$M_p = \frac{PL}{4} \dots\dots\dots (5)$$

Whereas the inter-relationship between the various rotations at each of the plastic hinges within the structure have been easy to determine thus far, this will not necessarily be the case for the remaining failure modes.

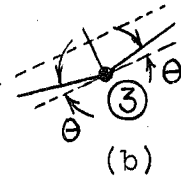
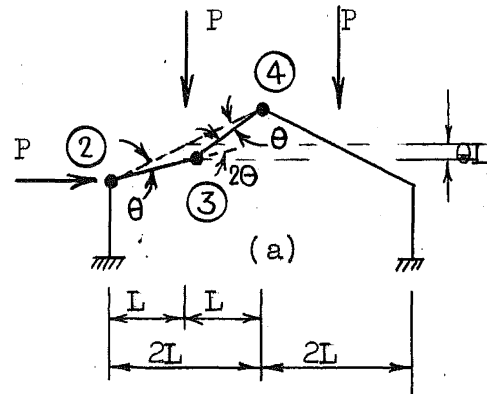


FIGURE 10

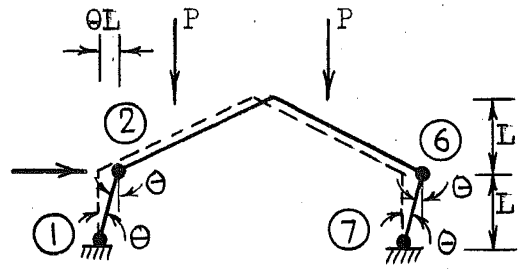


FIGURE 11

Consider the gable mechanism shown in Figure 12a. If it is assumed that the right hand column rotates through the virtual angle θ , then point (6) will move horizontally to the right a distance of θL . Because of the symmetric type of deformation pattern; that is, rafter (2)-(4) rotates through the same angle as rafter (4)-(6); the horizontal projection of the movement of point (4) will be one-half that at point (6) or $\frac{1}{2}\theta L$ as shown. In so doing (see Figure 12b) the movement of point (4) has a vertical project equal to θL . This requires that each of the rafters rotate through angles of $\theta L/2L$ or $\theta/2$ with respect to their original positions.

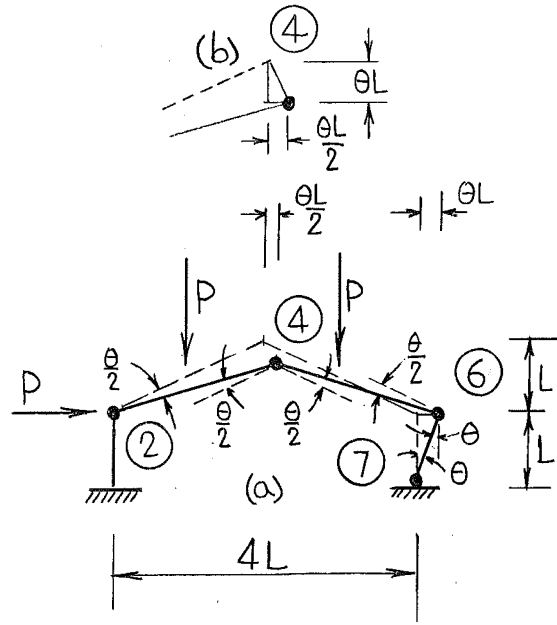


FIGURE 12

The total rotations at the various hinges are therefore as follows:

- Hinge 2 $\theta/2$
- Hinge 4 $\theta/2 + \theta/2 = \theta$
- Hinge 6 $\theta/2 + \theta = 3\theta/2$
- Hinge 7 θ

The distances traveled by each of the vertical forces P in the direction of the force are $(L)(\theta/2)$. The critical load is then

$$W_{int} = W_{ext}$$

$$M_p(\theta/2 + \theta + 3\theta/2 + \theta) = P(L\theta/2) + P(L\theta/2)$$

or
$$M_p = \frac{PL}{4} \dots\dots\dots(6)$$

We will now solve this same problem by a slightly different method, one that is usually referred to as the INSTANTANEOUS CENTER method⁽⁹⁾⁽²⁰⁾. (It should be pointed out that we are not here talking about a change in the mechanism method of solution as such but rather a change in the method of defining the geometry associated with any chosen virtual deformation).

Consider first the structure from an over-all point of view. For the failure mechanism being investigated the left hand column is assumed to remain vertical. Rafter (2)-(4) will therefore rotate about point (2) as its center. Likewise the right hand column (6)-(7) is constrained to rotate about its base, point (7). As to the point

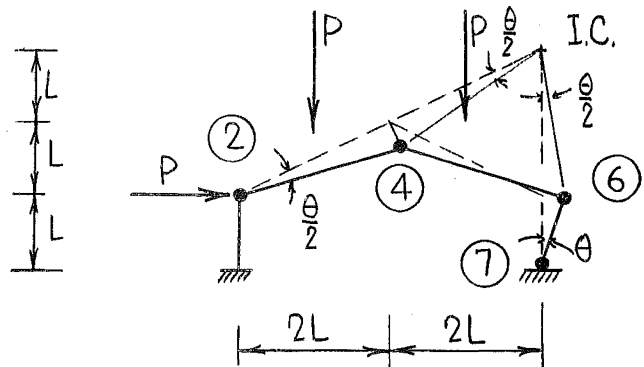


FIGURE 13

about which the rafter ④ - ⑥ will rotate, end ④ of the rafter must move in a direction perpendicular to member ② - ④, whereas end ⑥ must move horizontally to the right. With this information it can be shown that member ④ - ⑥ rotates about I.C., its instantaneous center of rotation. (The location of this point is from purely geometrical considerations).

If the base of the right hand column is again selected as the starting point, and the member ⑥ - ⑦ is subjected to a virtual rotation of θ , then point ⑥ will move to the right through a distance θL . In so doing it requires that end ⑥ of the rafter ④ - ⑥ must rotate about I.C. (its instantaneous center) through an angle $\theta L/2L = \theta/2$. At the same time point ④ moves to its new location; which is $\theta/2$ times the distance from ④ to I.C. below and to the right of its original position. Since the length of rafter ② - ④ is the same as the length ④ - I.C., member ② - ④ will rotate through an angle of $\theta/2$ at plastic hinge ②.

The total rotation at plastic hinge ② then is $\theta/2$; at plastic hinge ④ it will be the sum of that occurring at ② and at I.C., i.e. $\theta/2 + \theta/2 = \theta$; and at plastic hinge ⑥ the sum of that at I.C. and at ⑦, or in other words $\theta/2 + \theta = 3\theta/2$. These values are exactly the same as the ones previously obtained. The resulting solution for M_p in terms of P will therefore also be the same.

Using the instantaneous center method of defining the geometric changes associated with a given virtual displacement,

consider now the solution to composite mechanisms shown in Figure 9.

Since for the mechanism shown in Figure 14 the left hand column is assumed to remain vertical, the instantaneous center of linkage ③ - ⑥ is located a distance of $2L$ vertically above plastic hinge ⑥.

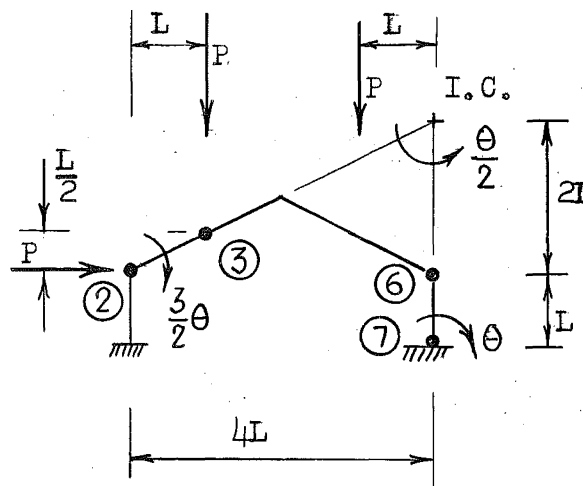


FIGURE 14

Assuming a virtual rotation equal to θ at plastic hinge ⑦, linkage ③ - ⑥ rotates about its instantaneous center, I.C., through an angle of $\theta/2$. For this to occur linkage ② - ③ is required to rotate through an angle of $\frac{3}{2}\theta$ since the distance from I.C. to 3 is three times that from ② to ③ (note the horizontal projections). The total rotations at each of the plastic hinges are therefore as follows:

- Hinge ② $3\theta/2$
- Hinge ③ $3\theta/2 + \theta/2 = 2\theta$
- Hinge ⑥ $\theta/2 + \theta = 3\theta/2$
- Hinge ⑦ θ

The solution to the problem is therefore,

$$W_{int} = W_{ext}$$

$$M_p \left[3\theta/2 + 2\theta + 3\theta/2 + \theta \right] = \underbrace{P(3\theta/2)(L)}_{(3)} + \underbrace{P(\theta/2)(L)}_{(5)}$$

or

$$M_p = \frac{PL}{3} \dots\dots\dots (7)$$

For the mechanism shown in Figure 15 the I.C. of linkage (5) - (6) is located $2L/3$ vertically above point (6). Assuming then a rotation of θ at hinge (7) the rotation at I.C. will equal $\frac{3}{2}\theta$ while the rotation at hinge (2) equals $\theta/2$. To obtain the solution

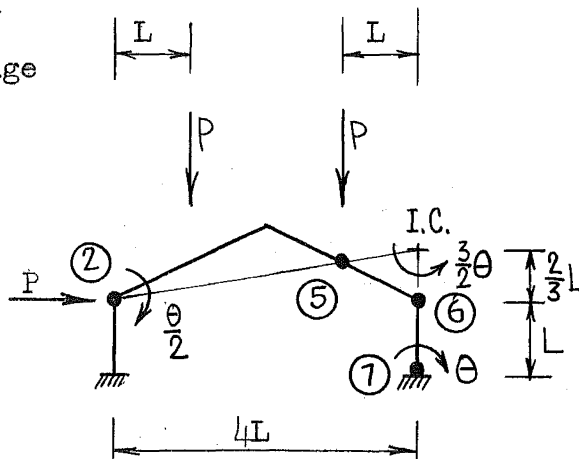


FIGURE 15

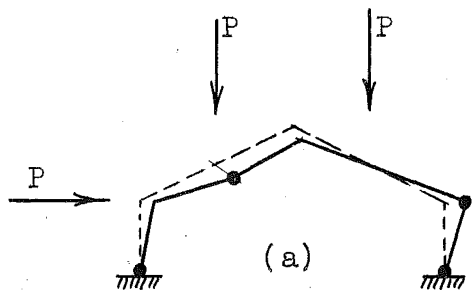
$$W_{int} = W_{ext}$$

$$M_p \left(\underbrace{\theta/2}_{@ (2)} + \underbrace{\theta/2 + 3\theta/2}_{@ (5)} + \underbrace{3\theta/2 + \theta + \theta}_{@ (6) @ (7)} \right) = PL\theta/2 + PL(3\theta/2)$$

or

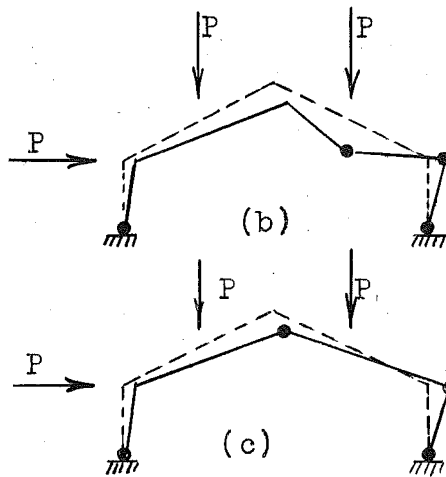
$$M_p = \frac{PL}{3} \dots\dots\dots (8)$$

Going through the same process for the remaining mechanisms, the solutions shown in Figure 16 are obtained.



$$M_p = \frac{7}{18} PL \dots\dots\dots (9)$$

FIGURE 16a



$$M_p = \frac{5}{14} \dots \dots \dots (10)$$

$$M_p = \frac{3}{10} PL \dots \dots \dots (11)$$

FIGURE 16b

Assume now that all possible failure modes have been examined. From the resulting equations (4) through (11) it is noted that equation (9) requires the greatest M_p value. and it is therefore assumed that this is the correct solution. To be certain that such is the case, a moment diagram for the supposed solution must be drawn. (see Figure 17*).

Considering the right hand columns as a free body and taking moments about the top of the column, the horizontal reaction B_H is found to be

$$B_H = 2 \frac{M_p}{L}$$

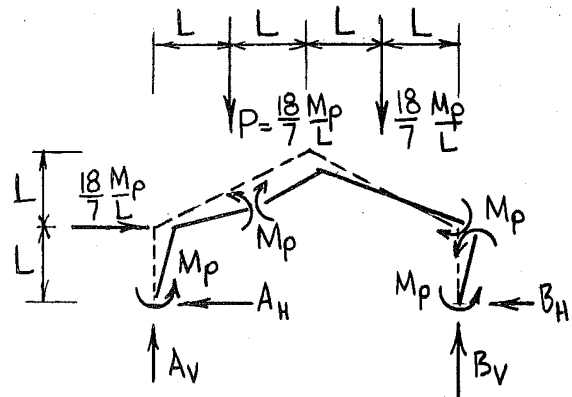


FIGURE 17

*It should be noted that the M_p moments act to oppose the deformation.

For the complete structure as a free body (taking moments about (A))

$$B_V = 2.71 \frac{M_p}{L}$$

The remaining reactions are therefore

$$A_H = 0.57 \frac{M_p}{L}$$

and

$$A_V = 2.43 \frac{M_p}{L}$$

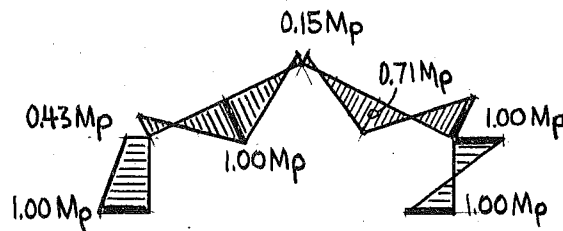


FIGURE 18

The moment diagram is as

shown in Figure 18. (Note:

moments are plotted on the tension side of the members).

Since the structure is in equilibrium with the applied loads, since a mechanism is formed and since nowhere does the moment exceed the full plastic value; this is the correct solution.

6. Concentrated versus Distributed Loads

In the preceding discussion the problem was straight forward since it was possible to ascertain at the start the exact location of all possible plastic hinges. Such will always be the case when the structure under consideration is subjected to concentrated loads.

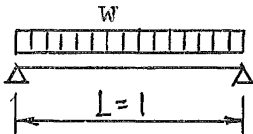

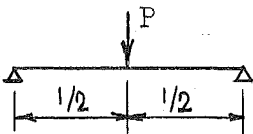
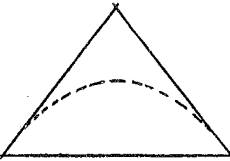
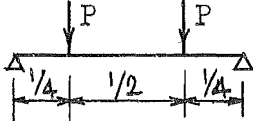

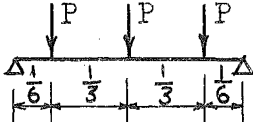



Where distributed loads are involved, however, the location of the plastic hinge must be written in generalized form and a solution to M_p obtained in terms of the unknown distance to the hinge. By differentiating this general

expression for M_p with respect to the unknown distance and setting it equal to zero the true location of the hinge can be determined. Such a procedure will be used in solving the generalized multi-span problem.

For an approximation the uniformly distributed load could be replaced by concentrated load. To ensure a safe answer the criterion for selection of these equivalent loads should be that the moment diagram due to the concentrated loads must circumscribe that due to the uniformly distributed ones. (This would require that the structure be subjected to at least as severe a moment condition as that of the uniform load case). Table 2 summarizes several equivalent loads systems that could be used. The derivation of these values is given in Appendix A to this report.

TABLE 2

EQUIVALENT CONCENTRATED LOADS

LOADING DIAGRAM	MOMENT DIAGRAM	EQUIVALENT LOAD
		
		$P = wL$
		$P = \frac{1}{2} wL$
		$P = \frac{1}{3} wL$
		$P = \frac{1}{4} wL$

7. Modifying Factors (8)

In the derivation of the simple plastic theory and consequently in the solutions presented in this paper several important assumptions were made. It was assumed that

1. normal force does not influence the ultimate bending resistance of a member (i.e. its M_p value),
2. the influence of shear on the full plastic moment may be disregarded,
3. no instability occurs prior to the development of a mechanism,
4. the loads are increased proportionally,
and
5. failure will not occur due to brittle fracture.

Regarding the first two of these factors, a solution to a given problem could be obtained on the assumption that the members in question will develop a certain M_p . After solving the problem for the required moment value, a member would be selected that will deliver this required moment value while sustaining the shear or thrust. Methods for handling such problems are discussed in reference (8).

Local instability can be prevented by placing certain restriction on the geometric proportions that a cross-section may have if it is to be used in plastic design. For lateral buckling a means of defining adequate lateral support is

needed. Further research work is required to be able to adequately handle the problem of column instability. The possibility of such a failure prior to the attainment of the full plastic load must at this time be avoided.

Concerning the problem of proportional loads, Symonds and Neal^{(11), (15)} have shown that this provision is not as restrictive as would be anticipated. For most structures and loadings found in practice the true maximum load including the influence of variable repeated load is only slightly below that predicted on the basis of simple plastic theory. Another point with regard to this problem is that the ratio of live load to dead load for a given structure is important. If this ratio is small, the influence of the live load variation will be of lesser importance. Another possibility is that if wind is responsible for the variation in load, and if it is assumed that smaller factors of safety are to be used when the influence of wind is included in the analysis, then it is quite possible that the design will not be governed by the loading condition that includes wind force even when modified to include the influence of variable repeated loading.

To ensure a safe structure against brittle fracture, attention must be given to design details.⁽¹⁹⁾ The material and type of fabrication should also be considered.

II. PLASTIC DESIGN OF SINGLE-SPAN GABLE FRAMES

In general, it can be reasoned from economic considerations that the better design is the one that requires the larger number of members within the structure to sustain the ultimate load at their maximum strengths. Such a design, however, will not necessarily be practical. For example, a portal frame subjected to vertical loads and wind from the left could be designed for "least weight" under this one loading condition. The wind, however, could for most structures just as well have occurred from the right. Had this been the case, the previously designed structure would have failed at a much lower load depending on the ratios of the horizontal to vertical load, the height to span, etc.

For the gabled frames considered in this section it is assumed that the rafters are of equal strength, their full plastic moment value being M_p . The columns are also assumed to be equal. The structure then is symmetric insofar as the member sizes are concerned. Moreover, for the majority of structures encountered in practice it can be shown that the most economical ("least weight") solution will occur when the delivered plastic moment value of the columns equal that of the rafter. Therefore, such an assumption is also made. The structures to be investigated then are as shown in Figure 19. Both the pinned base and the fixed base cases will be considered.

The loading to which these structures will be subjected is as shown in Figure 20: a uniform vertical load of w lbs/ft and a concentrated horizontal load P acting at the eave. For most problems the horizontal force will not be concentrated. As will be shown later, however, if the P force is chosen such that its "over-turning"

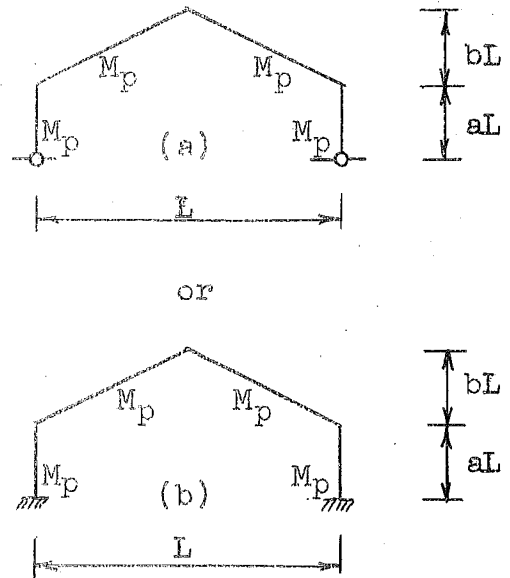


FIGURE 19

moment about the base of the structure is the same as that produced by the distributed load then a conservative answer will be obtained by solving the concentrated load problem.

1. Pinned-Base Gable Frames

Considering first the pinned-base structure (see Figure 20) and following the procedure outlined in the previous section on the mechanism method, there are 5 points of possible plastic hinge formations in this one-time-statically-redundant structure. Therefore

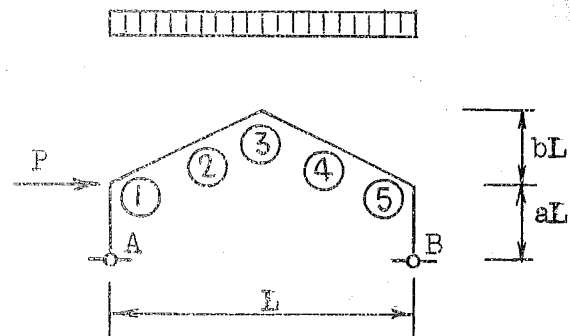


FIGURE 20

- 5 = number of possible plastic hinges
- 1 = number of redundants
- 4 = number of independent failure mechanisms

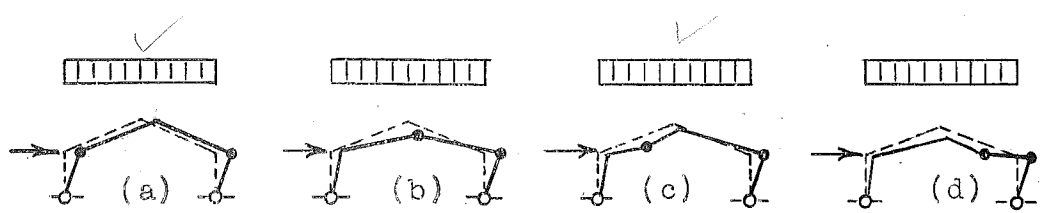


FIGURE 21

The chosen independent failure forms are as shown in Figure 21*. In cases (a) and (b) the positions of the plastic hinges are fixed. For (c) and (d), however, it is necessary that the correct distance to the hinge also be determined.

For the panel mechanism shown in Figure 22, the P force alone does external work. Therefore,

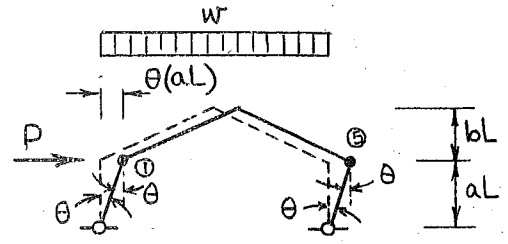


FIGURE 22

$$W_{int} = W_{ext}$$

$$M_p \theta(1+1) = P\theta(aL)$$

or

$$M_p = \frac{P(aL)}{2} \dots \dots \dots (12)$$

*It should be noted that if the structure is to sway to the right in failing then no combination of these mechanisms is geometrically possible. Should the P force be equal to zero, a panel mechanism movement (mechanism a of Figure 21) could be assumed to the left and combinations of failure modes thereby obtained.

The solution to mechanism (b) of Figure 21 is as shown in Figure 23. Since plastic hinges are assumed to form at (3) and (5), part (A)-(3) of the structure rotates about the base of the left hand column while part (B)-(5) rotates about the right hand base.

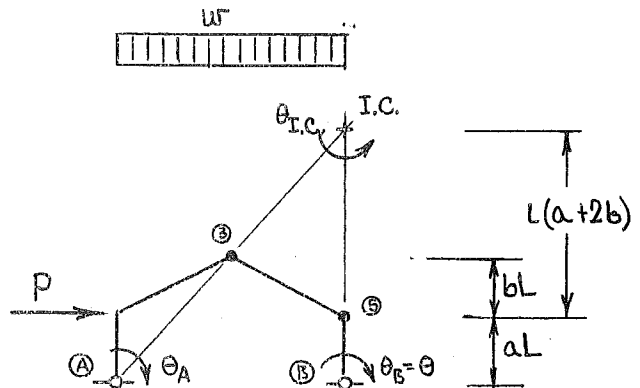


FIGURE 23

The instantaneous center of part (3)-(5) is therefore $L(a+2b)$ vertically above plastic hinge (5). Assuming now a virtual rotation θ_B equal to θ , the corresponding virtual rotations at other points in the structure are as follows:

$$\theta_{I.C.} = \theta \left[\frac{aL}{aL+2bL} \right] = \theta \left[\frac{1}{1+\frac{2b}{a}} \right]$$

$$\theta_A = \theta \left[\frac{1}{1+\frac{2b}{a}} \right] \left[\frac{2L}{2L} \right] = \theta \left[\frac{1}{1+\frac{2b}{a}} \right]$$

Plastic hinge (3) will therefore rotate through an angle of

$$\theta_3 = \theta \left[\frac{2}{1+\frac{2b}{a}} \right]$$

while

$$\theta_5 = \theta \left[\frac{1}{1+\frac{2b}{a}} + 1 \right]$$

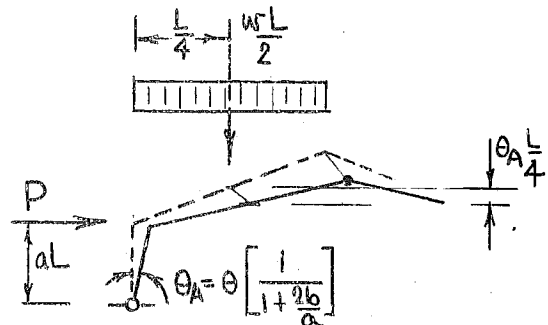


FIGURE 24

To compute the external work of the uniformly applied vertical load see Figure 24 . Since member ① - ③ remains rigid during the deformation, the uniform load on this part of the structure could be considered concentrated at its centroid. A similar situation exists for part ③ - ⑤. Solution therefore will be as follows:

$$W_{int} = W_{ext}$$

$$M_p \theta \left[\frac{2}{1 + \frac{2b}{a}} + \frac{1}{1 + \frac{2b}{a}} + 1 \right] = P \theta (aL) \left[\frac{1}{1 + \frac{2b}{a}} \right] + \frac{wL}{2} \left[\frac{L}{4} \right] \theta \left[\frac{1}{1 + \frac{2b}{a}} \right] + \frac{wL}{2} \left[\frac{L}{4} \right] \theta \left[\frac{1}{1 + \frac{2b}{a}} \right]$$

which gives

$$M_p = \frac{PaL + \frac{wL^2}{4}}{2(2 + \frac{b}{a})} \dots \dots \dots (13)$$

Rewriting the solution in another form, the over-turning moment, PaL, could be equated to a function of wL². For example,

$$PaL = A \frac{wL^2}{2} \dots \dots \dots (14)$$

Therefore

$$A = 2a \frac{P}{wL} \dots \dots \dots (15)$$

Substituting equation (14) in equation (13) and reducing gives

$$M_p = \frac{wL^2}{4} \left[\frac{A + 1/2}{2 + b/a} \right] \dots \dots \dots (16)$$

To further non-dimensionalize transpose the wL² term to the left of the equal sign,

$$\frac{M_p}{wL^2} = \frac{1}{4} \left[\frac{A + 1/2}{2 + b/a} \right] \dots \dots \dots (17)$$

Equation (17) then defines the non-dimensional quantity M_p/wL^2 in terms of the ratio of the total rise of the rafter to the height of the column (i.e. b/a) and the load parameter "A" defined by equation (15).

Rewriting equation (12) (the solution to the panel mechanism problem) in the same "A" parameter form

$$\frac{M_p}{wL^2} = \left[\frac{A}{4} \right] \dots\dots\dots(18)$$

For the mechanism shown in Figure 21c (re-drawn as Figure 25) the horizontal distance to plastic hinge ② equals αL . From geometry it can then be shown that the distance cL , the vertical distance above ⑤ to the instantaneous center of part ② - ⑤, is given by

$$cL = L \left[\frac{a}{k} - a + 2b \right]$$

Consistent rotations at the various points within the structure are therefore as follows:

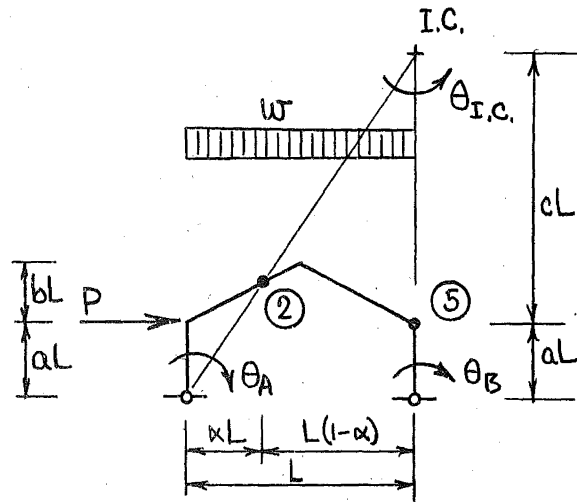


FIGURE 25

$$\left. \begin{aligned} \theta_B &= \theta \\ \theta_{I.C.} &= \theta \left[\frac{\alpha}{1-\alpha + \frac{2b}{a}\alpha} \right] \\ \theta_A &= \theta \left[\frac{1-\alpha}{1-\alpha + \frac{2b}{a}\alpha} \right] \end{aligned} \right\} \dots\dots\dots(19)$$

Total rotations at the plastic hinges equal

$$\left. \begin{aligned} \theta_2 &= \theta \left[\frac{1}{1-\alpha + \frac{2b}{a}\alpha} \right] \\ \theta_5 &= \theta \left[\frac{1 + \frac{2b}{a}\alpha}{1-\alpha + \frac{2b}{a}\alpha} \right] \end{aligned} \right\} \dots\dots\dots(20)$$

The expression for equalization of internal and external work therefore is as follows:

$$W_{int} = W_{ext}$$

$$M_p \theta \left[\frac{1}{1-\alpha + \frac{2b}{a}\alpha} + \frac{1 + \frac{2b}{a}\alpha}{1-\alpha + \frac{2b}{a}\alpha} \right] = PaL\theta \left[\frac{1-\alpha}{1-\alpha + \frac{2b}{a}\alpha} \right] + \frac{WL^2}{2} \alpha \left[\frac{1-\alpha}{1-\alpha + \frac{2b}{a}\alpha} \right] \theta + \frac{WL^2}{2} (1-\alpha)^2 \theta \left[\frac{\alpha}{1-\alpha + \frac{2b}{a}\alpha} \right]$$

This reduces to

$$\frac{M_p}{wL^2} = \frac{1}{4} \left[\frac{(1-\alpha)(A+\alpha)}{1 + \frac{b}{a}\alpha} \right], \dots\dots\dots(21)$$

where

$$A = 2a \left[\frac{P}{wL} \right]$$

It will be noted that equation (21) is in terms of the unknown distance αL . Since α is an independent variable

and since the structure will fail at its first opportunity, the correct α distance will be determined from the expression

$$\frac{\partial M_p}{\partial \alpha} = 0 \dots\dots\dots (22)$$

Equation (21) is of the general form "u/v". Therefore, the differentiation will be

$$d\left(\frac{u}{v}\right) = \frac{vdu - u dv}{v^2} \dots\dots\dots (23)$$

But since the expression is to equal zero,

$$vdu - u dv = 0$$

The correct α distance is therefore

$$\left. \begin{aligned} \alpha &= \frac{1}{\frac{b}{a}} \left[\sqrt{1 - \frac{b}{a} \left[A \left(1 + \frac{b}{a} \right) - 1 \right]} - 1 \right] \\ &\quad \text{for } \frac{b}{a} > 0 \\ \text{and } \alpha &= \left[\frac{1-A}{2} \right] \\ &\quad \text{for } \frac{b}{a} = 0 \end{aligned} \right\} \dots\dots\dots (24)$$

A substitution of these values for α in equation (21) will give the solution to this mechanism.

Going through the same process for the mechanism shown in Figure 26, it is found that

$$\frac{M_p}{wL^2} = \frac{1}{4} \left[\frac{\alpha(1-\alpha + A)}{1 + \frac{b}{a}\alpha} \right], \dots\dots (25)$$

where

$$\alpha = \frac{1}{\frac{b}{a}} \left[\sqrt{1 + \frac{b}{a}(1+A)} - 1 \right] \dots (26)$$

for $\frac{b}{a} > 0$

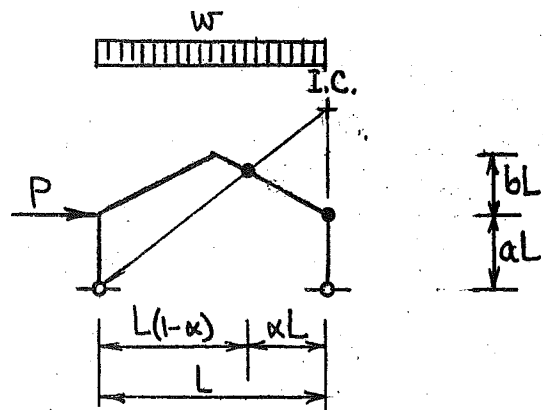


FIGURE 26

and

$$\alpha = \left[\frac{1+A}{2} \right] \dots\dots\dots \text{for } \frac{b}{a} = 0 \dots\dots\dots (27)$$

The problem now is to determine which of equations (17), (18), (21) and (25) requires (for a given loading condition) the larger plastic moment value. This will depend on the value of b/a and A under consideration. By assuming various values of b/a and A and solving each of these equations for the resulting M_p/wL^2 , ranges of applicability for each equation can be determined. If such a procedure is carried out it will be observed that only equations (18) and ⁽²¹⁾(25) govern the solution. Plotting the resulting values of b/a versus A versus M_p/wL^2 the design curve shown in Figure ⁽²¹⁾22 is obtained. Below the dashed line the governing equation is equation ⁽²¹⁾(25). Above this line equation (18) defines the solution. The corresponding α values are shown in Figure 27a.

These same curves are given to a larger scale as Design Charts I-1 and I-1a at the end of the dissertation. Their use will be described later.

2. Fixed-Base Gabled Frames

For the fixed-base frame shown in Figure 28

- 7 = number of possible plastic hinges
- 3 = number of redundants
- 4 = number of independent mechanisms.

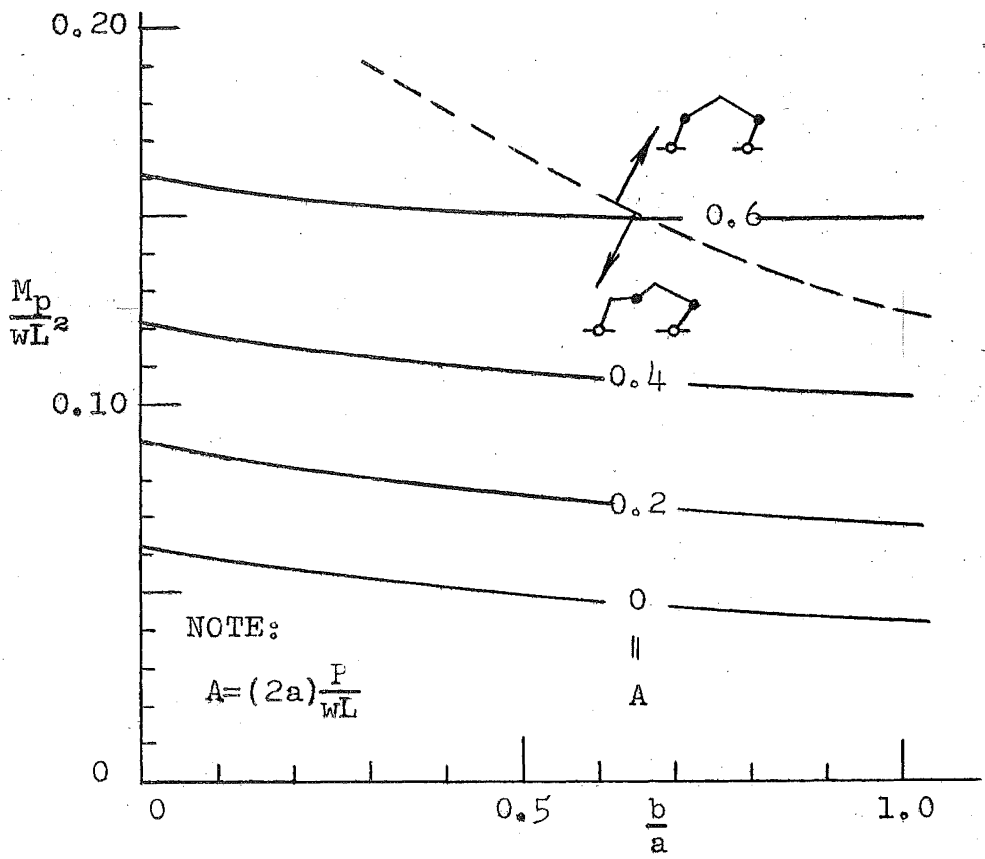


FIGURE 27

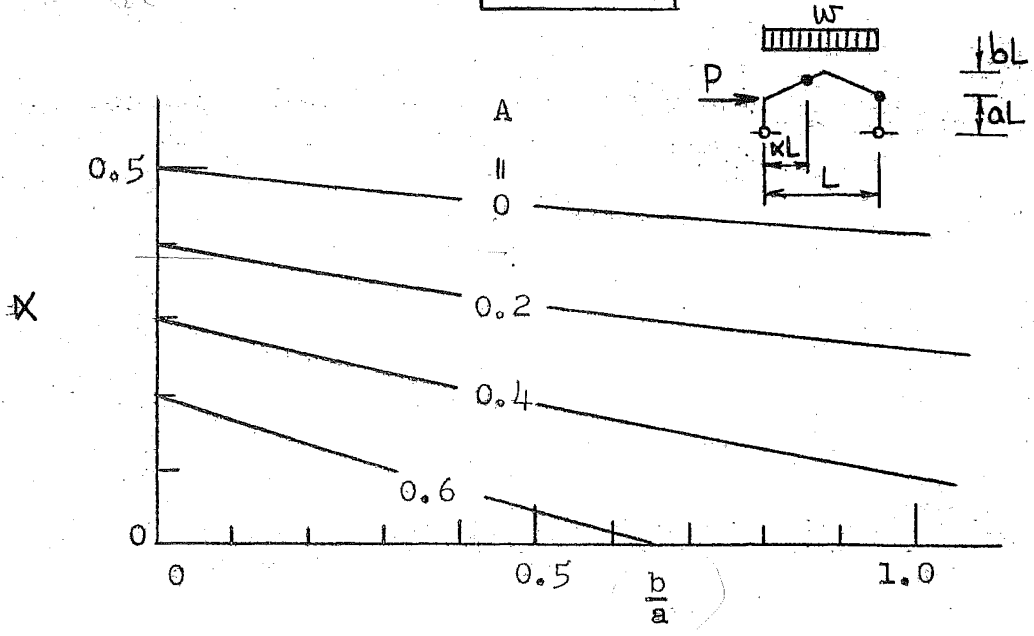


FIGURE 27a

The chosen independent mechanisms are those shown in Figure 29. These and their combinations would need to be investigated to solve the problem.

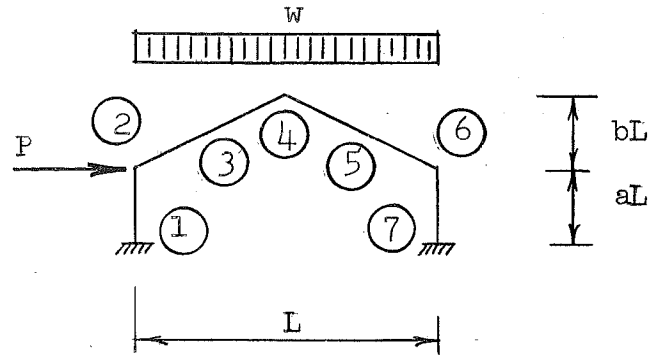


FIGURE 28

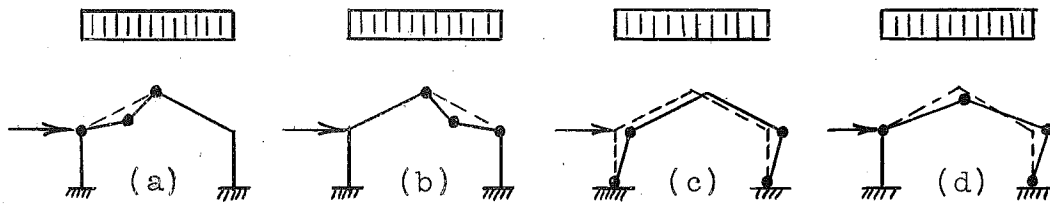


FIGURE 29

Going through the same procedure of investigation of all possible failure modes to determine the corresponding critical M_p/wL^3 values, a solution to this problem could be obtained as in the pinned-base case. The important equations that would govern the solution are tabulated as equations (4), (5), (6) and (7) of Appendix C.

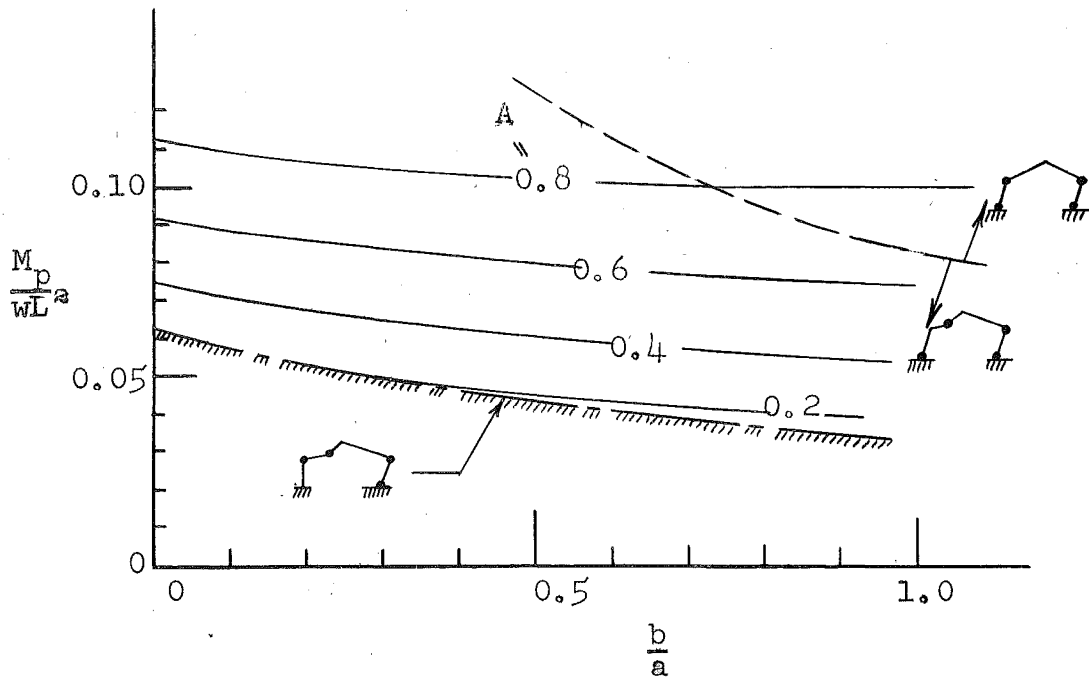


FIGURE 30

NOTE: $A = 2a(P/wL)$

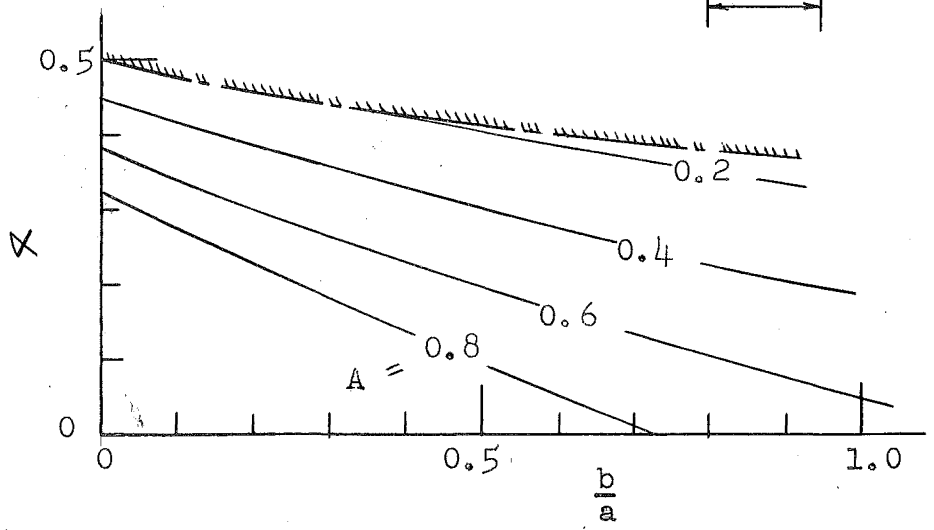
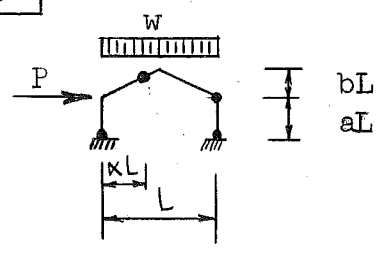


FIGURE 31

The resulting solutions in graphical form are Figures 30 and 31. (Here again it should be pointed out that design curves for this case are given to a larger scale in the section on Design Charts at the end of this report).

In Figures 30 and 31 there is shown a cross-hatched "cut-off" line. This line corresponds to equation 6 of Appendix C and represents the minimum M_p/wL^2 value that can occur. It will be noted that this equation is independent of A value (that is, independent of horizontal force).

3. The Problem of Distributed Horizontal Loads

As mentioned earlier, if the horizontal load acting on the structure is distributed rather than concentrated, a conservative answer can be obtained by selecting a P value for the concentrated load problem having an "over-turning" moment about the base of the structure equal to that of the distributed horizontal load (providing a hinge does not develop within the left hand column). Consider for example the two structures shown in Figure 32.

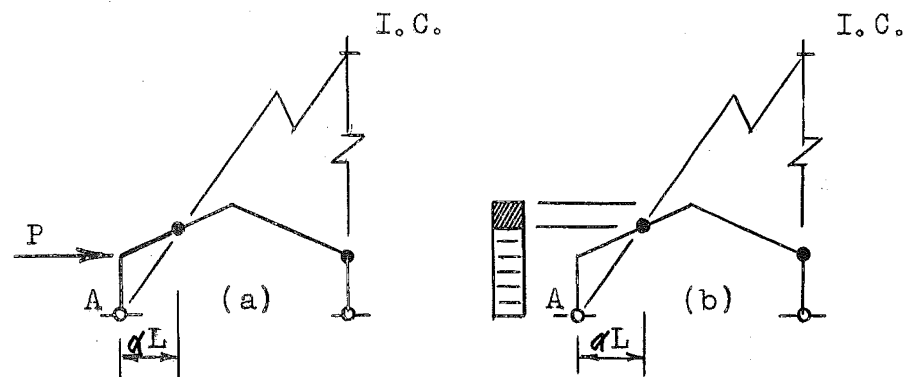


FIGURE 32

If these two structures are of equal size and shape and if the distances κL are also equal then the rotations corresponding to a virtual displacement and therefore the internal work will be the same for both structures. Since the external work due to equal vertical loading of both structures will be equal, these forces can be disregarded in this discussion.

Assume now that the moment of P about the base of the column ("A" in Figure 32a) is chosen equal to that of the distributed load of system "b" (see Figure 32b). The external work done by the P force will be greater than that of the distributed load of system "b". This can be seen by realizing that if they were equal the work done by the heavily cross-hatched portion of the distributed horizontal load shown in Figure 32b would need to be the same whether considered rotating about point A or point I.C.

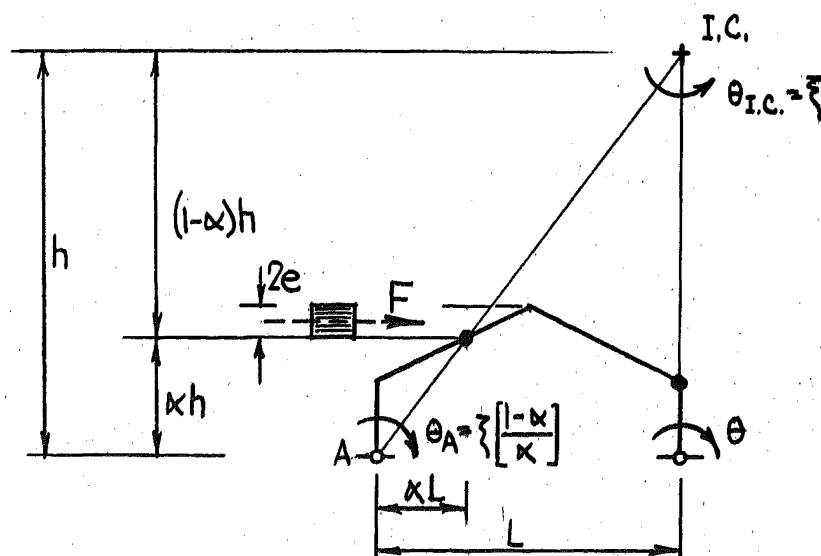


FIGURE 33

In Figure 33 it has been assumed that the virtual rotation at the instantaneous center equals ξ . The corresponding rotation at A is therefore

$$\theta_A = \xi \left(\frac{1-\alpha}{\alpha} \right).$$

If h is now assumed as the total vertical distance from the base of the structure to the instantaneous center I.C. then the vertical distances to the hinge in the left rafter will be given in terms of h and α as shown. For a distributed load block 2e in height the external work due to the concentrated force F equals

$$W_{\text{ext}}^{\text{I.C.}} = F \left[(1-\alpha)h - e \right] \xi \dots\dots\dots (28)$$

if considered rotating about I.C.

Assuming the force block rotates about the base of the column (i.e. about A)

$$W_{\text{ext}}^{\text{A}} = F \left[\alpha h + e \right] \xi \left[\frac{1-\alpha}{\alpha} \right] \dots\dots\dots (29)$$

The question is, is the external work defined by equation (29) greater than that of equation (28). If it is then system "a" of Figure 32a is the more conservative system (that is, it requires a greater value of M_p).

$$\begin{aligned} W_{\text{ext}}^{\text{A}} & \stackrel{?}{=} W_{\text{ext}}^{\text{I.C.}} \\ F \xi \left[\alpha h + e \right] \left[\frac{1-\alpha}{\alpha} \right] & \stackrel{?}{=} F \xi \left[(1-\alpha)h - e \right] \\ h + \frac{e}{\alpha} - \alpha h - e & \stackrel{?}{=} h - \alpha h - e \\ \frac{e}{\alpha} & > 0 \end{aligned}$$

Therefore

$$W_{\text{ext}}^{\text{A}} > W_{\text{ext}}^{\text{I.C.}} \dots\dots\dots (30)$$

and the concentrated load solution as assumed gives a conservative answer. This same qualitative answer could have been obtained by a consideration of the deformed structure.

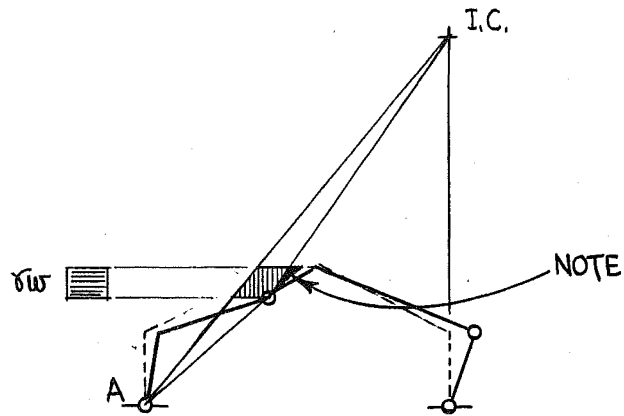


FIGURE 34

For the correct solution for external work due to the distributed horizontal load block in question, the force would be integrated over the deflection shown with vertical cross-hatching (see Figure 34). Assuming, however, that rotation and therefore the deflection through which this force moves was determined from rotation about A, the additional deflection shown heavily cross-hatched would have resulted. Obviously this system results in a greater external work.

For the sake of completeness, the exact answer to this distributed horizontal load problem is given by equations (31) and (32). The structure is as shown in Figure 35.

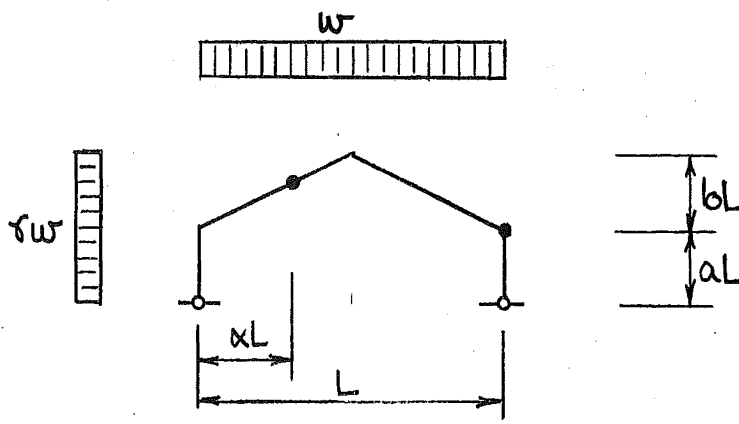


FIGURE 35

$$\frac{M_p}{wL^2} = \frac{1}{4} \left[\frac{\alpha(1-\alpha) + \frac{A}{(1+b/a)^2} \left\{ (1-\alpha)(1+2\frac{b}{a}) + \alpha(\frac{b}{a})^2(3-4\alpha) \right\}}{(1 + \frac{b}{a}\alpha)} \right] \dots\dots\dots (31)$$

$$\alpha = \frac{1}{\frac{b}{a}} \left[\sqrt{1 + \frac{b}{a} \left[1 - \frac{A \left\{ 1 + 3\frac{b}{a} + 3(\frac{b}{a})^2 \right\}}{(1+\frac{b}{a})^2 + 4A(\frac{b}{a})^2} \right]} - 1 \right] \dots\dots\dots (32)$$

where

$$\frac{AWL^2}{2} = \frac{\gamma w}{2} \cdot L^2 \cdot (a + b)^2$$

III. PLASTIC DESIGN OF MULTI-SPAN RIGID FRAMES

1. Direct Procedure

Having solved the pinned-base and fixed-base, single-span, gabled frame problem, and having found that for a major range of variables the mechanism that will control the design is the one where hinges develop in the windward rafter and at the top of the right hand column, a logical first attempt at a mechanism for the multi-span problem might be that shown in Figure 36.

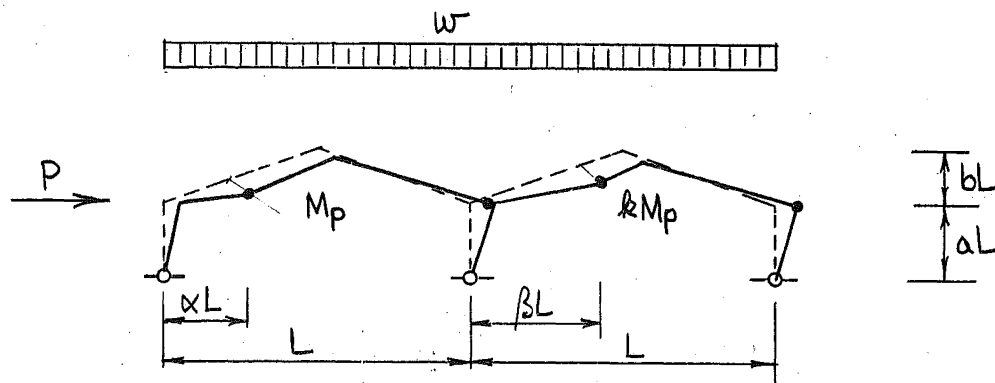
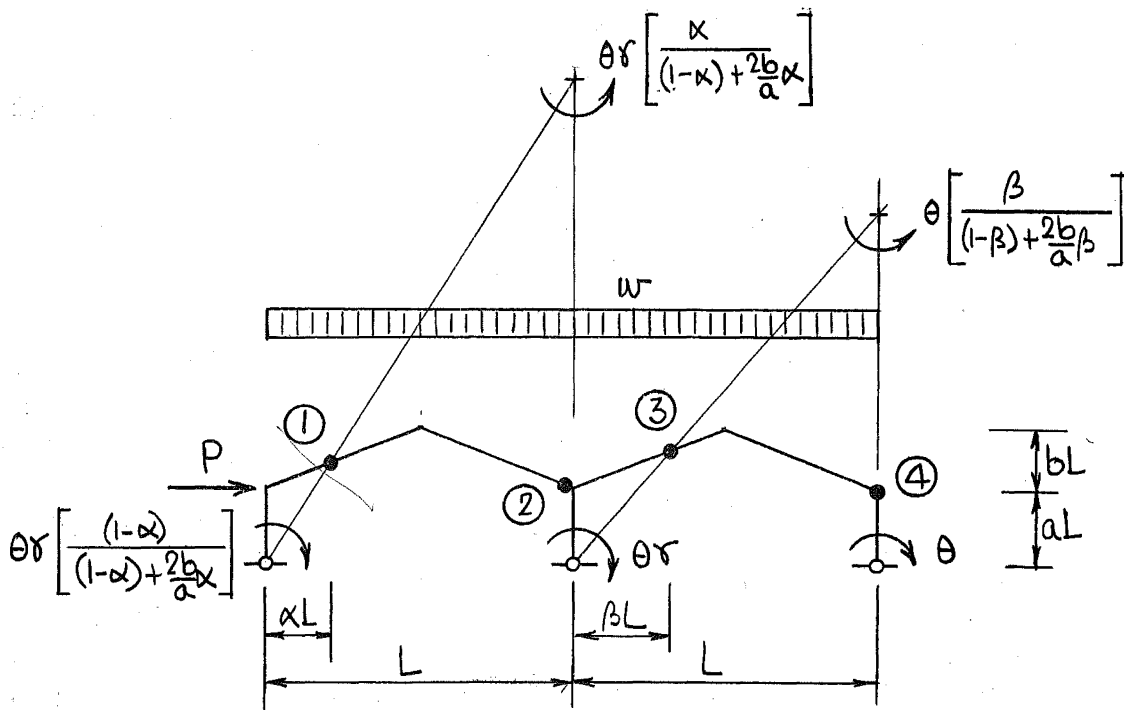


FIGURE 36

For the problem under consideration that part of the structure to the left of the center column is assumed to have a plastic moment value equal to M_p whereas the right hand part was chosen as kM_p . Lengths of span, heights of columns and total rise of rafters are chosen equal. It cannot be assumed, however, that the distances to the hinges in the windward rafters will be equal. The resulting expression for M_p will therefore contain the variables α and β .

Since each of these variables are independent, two separate differentiations (one of the form $\frac{\partial M_p}{\partial \alpha} = 0$ and the other $\frac{\partial M_p}{\partial \beta} = 0$) will be needed to solve for the correct α and β values.

The consistent virtual rotations as determined from a consideration of the instantaneous centers are shown in Figure 37.



NOTE:

$$r = \left[\frac{(1-\beta)}{(1-\beta) + \frac{2b}{a}\beta} \right]$$

FIGURE 37

The total rotations at the various plastic hinges are therefore as follows:

$$\begin{aligned}
 \text{Hinge } \textcircled{1} &= \theta \left[\frac{(1-\beta)}{(1-\beta) + \frac{2b}{a}\beta} \right] \left[\frac{1}{(1-\alpha) + \frac{2b}{a}\alpha} \right] \\
 \text{Hinge } \textcircled{2} &= \theta \left[\frac{(1-\beta)}{(1-\beta) + \frac{2b}{a}\beta} \right] \left[1 + \frac{\alpha}{(1-\alpha) + \frac{2b}{a}\alpha} \right] \\
 \text{Hinge } \textcircled{3} &= \theta \left[\frac{1}{(1-\beta) + \frac{2b}{a}\beta} \right] \\
 \text{Hinge } \textcircled{4} &= \theta \left[\frac{1}{(1-\beta) + \frac{2b}{a}\beta} \right]
 \end{aligned}
 \left. \vphantom{\begin{aligned} \text{Hinge } \textcircled{1} \\ \text{Hinge } \textcircled{2} \\ \text{Hinge } \textcircled{3} \\ \text{Hinge } \textcircled{4} \end{aligned}} \right\} \dots\dots\dots (33)$$

Equating the internal work and the external work

$$W_{int} = W_{ext}$$

$$\begin{aligned}
 &M_p \theta \left[\frac{(1-\beta)}{(1-\beta) + \frac{2b}{a}\beta} \right] \left[\frac{1}{(1-\alpha) + \frac{2b}{a}\alpha} \right] + M_p \theta \left[\frac{(1-\beta)}{(1-\beta) + \frac{2b}{a}\beta} \right] \\
 &\left[1 + \frac{\alpha}{(1-\alpha) + \frac{2b}{a}\alpha} \right] + kM_p \theta \left[\frac{1}{(1-\beta) + \frac{2b}{a}\beta} \right] + kM_p \theta \left[1 + \frac{\beta}{(1-\beta) + \frac{2b}{a}\beta} \right] \\
 &= PaL\theta \left[\frac{(1-\beta)}{(1-\beta) + \frac{2b}{a}\beta} \right] \left[\frac{(1-\alpha)}{(1-\alpha) + \frac{2b}{a}\alpha} \right] + \frac{wL^2}{2} (\alpha)^2 \theta \left[\frac{(1-\beta)}{(1-\beta) + \frac{2b}{a}\beta} \right] \\
 &\left[\frac{(1-\alpha)}{(1-\alpha) + \frac{2b}{a}\alpha} \right] + \frac{wL^2}{2} (1-\alpha)^2 \theta \left[\frac{(1-\beta)}{(1-\beta) + \frac{2b}{a}\beta} \right] \left[\frac{\alpha}{(1-\alpha) + \frac{2b}{a}\alpha} \right] \\
 &+ \frac{wL^2}{2} (\beta)^2 \theta \left[\frac{(1-\beta)}{(1-\beta) + \frac{2b}{a}\beta} \right] + \frac{wL^2}{2} (1-\beta)^2 \theta \left[\frac{\beta}{(1-\beta) + \frac{2b}{a}\beta} \right] \\
 &\dots\dots\dots (34)
 \end{aligned}$$

Again replace the concentrated horizontal force P acting at the eave by the non-dimensional "A" parametric form. The relationship assumed is the same as that previously used, i.e.

$$A = 2a \left[\frac{P}{wL} \right]$$

For the special case where $k=1$ the expression for internal and external work equalization (equation 34) reduces to

$$\frac{M_p}{wL^2} = \frac{1}{4} \left[\frac{-\alpha^2 - 2\alpha\beta - \beta^2 + \beta + \alpha + \beta^2\alpha + \beta\alpha^2 + \frac{2b}{a}\alpha\beta + \frac{2b}{a}\beta^2\alpha + A - A\beta - A\alpha - A\alpha\beta}{2 - \beta + \frac{4b}{a}\alpha - \frac{2b}{a}\alpha\beta - \alpha + \frac{b}{a}\beta + 2\left(\frac{b}{a}\right)^2\alpha\beta} \right] \dots\dots\dots (35)$$

Needless to say, the differentiation of this expression and the subsequent solution for α and β is not readily obtained. Even if an explicit solution of α and β were obtained, it is questionable if such an equation as (35) could be used in design.

Another possibility exists however. Since the variables involved are α , β and M_p an implicit differentiation of the work expression rather than the explicit one just considered may lead to an easier solution. As shown in Appendix B of this paper if $\frac{\partial M_p}{\partial \alpha} = 0$ then the corresponding differentiation of the function value, F, with respect to α must also equal zero; that is

$$\frac{\partial F}{\partial \alpha} = 0$$

In similar manner (36)

$$\frac{\partial F}{\partial \beta} = 0$$

Rewriting the internal and external work expressions (Eq. 34) in the form

$$W_{int} - W_{ext} = 0 \dots\dots\dots(37)$$

and keeping the γ parameter as defined in Figure 37 the following equation results:

$$\gamma \left[\frac{PaL(1-\alpha) + \frac{wL^2}{2}(\alpha-\alpha^2) - 2M_p \left\{ 1 + \frac{b}{a}\alpha \right\}}{(1-\alpha) + \frac{2b}{a}\alpha} \right] + \left[\frac{\frac{wL^2}{2}(\beta-\beta^2) - 2kM_p \left\{ 1 + \frac{b}{a}\beta \right\}}{(1-\beta) + \frac{2b}{a}\beta} \right] = 0 \dots\dots\dots(38)$$

Dividing through by γ , substituting in its value and reducing the resulting expression gives

$$\left[\frac{PaL(1-\alpha) + \frac{wL^2}{2}\alpha(1-\alpha) - 2M_p \left(1 + \frac{b}{a}\alpha \right)}{(1-\alpha) + \frac{2b}{a}\alpha} \right] + \left[\frac{\frac{wL^2}{2}\beta - 2kM_p \left\{ \frac{1 + \frac{b}{a}\beta}{1-\beta} \right\}}{1-\beta} \right] = 0 \dots\dots\dots(39)$$

This indicates that the function value is made up of two separate parts:

$$F(\alpha, \beta, M_p) = R(\alpha, M_p) + S(\beta, M_p) \dots\dots\dots(40)$$

Differentiation of this new expression (equation 39) according to equations 36 is therefore more easily obtained, than an explicit differentiation of M_p .

It should be remembered that only one possible failure configuration has been considered for the multi-span problem thus far. To solve a particular problem in question other modes would also need to be examined, to determine the one that would actually develop.

2. Solution by Separation

Based on the preceding discussion it could be reasoned that since for the problem under consideration the variables separate into two groups (one having to do with the loading and resistance of only the left hand portion, the other with only the right hand part) a solution might be more readily obtained by physically dividing the structure into two parts. If this division is made at the junction of the right hand rafter of the left structure and the center column, then the loading condition would be as shown in Figure 38.

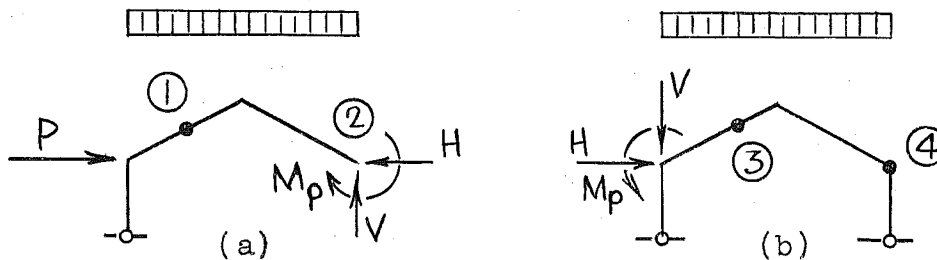


FIGURE 38

A solution to the multiple span case could be realized by solving each of these separate parts in terms of the loading parameters at the cut section and then in the final stage equating the parameters.

For the left hand part of the structure (see Figure 39), the resulting equation for M_p would be of the form

$$M_p = f(P, w, \alpha, H, \text{dimensions}) \dots (41)$$

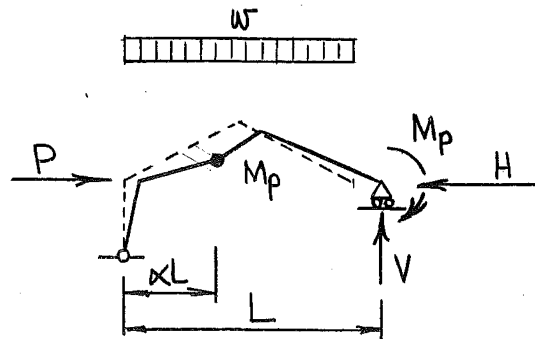


FIGURE 39

Since the structure does not move in the V direction at the cut section, this force will not enter the solution.

The equation for the right hand structure is $M_p = g(H, w, \beta, k, \text{dimensions}) \dots (42)$

From a virtual displacement consideration it is seen that as the structure fails the external work due to the H force on each of these parts will be equal since the deflections are equal.

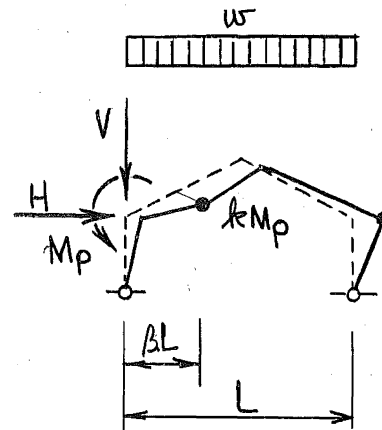


FIGURE 40

Assuming that the method of solution is the one shown in Figure 38 (i.e. the separation of the structure into two parts as shown) it is now necessary to write the equations corresponding to expression (41) and (42). Looking at (42) for a moment, it is seen that the derived equation for the strength of the right hand sub-structure would contain an expression involving the stiffness of the left hand part. Since it would be more desirable to have the resulting solution a function of the stiffness of that part of the structure in question only, consider the conditions that prevail as the structure fails.

As the structure deforms according to the assumed virtual displacement the only quantity of interest at the cut section is the work done. Therefore, why not consider a sub-division of the structure according to that shown in Figure 41?

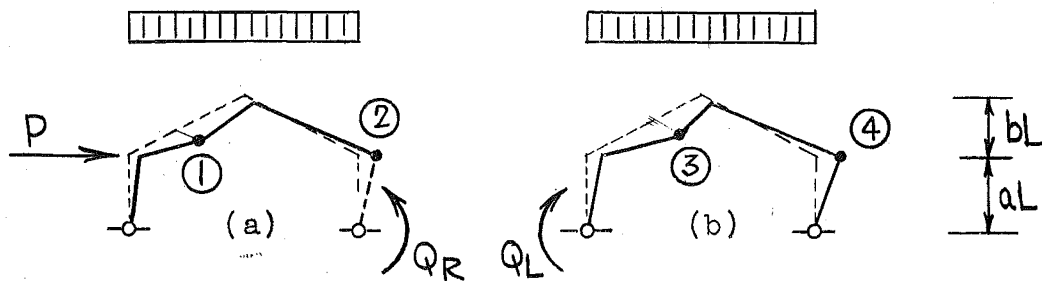


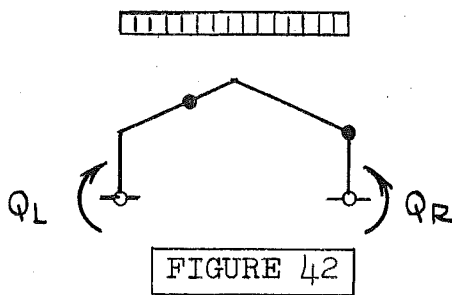
FIGURE 41

Here a hypothetical moment Q has been introduced. The reason is that since each of these Q 's rotate through the same angle in each sub-structure there will be work equalization at the divided section if the Q 's are equal. It should be remembered, however, that statically this Q does not necessarily tell the full story. It could be composed of just a moment, just a horizontal thrust having a moment Q about the base of the structure equal to Q or any combination of these.

It should also be noted that in Figure 41 the total internal work at plastic hinge ② is assumed to act in the left hand sub-structure. This is as justifiable an assumption as that shown in Figure 38. It has the advantage, however, of keeping all loads and moments resisting these

loads in the left structure together. The right sub-structure is therefore subjected to only the load w and the Q_L moment.

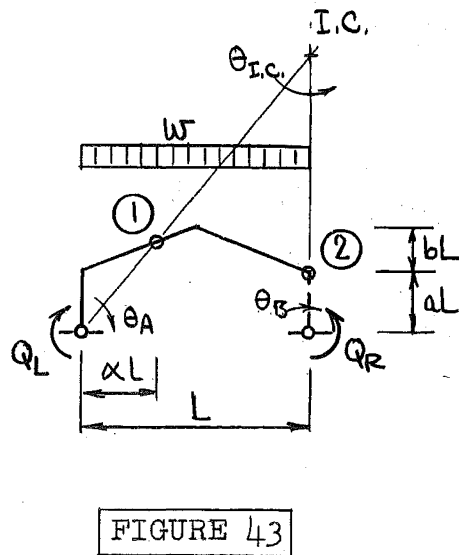
If a general structure and loading as shown in Figure 42 is now assumed, either of the two cases shown in Figure 41 can be represented.



For case (a) (the left hand sub-structure), Q_L would be chosen equal to PaL . For case (b), Q_R would equal zero.

From a consideration of the instantaneous center (see Figure 43), it is found that the following rotational relationships exist. (Note: these are the same as given in equation 19.)

$$\left. \begin{aligned} \theta_B &= \theta \\ \theta_{I.C.} &= \theta \left[\frac{\kappa}{(1-\kappa) + \frac{2b}{a}\kappa} \right] \\ \theta_A &= \theta \left[\frac{1-\kappa}{(1-\kappa) + \frac{2b}{a}\kappa} \right] \\ \theta_1 &= \theta \left[\frac{1}{(1-\kappa) + \frac{2b}{a}\kappa} \right] \\ \theta_2 &= \theta \left[\frac{1 + \frac{2b}{a}\kappa}{(1-\kappa) + \frac{2b}{a}\kappa} \right] \end{aligned} \right\}$$



.....(43)

Therefore,

$$\begin{aligned}
 & W_{int} = W_{ext} \\
 M_p \theta & \left[\frac{1}{(1-\alpha) + \frac{2b}{a}\alpha} + \frac{1 + \frac{2b}{a}\alpha}{(1-\alpha) + \frac{2b}{a}\alpha} \right] = \frac{wL^3}{2} \alpha^2 \theta \left[\frac{1-\alpha}{(1-\alpha) + \frac{2b}{a}\alpha} \right] \\
 & + \frac{wL^3}{2} (1-\alpha)^2 \theta \left[\frac{\alpha}{(1-\alpha) + \frac{2b}{a}\alpha} \right] + Q_L \theta \left[\frac{1-\alpha}{(1-\alpha) + \frac{2b}{a}\alpha} \right] \\
 & - Q_R \theta [1] \dots \dots \dots (44)
 \end{aligned}$$

Introducing the nondimensional form for the Q's,

$$\left. \begin{aligned}
 Q_L &= A \frac{wL^3}{2} \\
 Q_R &= D \frac{wL^3}{2}
 \end{aligned} \right\} \dots \dots \dots (45)$$

the following expression is obtained:

$$\frac{M_p}{wL^3} = \frac{1}{4} \left[\frac{(1-\alpha) (A + \alpha - D) - D(\frac{2b}{a})\alpha}{1 + \frac{b}{a}\alpha} \right] \dots \dots \dots (46)$$

where
$$\alpha = \frac{1}{\frac{b}{a}} \left[\sqrt{1 - \frac{b}{a} \left[A(1 + \frac{b}{a}) - D(1 - \frac{b}{a}) - 1 \right]} - 1 \right] \dots \dots \dots (47)$$

for $\frac{b}{a} > 0$

and
$$\alpha = \left[\frac{1-A+D}{2} \right] \dots \dots \dots \text{for } \frac{b}{a} = 0 \dots \dots \dots (48)$$

Solving these equations for various values of $\frac{b}{a}$, A and D and plotting the results in the form of curves, solutions to design problems are readily obtained.

Here again it should be pointed out that only one possible type of failure configuration has been investigated. Other possible modes must also be examined. The equations

that would result for such a structure are tabulated in Appendix C as equations 8 through 13.

Assume for illustration that the structure and loading to be investigated is that shown in Figure 44.

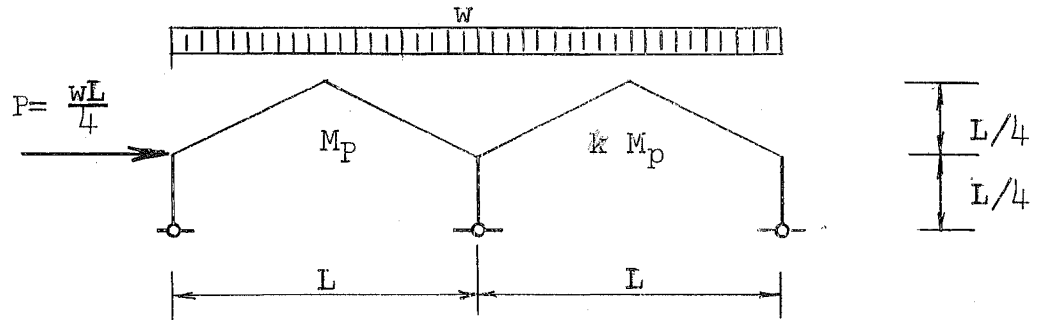


FIGURE 44

The b/a value for this structure equals 1.0. The corresponding design curves obtained by solving equations 8 through 12 (Appendix C) are given as Figure 45 (where M_p , A and D are plotted) and Figure 46 (where λ , the distance to the plastic hinge, is determined).

If this multi-span frame is now divided into two parts as shown in Figure 47

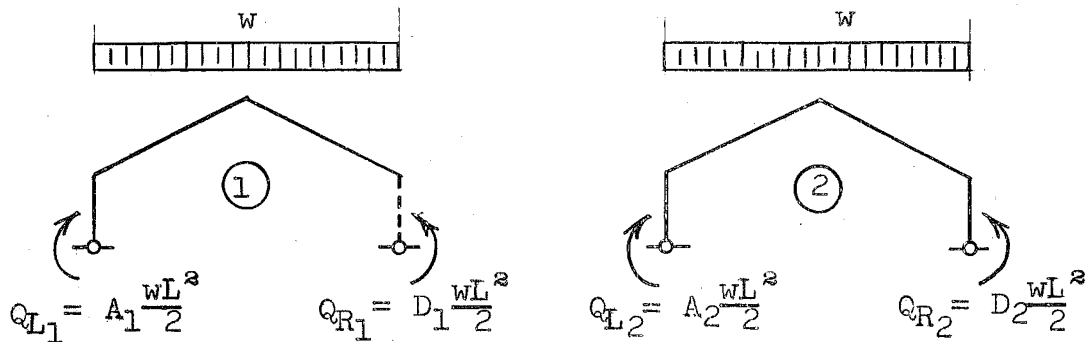
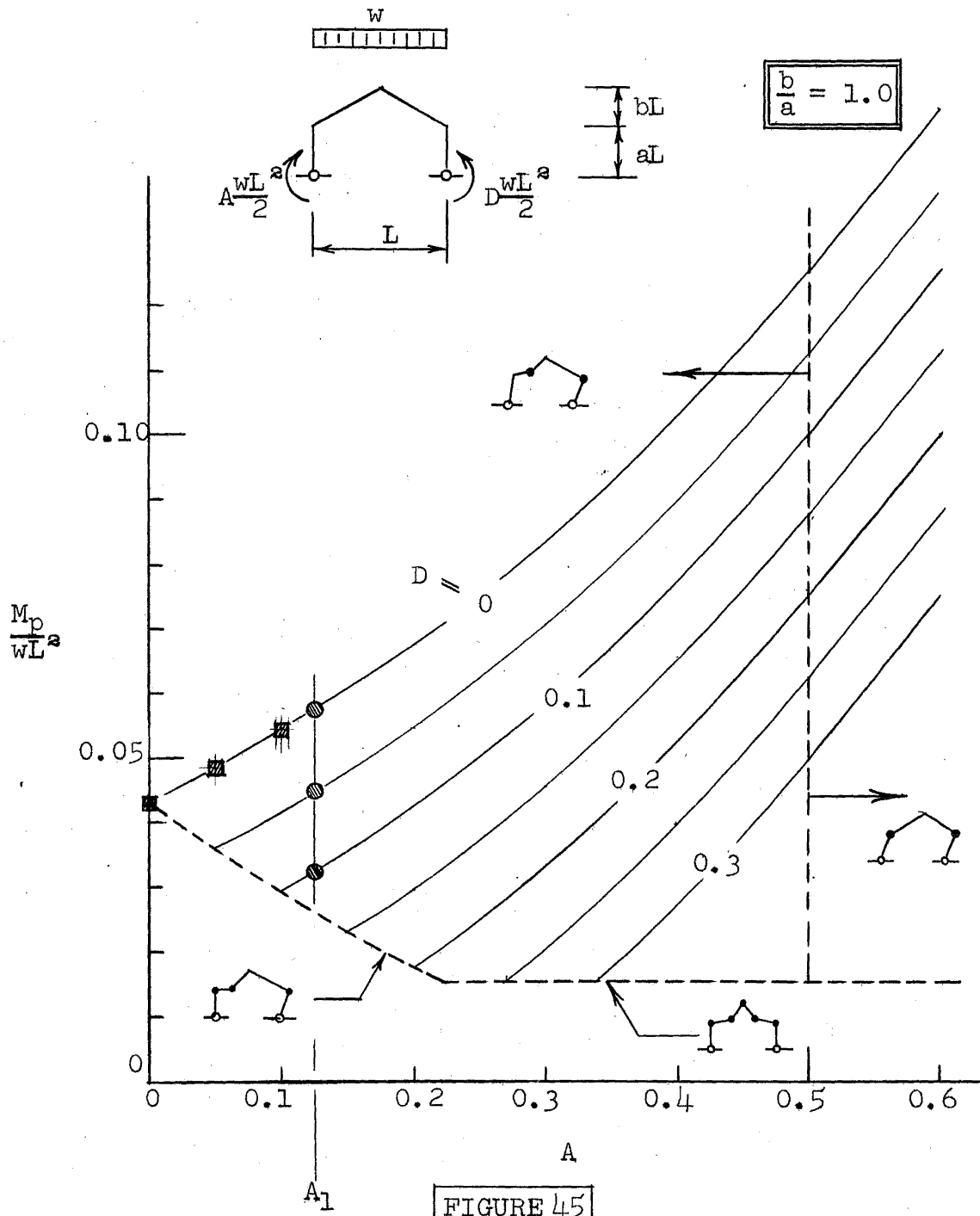


FIGURE 47



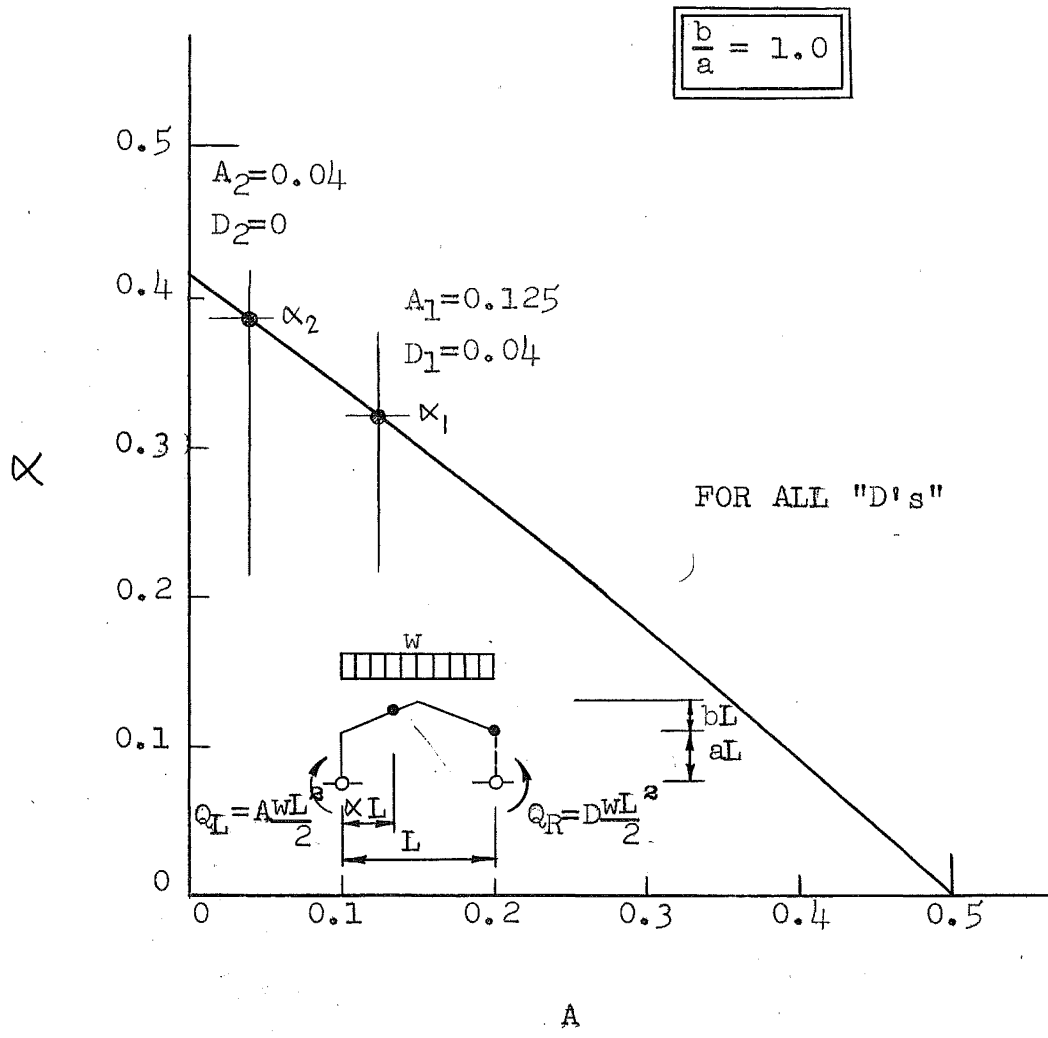


FIGURE 46

the left hand moment, Q_L , must equal the moment of the applied horizontal force P about the base of the structures; that is,

$$A_1 \frac{WL^2}{2} = P(aL)$$

$$A_1 \frac{wL^3}{2} = P(aL) = \frac{wL}{4} \left(\frac{L}{4}\right)$$

or

$$A_1 = 0.125 \dots \dots \dots (49)$$

Since $Q_{R2} = 0$, $D_2 = 0$

For each part then, the following exists:

- | <u>Part 1</u> | <u>Part 2</u> |
|----------------------|----------------------|
| (a) $b/a = 1.0$ | (a) $b/a = 1.0$ |
| (b) $A_1 = 0.125$ | (b) $A_2 = (?)$ |
| (c) $D_1 = (?)$ | (c) $D_2 = 0$ |
| (d) $M_p/wL^3 = (?)$ | (d) $M_p/wL^3 = (?)$ |

It is noted that in each case two unknowns are present; one defining the size of the member, the other the restraining or loading moments at the center column. From Figure 45 the curves shown in Figure 48 could be plotted

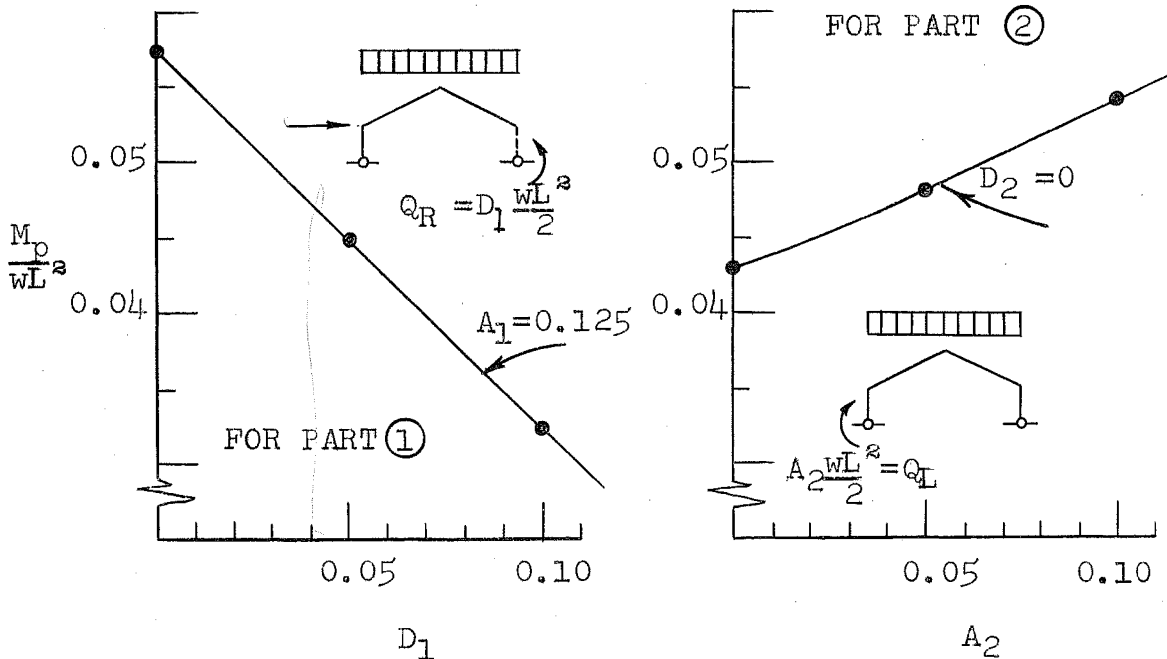


FIGURE 48

Since the Q values at the cut section of each of these must be equal in order that the work cancels when the structure is "put together"

$$Q_L = Q_R$$

or

$$A_2 = D_1 \dots\dots\dots(50)$$

These curves could therefore be plotted on the same ordinate and abscissa and their intersection would give the correct value of A_2 (or D_1) and M_p/wL^2 . This is shown in Figure 49.

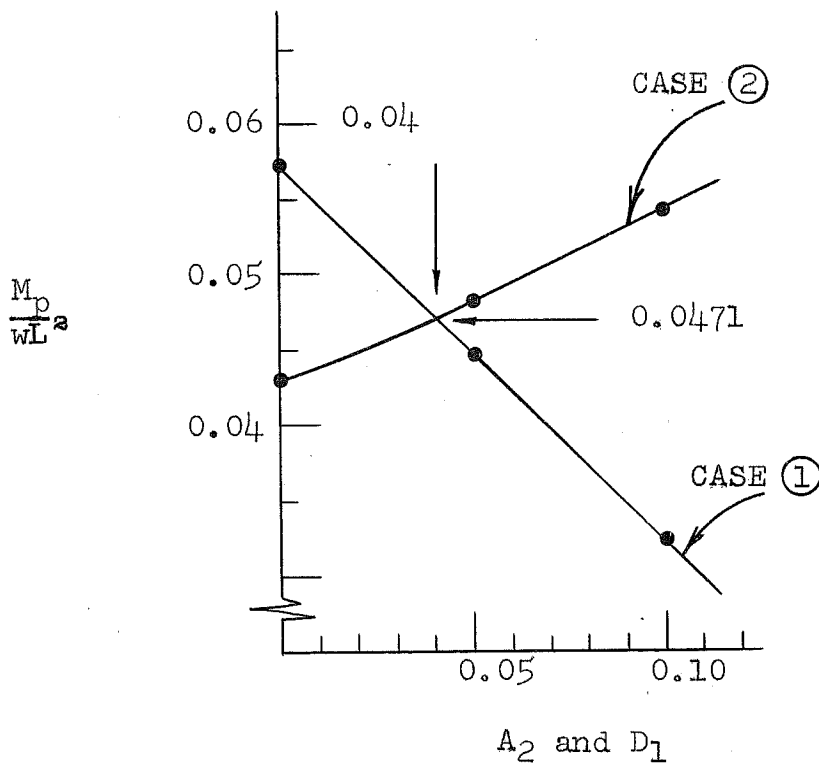


FIGURE 49

Having found the required M_p/wL^2 value, the next step would be to plot the corresponding moment diagram. From Figure 46 the location of the plastic hinges are found to be as shown in Figure 50.

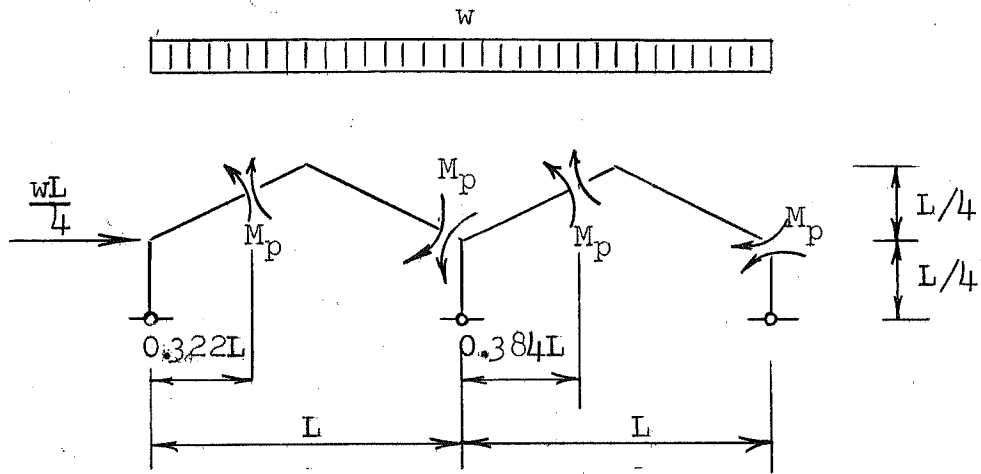


FIGURE 50

The moment diagram is given in Figure 51 where moments are plotted on the tension side of the members.

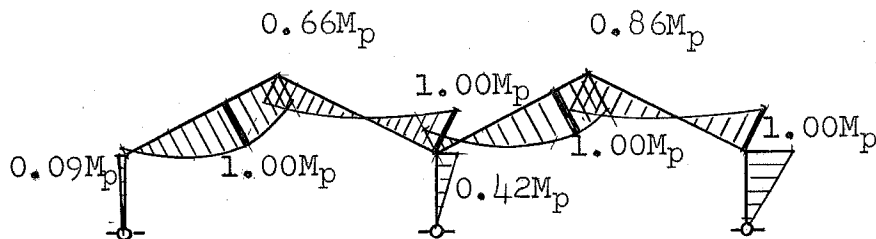


FIGURE 51

Since the structure is in equilibrium with the applied loads, since a mechanism forms and since nowhere is the full plastic moment of the section exceeded - this is the correct solution.

It will be noted from Figure 51 that the maximum moment to which the center column is subjected is $0.48M_p$. Should this be the only loading condition under consideration a smaller member could be used: one that when modified to sustain the axial thrust would deliver $0.48M_p$.

Had the horizontal force been substantially greater than that considered, it would have been found that the moment at the top of the center column would be in excess of M_p . In fact, it might have been as high as $2M_p$. For such a case (assuming that the center column has a moment capacity of only M_p) it is obvious that the investigated mechanism is not the correct one and the corresponding value of M_p is too small. The actual failure mode

would more than likely be the one shown in Figure 52. Since the solution of such a failure pattern would result in a greater M_p value for all the members of the structure, the new design would in almost all cases be less economical (in terms of "least weight") than

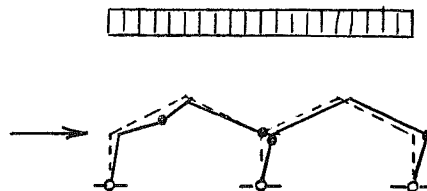


FIGURE 52

that design based on the assumption that the center column could supply whatever was needed. (Note the relative length of the center column to the remainder of the structure.) From economic considerations then the type of failure shown

in Figure 52 should be excluded, and the exact size of these "center type columns" be determined from a moment diagram assuming a more general failure configuration.

3. Development of Design Charts

To be able to solve all types of multiple span problems by this method it is necessary that all of the various possible sub-structures (or assemblages) be ascertained. For example, if a three span symmetrical,

pinned base, gable frame (see Figure 53a) were subjected to only vertical loads then the two types of sub-structure failure shown in Figure 53b could occur.

For the center span each of the "columns" would spread equal amounts. The outside spans would fail as assumed in the preceding problem (see Figure 41b).

Had the structure under consideration been a four span symmetrical frame

as shown in Figure 54a, the center two spans would have failed with their outside columns spreading. Due to the symmetry, the center column would remain vertical. A fourth

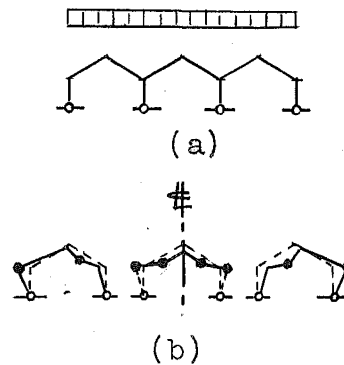


FIGURE 53

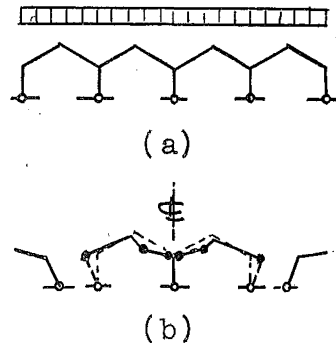


FIGURE 54

type of failure condition results when a three span, un-symmetrical frame fails. For such a case the center two columns may spread through different angles. Therefore, this condition must also be investigated.

The five types of sub-structures and loadings that must be considered for the solution to pinned base, gable frame problems are therefore as shown in Figure 55.

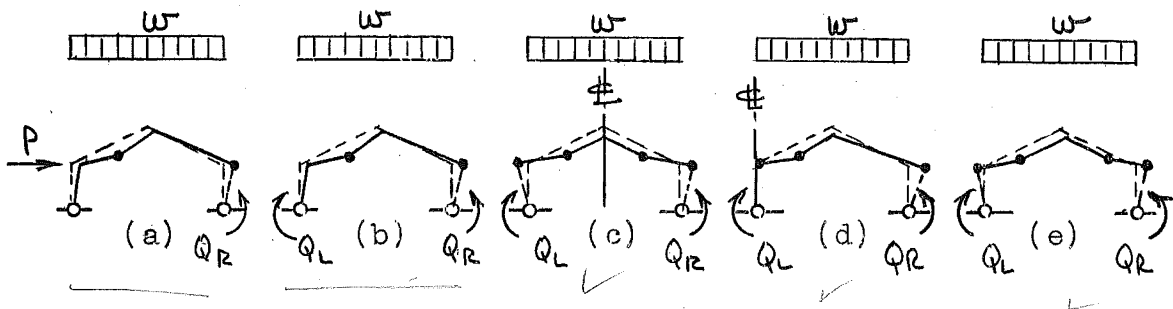


FIGURE 55

By selecting a value of the left hand "Q moment" in case (b) equal to the moment produced by the concentrated horizontal force of case (a), these two problems reduce to one. The equations governing their solution are tabulated in Appendix C as equations (1) through (4) and (11) through (13). The resulting design charts for various values of b/a (0, 0.2, 0.4, 0.6, 0.8, and 1.0) are given at the end of this report as Charts III-1 through III-6 and III-1a through III-6a.

For cases (c), (d), and (e) it can be shown that each reduces to the same solution. (See equations (8), (9) and (10) of Appendix C.) While the proof of this is straight forward for (c) and (d), case (e) presents an added problem.

Consider the failure mode and structure shown in Figure 56.

If it is assumed that the left hand column rotates to the left through an angle equal δ then the right hand column would rotate through an angle $\theta - \delta$ if θ is chosen as the virtual angle at B when the left column remains vertical. Since the structure

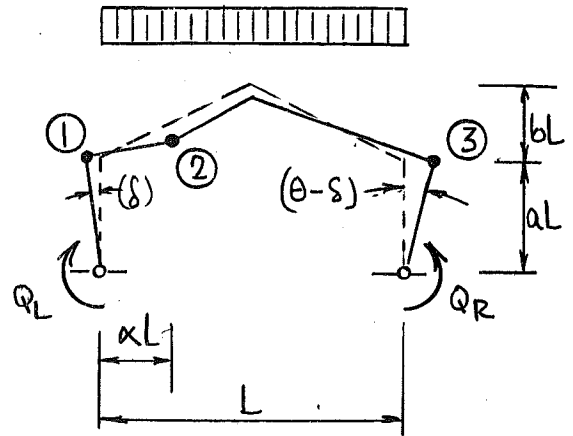


FIGURE 56

is over determinate (that is, there are more hinges developed than needed to produce a mechanism), the total virtual angle change at plastic hinge (2) is not a function of δ . The internal work at hinges (1) and (3), however, will change. (It should be noted, however, that as one decreases the other increases an equal amount thus keeping the internal work constant.) Equating the internal and external work for this condition gives equation 51.

$$\frac{M_p}{wL^2} = \frac{1}{4} \left[\frac{\alpha(1-\alpha) - \alpha \left\{ \frac{2b}{a} D_2 + \frac{2b}{a} (D_1 - D) \frac{\delta}{\theta} \right\}}{1 + \frac{b}{a} \alpha} \right] \dots \dots \dots (51)$$

where

$$D_2 = \left(\frac{2}{wL^2} \right) Q_R$$

$$D_1 = \left(\frac{2}{wL^2} \right) Q_L$$

The D_1 parameter is used to define Q_L , rather than A as previously.

This has been done to try to achieve a uniformity throughout the paper of always using "A's" when the structure fails with the "Q moment" and "D's" when negative work is done by the Q moment.

Since it is required to have the maximum value of M_p for all possible values of δ/θ ,

$$\frac{\partial M_p}{\partial(\delta/\theta)} = 0$$

This gives

$$\frac{2b}{a} (D_1 - D) = 0$$

or

$$D_1 = D \dots\dots\dots(52)$$

The solution to this case then is identical to cases (c) and (d) of Figure 55 with the Q moments on each side being equal. The solution to all three possibilities is graphically given by Design Charts II-1 and II-1a at the end of the report.

For fixed base types of gabled frames the sub-assemblages shown in Figure 57 must be solved.

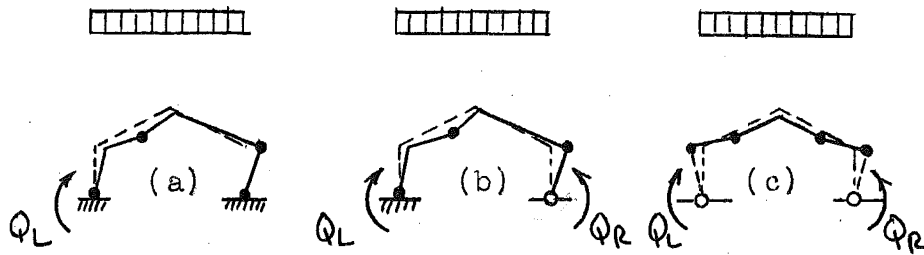


FIGURE 57

The solution to 57(a) is given by Design Chart I-2 and I-2a. 57(b) is considered in charts IV-1 through IV-6 and IV-1a through IV-6a.

57(c) is identical to 55(c), (d) and (e). Its solution is therefore shown in Charts II-1 and II-1a.

For lean-to types of structures, the configurations as shown in Figure 58 must be considered.

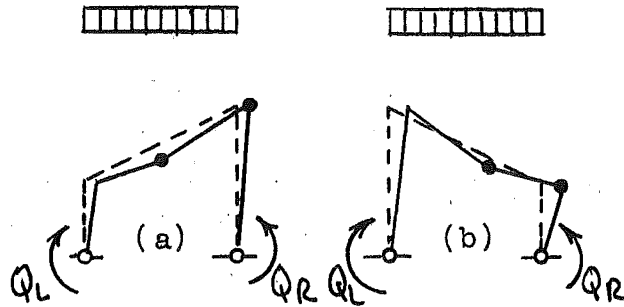


FIGURE 58

Design charts V-1 and V-1a through V-6 and V-6a, and VI-1 and VI-1a through VI-6 and VI-6a give the solutions to these types of problems. The equations on which these charts are based are given as equations 16 through 20 of Appendix C.

IV. DISCUSSION

1. Factor of Safety

Since plastic design results in a structure that will just sustain the imposed loading at the structures ultimate strength, there must be included in the design load a certain margin of safety above the antitipated working value. This margin would then truly be a load factor of safety since it would indicate the amount of overload the structure could sustain prior to collapse. Accepting this philosophy, the next step is the selection of a criterion for determining the numerical value of this safety factor.

If it is assumed that it is desirable to have the load factor of safety of a continuous structure equal to that of a statically determinate one, and if it is further assumed that a simple beam designed according to the present AISC Specification⁽¹⁶⁾ has an adequate reserve in strength, then the load factor of safety would be computed as follows.⁽¹⁷⁾ Consider the simple beam shown in Figure 59. If it is assumed that the allowable bending stress is 20,000 psi (AISC Specifications--Section 15c), and that the yield stress is 33,000 psi (minimum allowable by ASTM for A-7 type steels), then M_y , the initial yield moment, is 1.65 times greater than the working moment, M_w . It then follows that P_y , the initial yield load, is 1.65 times greater than P_w , the working load. Since the full plastic moment equals $Z\sigma_y$ and

the initial yield moment equals $S\sigma_y$,

$$\frac{M_p}{M_y} = \frac{Z\sigma_y}{S\sigma_y} = \frac{Z}{S} = f$$

where f is termed the shape factor of the section. Values of " f " for rolled symmetrical shapes are given in Appendix D of this report. The average " f " value of these is 1.14 with a high of 1.23 for the 5I14.75 and a low of 1.11 for several different sections. Assuming the average case:

$$M_p = 1.14 M_y = (1.65)(1.14)M_w = 1.88 M_w$$

Since a one-to-one relationship exists between the loads and the centerline moment values, the load factor of safety, F , is then 1.88.

Assuming the minimum " f " value:

$$M_p = 1.11 M_y = (1.65)(1.11)(M_w) = 1.81 M_w$$

The AISC specifies another allowable stress value when stresses are caused by wind, earthquake, etc. in combination with "real" loads. For these cases the allowable stress is increased by 33 1/3%. The corresponding load factors of safety are therefore as shown in Table 3.

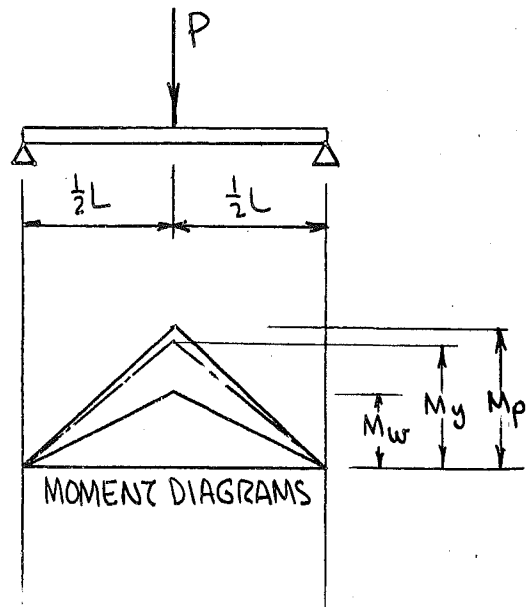


FIGURE 59

TABLE 3

	AVERAGE SECTION	MINIMUM SECTION
F including wind, earthquake, etc.	1.41	1.36
F excluding wind, earthquake, etc.	1.88	1.81

A somewhat different approach to the general problem of safety can be based on the philosophy that a structure is no better than the load analysis. Therefore, this factor should play a major part in the determination of the factor of safety of any given structure. Furthermore, the ability to predict loads is dependent on the type of loading. For example, the maximum load to which a water tank may be subjected can be computed with a high degree of certainty. The live load for a warehouse, however, is not too well defined. The uncertainty in each of the loads making up the total could be taken into account separately.

While the question of safety is important it is not unique to plastic analysis. It is therefore felt that further discussion in this paper is not warranted.

2. Economical Designs

As specified earlier many factors enter into the selection of an "economical design" not the least of which

is the availability of a certain desired shape. In this paper "least weight" of main member is chosen as the criterion.

Since in a plastic design the section property most often encountered is the full plastic moment, M_p , it would be desirable to have an expression relating this property and the weight/unit lengths of the member. Two designs could then be compared by knowing M_p values, lengths of the various elements, etc.

Unfortunately the plastic modulus (which is directly related to the full plastic moment) not only takes into account the area of the section but also the moment of this area. The relationship therefore will not be linear. Assuming that the relationship must be one of a power, the plastic modulus values have been plotted versus unit weights in Figures 60 (for WF sections) and 61 (for I Sections).

From Figure 60 it is noted that an equation of the form

$$W = CZ^{0.50}$$

gives a fair average through all the wide-flange sections. The most economical (that is the largest Z for the smallest W) is approximately

$$W = CZ^{0.30}$$

For any one given depth of WF section the equation

$$W = CZ^{0.90}$$

is a comparatively good average value.

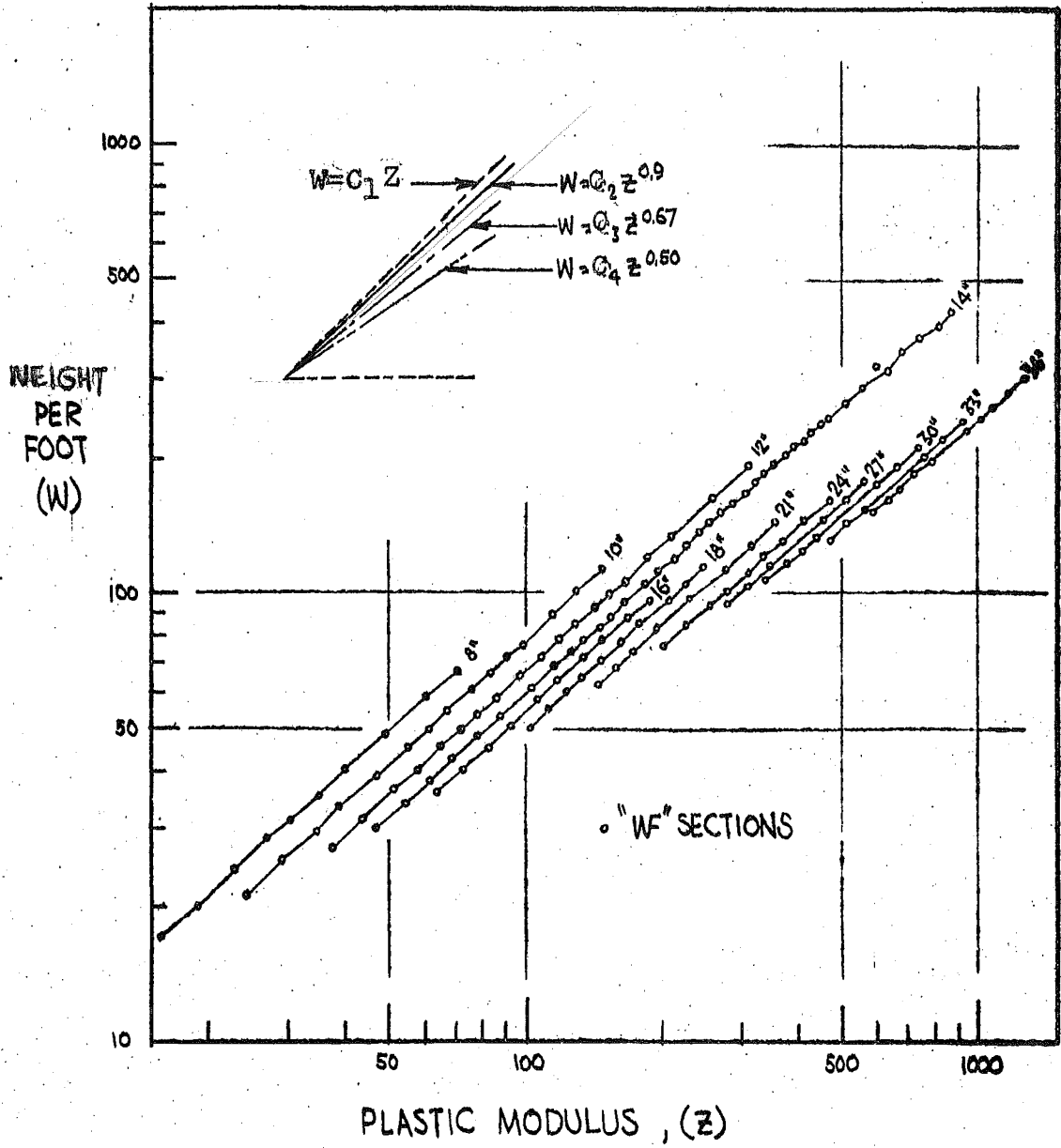


FIGURE 60

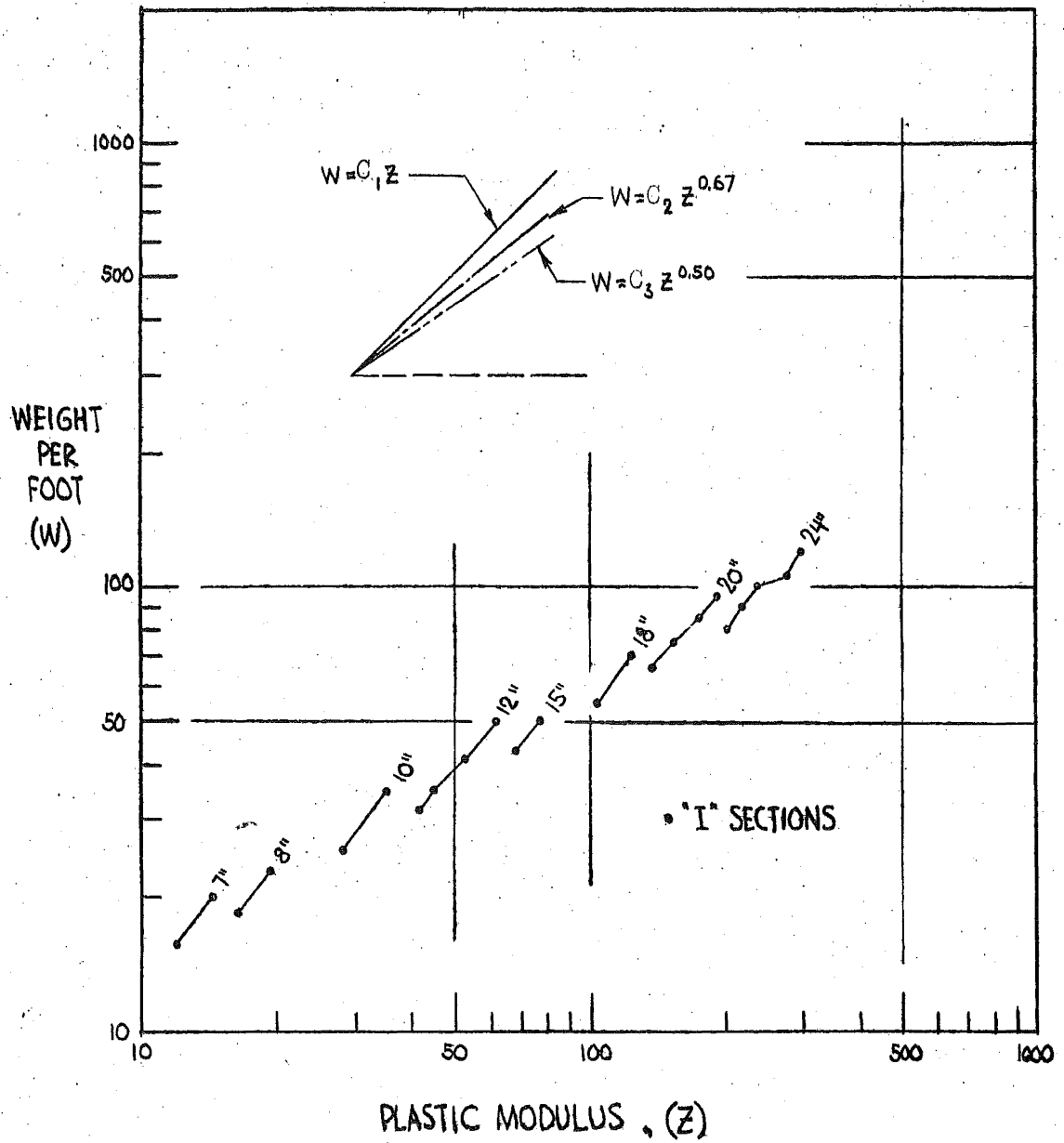


FIGURE 61

It is interesting to note that Heyman⁽¹⁸⁾ has used a value of
 $W = cz^{0.67}$

While the difference between an exponent of say 0.5 versus 1.0 is extremely large, the net effect on the isolation of the more economical choice of member sizes is rather small. In addition the assumption of equal rafter sizes in a given span, etc., will often over shadow the difference. Therefore, a one-to-one correspondence between weight and plastic modulus (or M_p) will be assumed in the remainder of this discussion.

3. Initial Choice of Members

As in the elastic case, design time can be saved by a judicious first choice of relative member sizes throughout the structure. It will be shown later, however, that this is not absolutely essential when using the plastic design charts.

V. DESIGN EXAMPLES

1. Design Example No.1

As a first design example consider the single span gable frame loaded as shown in Figure 62. Since b/a is equal to $7.5/15$ or 0.5 , the solution from Design Chart I-1 is

$$\frac{M_p}{wL^2} = 0.0505 \dots\dots\dots(53)$$

Therefore,

$$\begin{aligned} M_p &= (0.0505)wL^2 \\ &= (0.0505)(1.88)(1)(40)^2 \\ &\quad \underbrace{\hspace{10em}}_{\text{Factor of Safety}} \\ &= 152.0 \text{ ft.kips} \\ &= 1825 \text{ inch kips} \end{aligned}$$

The required plastic modulus then equals

$$Z = \frac{M_p}{\sigma_y} = \frac{1825}{33} = 55.3 \text{ in}^3$$

From Appendix D, the most economical section is the 16WF36 supplying 63.9 in^3 .

Design Example 1a

Assume now that this same structure is to be subjected to a combination of vertical and horizontal loads as shown in Figure 63. Here again the b/a value is 0.5 . The

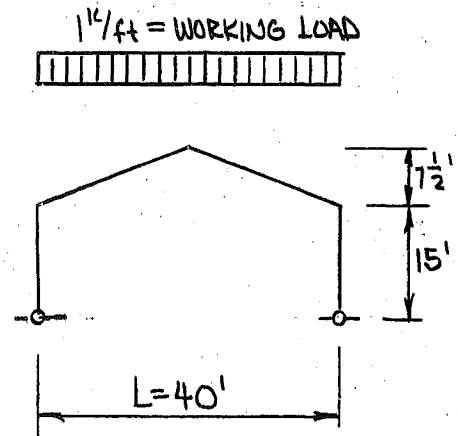


FIGURE 62

"A" parameter is given as

$$A = (2a)(P/wL)$$

$$= (0.75)(10.7/40) = 0.20$$

From Design Chart I-1 it is found that

$$M_p/wL^2 = 0.0762 \dots\dots (54)$$

This gives for a moment value

$$M_p = (0.0762)(1.41)(1)(1600)$$

⏟
Load Factor of Safety
(including influence of wind)

$$= 172 \text{ ft. kips}$$

$$= 2060 \text{ in. kips}$$

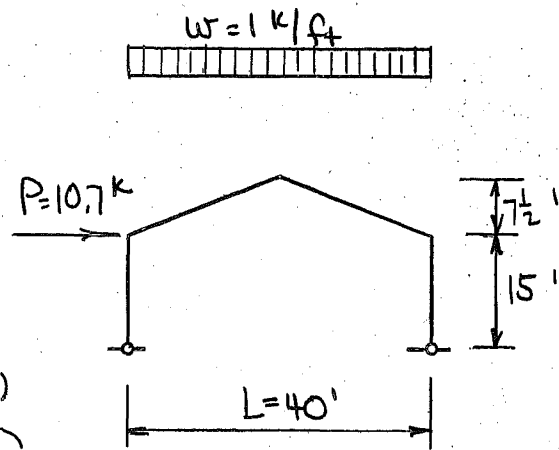


FIGURE 63

The required Z value is therefore

$$Z = M_p/\sigma_y = 2060/33 = 62.4 \text{ in}^3$$

and the most economical section supplying this value is the 16WF36 ($Z=63.9 \text{ in}^3$).

This example illustrates one of the arguments against talking about a most economical design. It will be noted that both loadings resulted in the same section, however, the required Z values were quite different.

To help eliminate some of the confusion that results from situations of this type the answers for the remaining examples will be left in required M_p form.

2. Design Example No.2

As a second example consider the two span rectangular portal frame of Figure 64a. Dividing the structure into two

sub-assemblages as shown in Figure 64b a solution can be obtained by using Design Chart III-1 for both parts.

Considering part ①, since there are no horizontal forces acting on the structure, the "A" for this part equals zero. From Chart III-1 it is seen that for $A = 0 \rightarrow D$ must also equal zero and the failure will be of the "beam type". The same condition holds for the ② part of the structure.

The solution is therefore given by the two following equations

$$\left. \begin{aligned} \frac{M_p}{wL_1^2} a &= 0.0625 \\ \frac{kM_p}{wL_2^2} a &= 0.0625 \end{aligned} \right\} \dots\dots\dots (55)$$

Substituting into equations 55 the values of L_1 and L_2 in terms of L

$$\left. \begin{aligned} \frac{M_p}{wL^2} a &= (0.0625)(9) = 0.563 \\ \text{and} \\ \frac{kM_p}{wL^2} a &= (0.0625)(25) = 1.562 \end{aligned} \right\} \dots\dots\dots (56)$$

This gives for a value of relative members sizes

$$k = 2.78 \dots\dots\dots (57)$$

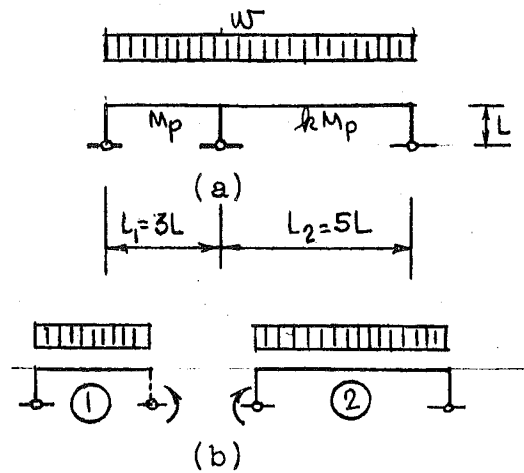


FIGURE 64

It should be noted that this value of k is equal to the ratio of the squares of the span lengths. Such will always be the case for uniformly loaded (vertical loading) rectangular portal frames or continuous beams.

The moment diagram corresponding to the ultimate carrying capacity is as shown in Figure 65.

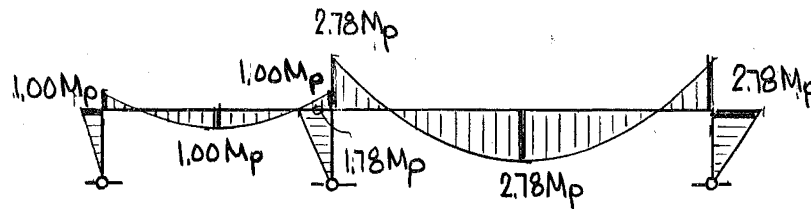


FIGURE 65

From this diagram it is seen that the plastic moment of the center column must equal $1.78 M_p$.

3. Design Example No. 3

The third design example is a three span symmetrical gabled frame subjected to a uniform load of w lbs/ft and a concentrated horizontal load of $wL/4$ at the windward eave. (see Figure 66).

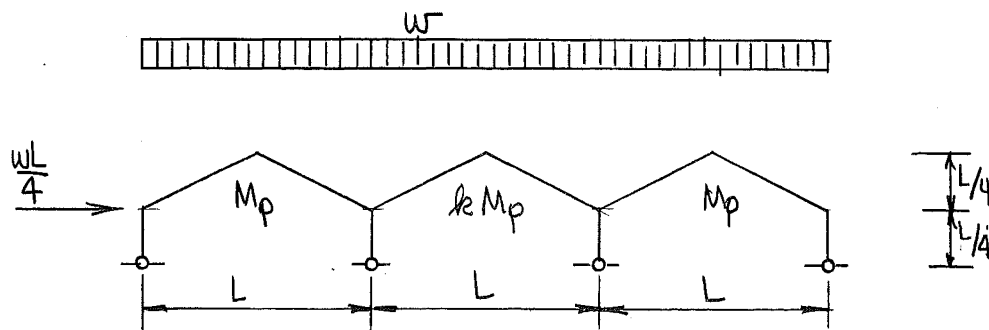


FIGURE 66

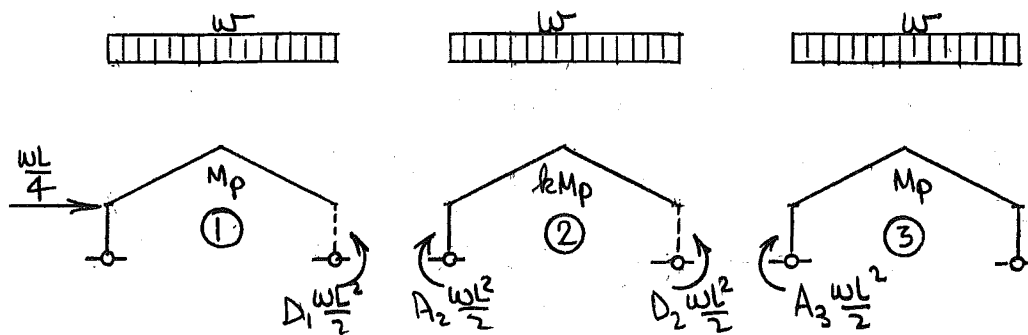


FIGURE 67

Equating the moment of the horizontal force, $wL/4$, to $A_1 wL^2/2$, the value of A_1 equals

$$A_1 = 0.125 \dots\dots\dots (58)$$

For equilibrium at the cut sections

$$\left. \begin{aligned} D_1 \frac{wL^2}{2} &= A_2 \frac{wL^2}{2} \\ D_2 \frac{wL^2}{2} &= A_3 \frac{wL^2}{2} \end{aligned} \right\} \dots\dots\dots (59)$$

These give

$$A_2 = D_1 \dots\dots\dots (60)$$

and

$$D_2 = A_3$$

Selecting equal values of M_p/wL^2 (and therefore M_p values) for spans ① and ③ — enter Design Chart III-6 (b/a=1.0) and read off suitable D_1 and A_3 values. With these values reenter this same design charts with the values of A_2 and D_2 and read off the corresponding kM_p/wL^2 for the center span. A table of the following type is desirable.

TABLE 4

$\frac{M_p}{wL^2}$	$D_1=A_2$	$A_3=D_2$	$\frac{kM_p}{wL^2}$	k
0.0446	0.050	0.016	0.0442	0.991
0.0435	0.0905	0.006	0.0527	1.212
0.0440	0.0635	0.011	0.0494	1.123

For each of these three solutions one must now compute the moment diagram to select the size of the center columns. With this information, it is then possible to plot a curve of the summation of the $(M_p/wL^2)_i$ with respect to the various lengths and plot these against k values. Such a curve is shown in Figure 68.

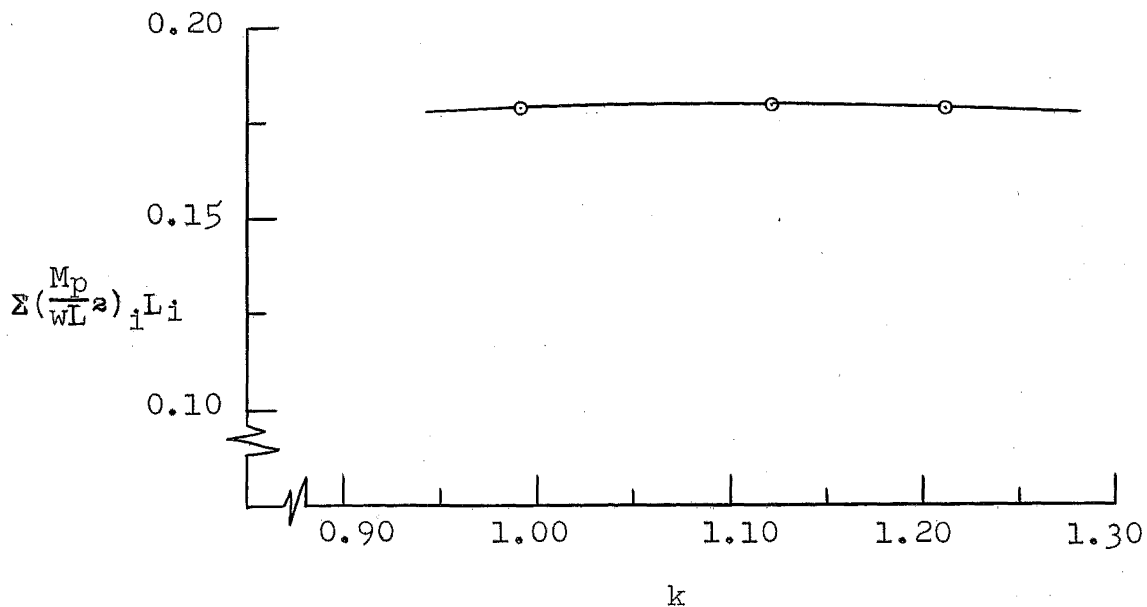


FIGURE 68

From Figure 68 it is noted that total weight of this structure (as measured by $\sum (M_p/wL^2)_i L_i$) is only slightly affected by a change in k value.

4. Design Example No.4

As a fourth design example consider the three span unsymmetrical gable frame of Figure 69.

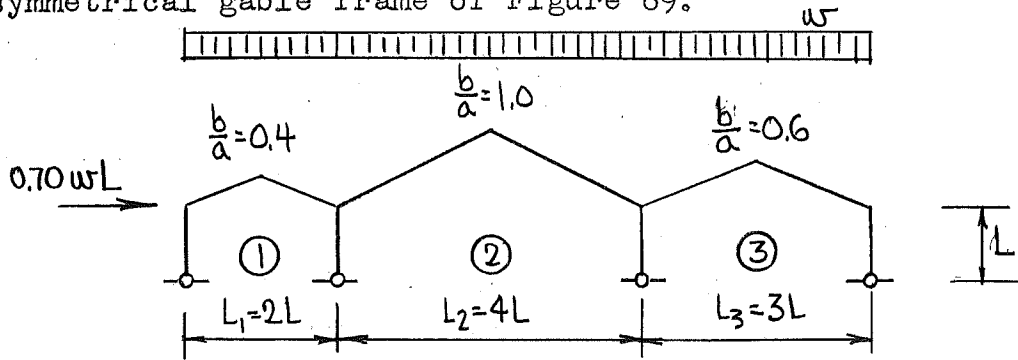


FIGURE 69

Dividing the structure into three parts

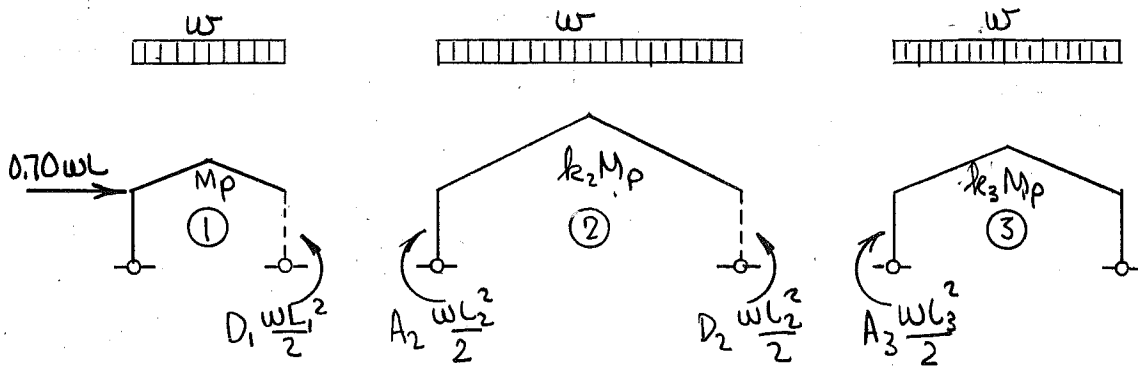


FIGURE 70

$$\left. \begin{aligned} A_1 &= 0.350 \\ D_1 &= 4A_2 \\ A_3 &= 1.778 D_2 \end{aligned} \right\} \dots\dots\dots (61)$$

By preparing a table of the following type and by solving for selected values of D_1 versus A_3 , solution to the problem is found.

TABLE 5

1	2	3	4	5	6	7	8	9	10	11
A_1	$\frac{M_p}{wL_1^2}$	D_1	$\frac{k_3 M_p}{wL_3^2}$	A_3	A_2	D_2	$\frac{k_2 M_p}{wL_2^2}$	$\frac{M_p}{wL^2}$	$k_2 \frac{M_p}{wL^2}$	$k_3 \frac{M_p}{wL^2}$

12	13
k_2	k_3

Plotting a curve of k_2 -vs- k_3 for various values of M_p/wL^2 , the solutions shown in Figure 71 are obtained. For the structure to fail as one complete unit the values of k_2 and k_3 must be such that they fall within the triangular area. Furthermore, since each of these three lines defining the permissible region represent a case where one of the parts of the structure becomes "over-determinate", their intersections represent the points of most probable "least weight". This can be seen by realizing that the M_p/wL^2 is a minimum for that sub-structure when it becomes "over-determinate". Therefore two sub-assembly minimums will give a minimum for the total structure. For the case in question the "least weight" design is as shown.

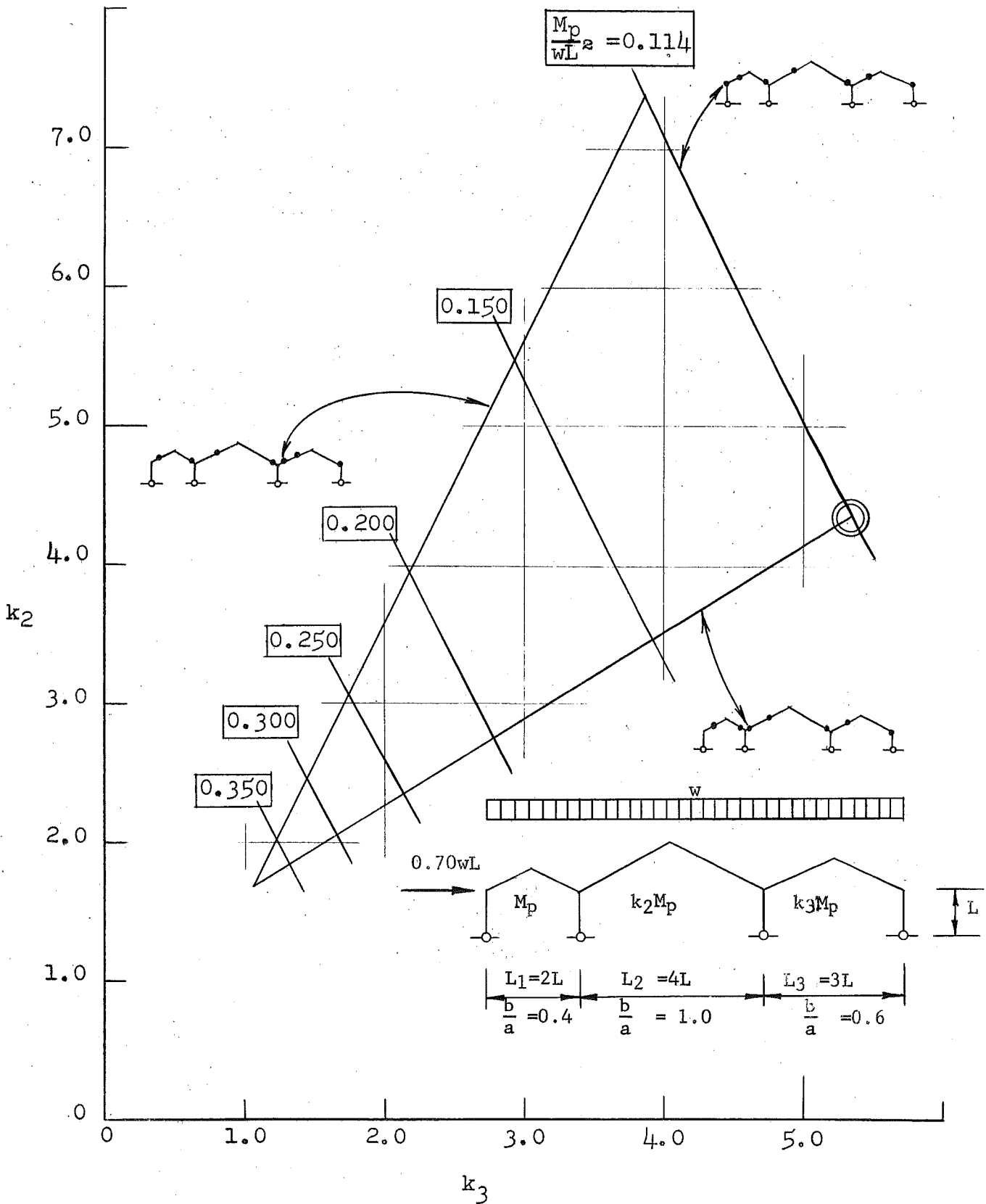


FIGURE 71

5. Design Example No.5

As a final design example, solutions to the mill-type building shown in Figure 72 will be obtained.

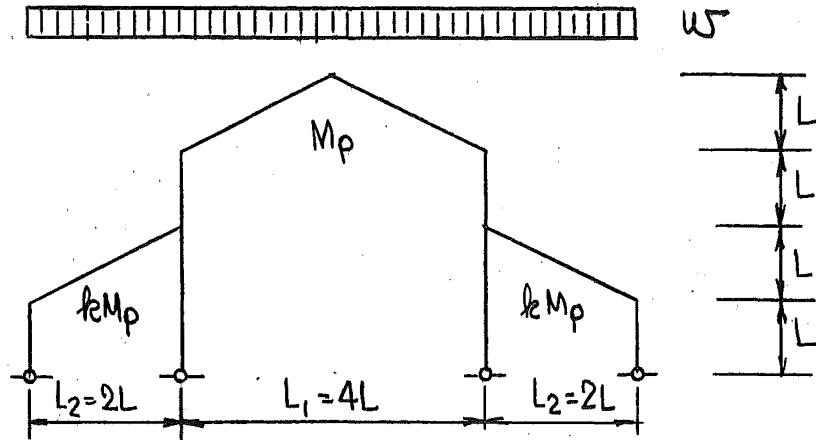


FIGURE 72

Because of symmetry, only one half of the structure need be considered. Solution to the ① part is given by Design Chart II-1, whereas part ② is given by Design Chart VI-6.

Again by using a tabular form and noting that

$$A_2 = 4D_1,$$

solutions can be obtained (see Table 6).

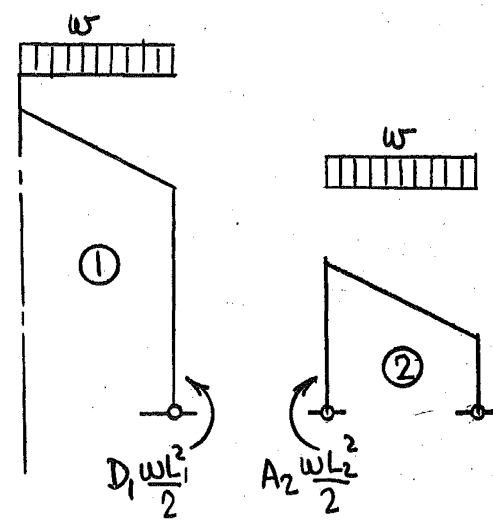


FIGURE 73

TABLE 6

$\frac{M_p}{wL_1^2}$	D_1	A_2	$\frac{kM_p}{wL_1^2}$	$\frac{M_p}{wL^2}$	$\frac{kM_p}{wL^2}$	k
0.0537	0	0	0.0625	0.859	0.250	0.291
0.0506	0.05	0.20	0.0702	0.810	0.281	0.347
0.0474	0.10	0.40	0.0923	0.758	0.369	0.487
0.0443	0.15	0.60	0.1167	0.709	0.467	0.659
0.0414	0.20	0.80	0.1431	0.662	0.572	0.864

M_p/wL^2 versus k values are shown in Figure 74.

It should be pointed out that for each of the designs carried out in this section it is necessary to check for "Additional Considerations"⁽⁹⁾ as discussed in section 6 of the INTRODUCTION of this dissertation.

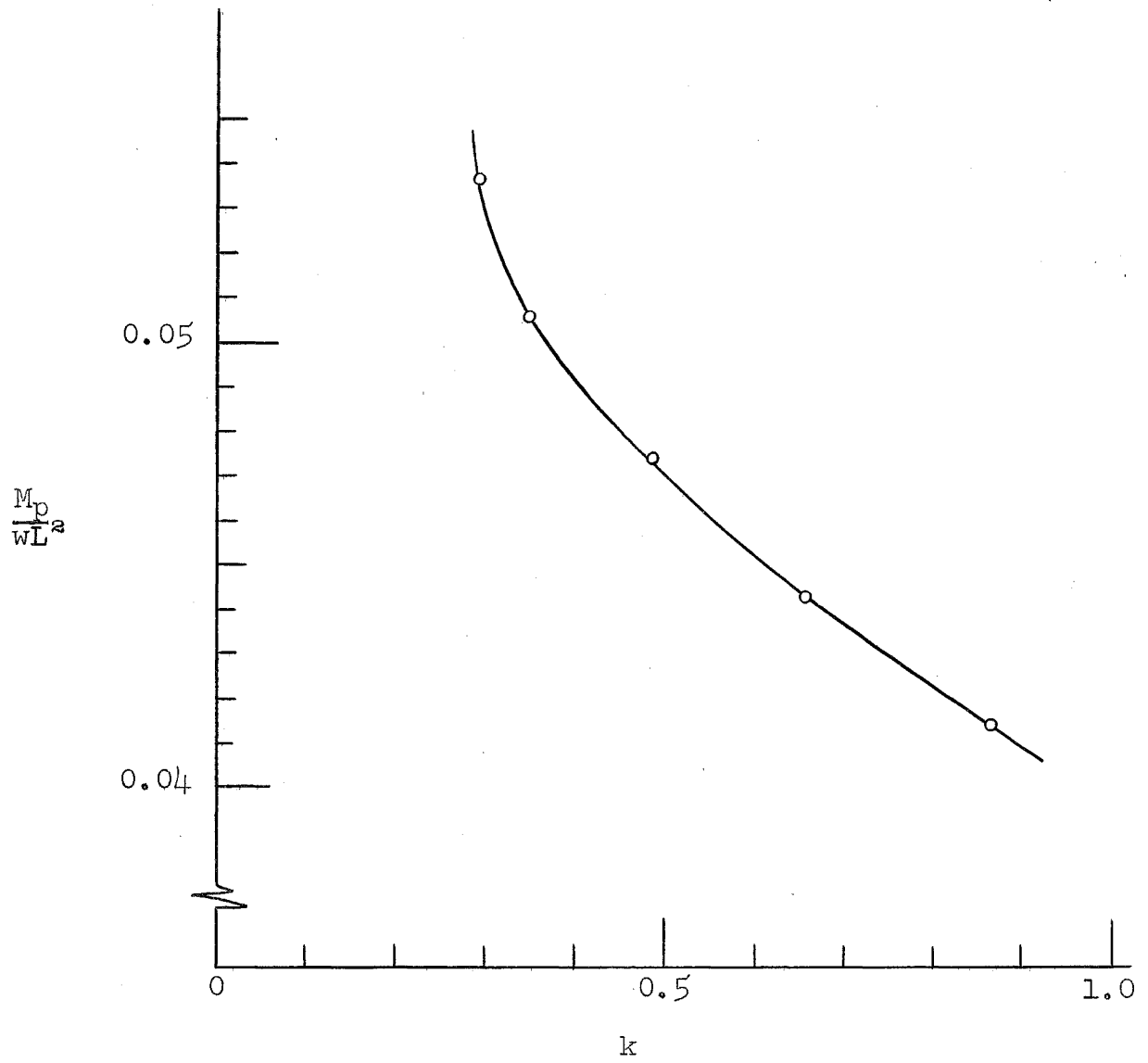


FIGURE 74

VI. SUMMARY

After reviewing the assumptions of the simple plastic theory and discussing the various methods whereby a solution to problems in plastic analysis can be obtained, there is presented in this dissertation a method whereby plastic analysis solutions to the single or multiple span rigid frames can be obtained. The solution is based on the concept of dividing the structure into sub-assemblages and solving each of these separately in terms of the boundary conditions at the cut sections. By equating the unknown values at these boundaries a solution to the problem in question can be obtained.

To facilitate the solution of other problems there is presented design curves which give in graphical form the solution to the various sub-assemblage problems.

The problem of "least weight" design was also discussed and a method was presented whereby such a design can be approached.

By solving six typical structures, it was shown that the methods presented in this dissertation are usable. Furthermore, they result in a large saving in design time.

VII. NOMENCLATURE

- A = non-dimensional parameter relating the horizontal force acting on a structure (or the "over turning" moment of one part of a structure on the adjacent part) to the vertical loading. It is assumed that "A" results in positive work being done as the structure fails.
- C = constant
- D = non-dimensional parameter relating the horizontal resisting force or "over-turning" moment acting on a structure to its vertical loading. It is assumed that "D" results in negative work being done as the structure fails.
- E = Young's modulus of elasticity
- F = function value
= load factor of safety
- L = length measurement. Can be total span length, or a fractional part of it.
- M = bending moment
- M_p = full plastic moment of a cross-section
- M_w = bending moment corresponding to working loads
- M_y = bending moment corresponding to initial yield loads
- P = concentrated loads
- P_u = concentrated load corresponding to maximum carrying capacity of a structure
- P_w = concentrated load corresponding to working stress within structure
- P_y = concentrated load corresponding to initial yield within structure
- Q = hypothetical "over-turning" or resisting moment assumed acting about the base of a structure
- W = weight per unit length of a structural member

- W_{int} = internal work associated with a virtual displacement of an assumed mechanism.
- W_{ext} = external work associated with a virtual displacement of an assumed mechanism.
- a = non-dimensional parameter relating the height of a column to the span length.
- b = non-dimensional parameter relating the total rise of a rafter to the span length.
- b = flange width
- d = depth of section
- f = shape factor = Z/S
- f }
 g } = function values
 h }
- h = total vertical distance from the base of a structure to the instantaneous center (I.C.) of one of its linkages (which result from the formation of plastic hinges)
- k = ratio of the full plastic moment values of two spans
- m }
 n } = non-dimensional parameter defining the distance from a support to the placement of a concentrated load such that it is equivalent to a uniformly distributed load. (Appendix A)
- t = flange thickness
- w = web thickness
- w = distributed horizontal load per unit length
- α }
 β } = non-dimensional parameter defining the distance to the location of the plastic hinge in the rafter of a structure
- γ = ratio of the applied horizontal load per foot to the applied vertical load per foot
- δ = special virtual rotation (see page 67)
- ϵ = strain

ϵ_y = strain corresponding to the first attainment of the yield stress level

σ = normal stress

σ_y = yield stress level

θ = virtual rotation

ξ = special virtual rotation (see page 44, figure 33)

ϕ = curvature

VIII. REFERENCES

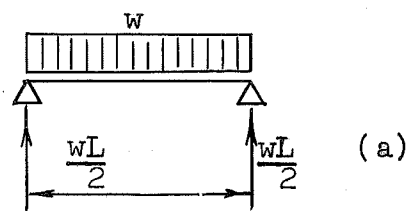
1. Hoff, N.J., Discussion of "AN EVALUATION OF PLASTIC ANALYSIS AS APPLIED TO STRUCTURAL DESIGN", Welding Journal, 33(1), p.14-s, January 1954.
2. Kazinczy, G.V., "KISERLETEK BEFALAZOTT TARTOKKAL", Betonzemle, 2, 68.(1914) Translated in part by N.J. Hoff, see Reference 1.
3. Baker, J.F., and Horne, M.R., "NEW METHODS IN THE ANALYSIS AND DESIGN OF STRUCTURES IN THE PLASTIC RANGE", British Welding Journal, 1(7), p.307, July, 1954.
4. "THE COLLAPSE METHOD OF DESIGN", British Constructional Steelwork Association, Publication No.5, London, 1952.
5. Van den Broek, "THEORY OF LIMIT DESIGN", John Wiley and Sons, Inc., New York, 1948.
6. Roderick, J.W., "THEORY OF PLASTICITY - ELEMENTS OF THE SIMPLE PLASTIC THEORY", Philosophical Magazine, Series 7, XXXIX, p. 529, July, 1948.
7. Luxion, W.W., and Johnston, B.G., "PLASTIC BEHAVIOR OF WIDE FLANGE BEAMS", Welding Research Supplement, Vol. XIII, p. 538, (1948)
8. Beedle, L.S., Thürlimann, B., and Ketter, R.L., "PLASTIC DESIGN IN STRUCTURAL STEEL - Lecture Notes of a Summer Course", Lehigh University - American Institute of Steel Construction, September, 1955.
9. Thürlimann, B., "ANALYSIS OF STEEL STRUCTURES FOR ULTIMATE STRENGTH" - Scheduled for publication as an American Society of Civil Engineers' Proceedings Paper.
10. Baker, J.F. Roderick, J.W., and Horne, M.R., "PLASTIC DESIGN OF SINGLE BAY PORTAL FRAMES", British Welding Research Association Report FE 1/2 (1947).
11. Symonds, P.S., and Neal, B.G., "RECENT PROGRESS IN THE PLASTIC METHODS OF STRUCTURAL ANALYSIS", Journal of Franklin Institute, 252(5), p. 383-407, November, 1951, and 252(6), p. 469-492, December 1951.

12. Neal, B.G., and Symonds, P.S., "THE COLLAPSE LOAD OF FRAME STRUCTURES", Journal of the Institution of Civil Engineers, No.1, November 1950, p.31.
13. Horne, M.R., "A MOMENT DISTRIBUTION METHOD FOR THE ANALYSIS AND DESIGN OF STRUCTURES BY THE PLASTIC THEORY", Proceedings of the Institution of Civil Engineers, 3 (part 3), 51, (1954).
14. English, J.M., "DESIGN OF FRAMES BY RELAXATION OF YIELD HINGES", Transactions, American Society of Civil Engineers, Vol. 119 (1954)
15. Neal, B.G., "PLASTIC COLLAPSE AND SHAKEDOWN THEOREMS FOR STRUCTURES OF STRAIN-HARDENING MATERIAL", Journal of Aeronautical Sciences, Vol. 17, No.5, May 1950.
16. "STEEL CONSTRUCTION MANUAL", American Institute of Steel Construction, New York, 1951.
17. Ketter, R.L., "LECTURE III - ANALYSIS AND DESIGN", Proceedings of the Sixth National Engineering Conference of the American Institute of Steel Construction, American Institute of Steel Construction, April 1956.
18. Heyman, J., "PLASTIC DESIGN OF PLANE FRAMES FOR MINIMUM WEIGHT", Structural Engineer, Vol.31, (1953), pp. 125-129
19. Thürlimann, B., "LECTURE IV - Modifications to 'SIMPLE PLASTIC THEORY'", Proceedings of the Sixth National Engineering Conference of the American Institute of Steel Construction, American Institute of Steel Construction, April 1956.
20. Neal, B.G., Discussion of Reference 13, Proceedings of the Institution of Civil Engineers, 3(part 3), 51, (1954).

APPENDIX A. DETERMINATION OF EQUIVALENT SYSTEM
OF CONCENTRATED LOADS TO REPLACE
UNIFORMLY DISTRIBUTED LOADS

In choosing the equivalent system, the necessary condition is that the moment diagram resulting from the concentrated loads circumscribe the moment diagram due to the distributed loads.

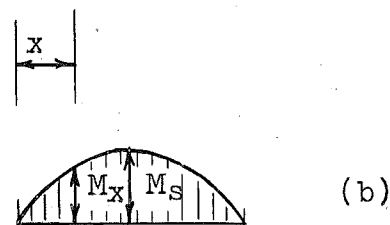
Figure A-1 (a) shows a simple beam loaded with a uniformly distributed load of w lbs/ft. Its moment diagram is as given in Figure A-1(b) with



$$M_x = \frac{wL}{2} x - \frac{wx^2}{2} \dots\dots\dots [A-1]$$

and

$$M_s = \frac{wL^2}{8} \dots\dots\dots [A-2]$$



Moment Diagram

FIGURE A-1

The slope of the moment diagram at each end equals

$$\frac{dM_x}{dx} = \text{Shear} = \frac{wL}{2} \dots\dots\dots [A-3]$$

1. EQUIVALENT CONCENTRATED LOAD AT MID-SPAN

Assuming a concentrated load at mid-span, the slope of the moment diagram at the ends will equal the shear or

$\frac{1}{2}P$. Equating this to

Equation A-3

$$\frac{P}{2} = \frac{wL}{2}$$

or

$$P = wL \dots\dots\dots [A-4]$$

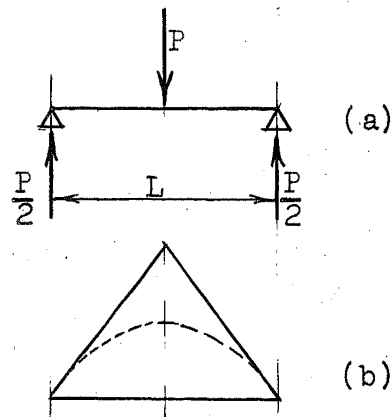


FIGURE A-2

From the moment diagram of Figure A-2 it is observed that the distributed load moment diagram is circumscribed.

2. EQUIVALENT CONCENTRATED LOADS

As shown in Figure A-3 two unknowns are involved in this problem: the equivalent load P and the distance from the ends of the beam to the points of load application, mL.

For the endslopes of the moment diagrams to be equal

$$P = \frac{wL}{2} \dots\dots\dots, [A-5]$$

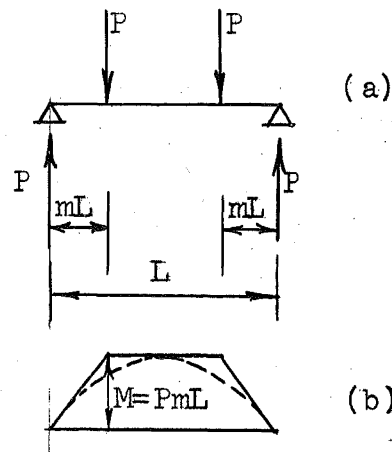


FIGURE A-3

Since the moments must also equal at the centerline section

$$PmL = \frac{wL^2}{8}$$

or $m = \frac{1}{4}$ [A-6]

3. CONCENTRATED LOADS

It has been assumed that each of the three loads are equal. Furthermore, the loads are placed symmetric about the centerline of the beam.

As seen from Figure A-4 two unknowns are to be evaluated, P and m. It is also noted that the two conditions controlling the determination of these quantities are

1. the slopes at the ends of the beams must be equal, and
2. the magnitudes of the moment values must be equal at the points within the beam where the slopes are also equal.

Using the first condition

$$\frac{3}{2}P = \frac{wL}{2}, \dots\dots\dots$$

or

$$P = \frac{wL}{3} \dots\dots\dots [A-6]$$

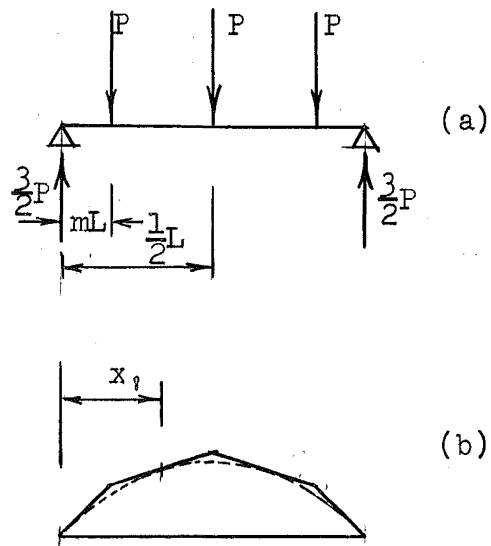


FIGURE A-4

To determine x_1 , the distance from the ends of the beam to the sections where the slopes of the two moment diagrams are equal,

$$\text{SHEAR} = \frac{1}{2}P = \frac{wL}{2} - wx,$$

which gives

$$x_1 = \frac{P}{w} \dots \dots \dots [A-7]$$

Equating the moment values at this location, it is found that

$$\frac{P}{w} - \frac{L}{2} = -mL$$

But since from Equation A-6 $P = \frac{1}{3} wL$

$$m = \frac{1}{6} \dots \dots \dots [A-8]$$

4. CONCENTRATED LOADS

Using the same procedure for the case of 4 equal concentrated loads as shown in Figure A-5, it is found that

$$P = \frac{wL}{4}, \dots \dots \dots [A-9]$$

$$m = \frac{1}{8}, \text{ and } \dots \dots \dots [A-10]$$

$$n = \frac{1}{4}.$$

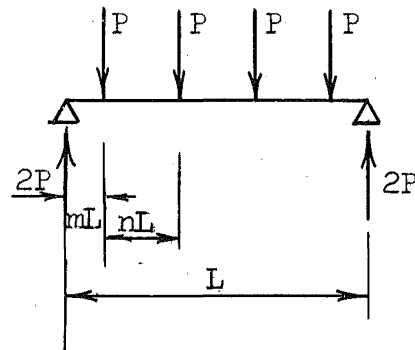


FIGURE A-5

APPENDIX B - IMPLICIT DIFFERENTIATION OF FUNCTION OF THREE VARIABLES*

Assuming that the three variables M_p , α and β are related according to the function

$$F(M_p, \alpha, \beta) = 0, \dots\dots\dots [B-1]$$

and further assume that α and β are the primary variables (M_p being an implicit function of α and β), the total differential of M_p can be expressed as

$$dM_p = \frac{\partial M_p}{\partial \alpha} d\alpha + \frac{\partial M_p}{\partial \beta} d\beta \dots\dots\dots [B-2]$$

In like manner the total differential of the function value itself is given by the expression

$$dF = \frac{\partial F}{\partial \alpha} d\alpha + \frac{\partial F}{\partial \beta} d\beta + \frac{\partial F}{\partial M_p} dM_p = 0 \dots\dots [B-3]$$

Substituting Equation B-2 in Equation B-3

$$\frac{\partial F}{\partial \alpha} d\alpha + \frac{\partial F}{\partial \beta} d\beta + \frac{\partial F}{\partial M_p} \left[\frac{\partial M_p}{\partial \alpha} d\alpha + \frac{\partial M_p}{\partial \beta} d\beta \right] = 0$$

Rearranging Terms

$$\left[\frac{\partial F}{\partial \alpha} + \frac{\partial F}{\partial M_p} \cdot \frac{\partial M_p}{\partial \alpha} \right] d\alpha + \left[\frac{\partial F}{\partial \beta} + \frac{\partial F}{\partial M_p} \cdot \frac{\partial M_p}{\partial \beta} \right] d\beta = 0 [B-4]$$

But since α and β are the assumed independent variables Equation B-4 must hold for all values of α and β .

*For further information on implicit differentiation see any text on Higher Mathematics; for example, "Higher Mathematics for Engineers and Physicists" by I.S. and E.S. Sokolnikoff, McGraw-Hill Book Company, New York, 1951 (page 138).

Therefore,

$$\frac{\partial F}{\partial \alpha} + \frac{\partial F}{\partial M_p} \cdot \frac{\partial M_p}{\partial \alpha} = 0$$

$$\frac{\partial F}{\partial \beta} + \frac{\partial F}{\partial M_p} \cdot \frac{\partial M_p}{\partial \beta} = 0$$

..... [B-5]

Transposing

$$\frac{\partial F}{\partial \alpha} = - \frac{\partial F}{\partial M_p} \cdot \frac{\partial M_p}{\partial \alpha}$$

$$\frac{\partial F}{\partial \beta} = - \frac{\partial F}{\partial M_p} \cdot \frac{\partial M_p}{\partial \beta}$$

..... [B-6]

For the problems considered in this paper it is known that

$$\frac{\partial M_p}{\partial \alpha} = 0$$

$$\frac{\partial M_p}{\partial \beta} = 0$$

..... [B-7]

Therefore,

$$\frac{\partial F}{\partial \alpha} = 0$$

$$\frac{\partial F}{\partial \beta} = 0$$

..... [B-8]

1.

$$\frac{M_p}{wL^2} = \frac{1}{4} \left[\frac{(1-\alpha)(A+\alpha)}{1 + \frac{b}{a}\alpha} \right], \text{ where } A = (2a) \left(\frac{P}{wL} \right)$$

$$\alpha = \frac{1}{\frac{b}{a}} \left[\sqrt{1 - \frac{b}{a} \left[A \left(1 + \frac{b}{a} \right) - 1 \right]} - 1 \right] \dots \text{for } \frac{b}{a} > 0$$

$$\alpha = \left[\frac{1-A}{2} \right] \dots \dots \dots \text{for } \frac{b}{a} = 0$$

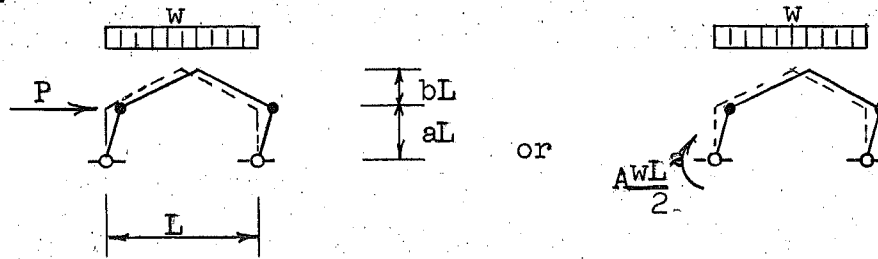
2.

$$\frac{M_p}{wL^2} = \frac{1}{4} \left[\frac{\alpha(1-\alpha)}{1 + \frac{b}{a}\alpha} \right], \text{ where } A = (2a) \left(\frac{P}{wL} \right)$$

$$\alpha = \frac{1}{\frac{b}{a}} \left[\sqrt{1 + \frac{b}{a}} - 1 \right] \dots \dots \dots \text{for } \frac{b}{a} > 0$$

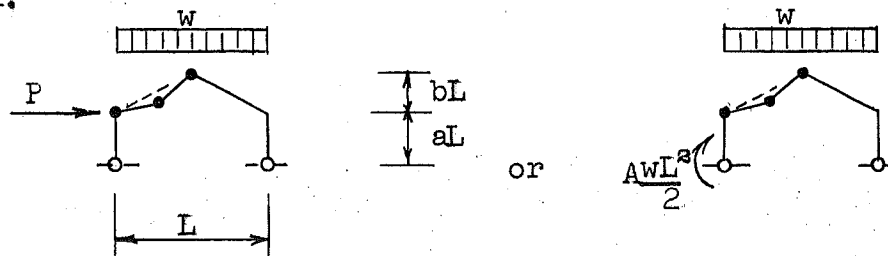
$$\alpha = \frac{1}{2} \dots \dots \dots \text{for } \frac{b}{a} = 0$$

3.



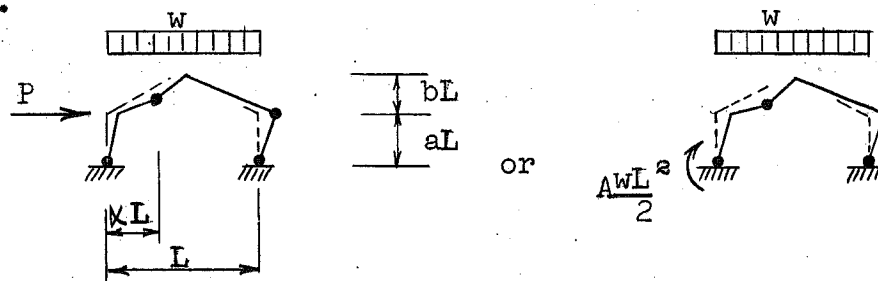
$$\frac{M_p}{wL^2} = \left[\frac{A}{4} \right] \quad \text{where } A = (2a) \left(\frac{P}{wL} \right)$$

4.



$$\frac{M_p}{wL^2} = 0.0156 \text{ for } \frac{b}{a} > 0, \quad \frac{M_p}{wL^2} = 0.0625 \text{ for } \frac{b}{a} = 0$$

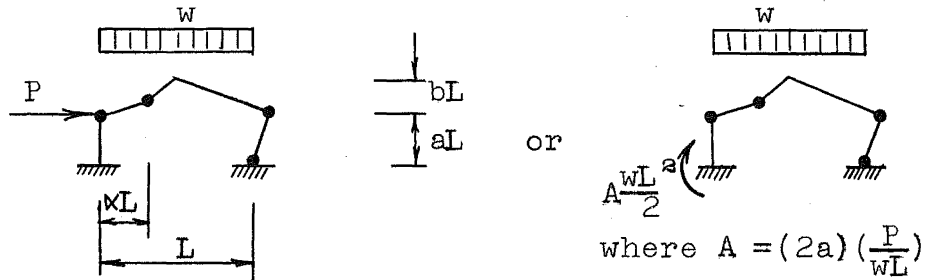
5.



$$\frac{M_p}{wL^2} = \frac{1}{4} \left[\frac{(1-\alpha)(A+\alpha)}{2 + \alpha \left(\frac{2b}{a} - 1 \right)} \right] \quad \text{where } A = (2a) \left(\frac{P}{wL} \right)$$

$$\alpha = \frac{2}{(1 - \frac{2b}{a})} \left[1 - \sqrt{\frac{1}{2} + \frac{A}{4} + \frac{b}{a} - A \left(\frac{b}{a} \right)^{2/3}} \right] \dots \frac{b}{a} \geq 0$$

6.

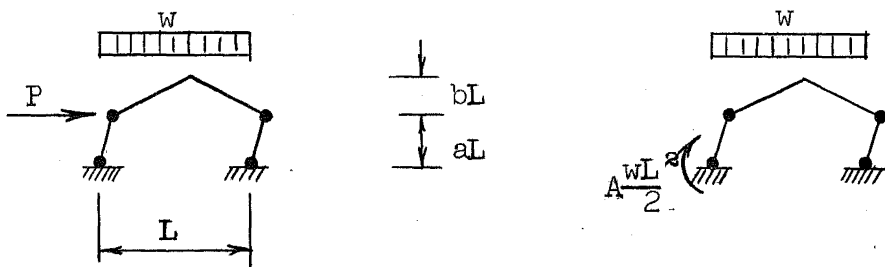


$$\frac{M_p}{wL^2 a} = \frac{1}{4} \left[\frac{x(1-x)}{1 + \frac{2b}{a}x} \right]$$

$$x = \frac{1}{\frac{2b}{a}} \left[\sqrt{1 + \frac{2b}{a}} - 1 \right] \dots \dots \dots \text{for } \frac{b}{a} > 0$$

$$x = \frac{1}{2} \dots \dots \dots \text{for } \frac{b}{a} = 0$$

7.



$$\frac{M_p}{wL^2 a} = \left[\frac{A}{8} \right] \text{ where } A = (2a) \cdot \left(\frac{P}{wL} \right)$$

8.

$$\frac{M_p}{wL^2} = \frac{1}{4} \left[\frac{\alpha \left(1 - \frac{2b}{a} D - \alpha\right)}{1 + \frac{b}{a} \alpha} \right]$$

$$\alpha = \frac{1}{\frac{b}{a}} \left[\sqrt{1 - \left(\frac{b}{a}\right) \left(2 \frac{b}{a} D - 1\right)} - 1 \right] \dots \dots \text{for } \frac{b}{a} > 0$$

$$\alpha = \frac{1}{2} \dots \dots \dots \text{for } \frac{b}{a} = 0$$

9.

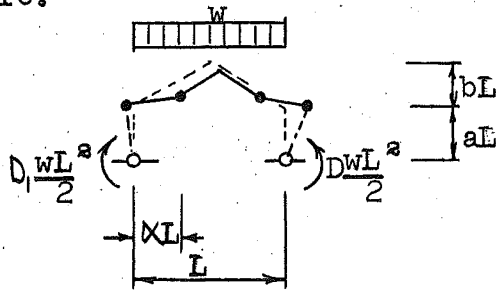
$$\frac{M_p}{wL^2} = \frac{1}{4} \left[\frac{\alpha \left(1 - \frac{2b}{a} D - \alpha\right)}{1 + \frac{b}{a} \alpha} \right]$$

$$\alpha = \frac{1}{\frac{b}{a}} \left[\sqrt{1 - \left(\frac{b}{a}\right) \left(2 \frac{b}{a} D - 1\right)} - 1 \right] \dots \dots \text{for } \frac{b}{a} > 0$$

$$\alpha = \frac{1}{2} \dots \dots \dots \text{for } \frac{b}{a} = 0$$

10.

NOTE: D, will be equal to D.

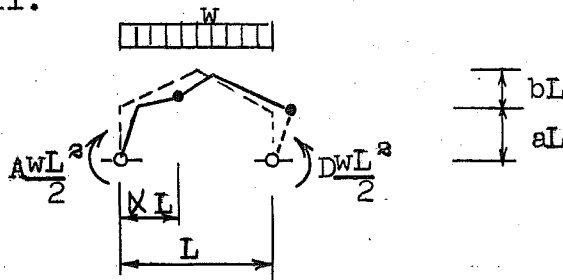


$$\frac{M_p}{wL^2} = \frac{1}{4} \left[\frac{x(1 - \frac{2b}{a}D - x)}{1 + \frac{b}{a}x} \right]$$

$$x = \frac{1}{\frac{b}{a}} \left[\sqrt{1 - (\frac{b}{a}) \cdot (2\frac{b}{a}D - 1)} - 1 \right] \dots \text{for } \frac{b}{a} > 0$$

$$x = \frac{1}{2} \dots \text{for } \frac{b}{a} = 0$$

11.

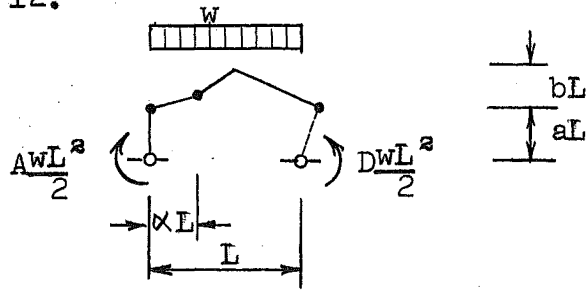


$$\frac{M_p}{wL^2} = \frac{1}{4} \left[\frac{(1-x)(A+x-D) - D(\frac{2b}{a})x}{1 + \frac{b}{a}x} \right]$$

$$x = \frac{1}{\frac{b}{a}} \left[\sqrt{1 - \frac{b}{a} \left[A(1 + \frac{b}{a}) - D(1 - \frac{b}{a}) - 1 \right]} - 1 \right] \dots \text{for } \frac{b}{a} > 0$$

$$x = \left[\frac{1 - A + D}{2} \right] \dots \text{for } \frac{b}{a} = 0$$

12.

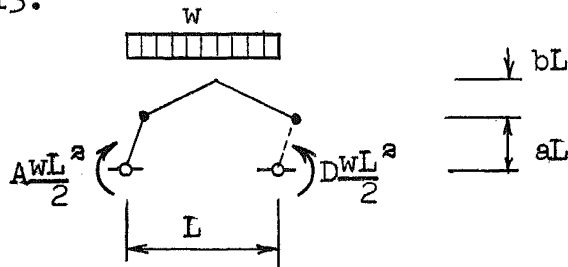


$$\frac{M_p}{wL^2} = \frac{1}{4} \left[\frac{\alpha \left(1 - D \frac{2b}{a} - \alpha \right)}{1 + \frac{b}{a} \alpha} \right]$$

$$\alpha = \frac{1}{\frac{b}{a}} \left[\sqrt{1 + \frac{b}{a} \left[1 - D \left(\frac{2b}{a} \right) \right]} - 1 \right] \quad \text{.. for } \frac{b}{a} > 0$$

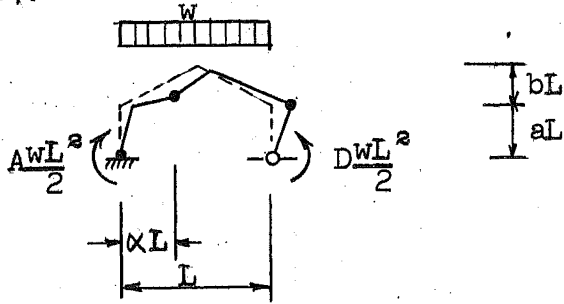
$$\alpha = \frac{1}{2} \quad \text{..... for } \frac{b}{a} = 0$$

13.



$$\frac{M_p}{wL^2} = \left[\frac{A-D}{4} \right]$$

14.

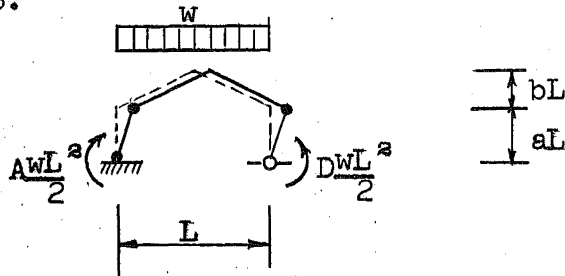


$$\frac{M_p}{wL^2} = \frac{1}{2} \left[\frac{(1-\alpha)(A-D+\alpha) - D\left(\frac{2b}{a}\right)\alpha}{3 + \alpha\left(\frac{2b}{a} - 1\right)} \right]$$

$$\alpha = \left[\frac{3}{\frac{2b}{a} - 1} \right] \left[\sqrt{1 - \frac{(2\frac{b}{a} - 1)}{9} \left[2A\left(1 + \frac{b}{a}\right) + 2D\left(2\frac{b}{a} - 1\right) - 3 \right]} - 1 \right]$$

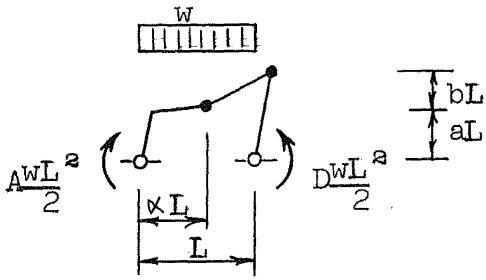
for $\frac{b}{a} \geq 0$

15.



$$\frac{M_p}{wL^2} = \left[\frac{A-D}{6} \right]$$

16.

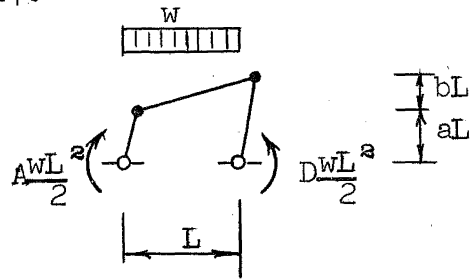


$$\frac{M_p}{wL^2} = \frac{1}{2} \left[\frac{(1-\alpha) \left\{ \left(1 + \frac{b}{a}\right) (A + \alpha) - D \right\}}{2 + \left(\frac{b}{a}\right) \cdot (1 + \alpha)} \right]$$

$$\alpha = \left[\frac{2 + \frac{b}{a}}{\frac{b}{a}} \right] \left[\left| 1 + \frac{b}{a} \left[\frac{\frac{b}{a} + 2 \left\{ 1 + D - A \left(1 + \frac{b}{a}\right) \right\}}{\left(2 + \frac{b}{a}\right)^2} \right] - 1 \right| \right] \text{ for } \frac{b}{a} > 0$$

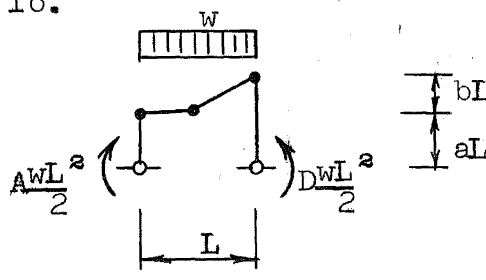
$$\alpha = \left[\frac{1 - A + D}{2} \right] \dots \dots \dots \text{ for } \frac{b}{a} = 0$$

17.



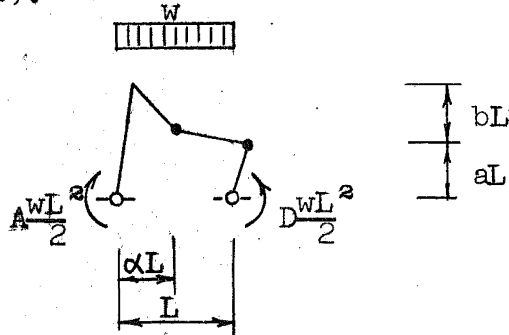
$$\frac{M_p}{wL^2} = \frac{1}{2} \left[\frac{A \left(1 + \frac{b}{a}\right) - D}{2 + \frac{b}{a}} \right]$$

18.



$$\frac{M_p}{wL^2} = 0.0625$$

19.

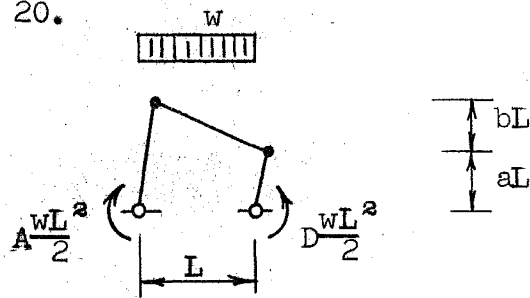


$$\frac{M_p}{WL^2} = \frac{1}{2} \left[\frac{(1-\alpha) \left\{ A - D \left(1 + \frac{b}{a} \right) + \alpha \right\}}{2 + \frac{b}{a} (1-\alpha)} \right]$$

$$\alpha = 1 - \frac{2}{a} \left[\sqrt{1 + \frac{b}{a} \left[A - D \left(1 + \frac{b}{a} \right) + 1 \right]} - 1 \right] \dots \dots \text{for } \frac{b}{a} \neq 0$$

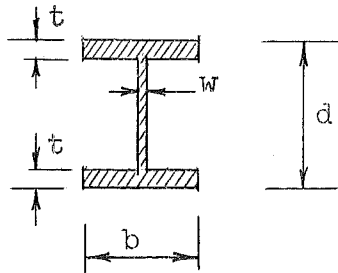
$$\alpha = \left[\frac{1 - A + D}{2} \right] \dots \dots \dots \text{for } \frac{b}{a} = 0$$

20.



$$\frac{M_p}{WL^2} = \frac{1}{2} \left[\frac{A - D \left(1 + \frac{b}{a} \right)}{2 + \frac{b}{a}} \right]$$

PLASTIC MODULUS TABLE



PLASTIC MODULUS	f	SECTION	AREA	b/t	d/w
1255.0	1.14	36 WF 300	88.17	9.91	38.9
1167.0	1.13	36 WF 280	82.32	10.57	41.2
1076.0	1.13	36 WF 260	76.56	11.50	42.9
1008.0	1.13	36 WF 245	72.03	12.23	45.0
942.7	1.13	36 WF 230	67.73	13.08	46.9
918.2	1.13	33 WF 240	70.52	11.33	40.4
869.3	1.23	14 WF 426	125.25	5.50	10.0
836.2	1.13	33 WF 220	64.73	12.40	42.9
803.0	1.22	14 WF 398	116.98	5.84	10.3
754.4	1.13	33 WF 200	58.79	13.70	46.2
767.2	1.16	36 WF 194	57.11	9.62	47.4
733.9	1.13	30 WF 210	61.78	11.49	39.2
716.9	1.15	36 WF 182	53.54	10.23	50.1
673.7	1.21	14 WF 370	108.78	6.20	10.8
659.6	1.13	30 WF 190	55.90	12.69	42.4
666.7	1.15	36 WF 170	49.98	10.93	53.2
623.3	1.15	36 WF 160	47.09	11.76	55.1
611.5	1.19	14 WF 314	92.30	7.11	12.1
593.0	1.13	30 WF 172	50.65	14.07	45.6
592.2	1.20	14 WF 320	94.12	7.98	8.9
579.8	1.15	36 WF 150	44.16	12.74	57.3
558.3	1.15	33 WF 152	44.71	10.96	52.8
556.9	1.13	27 WF 177	52.10	11.84	37.7
551.6	1.18	14 WF 287	84.37	7.71	12.8

PLASTIC MODULUS	f	SECTION	AREA	b/t	d/w
513.2	1.15	33 WF 141	41.51	12.02	55.1
504.3	1.14	27 WF 160	47.04	13.04	41.2
502.4	1.18	14 WF 264	77.63	8.27	13.7
466.0	1.15	33 WF 130	38.26	13.46	57.1
464.5	1.17	14 WF 246	72.33	8.80	14.4
463.7	1.12	24 WF 160	47.04	12.41	37.7
452.0	1.12	24 WF 145	42.68	14.32	44.8
445.4	1.17	14 WF 237	69.69	9.10	14.8
436.7	1.15	30 WF 132	38.83	10.55	49.3
427.2	1.16	14 WF 228	67.06	9.40	15.3
416.0	1.12	24 WF 145	42.62	13.78	40.3
408.0	1.15	14 WF 219	64.36	9.75	15.8
407.4	1.15	30 WF 124	36.45	11.31	52.0
391.7	1.16	14 WF 211	62.07	10.11	16.1
377.6	1.15	30 WF 116	34.13	12.35	53.2
373.6	1.15	14 WF 202	59.39	10.48	16.8
369.2	1.12	24 WF 130	38.21	15.56	42.9
357.0	1.13	21 WF 142	41.76	11.99	32.6
355.1	1.15	14 WF 193	56.73	10.92	17.4
345.5	1.16	30 WF 108	31.77	13.79	54.4
342.8	1.15	27 WF 114	33.53	11.48	47.9
337.5	1.14	14 WF 184	54.07	11.36	18.3
336.6	1.13	24 WF 120	35.29	13.00	43.7
321.3	1.14	14 WF 176	51.73	11.91	18.6
317.8	1.12	21 WF 127	37.34	13.26	36.1
311.5	1.18	12 WF 190	55.86	7.30	13.6
307.7	1.12	24 WF 110	32.36	14.08	47.4
304.4	1.14	27 WF 102	30.01	12.11	52.3
302.9	1.13	14 WF 167	49.09	12.50	19.4
298.0	1.19	24 I 120	35.13	7.30	30.1
286.3	1.13	14 WF 158	46.47	13.10	20.5
278.0	1.11	21 WF 112	32.93	15.03	39.8
278.3	1.12	24 WF 100	29.43	15.48	51.3
277.7	1.14	27 WF 94	26.91	13.37	54.9
273.0	1.17	24 I 105.9	30.98	7.15	38.4
270.2	1.13	14 WF 150	44.08	13.75	21.4
259.2	1.17	12 WF 161	47.38	8.42	15.3
254.8	1.12	14 WF 142	41.85	14.58	21.7

APPENDIX D

D-3

PLASTIC MODULUS	f	SECTION	AREA	b/t	d/w
253.0	1.15	24 WF 94	27.63	10.39	47.1
247.9	1.13	18 WF 114	33.51	11.94	31.1
242.7	1.12	14 WF 136	39.98	13.87	22.3
238.8	1.21	24 I 100	29.25	8.32	32.1
226.5	1.12	18 WF 105	30.86	12.94	33.1
226.3	1.15	21 WF 96	28.21	9.67	36.8
225.9	1.12	14 WF 127	37.33	14.72	24.0
224.0	1.14	24 WF 84	24.71	11.68	51.3
220.5	1.14	24 I 90	26.30	8.18	38.5
210.9	1.11	14 WF 119	34.99	15.62	25.4
209.7	1.15	12 WF 133	39.11	10.00	17.7
206.0	1.12	18 WF 96	28.22	14.14	35.5
203.0	1.17	24 I 79.9	23.33	8.04	48.0
200.1	1.14	24 WF 76	22.37	13.17	54.3
196.0	1.11	14 WF 111	32.65	16.75	26.6
192.0	1.20	20 I 95	27.74	7.86	25.0
191.6	1.14	21 WF 82	24.10	11.27	41.8
186.4	1.14	12 WF 120	35.31	11.14	18.5
186.0	1.12	16 WF 96	28.22	13.18	30.5
181.0	1.11	14 WF 103	30.26	17.93	28.8
177.6	1.14	18 WF 85	24.97	9.70	34.8
177.3	1.18	20 I 85	24.80	7.70	30.6
172.1	1.14	21 WF 73	21.46	11.21	46.7
169.0	1.12	16 WF 88	25.87	14.47	32.1
166.6	1.11	14 WF 95	27.94	19.45	30.4
163.4	1.13	12 WF 106	31.19	12.40	20.8
160.5	1.13	18 WF 77	22.62	10.57	38.2
159.8	1.14	21 WF 68	20.02	12.07	49.1
151.8	1.13	12 WF 99	29.09	13.24	22.0
151.5	1.20	20 I 75	21.90	8.10	31.2
151.3	1.10	14 WF 87	25.56	21.08	33.3
147.5	1.17	10 WF 112	32.96	8.35	15.1
145.5	1.14	16 WF 78	22.92	9.81	30.9
145.4	1.11	14 WF 84	24.71	15.45	31.4
144.7	1.13	18 WF 70	20.56	11.65	41.1

PLASTIC MODULUS	f	SECTION	AREA	b/t	d/w
144.1	1.14	21 WF 62	18.23	13.40	52.5
140.2	1.12	12 WF 92	27.06	14.20	23.2
137.3	1.17	20 I 65.4	19.08	7.92	40.0
134.0	1.11	14 WF 78	22.94	16.71	32.9
131.8	1.13	18 WF 64	18.80	12.70	44.3
131.6	1.14	16 WF 71	20.86	10.75	33.3
130.1	1.16	10 WF 100	29.43	9.25	16.2
129.1	1.12	12 WF 85	24.98	15.21	25.3
125.6	1.12	14 WF 74	21.76	12.86	31.5
123.8	1.21	18 I 70	20.46	9.05	25.3
122.6	1.14	18 WF 60	17.64	10.87	43.9
119.3	1.11	12 WF 79	23.22	16.41	26.3
117.9	1.13	16 WF 64	18.80	11.90	36.1
114.8	1.12	14 WF 68	20.00	13.98	33.6
114.4	1.15	10 WF 89	26.19	10.30	17.7
111.6	1.14	18 WF 55	16.19	11.96	46.5
108.1	1.11	12 WF 72	21.16	17.94	28.5
106.2	1.13	16 WF 58	17.04	13.12	39.0
103.5	1.17	18 I 54.7	15.94	8.68	39.1
102.4	1.11	14 WF 61	17.94	15.55	36.8
100.8	1.13	18 WF 50	14.71	13.16	50.3
97.7	1.13	10 WF 77	22.67	11.75	19.9
97.0	1.10	12 WF 65	19.11	19.80	31.1
92.7	1.15	16 WF 50	14.70	11.26	42.8
90.7	1.13	10 WF 72	21.18	12.59	20.6
87.1	1.12	14 WF 53	15.59	12.25	37.7
86.5	1.11	12 WF 58	17.06	15.62	34.0
82.8	1.12	10 WF 66	19.41	13.53	22.7
82.0	1.13	16 WF 45	13.24	12.50	46.6
78.51	1.12	14 WF 48	14.11	13.54	40.7
78.16	1.11	12 WF 53	15.59	17.36	35.0
76.5	1.19	15 I 50	14.59	9.07	27.3
75.1	1.21	10 WF 60	17.66	14.75	24.7
72.7	1.13	16 WF 40	11.77	13.92	52.1
72.57	1.12	12 WF 50	14.71	12.60	32.9
70.1	1.16	8 WF 67	19.70	8.88	15.7
69.65	1.11	14 WF 43	12.65	15.15	44.4
68.6	1.16	15 I 42.9	12.49	8.84	36.6
67.0	1.11	10 WF 54	15.88	16.23	27.5
64.88	1.12	12 WF 45	13.24	13.96	35.9

APPENDIX D

D-5

PLASTIC MODULUS	f	SECTION	AREA	b/t	d/w
63.9	1.14	16 WF 36	10.59	16.34	53.0
61.49	1.13	14 WF 38	11.17	13.21	45.1
60.65	1.21	12 I 50	14.57	8.31	17.5
60.3	1.11	10 WF 49	14.40	17.92	29.4
59.9	1.15	8 WF 58	17.06	10.18	17.2
57.6	1.11	12 WF 40	11.77	15.50	40.6
54.95	1.12	10 WF 45	13.24	12.98	28.9
54.5	1.12	14 WF 34	10.00	14.90	48.8
52.45	1.17	12 I 40.8	11.84	7.97	26.1
51.42	1.12	12 WF 36	10.59	12.16	40.1
49.0	1.13	8 WF 48	14.11	11.88	21.0
47.1	1.13	14 WF 30	8.81	17.58	51.3
46.95	1.11	10 WF 39	11.48	15.13	31.3
44.37	1.17	12 I 35	10.20	9.33	28.0
43.96	1.12	12 WF 31	9.12	14.03	45.6
41.58	1.16	12 I 31.8	9.26	9.19	34.3
39.9	1.12	8 WF 40	11.76	14.47	22.6
38.8	1.11	10 WF 33	9.71	18.39	33.4
37.97	1.11	12 WF 27	7.97	16.25	49.8
35.16	1.20	10 I 35	10.22	10.07	16.8
34.70	1.12	8 WF 35	10.30	16.28	25.8
34.70	1.13	10 WF 29	8.53	11.60	35.4
32.8	1.14	8 M 34.3	10.09	18.26	21.3
30.4	1.11	8 WF 31	9.12	18.48	27.8
29.5	1.12	10 WF 25	7.35	13.40	40.0
29.35	1.16	12 B 22	6.47	9.50	47.3
28.04	1.15	10 I 25.4	7.38	9.49	32.3
27.1	1.12	8 WF 28	8.23	14.13	28.3
24.78	1.16	12 B 19	5.62	11.50	50.7
24.1	1.12	10 WF 21	6.19	16.91	41.3
23.42	1.12	8 M 24	7.06	17.33	33.3
23.1	1.11	8 WF 24	7.06	16.33	32.4
21.56	1.15	10 B 19	5.61	10.20	41.0
20.61	1.18	12 B 16.5	4.86	14.87	52.2
19.15	1.20	8 I 23	6.71	9.81	18.1
19.1	1.12	8 WF 20	5.88	13.94	32.8
19.03	1.13	6 WF 25	7.37	13.33	19.9
18.63	1.15	10 B 17	4.98	12.19	42.2
17.86	1.14	6 M 25	7.35	11.88	19.2
17.46	1.15	8 M 20	5.88	17.12	22.9

PLASTIC MODULUS	f	SECTION	AREA	b/t	d/w
17.39	1.18	12 B 14	4.14	17.72	59.6
16.34	1.15	8 I 18.4	5.34	9.41	29.6
15.97	1.16	10 B 15	4.40	14.87	43.5
15.8	1.12	8 WF 17	5.00	17.05	34.8
15.70	1.12	8 M 17	5.00	16.77	33.3
15.04	1.12	6 WF 20	5.90	16.40	24.0
14.56	1.14	6 M 20	5.88	15.83	24.0
14.37	1.20	7 I 20	5.83	9.85	15.6
14.21	1.18	12 JR 11.8	3.45	12.25	68.6
13.59	1.15	8 B 15	4.43	12.79	33.1
12.13	1.16	10 B 11.5	3.39	19.36	54.8
11.94	1.15	7 I 15.3	4.43	9.33	28.0
11.61	1.12	6 B 16	4.72	9.98	24.0
11.35	1.15	8 B 13	3.83	15.75	34.8
11.35	1.14	5 WF 18.5	5.45	11.96	19.3
11.29	1.12	6 WF 15.5	4.43	9.33	28.0
11.06	1.16	5 M 18.9	5.56	11.42	16.0
10.49	1.21	6 I 17.25	5.02	9.93	12.9
9.62	1.13	5 WF 16	4.70	13.89	20.8
9.23	1.18	10 JR 9	2.64	14.30	64.5
8.85	1.14	8 B 10	2.95	19.31	46.5
8.36	1.15	6 I 12.5	3.61	9.28	26.1
8.25	1.14	6 B 12	3.53	14.34	26.1
7.37	1.23	5 I 14.75	4.29	10.07	10.1
6.29	1.15	4 WF 13	3.82	11.77	14.9
6.11	1.17	4 M 13	3.82	10.67	16.0
5.70	1.12	6 B 8.5	2.50	20.30	34.3
5.57	1.16	5 I 10	2.87	9.20	23.8
5.44	1.16	8 JR 6.5	1.92	12.13	59.3
4.03	1.15	7 JR 5.5	1.61	11.05	55.6
4.02	1.22	4 I 9.5	2.76	9.54	12.3
3.46	1.15	4 I 7.7	2.21	9.08	21.1
2.82	1.18	6 JR 4.4	1.30	9.81	52.6
2.31	1.22	3 I 7.5	2.17	9.65	8.6
1.93	1.14	3 I 5.7	1.64	8.96	17.6

DESIGN CHART

TABLE
INDEX TO DESIGN CHARTS

STRUCTURE	$\frac{b}{a}$	0	0.2	0.4	0.6	0.8	1.0
		← I-1* →					
		← I-2 →					
		← II-1 →					
		III-1	III-2	III-3	III-4	III-5	III-6
		IV-1	IV-2	IV-3	IV-4	IV-5	IV-6
		V-1	V-2	V-3	V-4	V-5	V-6
		VI-1	VI-2	VI-3	VI-4	VI-5	VI-6

*These Are The Numbers Of The Design Charts That Determine The Size Of The Members. Corresponding Charts Locating The Plastic Hinge Are Denoted By The Additional Letter a, (e.g. I-1a).

DESIGN CHART

I-1

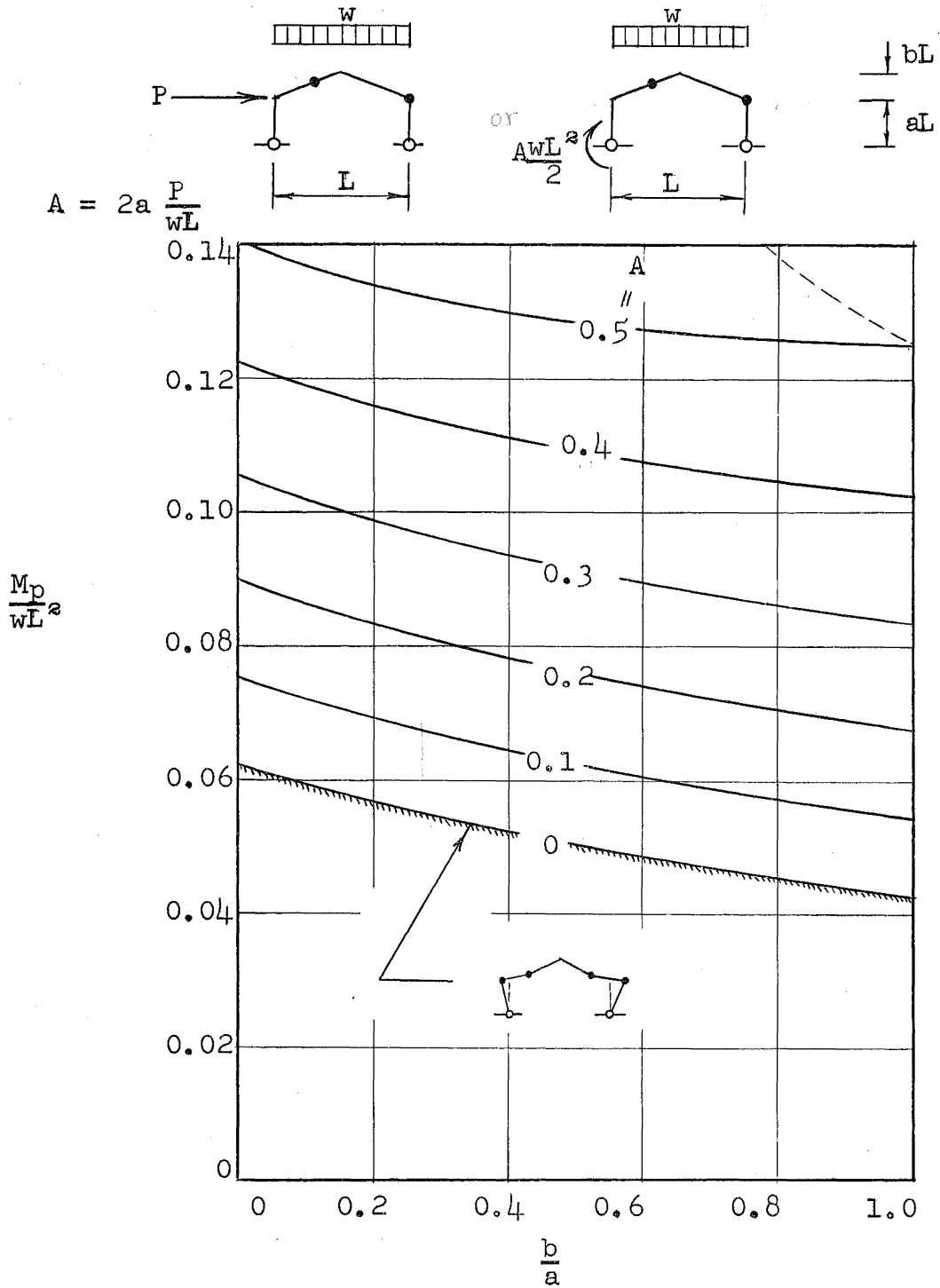


CHART I-1

DESIGN CURVES FOR "PINNED-BASE" GABLE FRAMES
DETERMINATION OF MEMBER SIZE

DESIGN CHART

I-2

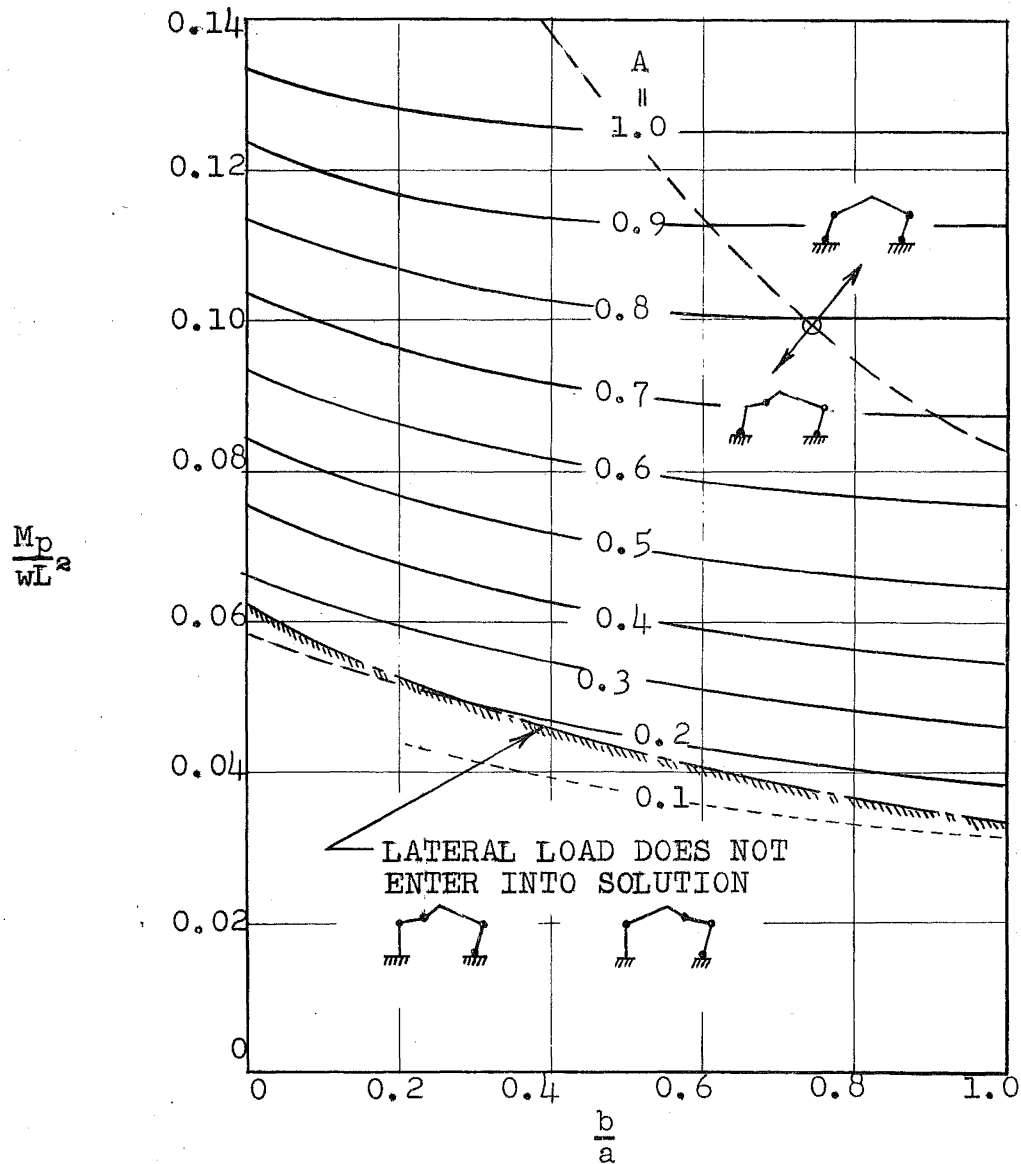
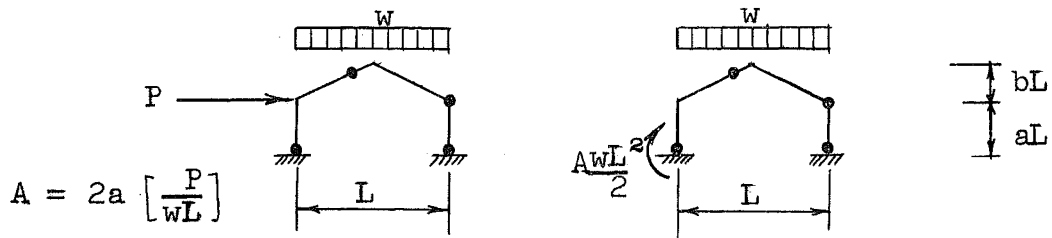
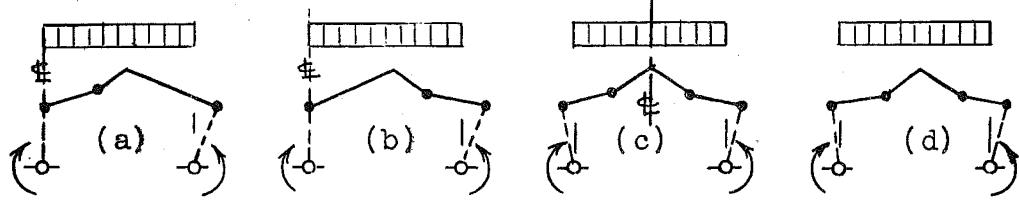


CHART I-2

DESIGN CURVES FOR "FIXED-BASE" GABLE FRAME
DETERMINATION OF MEMBER SIZE

DESIGN CHART

II-1



POSSIBLE FAILURE MODES

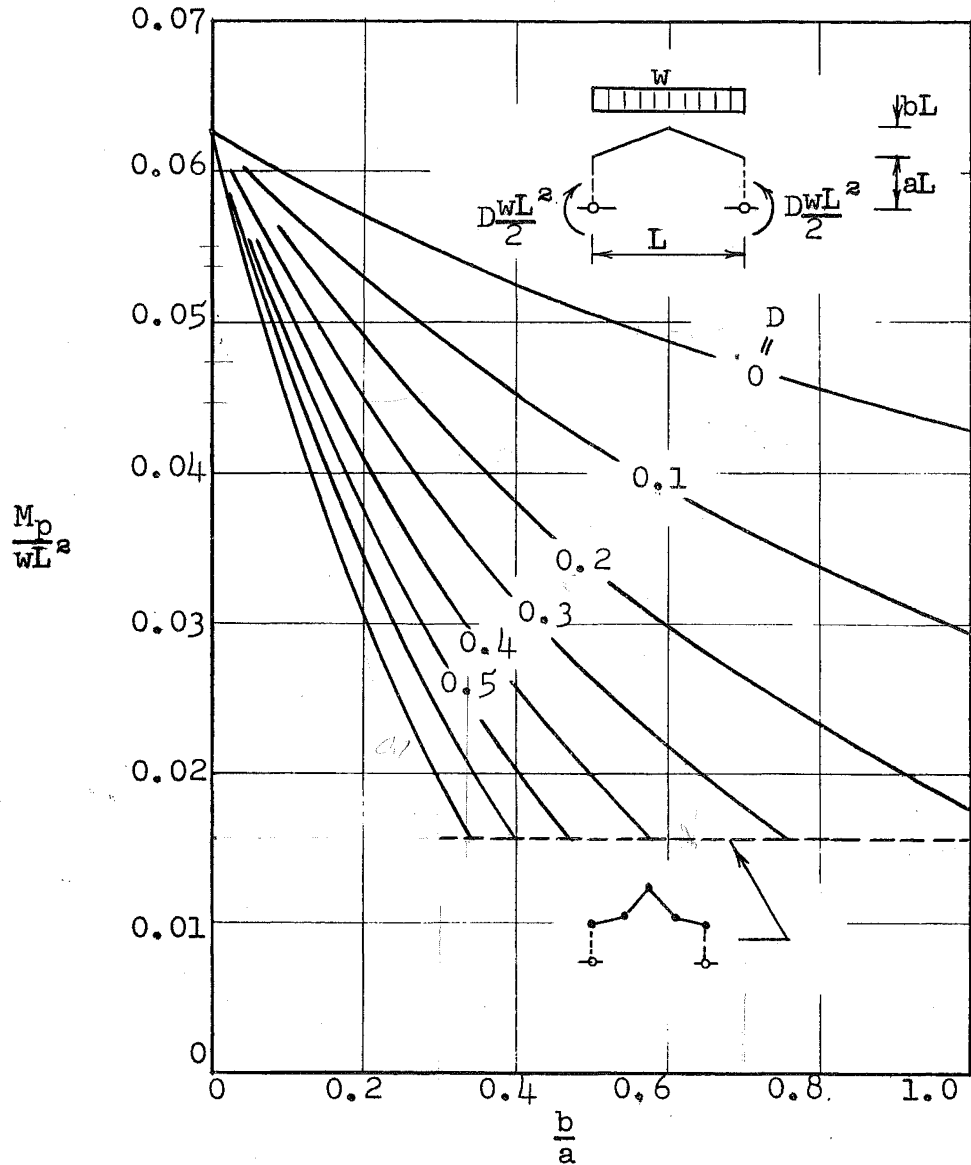


CHART II-1

DESIGN CURVES FOR GABLE FRAMES
DETERMINATION OF MEMBER SIZE

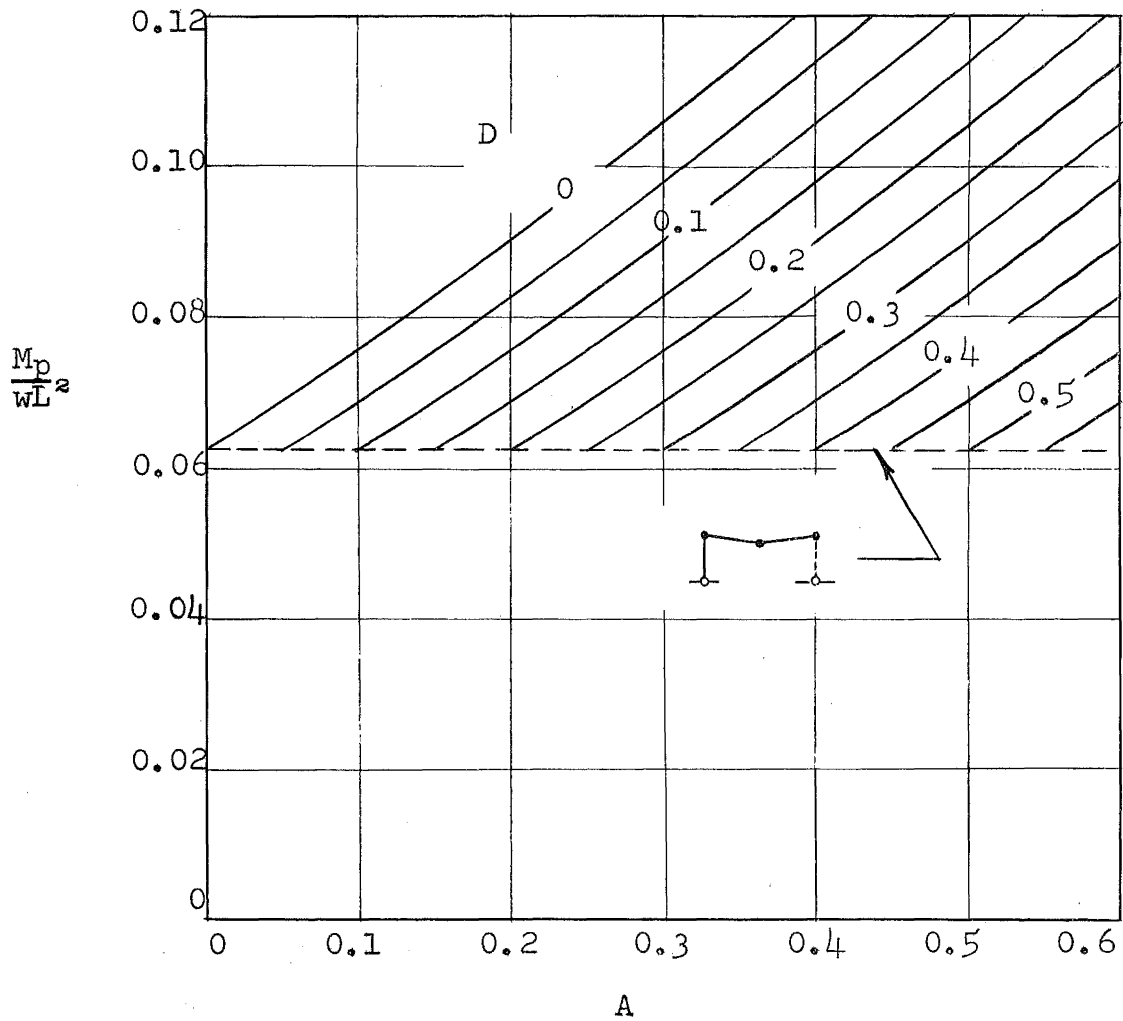
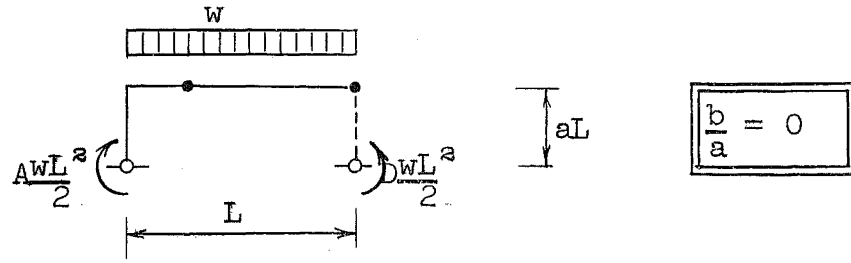


CHART III-1

DESIGN CURVES FOR "PINNED-BASE" GABLE FRAMES
DETERMINATION OF MEMBER SIZE

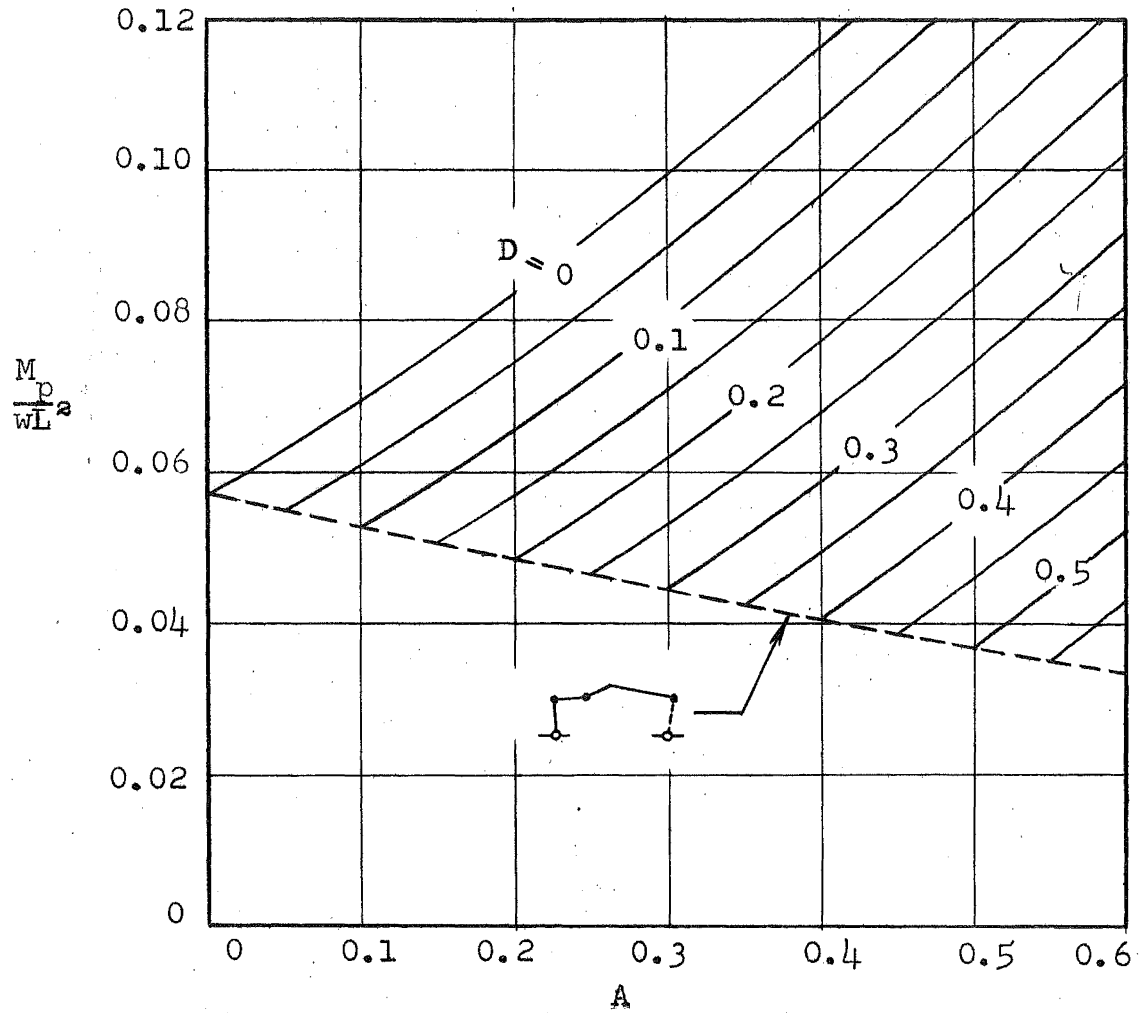
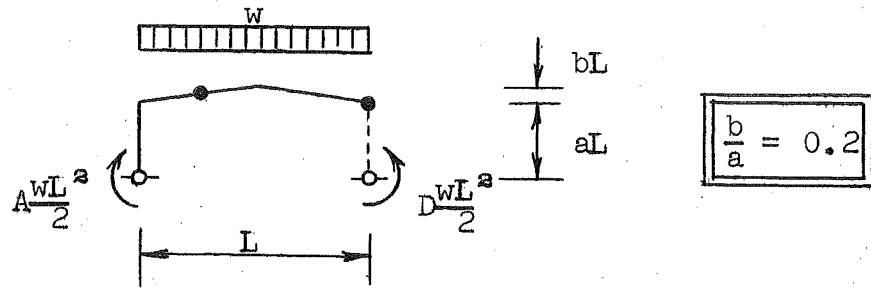


CHART III-2

DESIGN CURVES FOR "PINNED-BASE" GABLE FRAMES
 DETERMINATION OF MEMBER SIZE

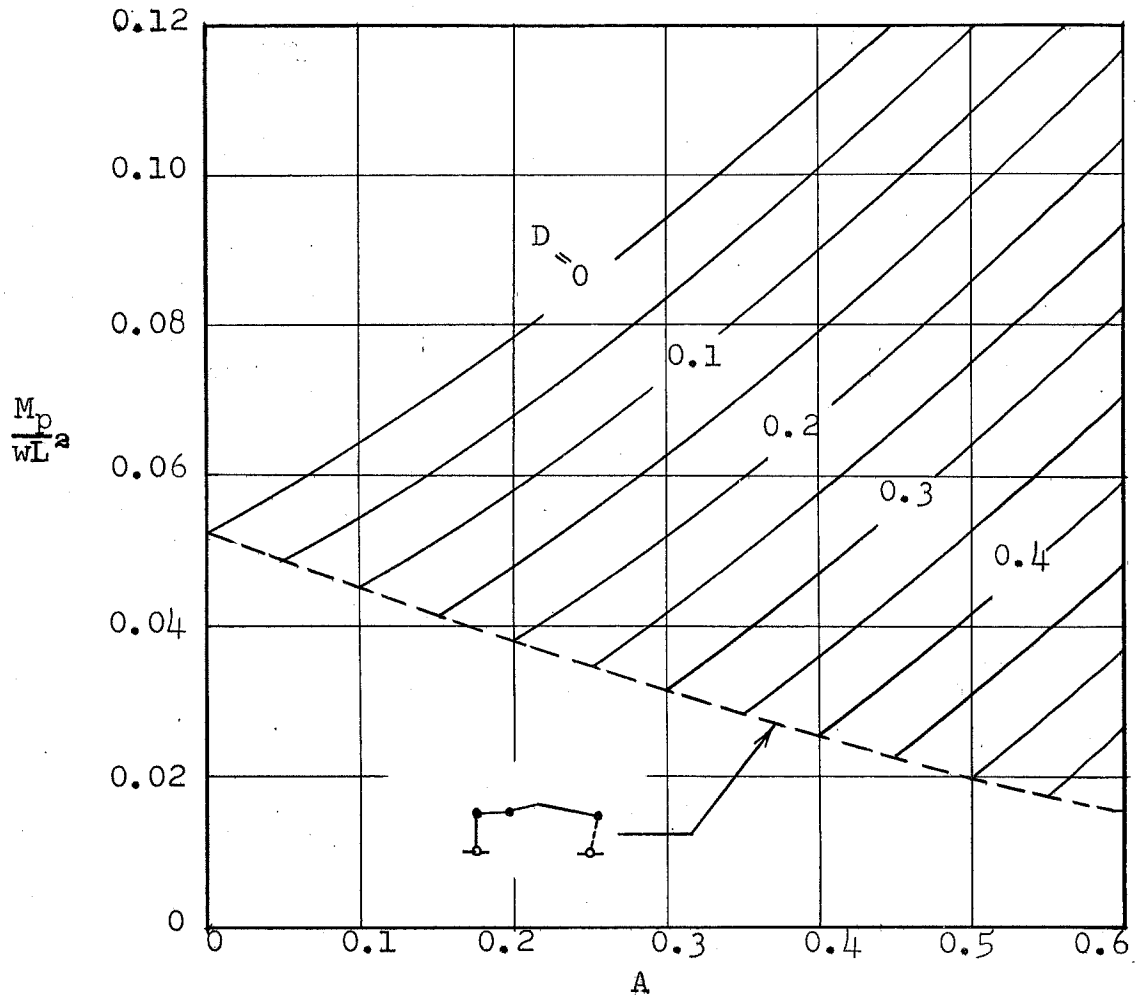
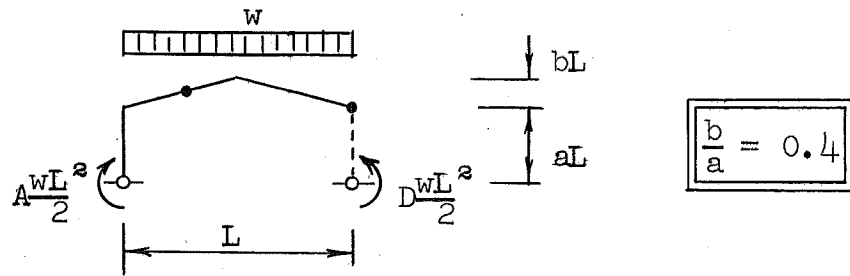


CHART III-3

DESIGN CURVES FOR "PINNED-BASE" GABLE FRAMES
 DETERMINATION OF MEMBER SIZE

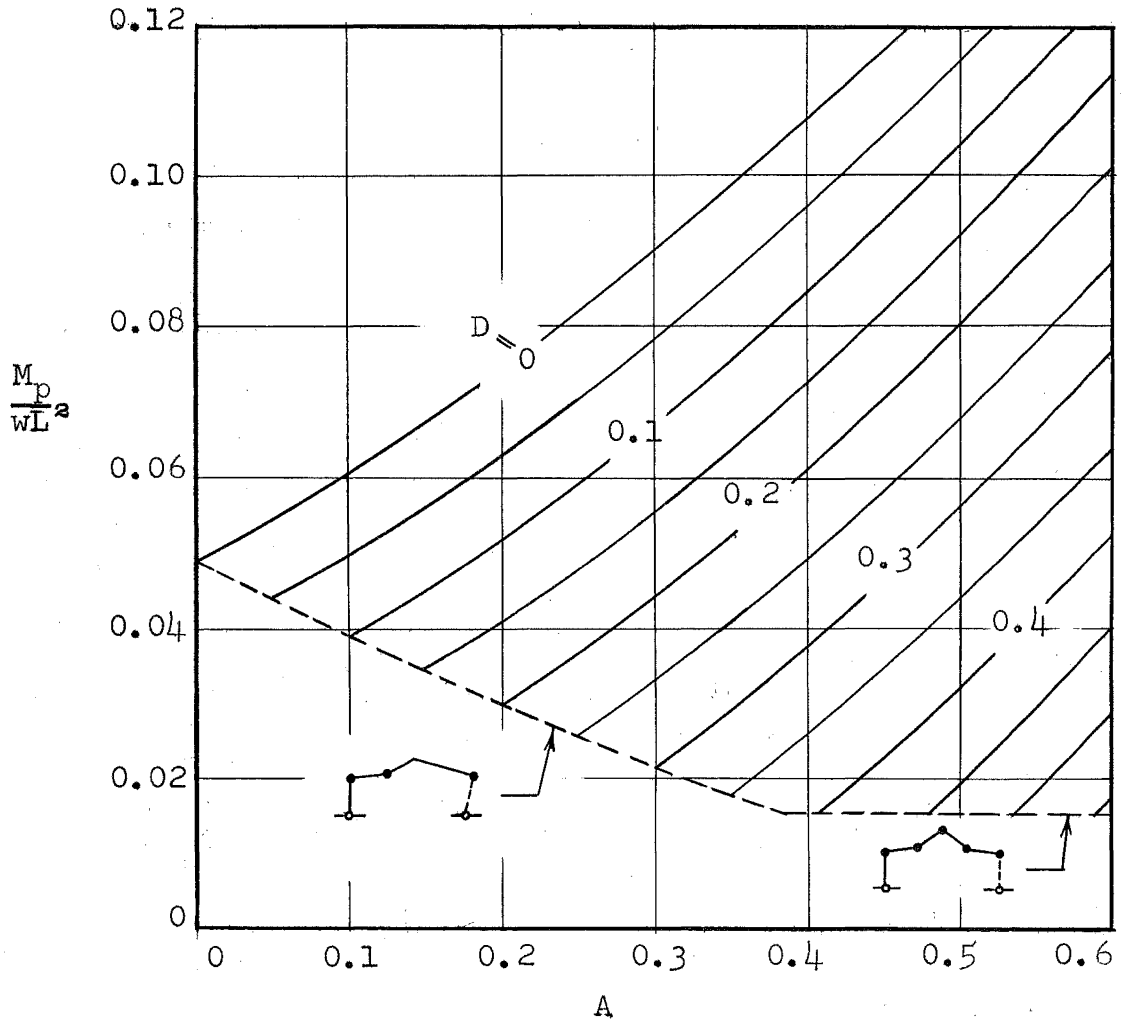
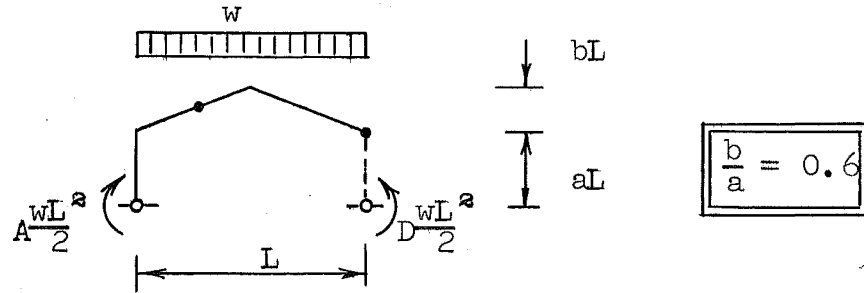


CHART III-4

DESIGN CURVES FOR "PINNED-BASE" GABLE FRAMES
DETERMINATION OF MEMBER SIZE

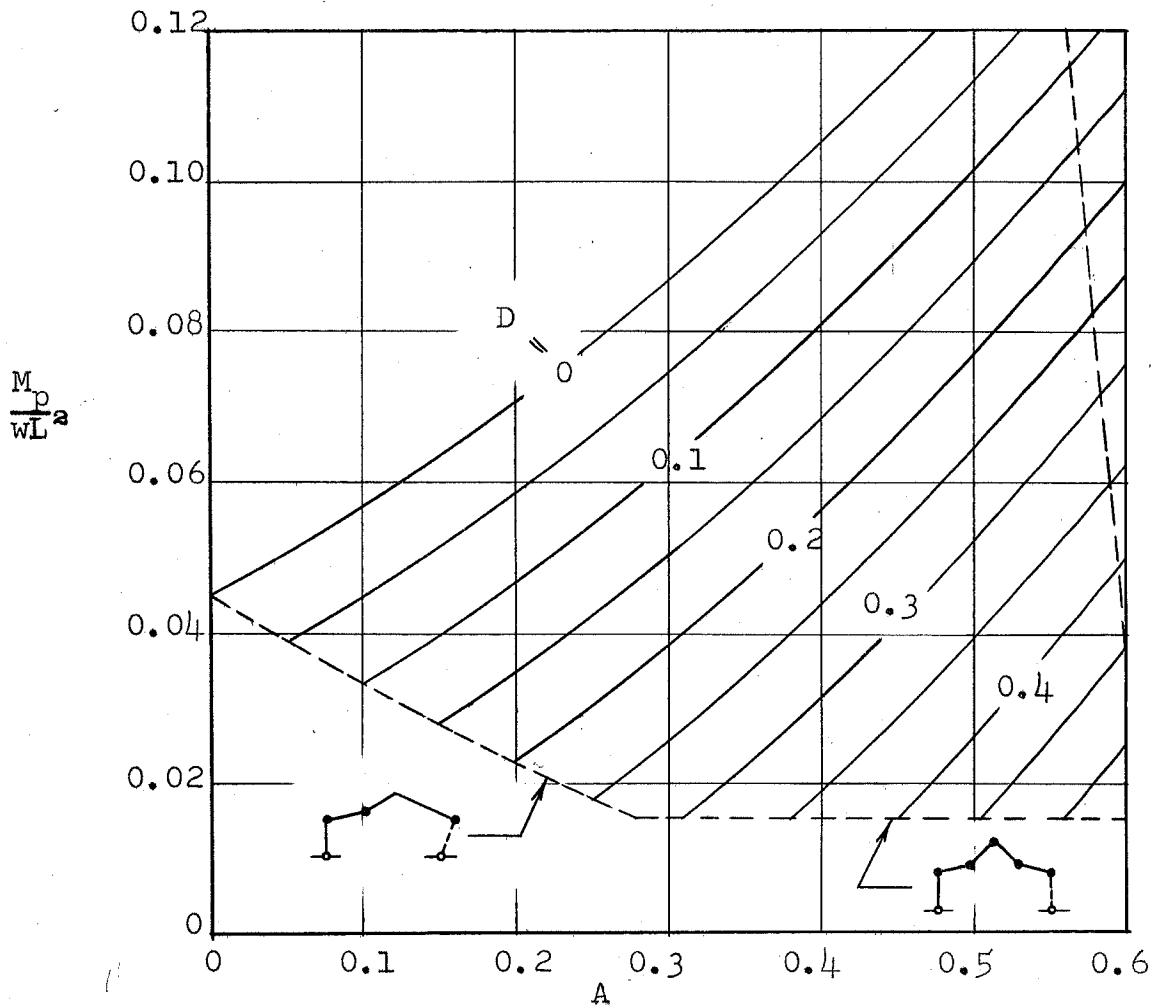
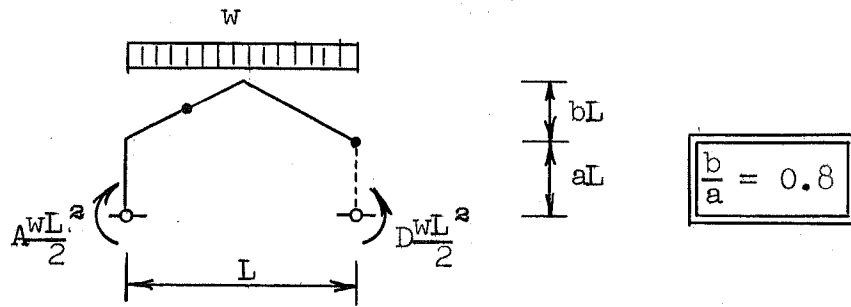


CHART III-5

DESIGN CURVES FOR "PINNED-BASE" GABLE FRAMES
 DETERMINATION OF MEMBER SIZE

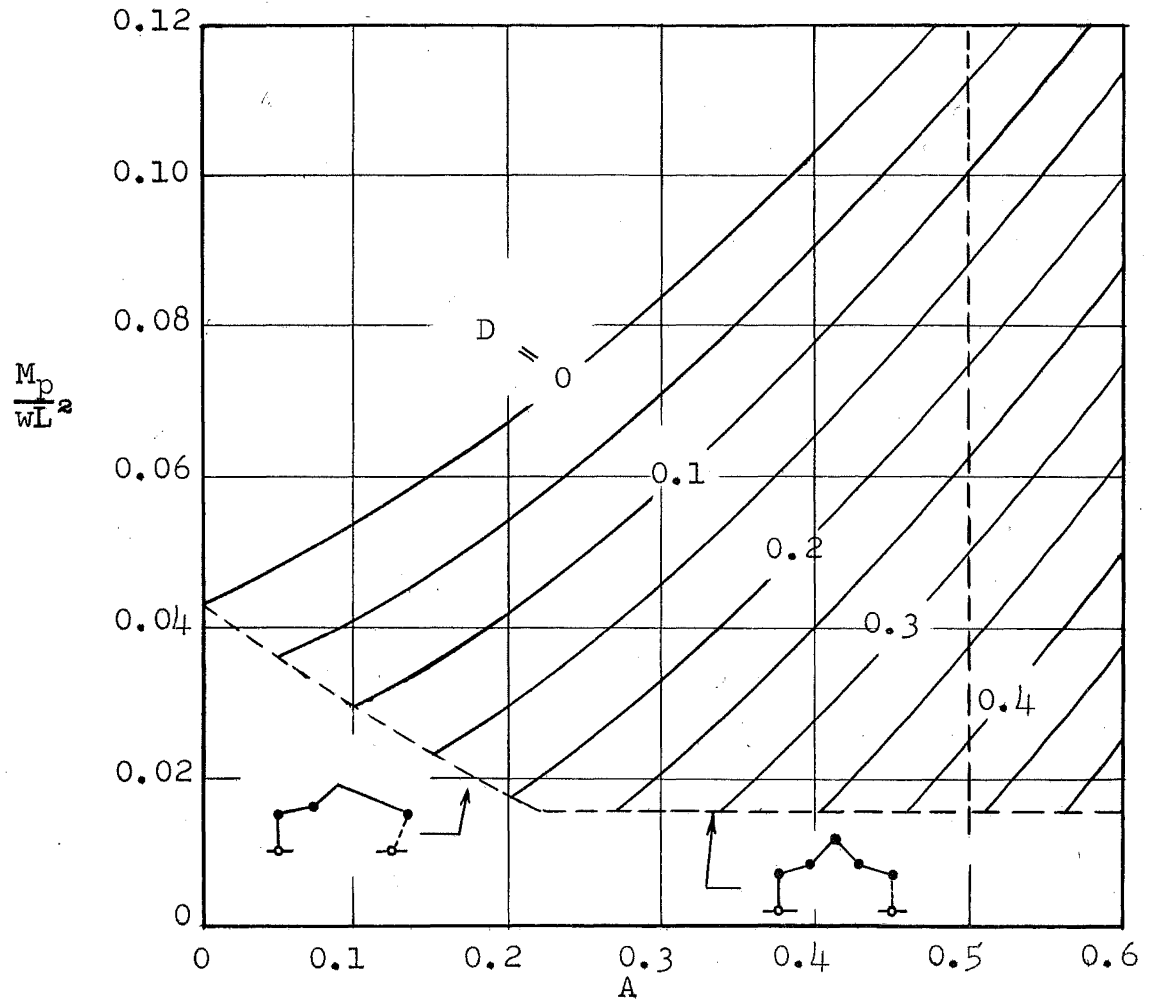
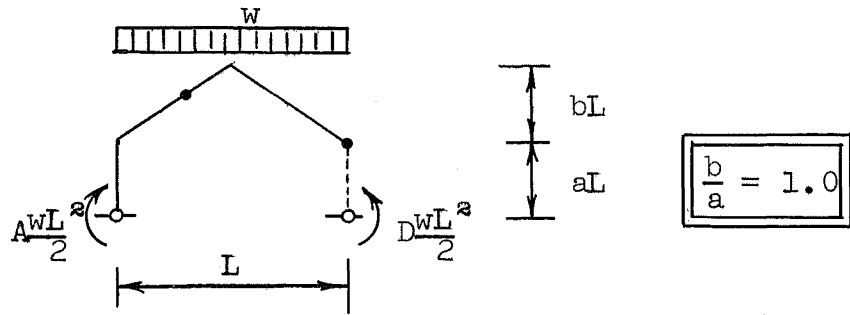


CHART III-6

DESIGN CURVES FOR "PINNED-BASE" GABLE FRAMES
 DETERMINATION OF MEMBER SIZE

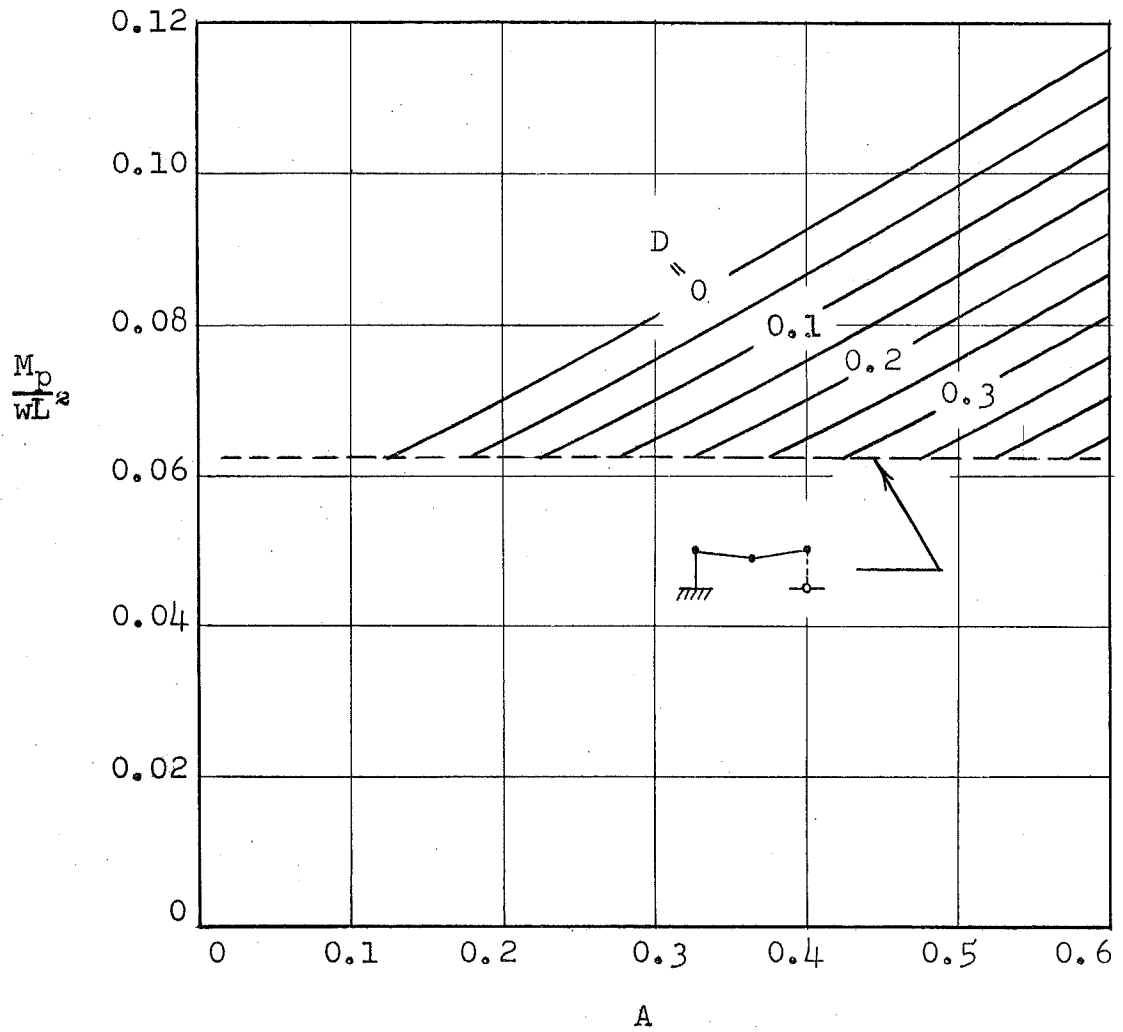
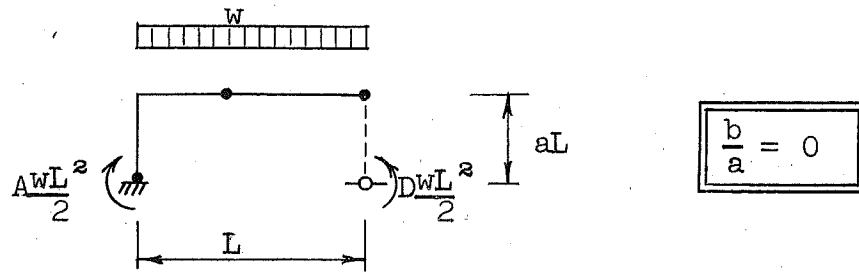


CHART IV-1

DESIGN CURVES FOR "FIXED-BASE" GABLE FRAMES
 DETERMINATION OF MEMBER SIZE

DESIGN CHART

IV-2

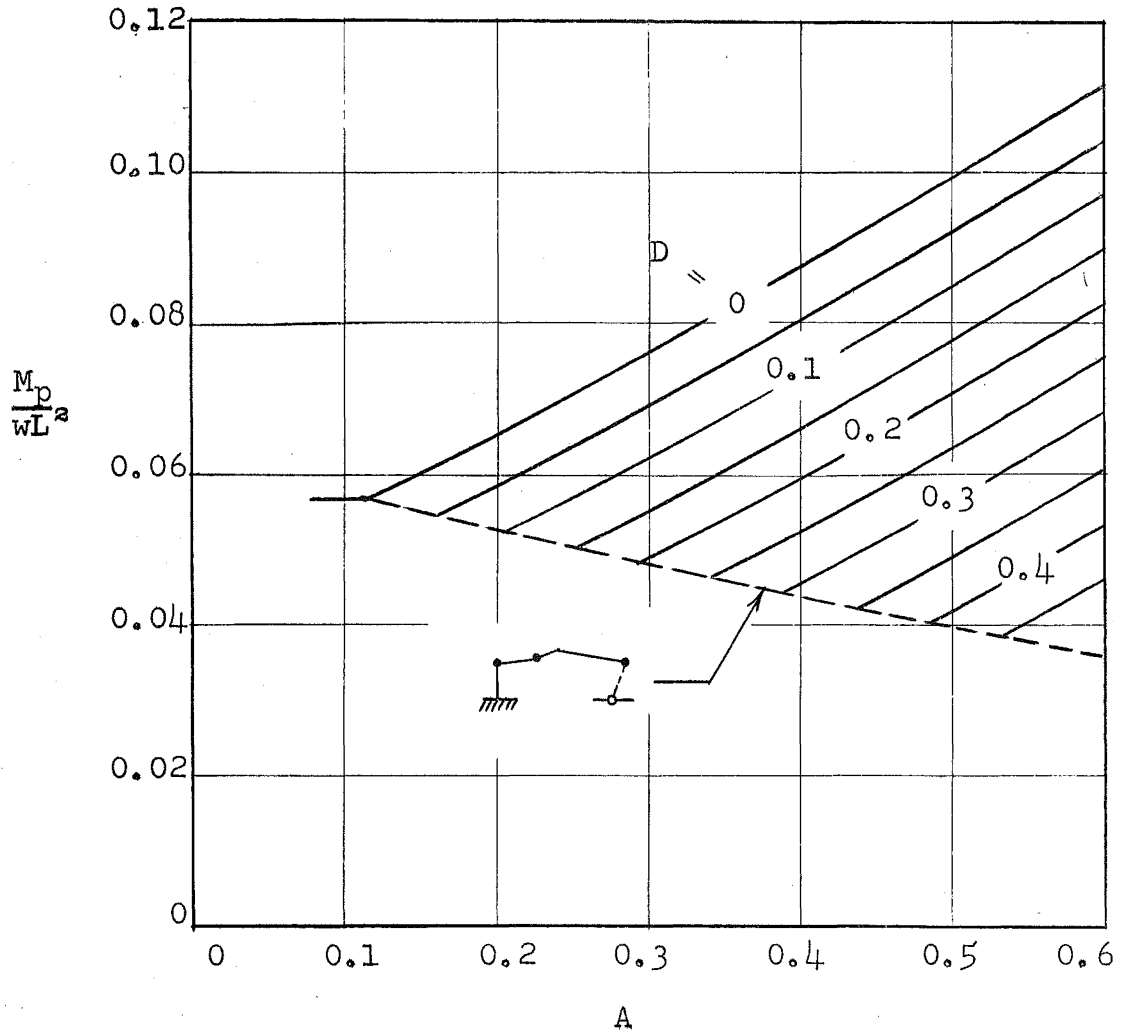
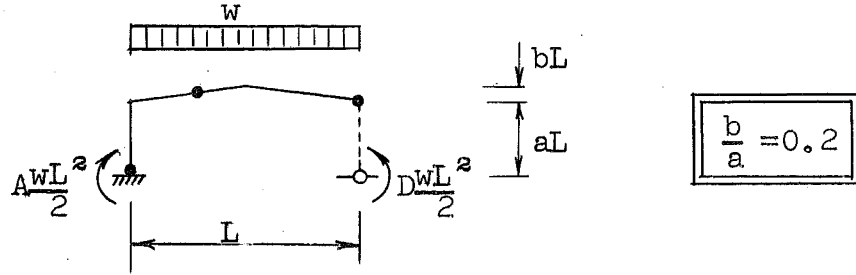


CHART IV-2

DESIGN CURVES FOR "FIXED-BASE" GABLE FRAMES
DETERMINATION OF MEMBER SIZE

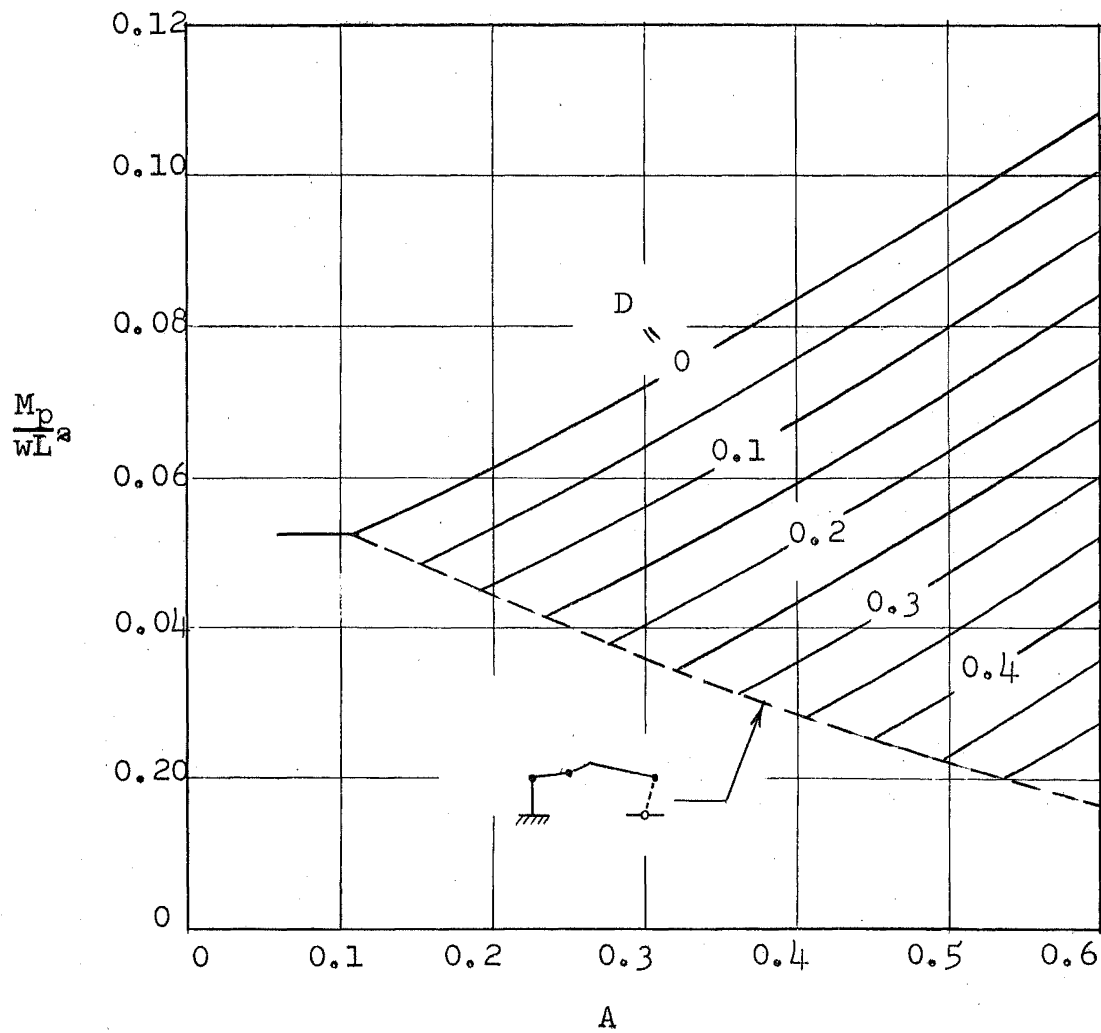
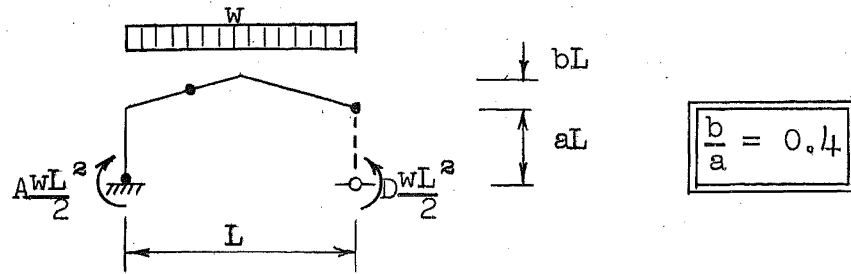


CHART IV-3

DESIGN CURVES FOR "FIXED-BASE" GABLE FRAMES
DETERMINATION OF MEMBER SIZE

DESIGN CHART

IV-4

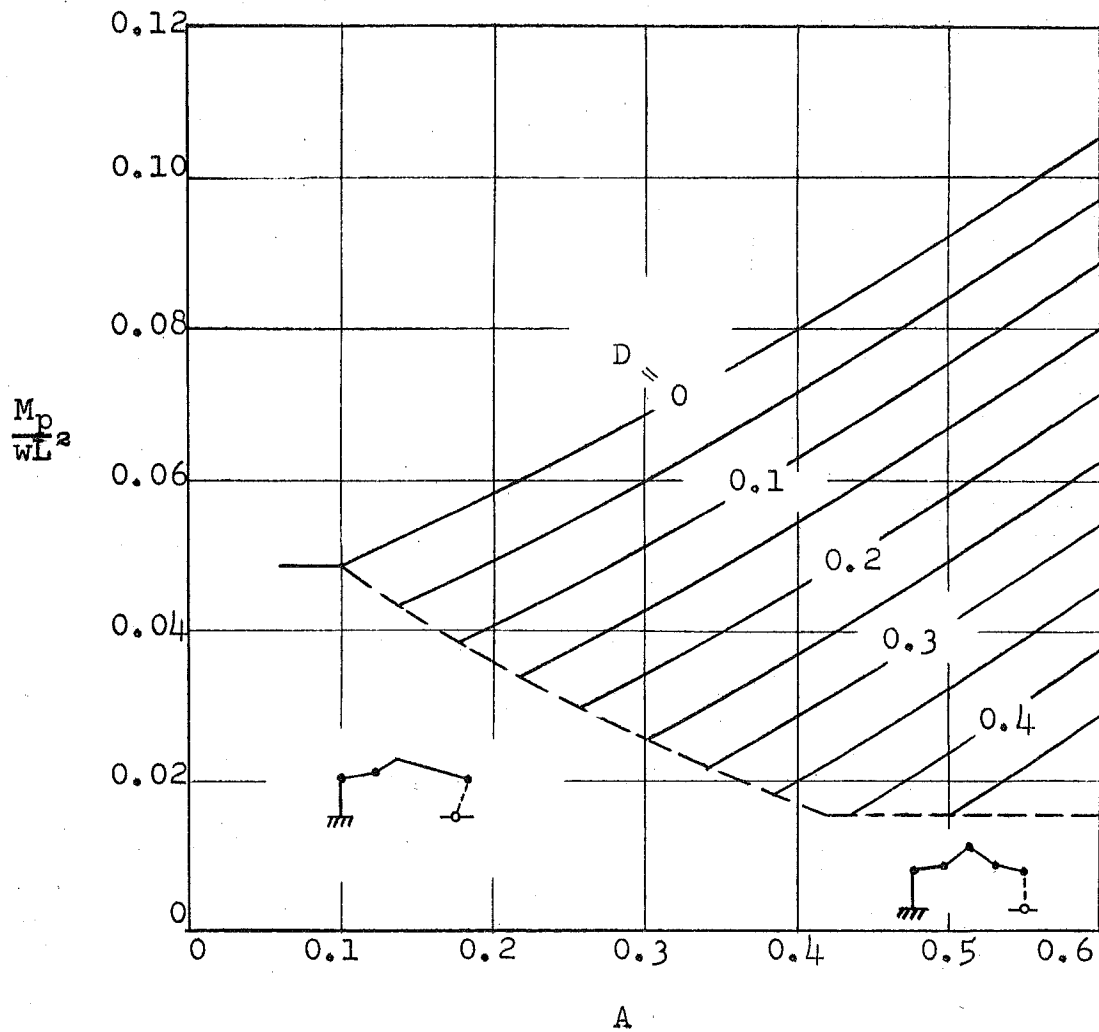
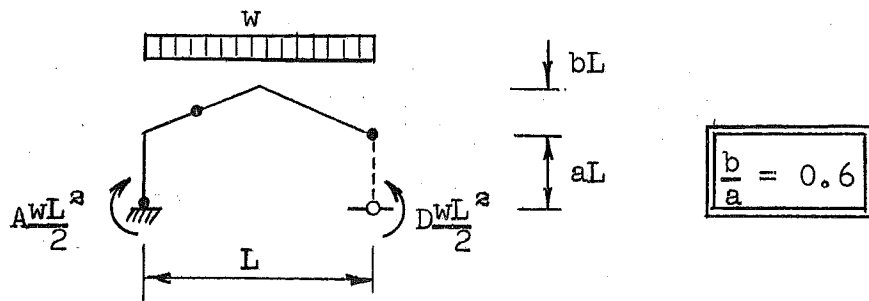


CHART IV-4

DESIGN CURVES FOR "FIXED-BASE" GABLE FRAMES
DETERMINATION OF MEMBER SIZE

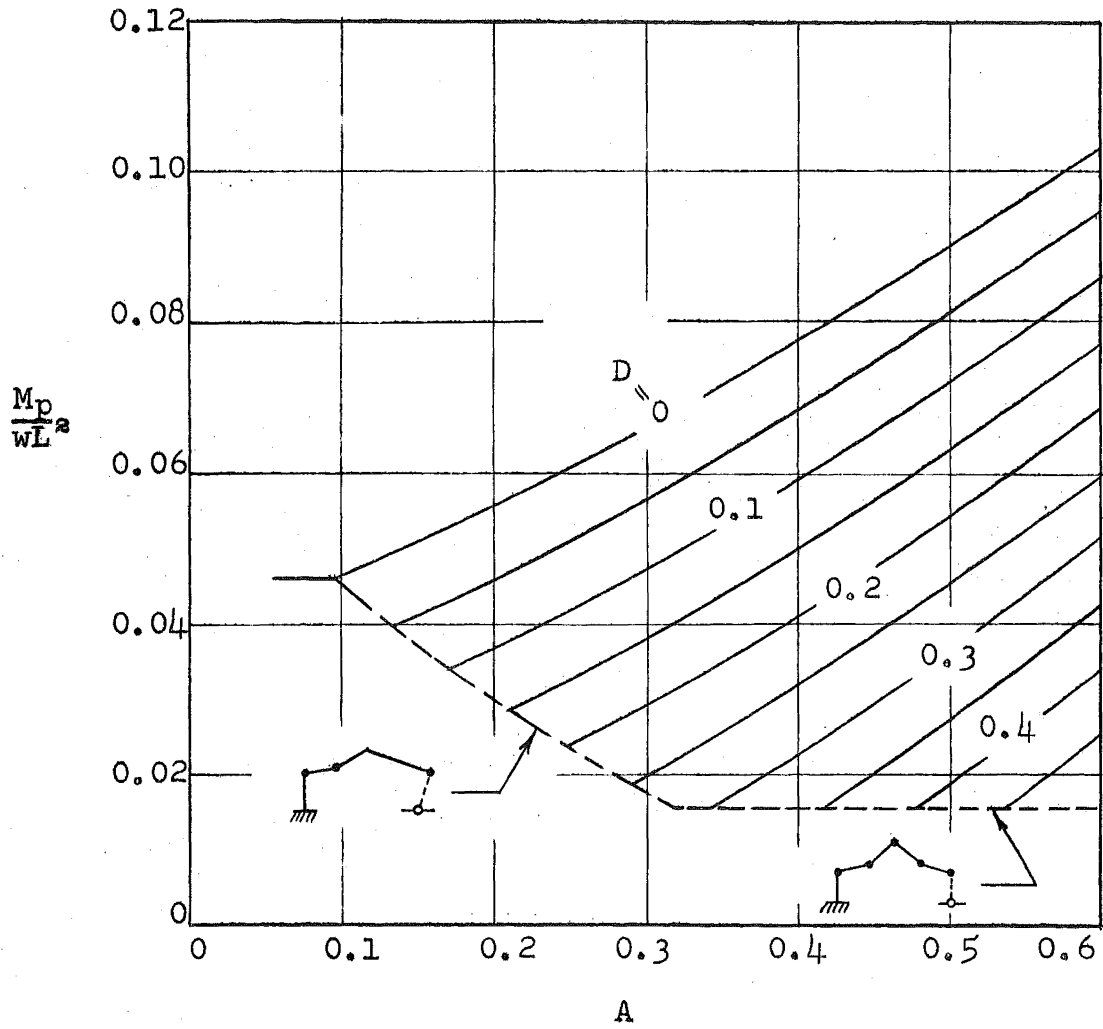
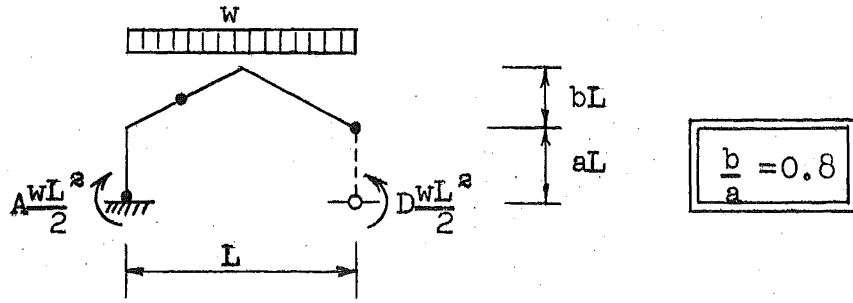


CHART IV-5

DESIGN CURVES FOR "FIXED-BASE" GABLE FRAMES
DETERMINATION OF MEMBER SIZE

DESIGN CHART

IV-6

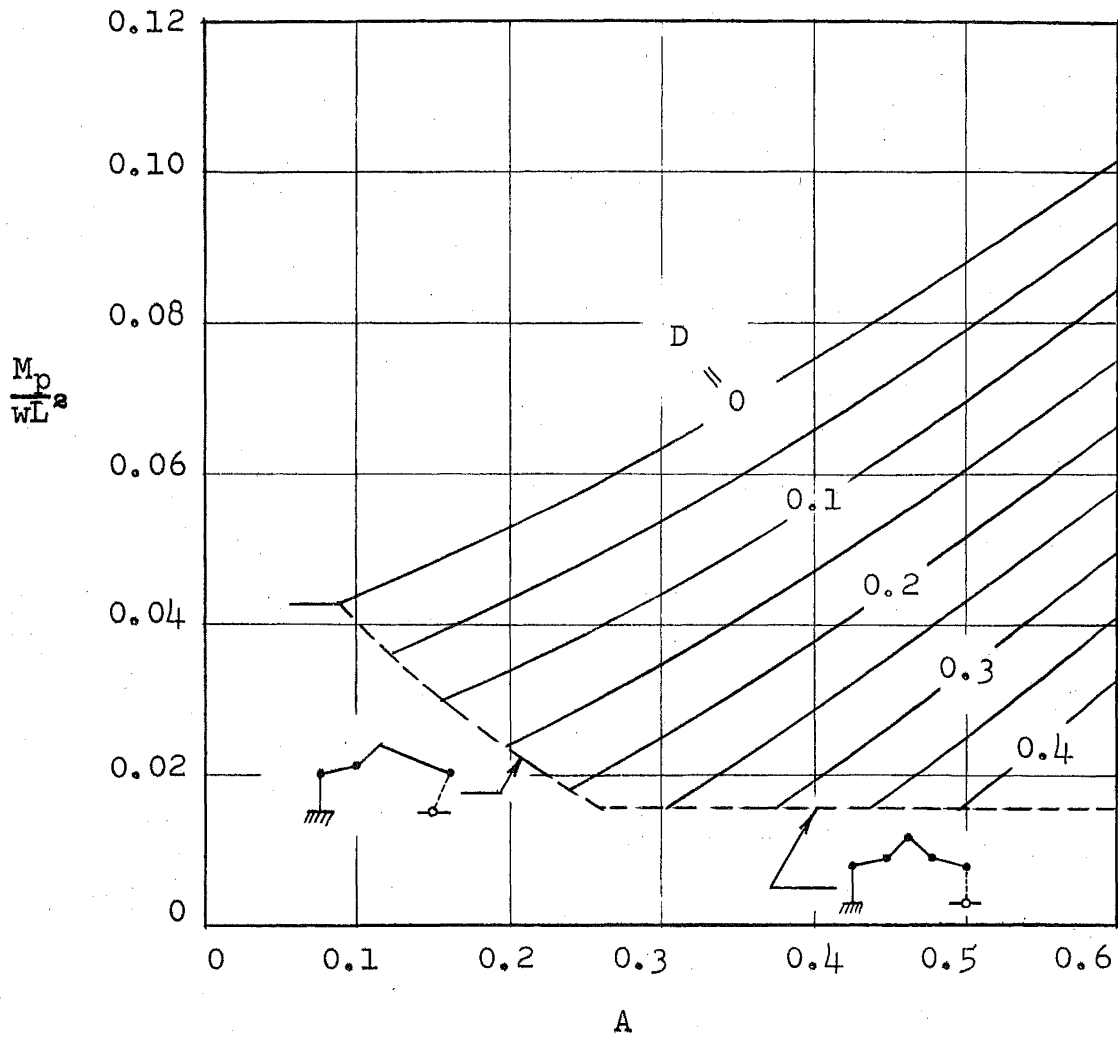
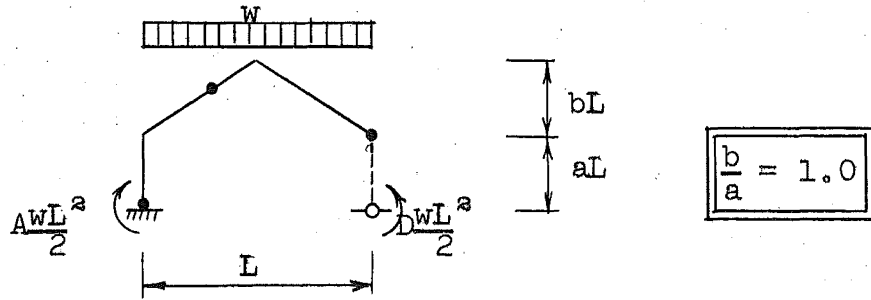


CHART IV-6

DESIGN CURVES FOR "FIXED-BASE" GABLE FRAMES
DETERMINATION OF MEMBER SIZE

DESIGN CHART

V-1

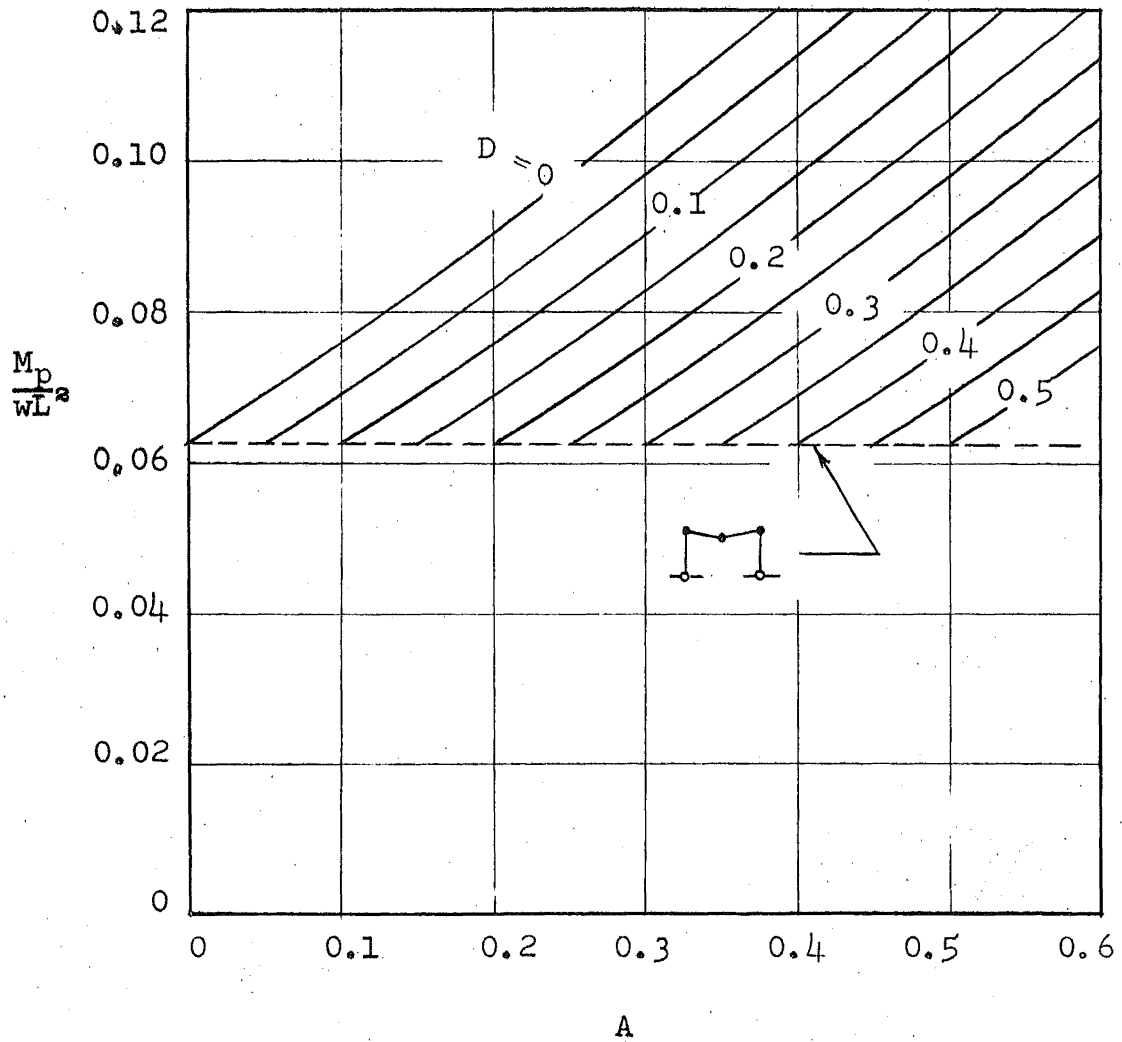
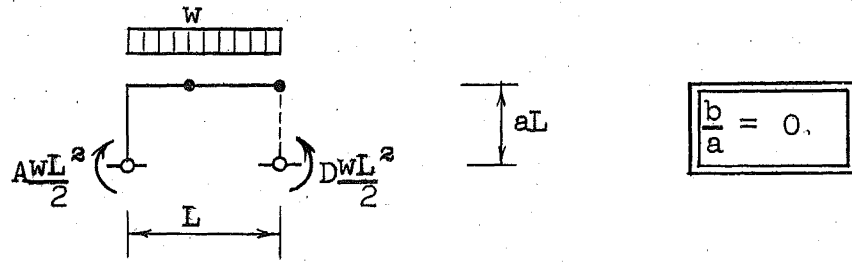


CHART V-1

DESIGN CURVES FOR "PINNED-BASE", LEAN-TO FRAMES
DETERMINATION OF MEMBER SIZE

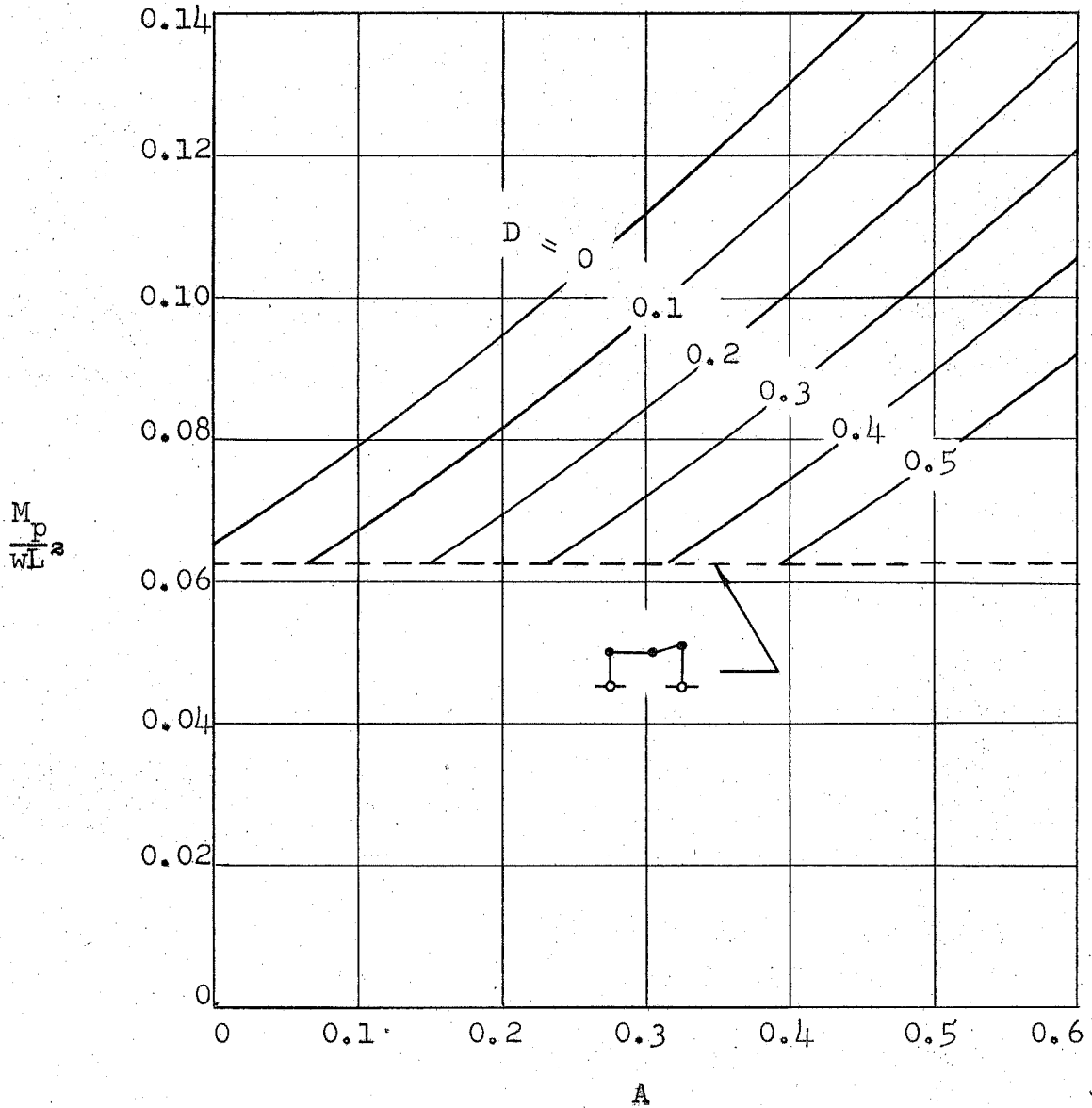
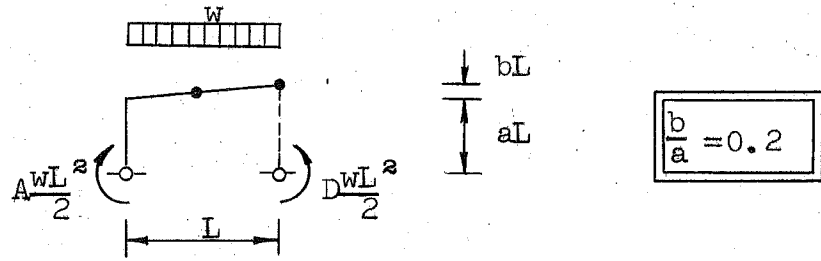


CHART V-2

DESIGN CURVES FOR "PINNED-BASE", LEAN-TO FRAMES
DETERMINATION OF MEMBER SIZE

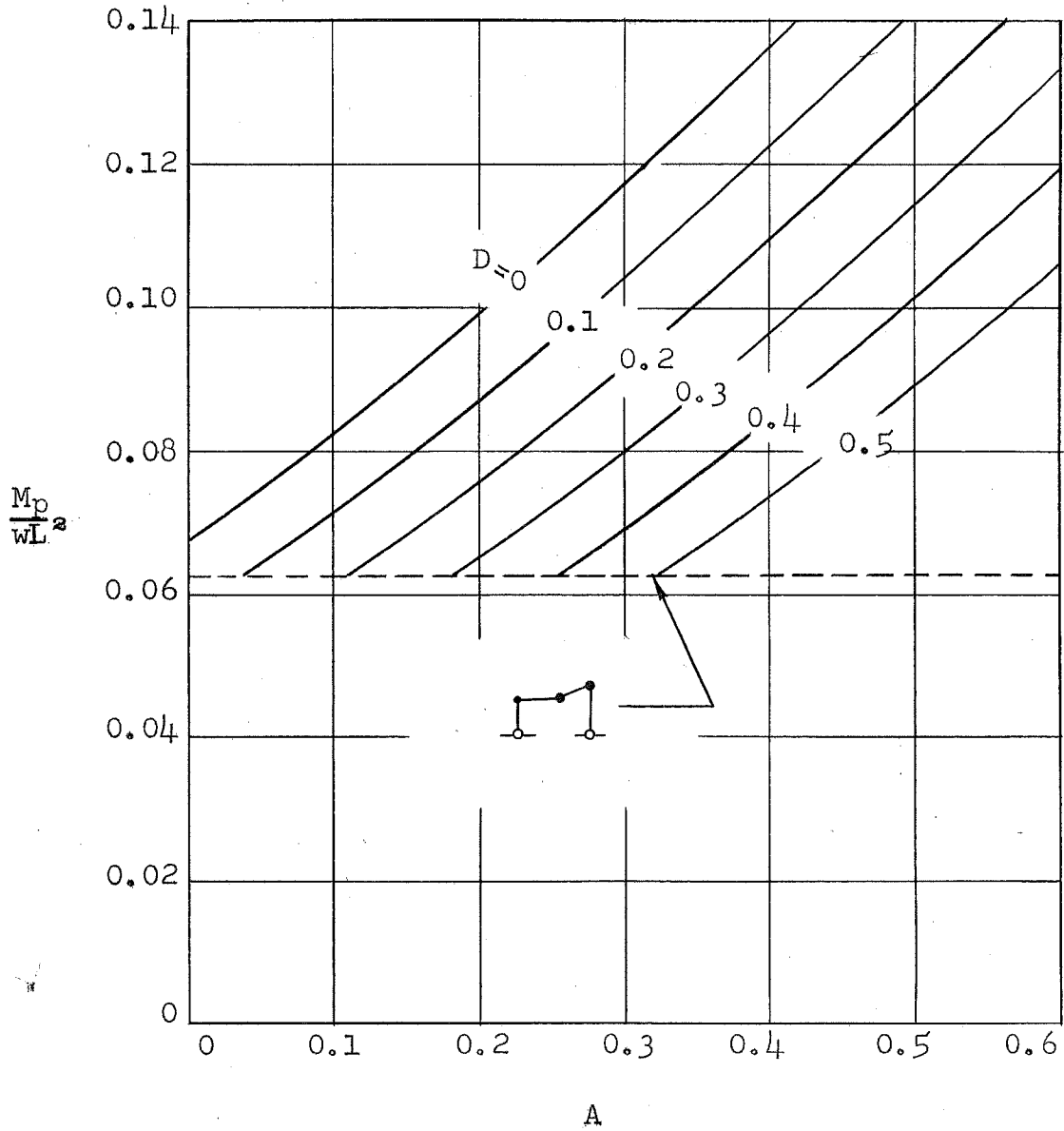
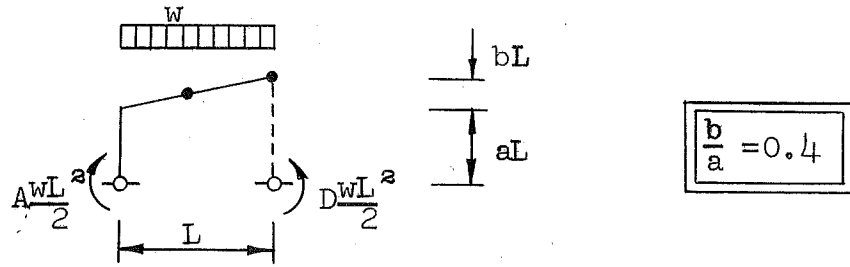


CHART V-3

DESIGN CURVES FOR "PINNED-BASE", LEAN-TO FRAMES
DETERMINATION OF MEMBER SIZE

DESIGN CHART

V-4

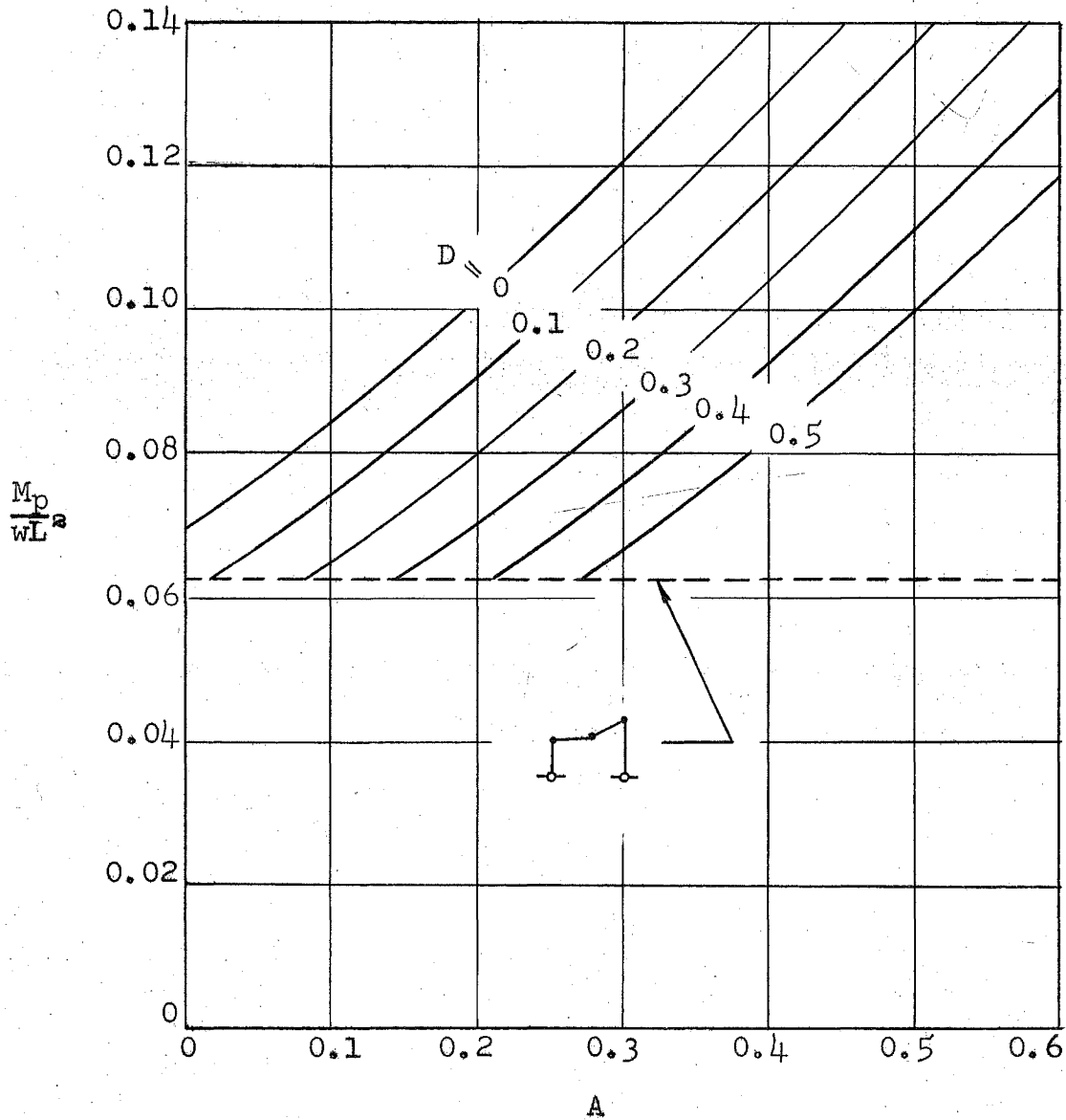
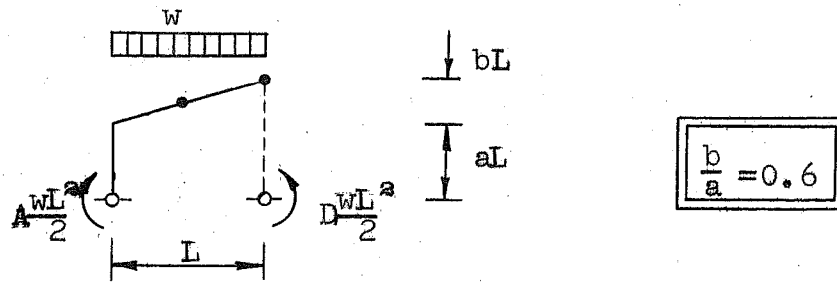


CHART V-4

DESIGN CURVES FOR "PINNED-BASE", LEAN-TO FRAMES
DETERMINATION OF MEMBER SIZE

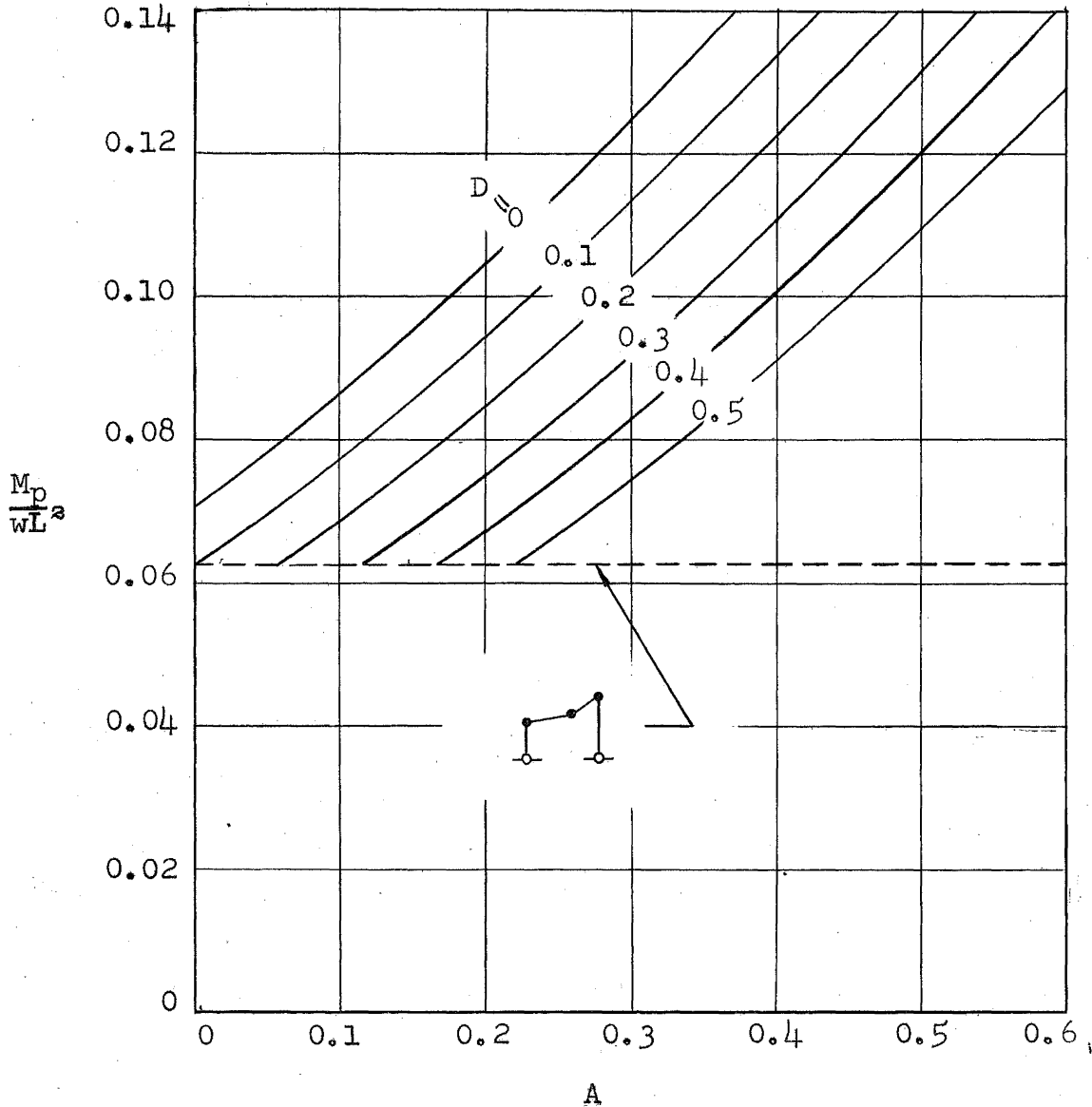
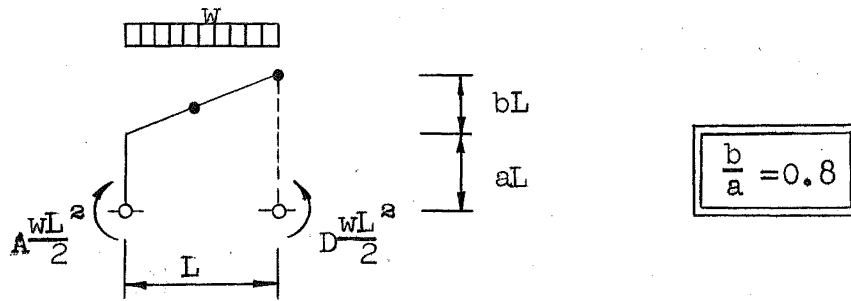


CHART V-5

DESIGN CURVES FOR "PINNED-BASE", LEAN-TO FRAMES
 DETERMINATION OF MEMBER SIZE

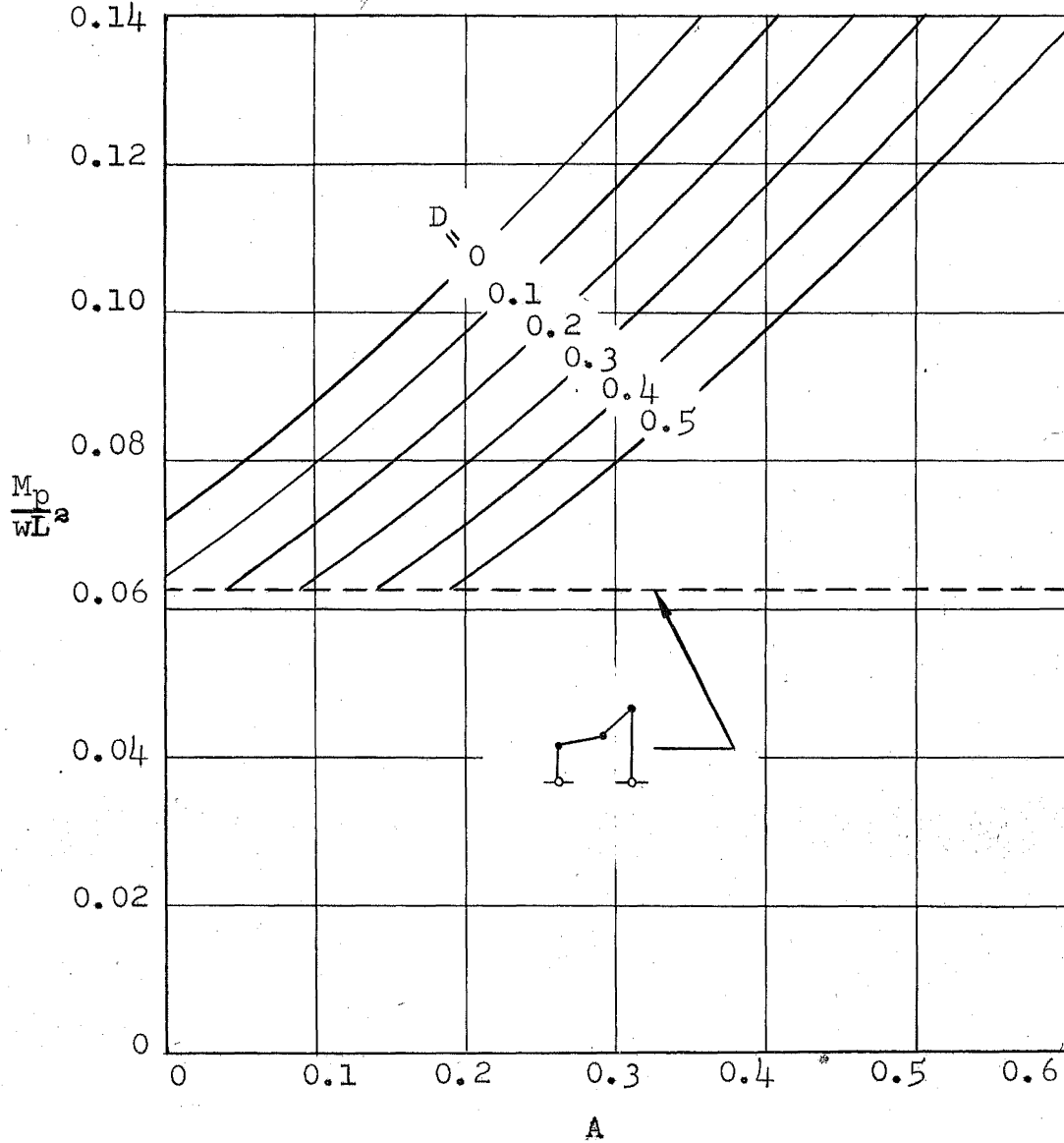
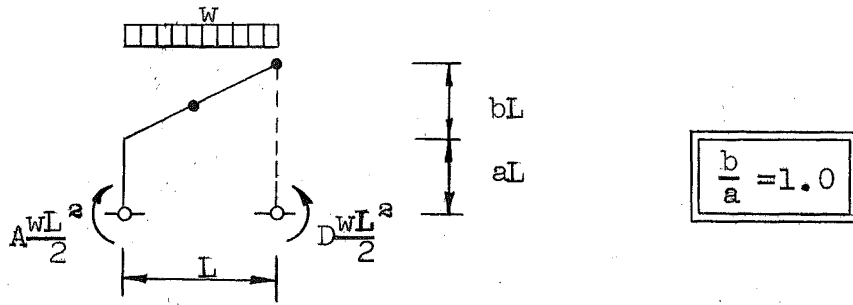


CHART V-6

DESIGN CURVES FOR "PINNED-BASE", LEAN-TO FRAMES
DETERMINATION OF MEMBER SIZE

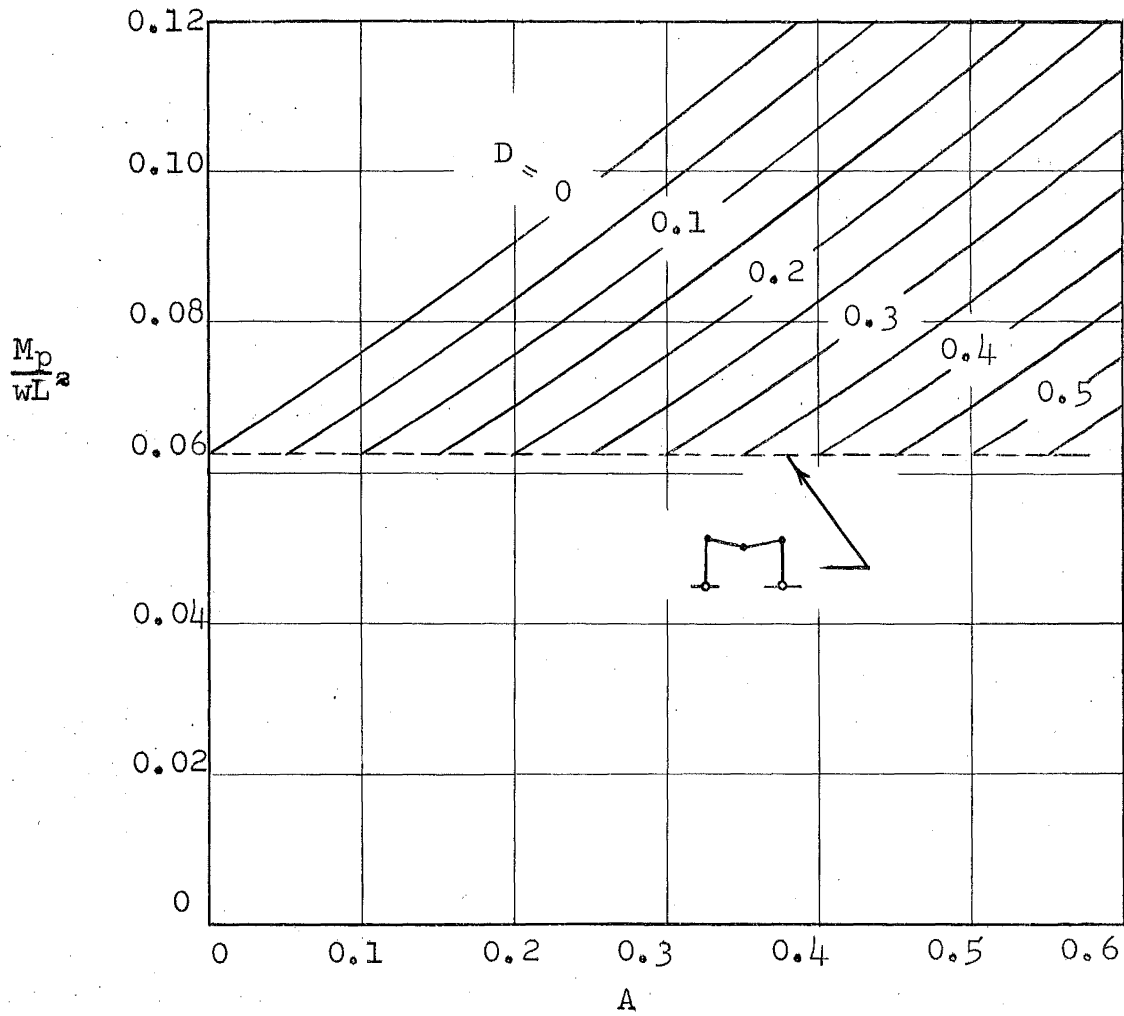
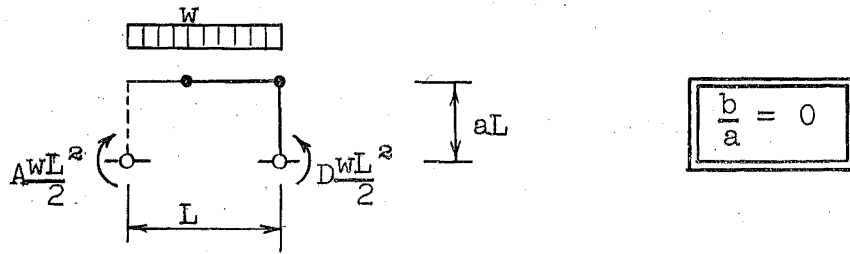
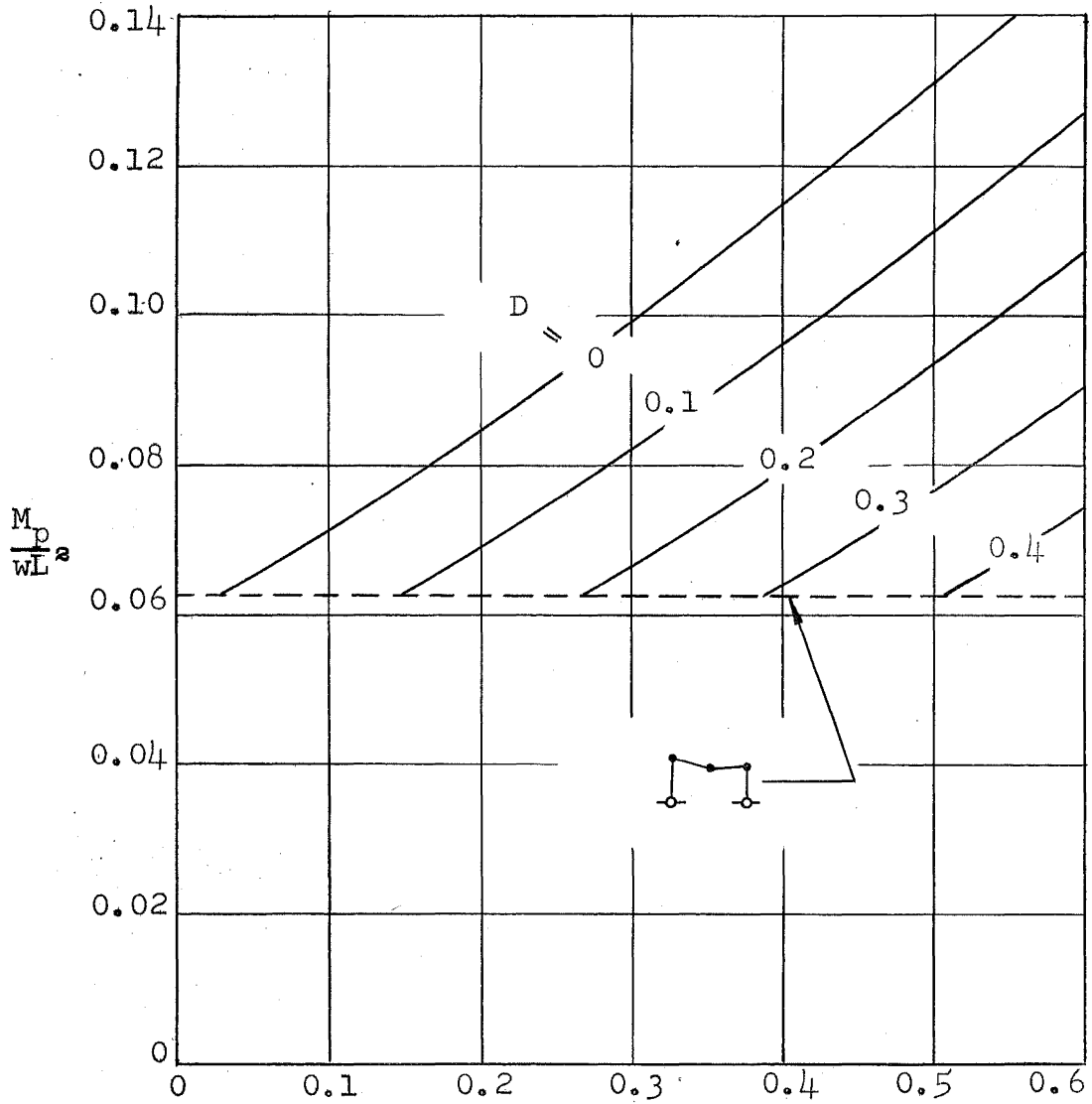
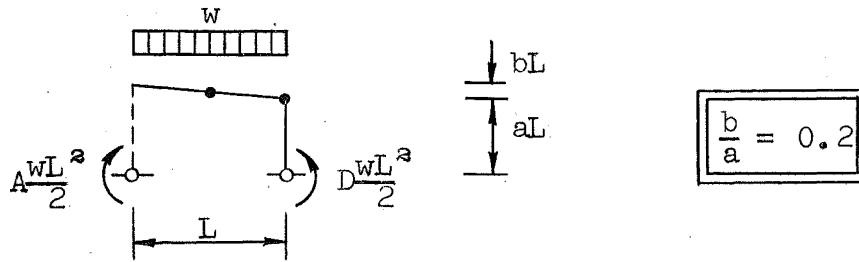


CHART VI-1

DESIGN CURVES FOR "PINNED-BASE", LEAN-TO FRAMES
 DETERMINATION OF MEMBER SIZE



A

CHART VI-2

DESIGN CURVES FOR "PINNED-BASE", LEAN-TO FRAMES
DETERMINATION OF MEMBER SIZE

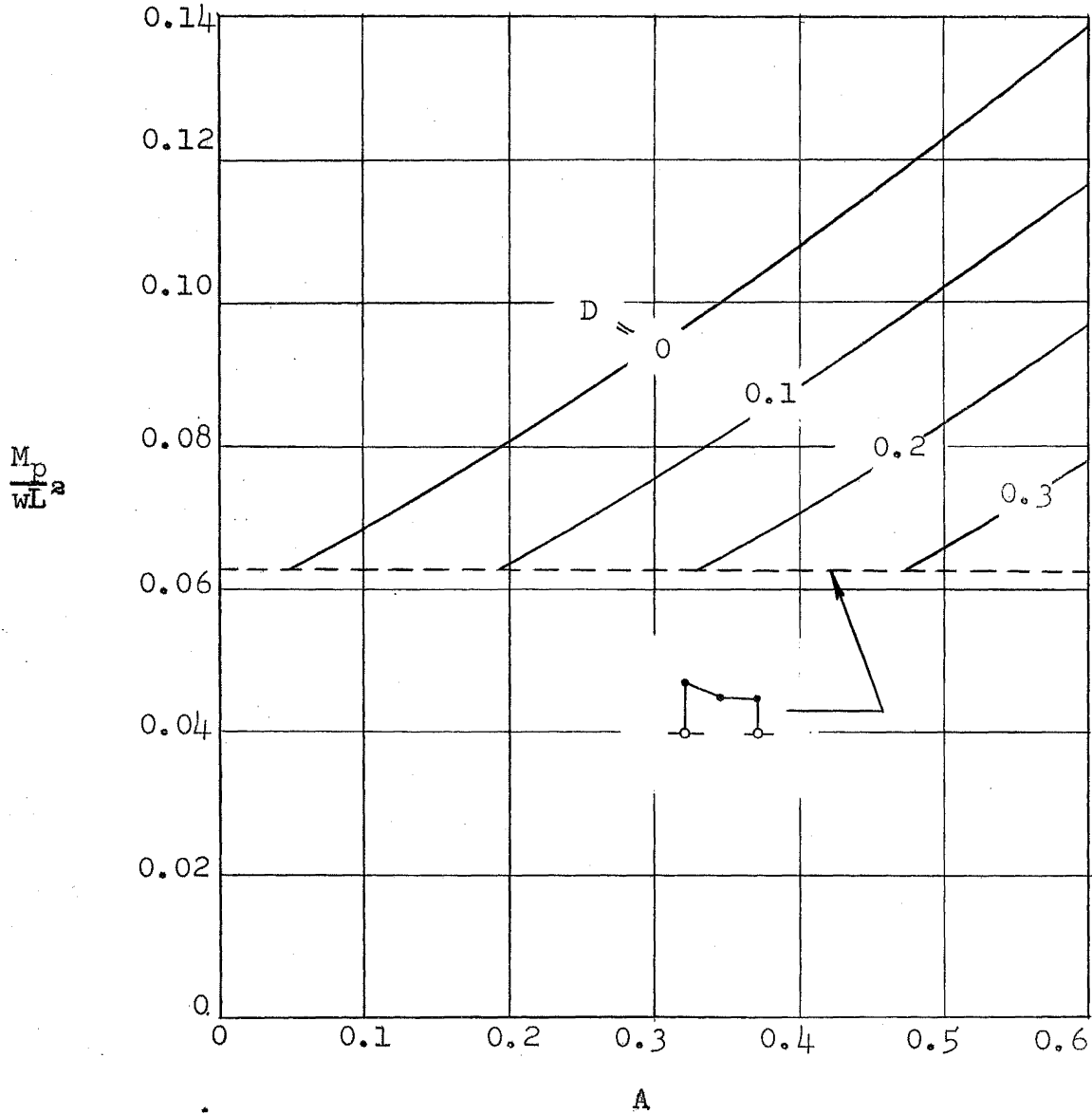
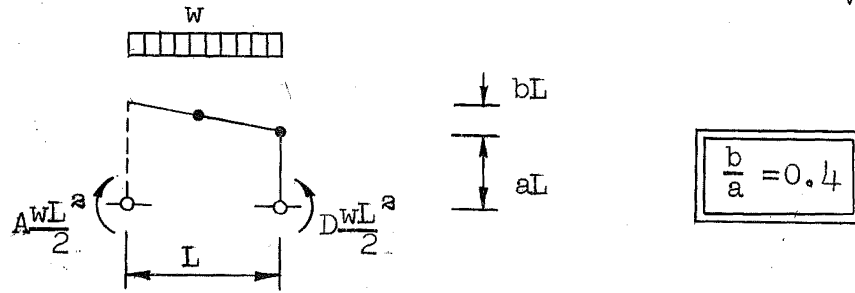


CHART VI-3

DESIGN CURVES FOR "PINNED-BASE", LEAN-TO FRAMES
DETERMINATION OF MEMBER SIZE

DESIGN CHART

VI-4

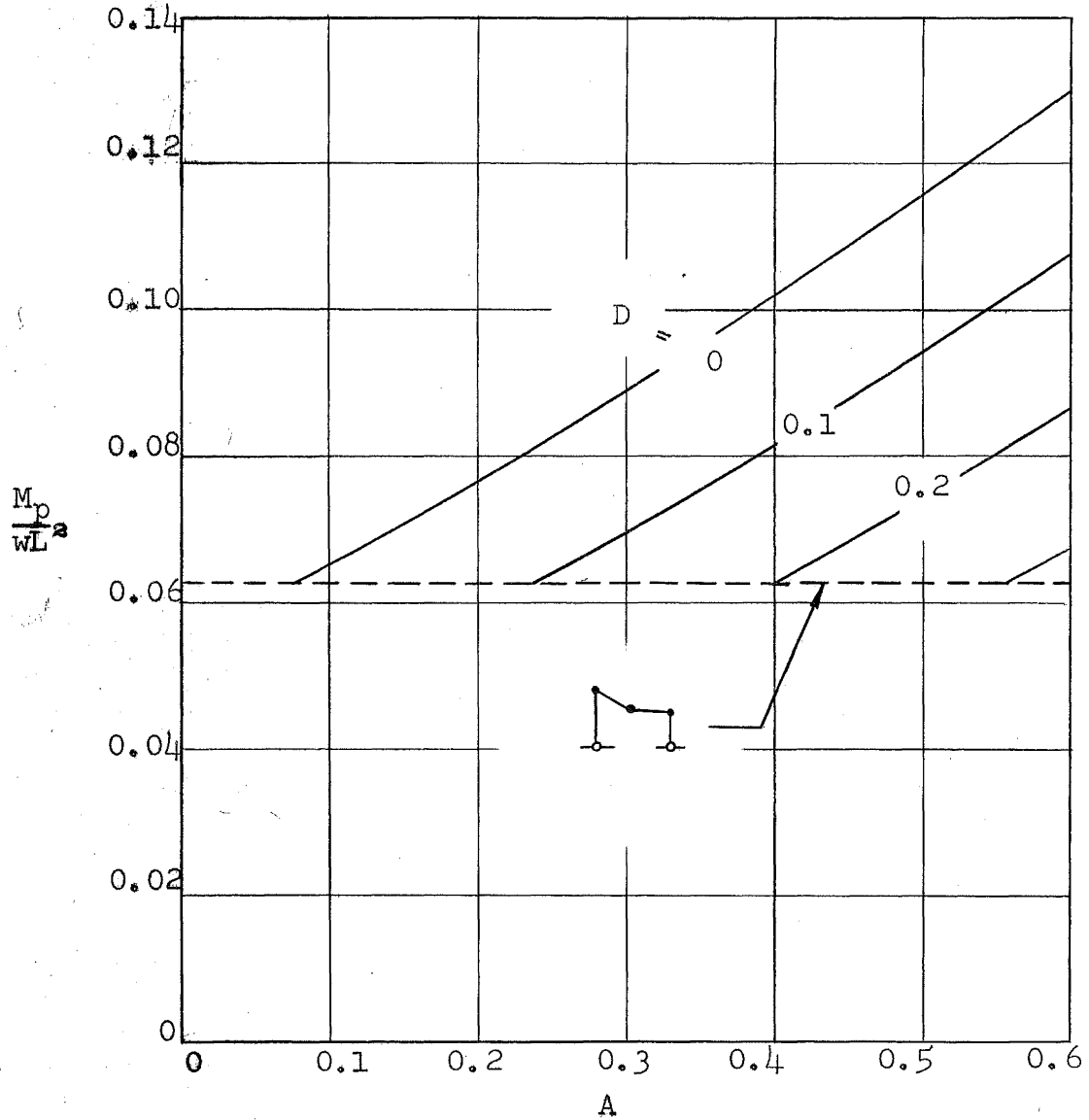
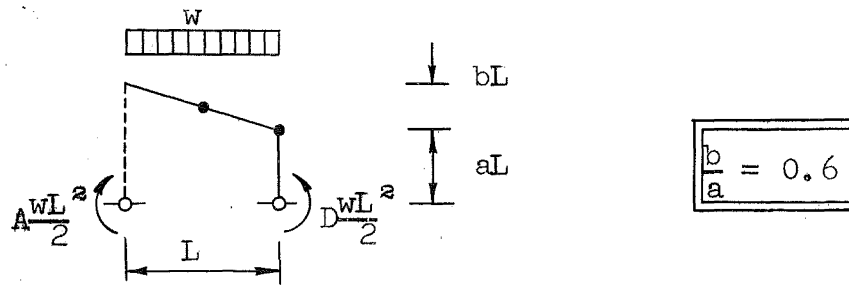


CHART VI-4

DESIGN CURVES FOR "PINNED-BASE", LEAN-TO FRAMES
DETERMINATION OF MEMBER SIZE

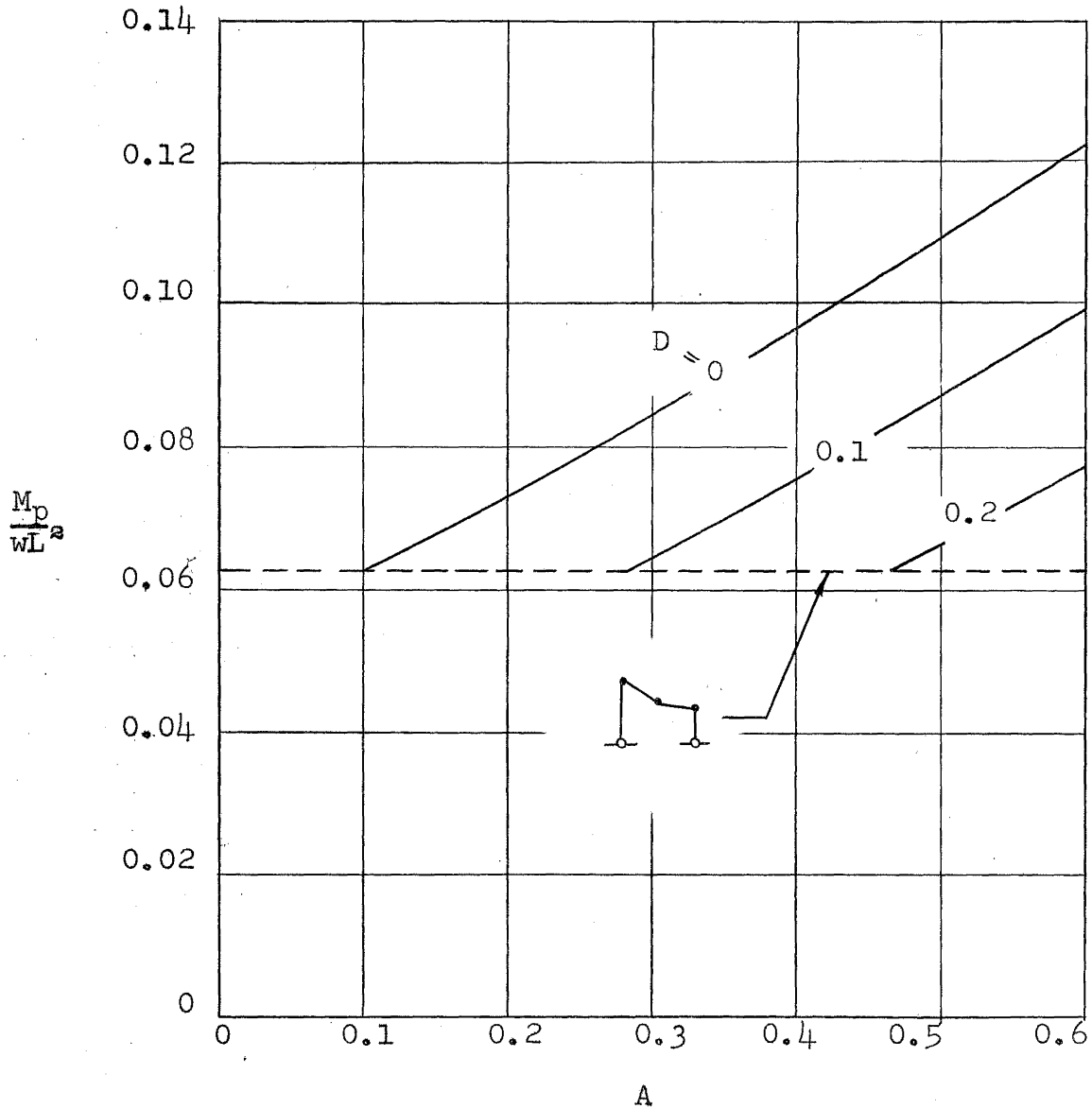
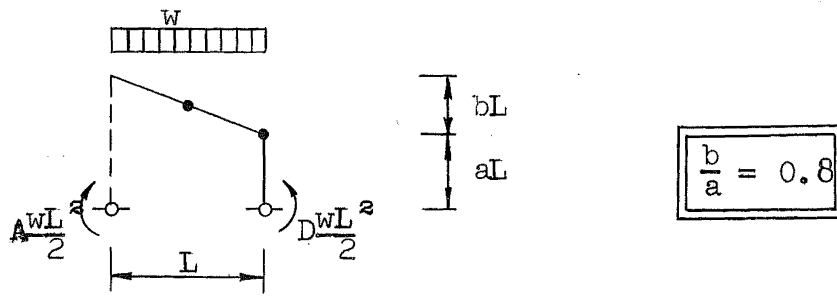


CHART VI-5

DESIGN CURVES FOR "PINNED-BASE", LEAN-TO FRAMES
 DETERMINATION OF MEMBER SIZE

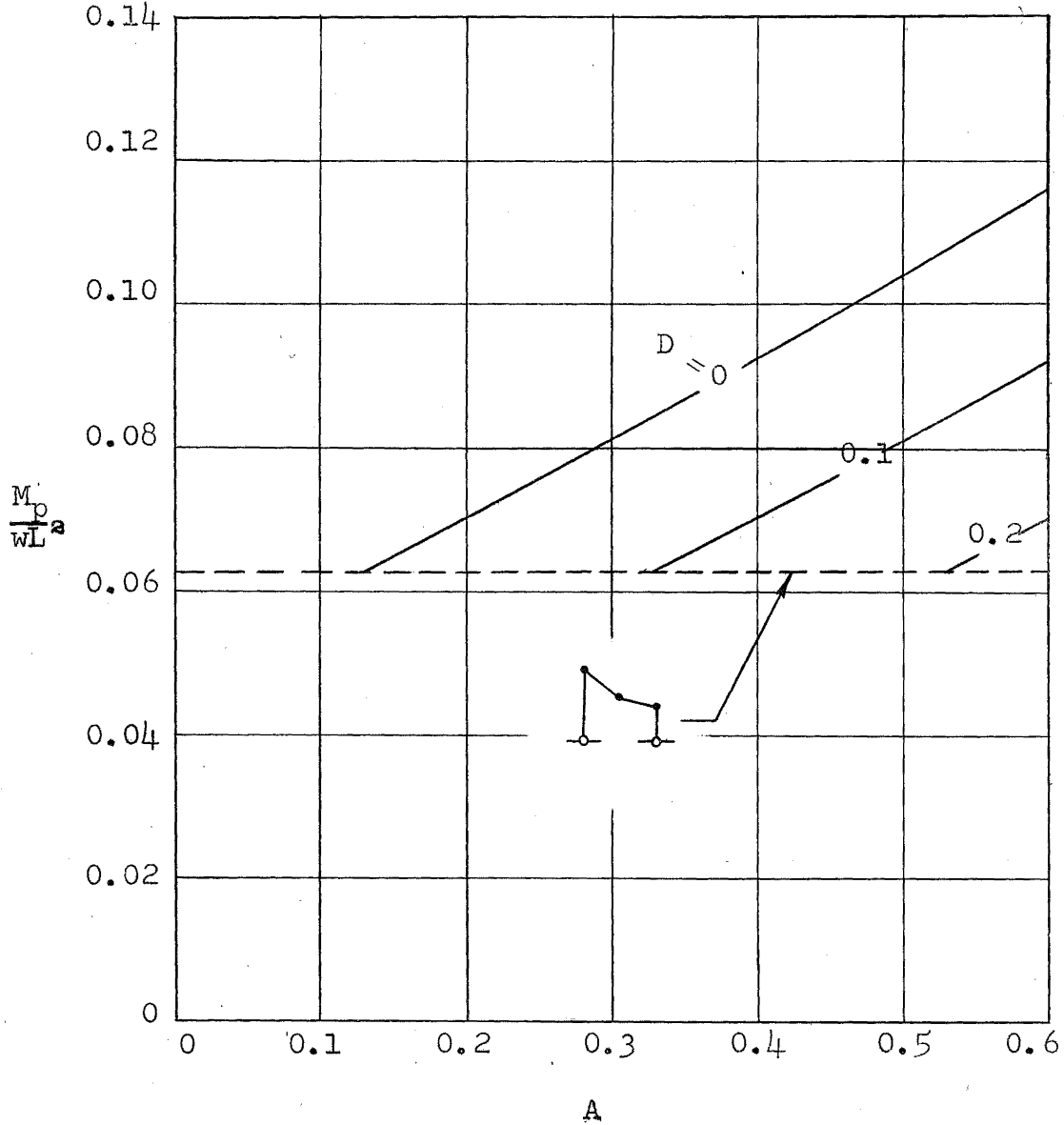
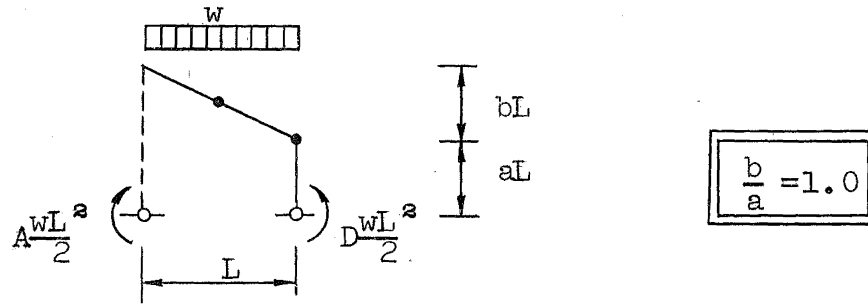


CHART VI-6

DESIGN CURVES FOR "PINNED-BASE", LEAN-TO FRAMES
DETERMINATION OF MEMBER SIZE

DESIGN CHART

I-1a

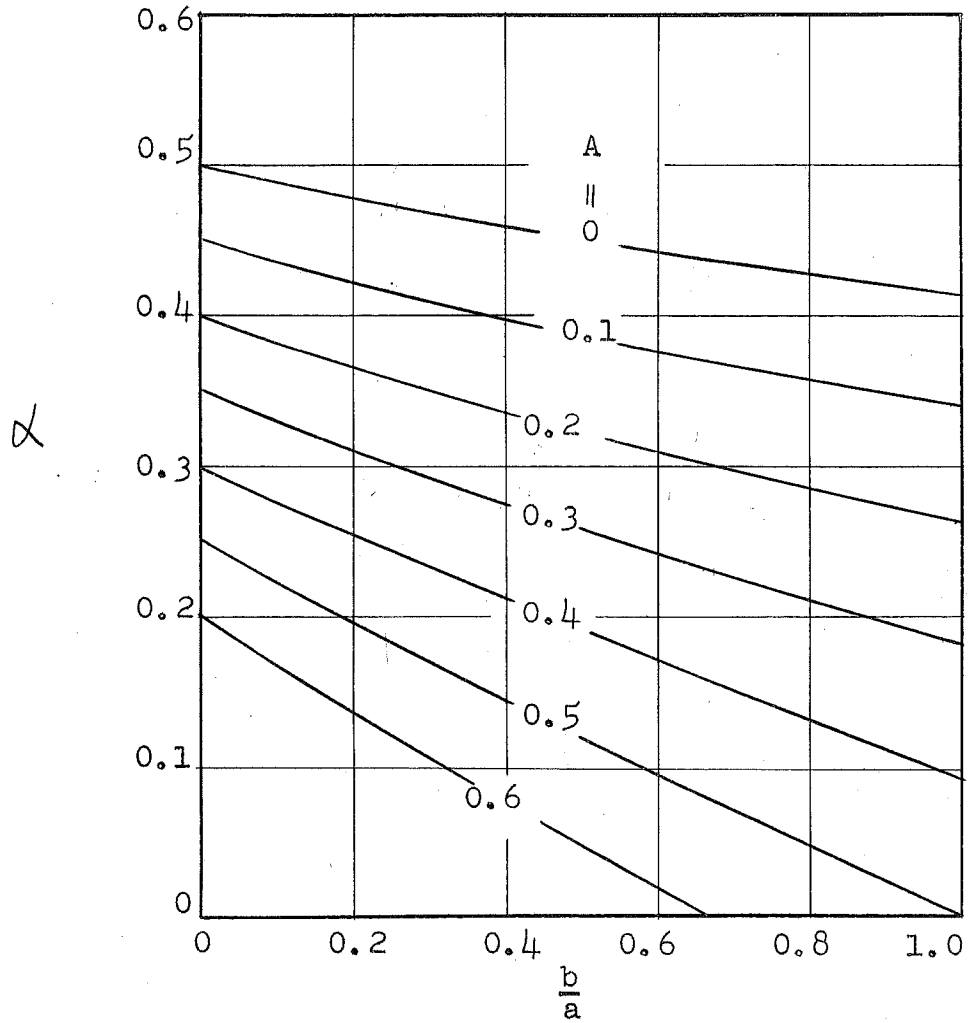
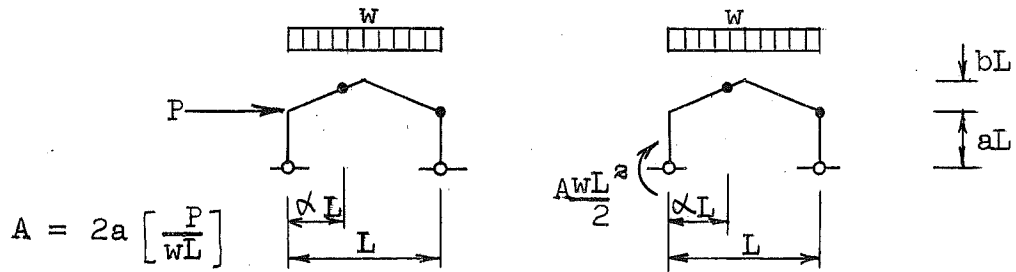


CHART I-1a

DESIGN CURVES FOR "PINNED-BASE" GABLE FRAMES
LOCATION OF PLASTIC HINGE

DESIGN CHART

I-2a

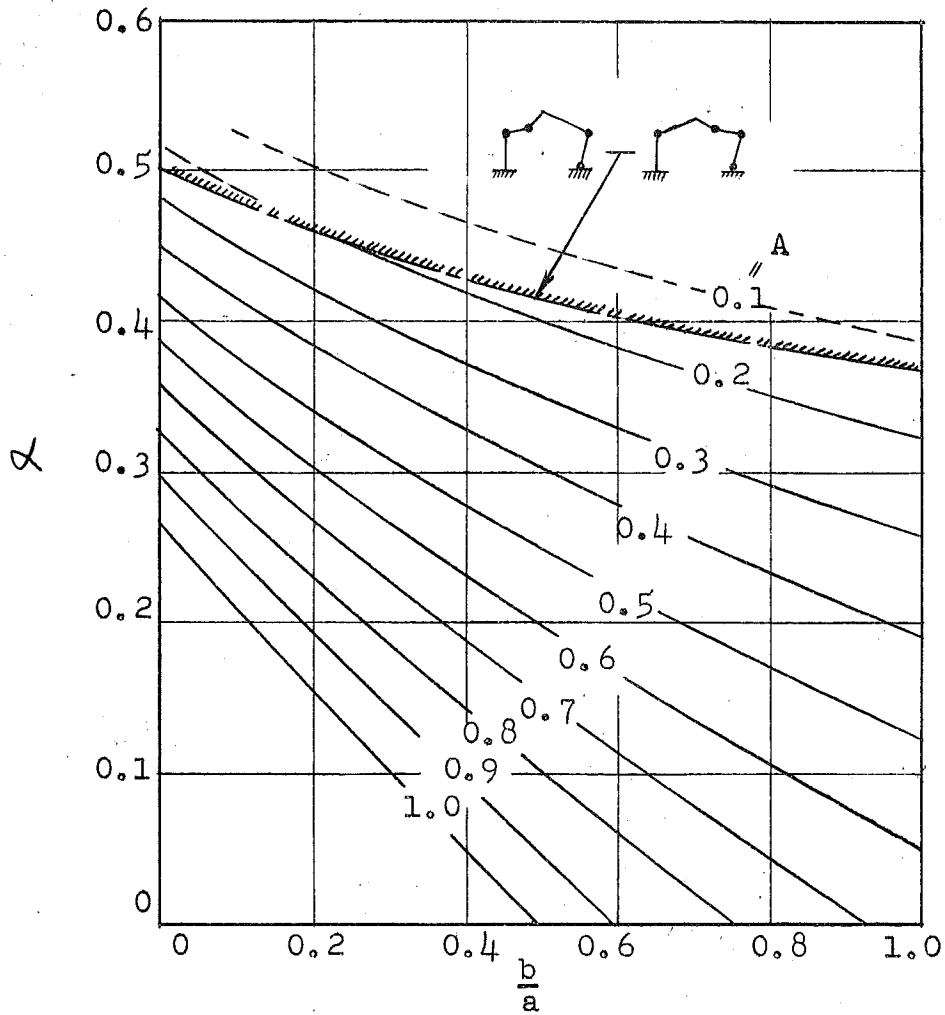
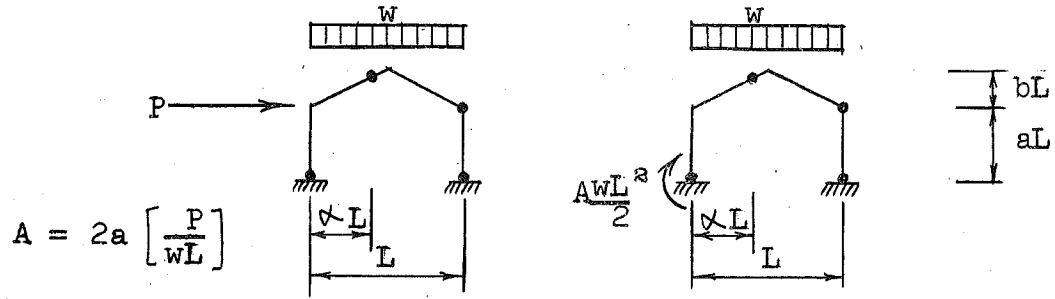
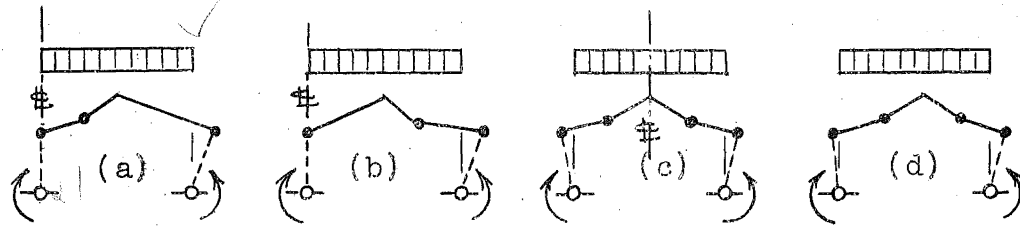


CHART I-2a

DESIGN CURVES FOR "FIXED-BASE" GABLE FRAME
LOCATION OF PLASTIC HINGE

DESIGN CHART

II-1a



POSSIBLE FAILURE MODES

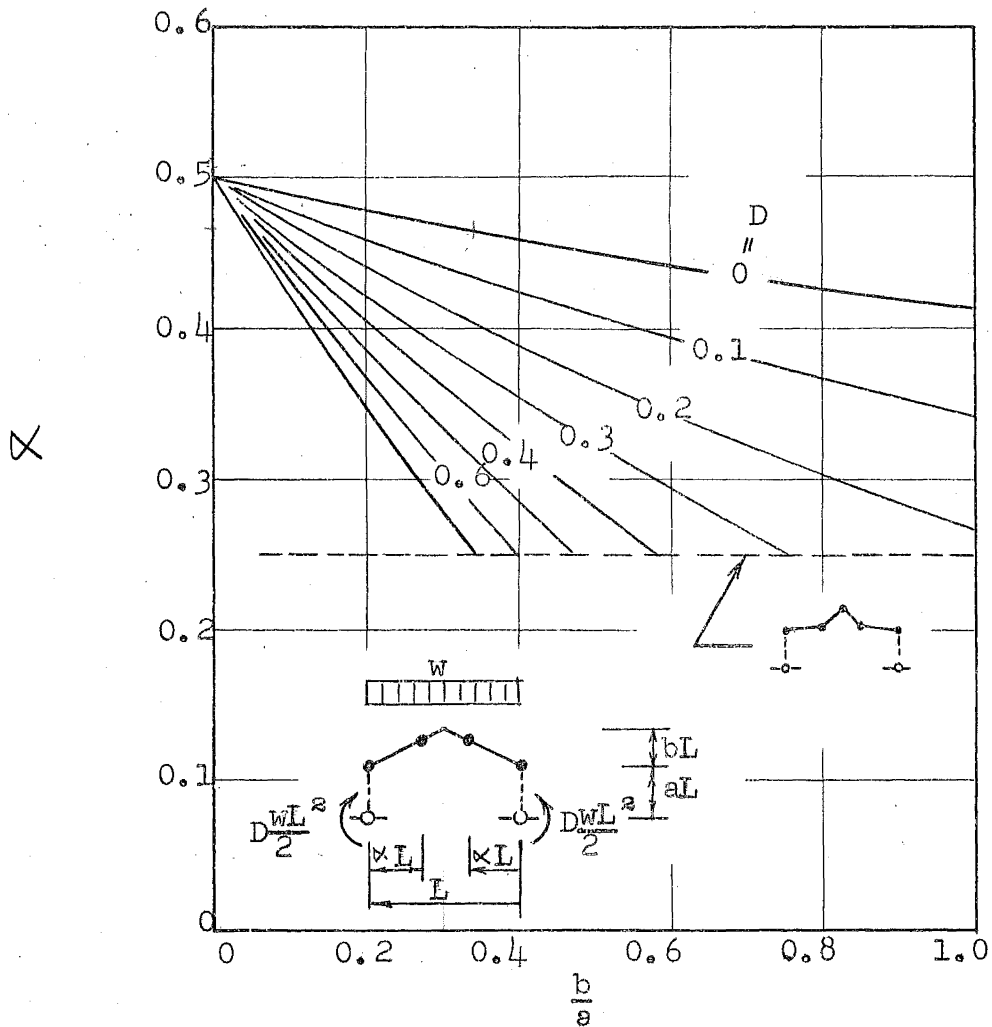


CHART II-1a

DESIGN CURVES FOR GABLE FRAMES
LOCATION OF PLASTIC HINGE

DESIGN CHART

III-1a

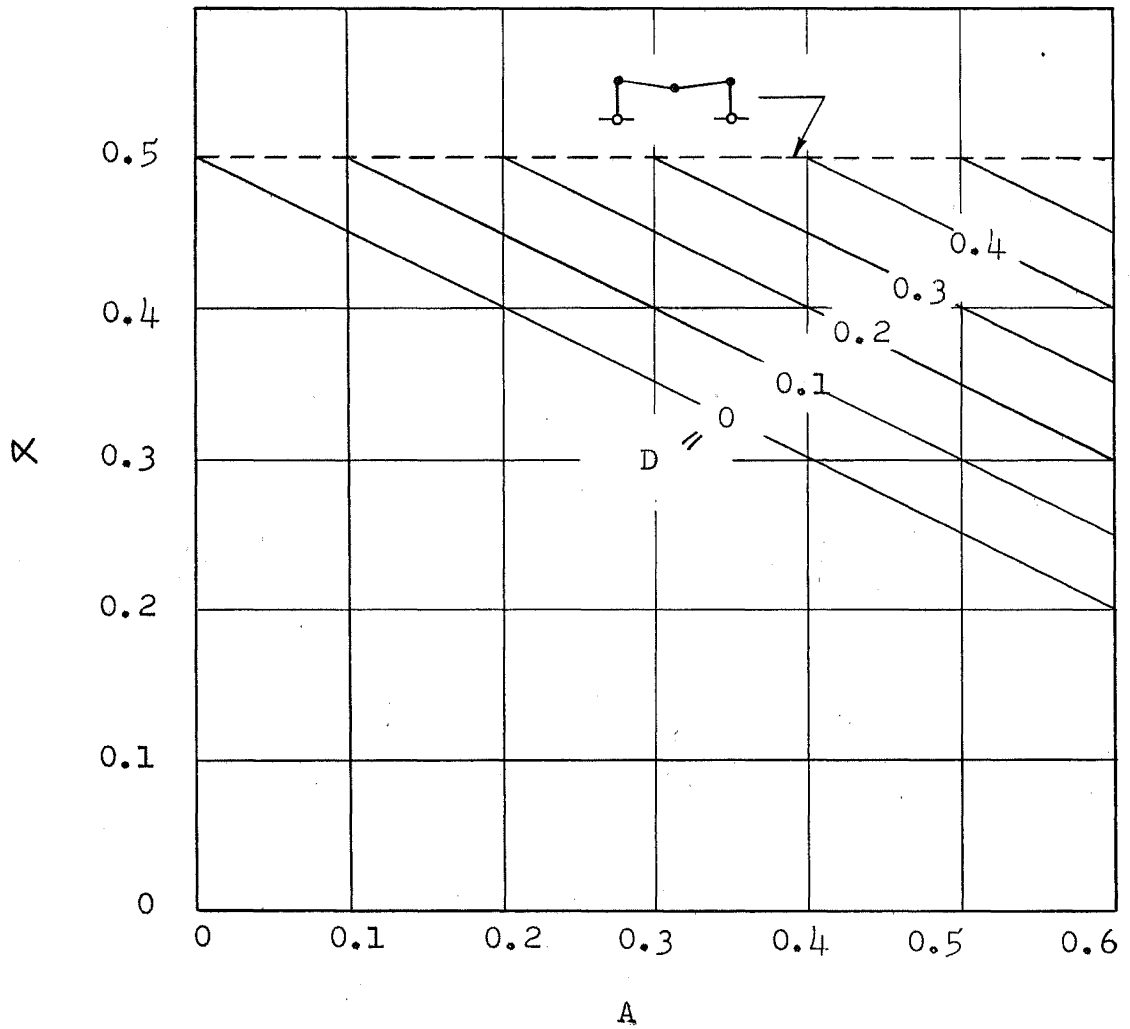
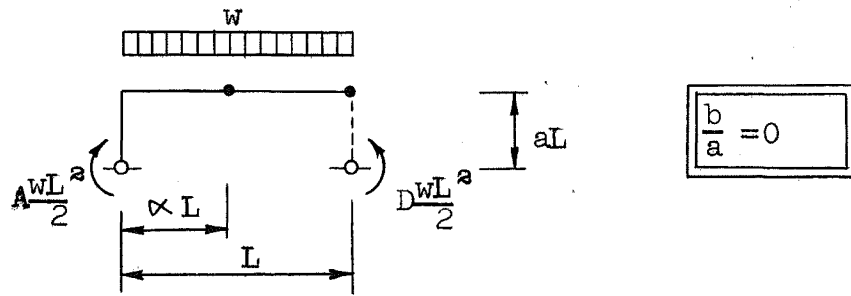


CHART III-1a

DESIGN CURVES FOR "PINNED-BASE", GABLE FRAMES
LOCATION OF PLASTIC HINGE

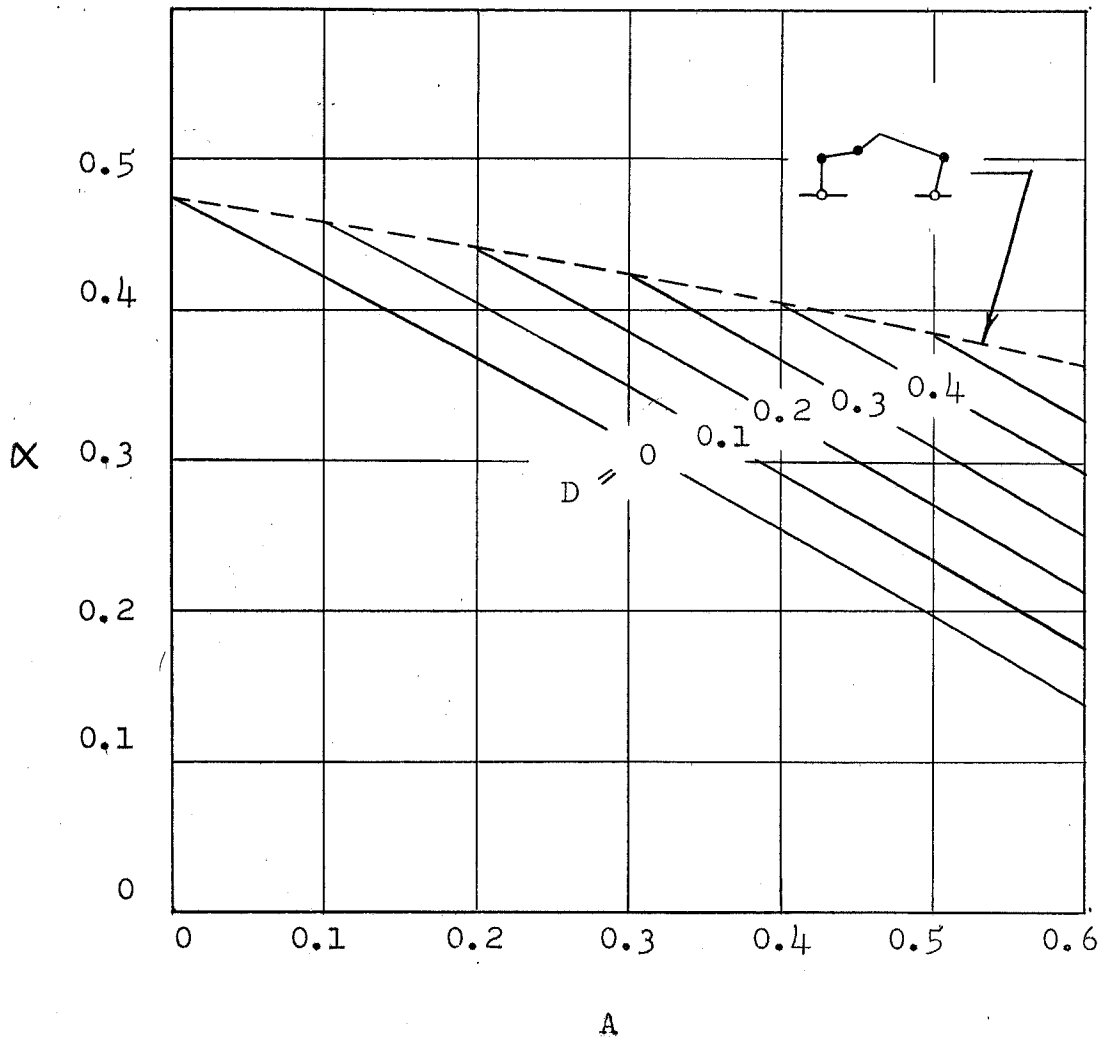
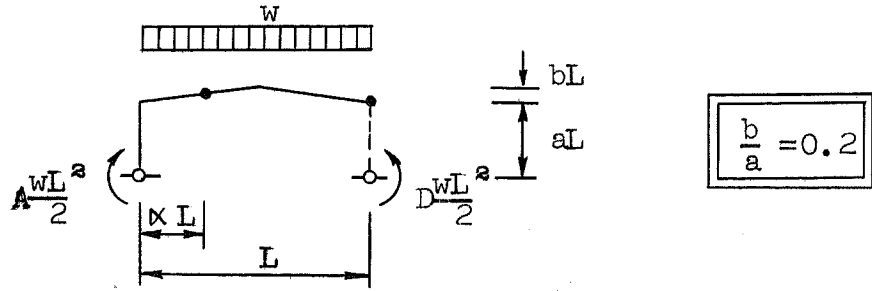


CHART III-2a

DESIGN CURVES FOR "PINNED-BASE" GABLE FRAMES
LOCATION OF PLASTIC HINGE

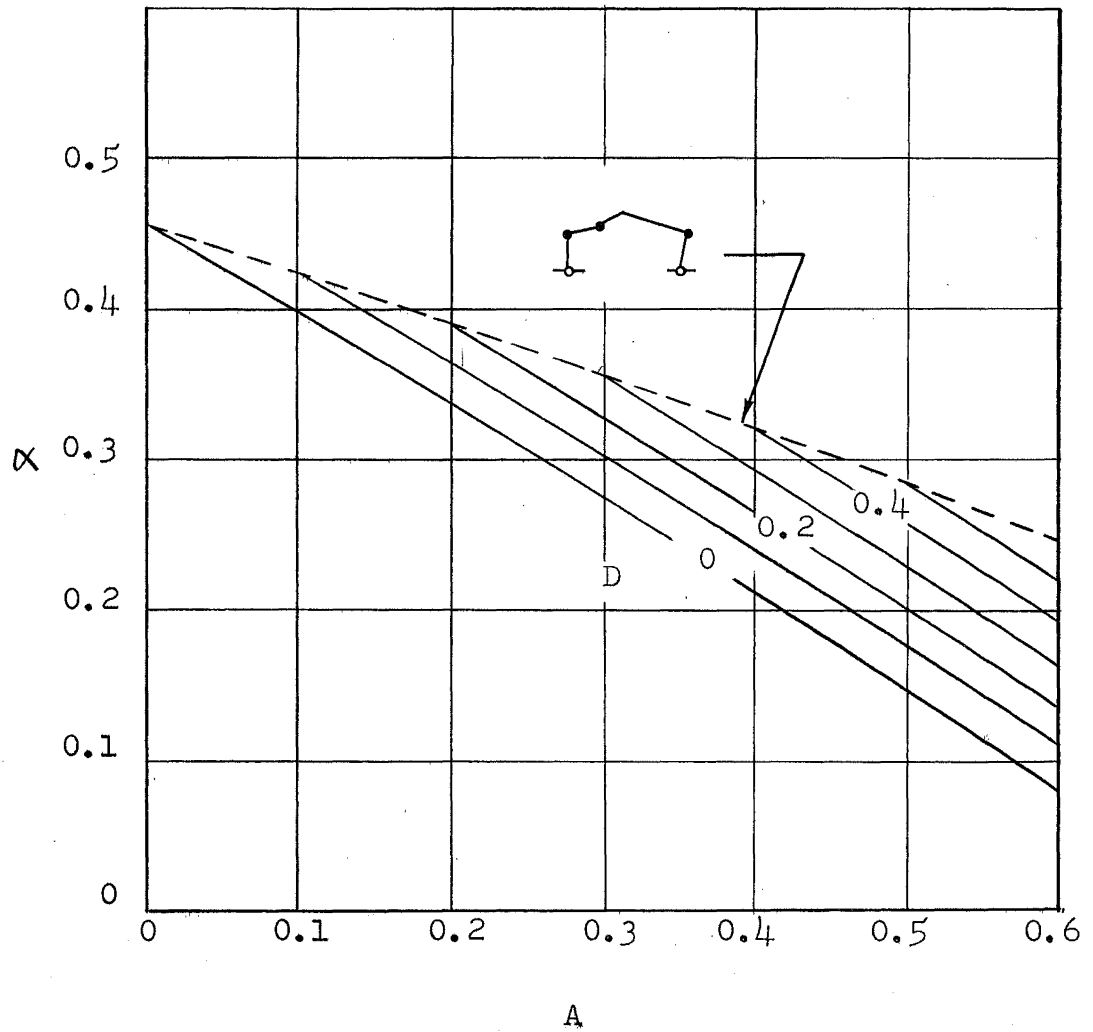
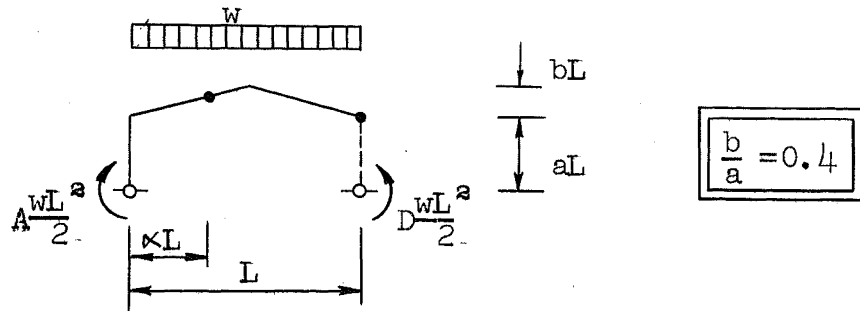


CHART III-3a

DESIGN CURVES FOR "PINNED-BASE" GABLE FRAMES
LOCATION OF PLASTIC HINGE

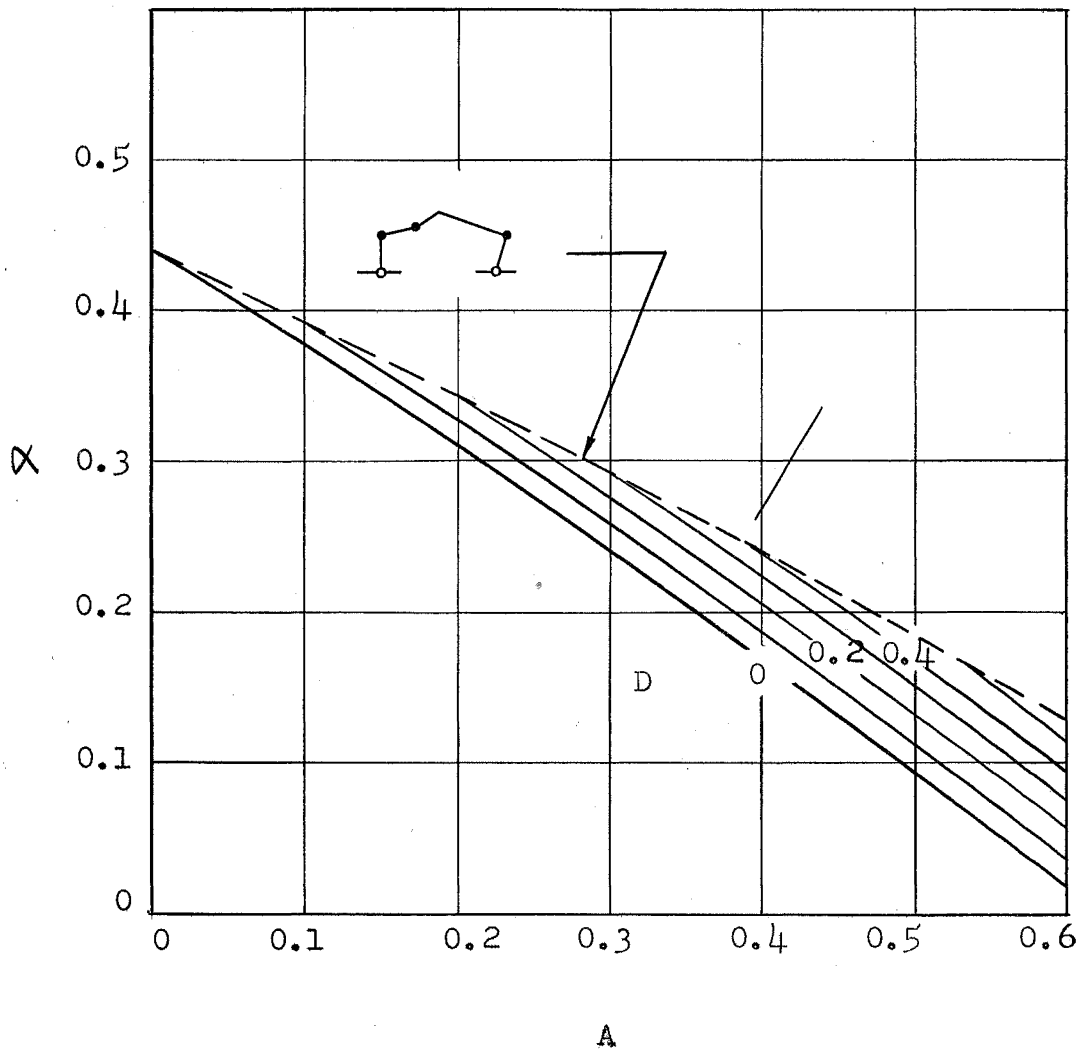
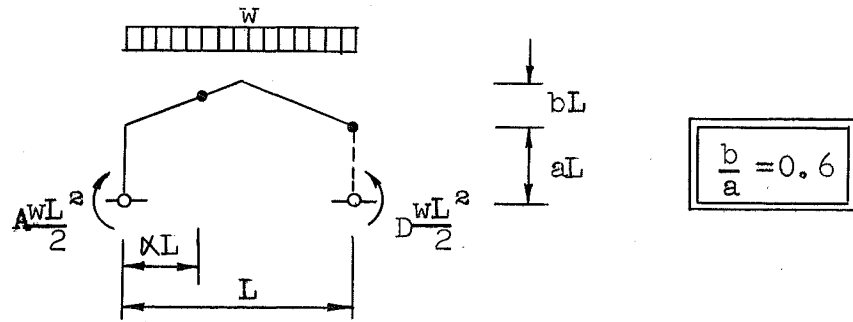


CHART III-4a

DESIGN CURVES FOR "PINNED-BASE" GABLE FRAMES
LOCATION OF PLASTIC HINGE

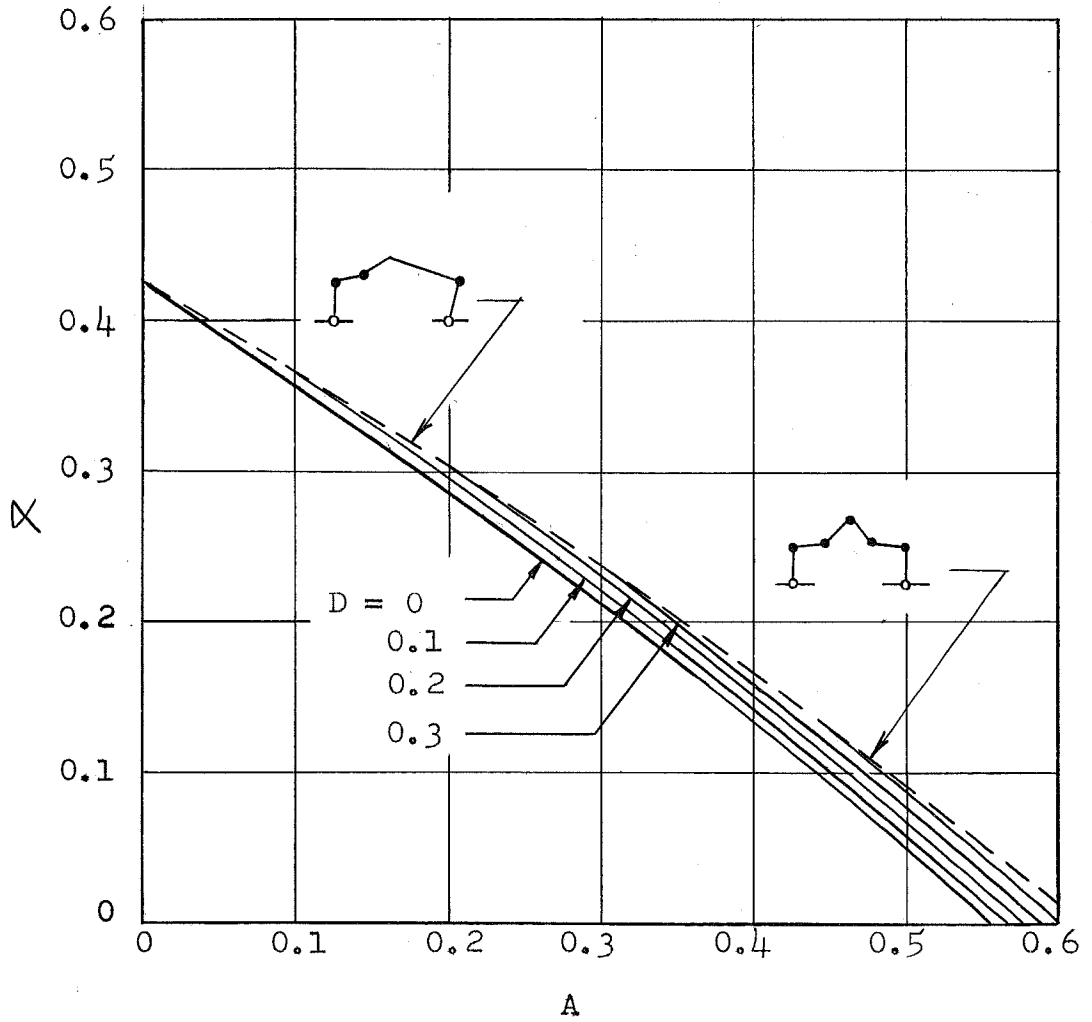
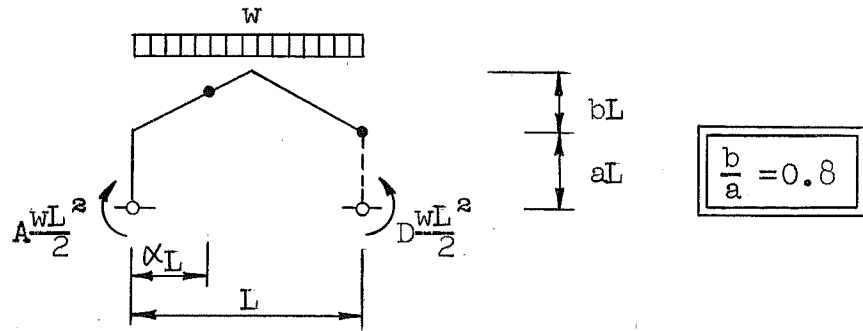
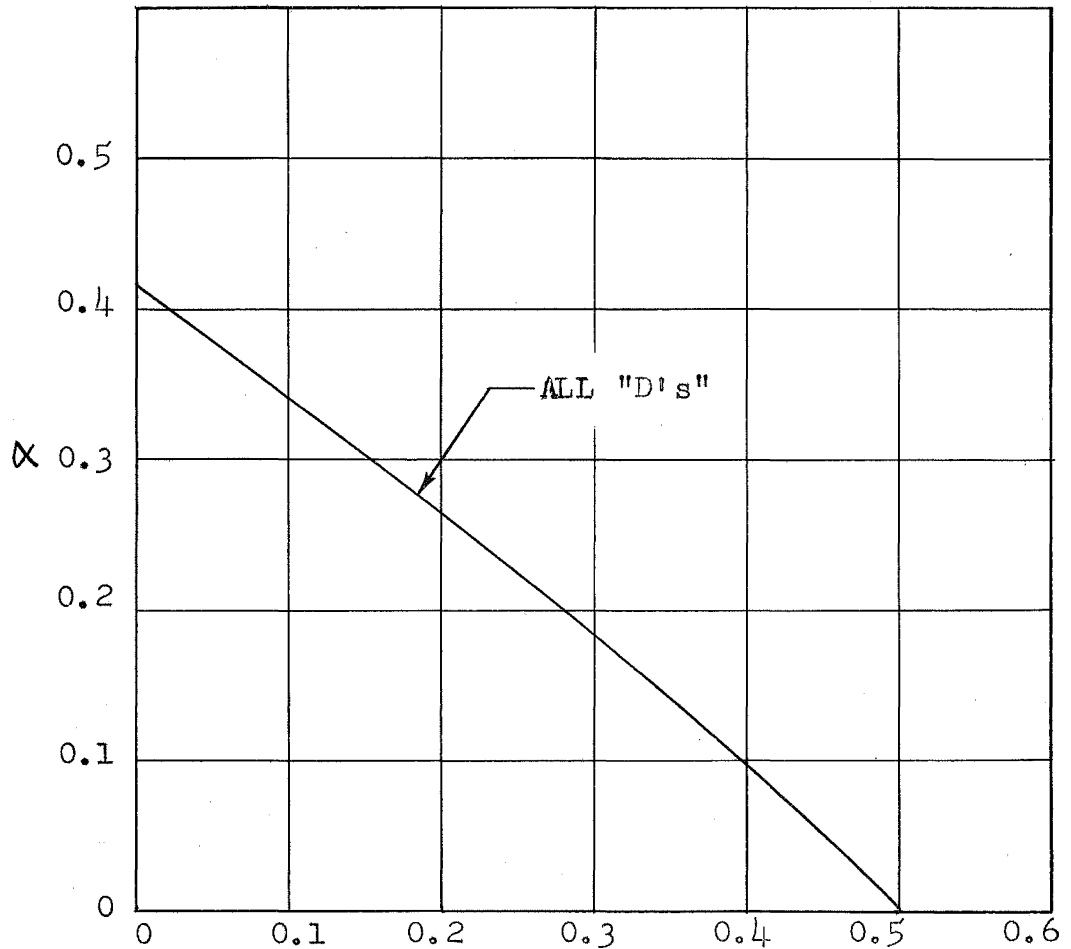
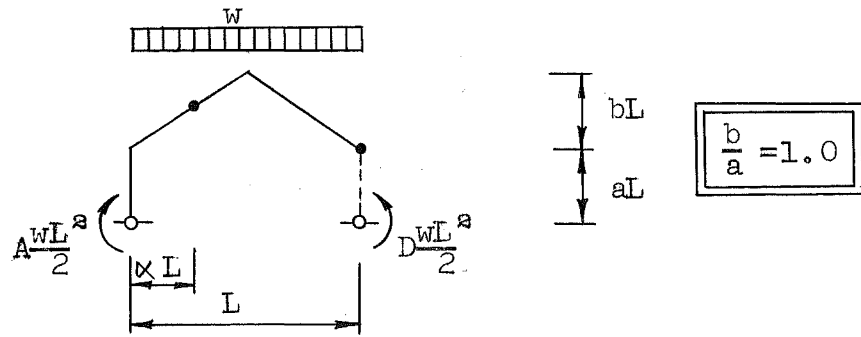


CHART III-5a

DESIGN CURVES FOR "PINNED-BASE" GABLE FRAMES
LOCATION OF PLASTIC HINGE



A

CHART III-6a

DESIGN CURVES FOR "PINNED-BASE" GABLE FRAMES
LOCATION OF PLASTIC HINGE

DESIGN CHART

IV-1a

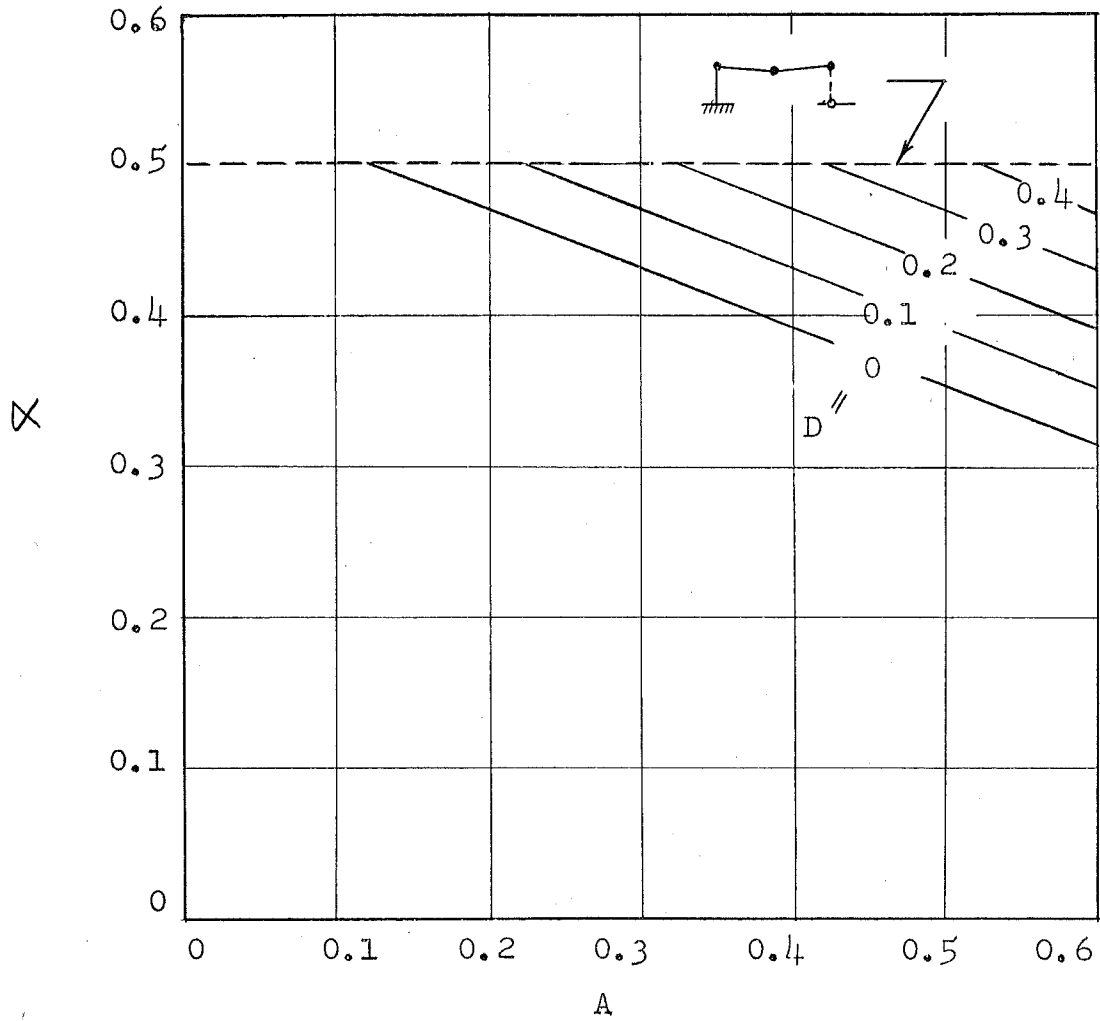
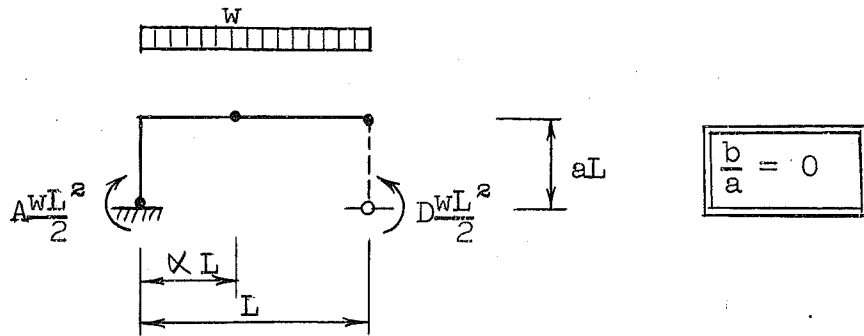


CHART IV-1a

DESIGN CURVES FOR "FIXED-BASE" GABLE FRAMES
LOCATION OF PLASTIC HINGE

DESIGN CHART

IV-2a

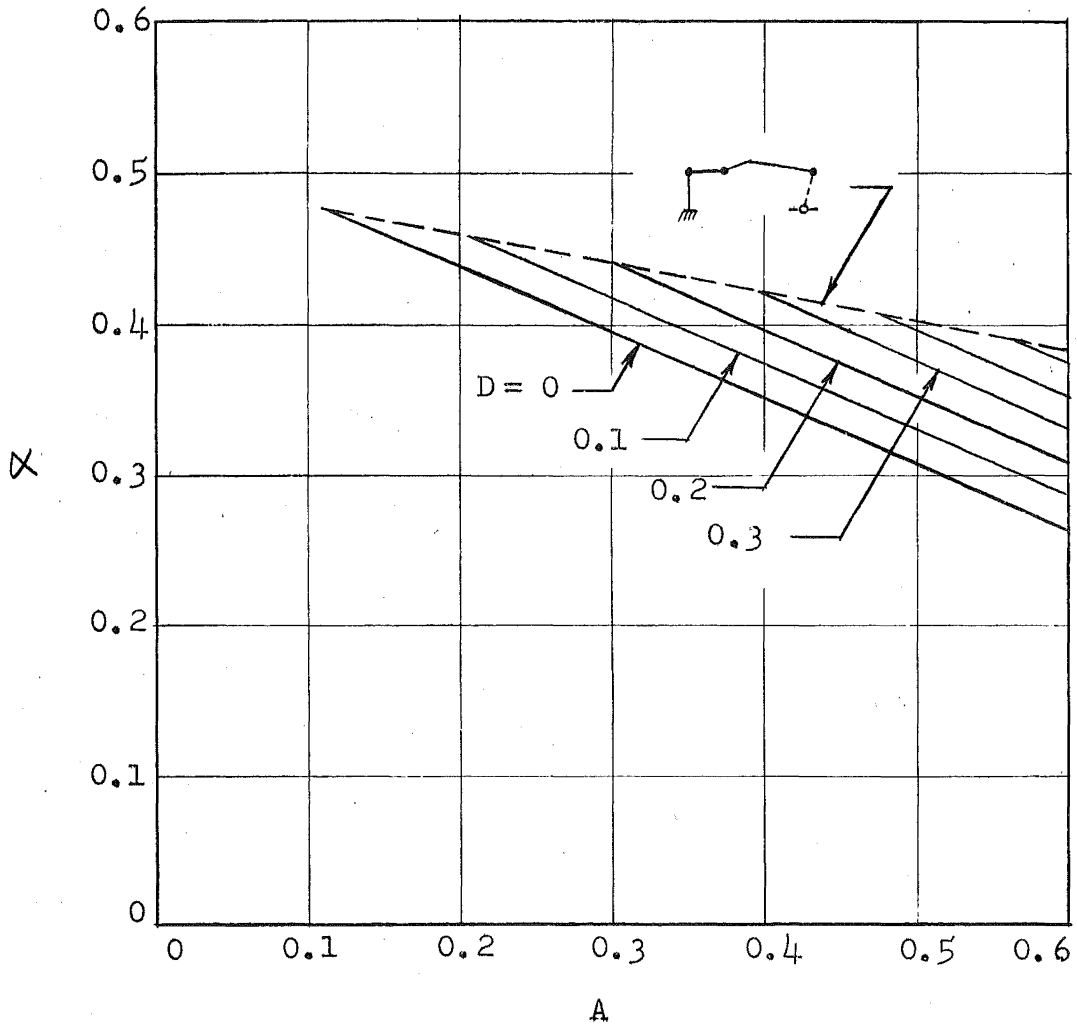
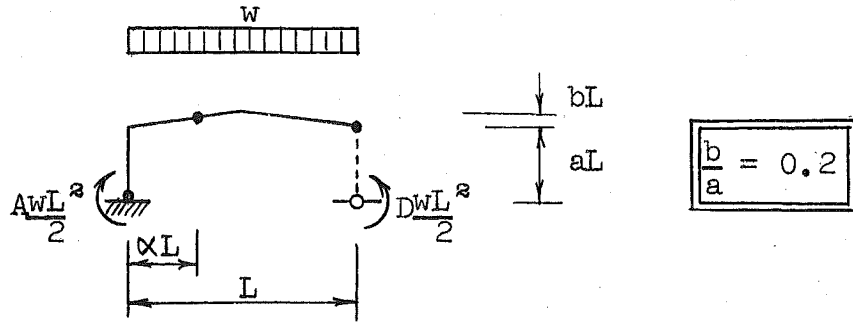


CHART IV-2a

DESIGN CURVES FOR "FIXED-BASE" GABLE FRAMES
LOCATION OF PLASTIC HINGE

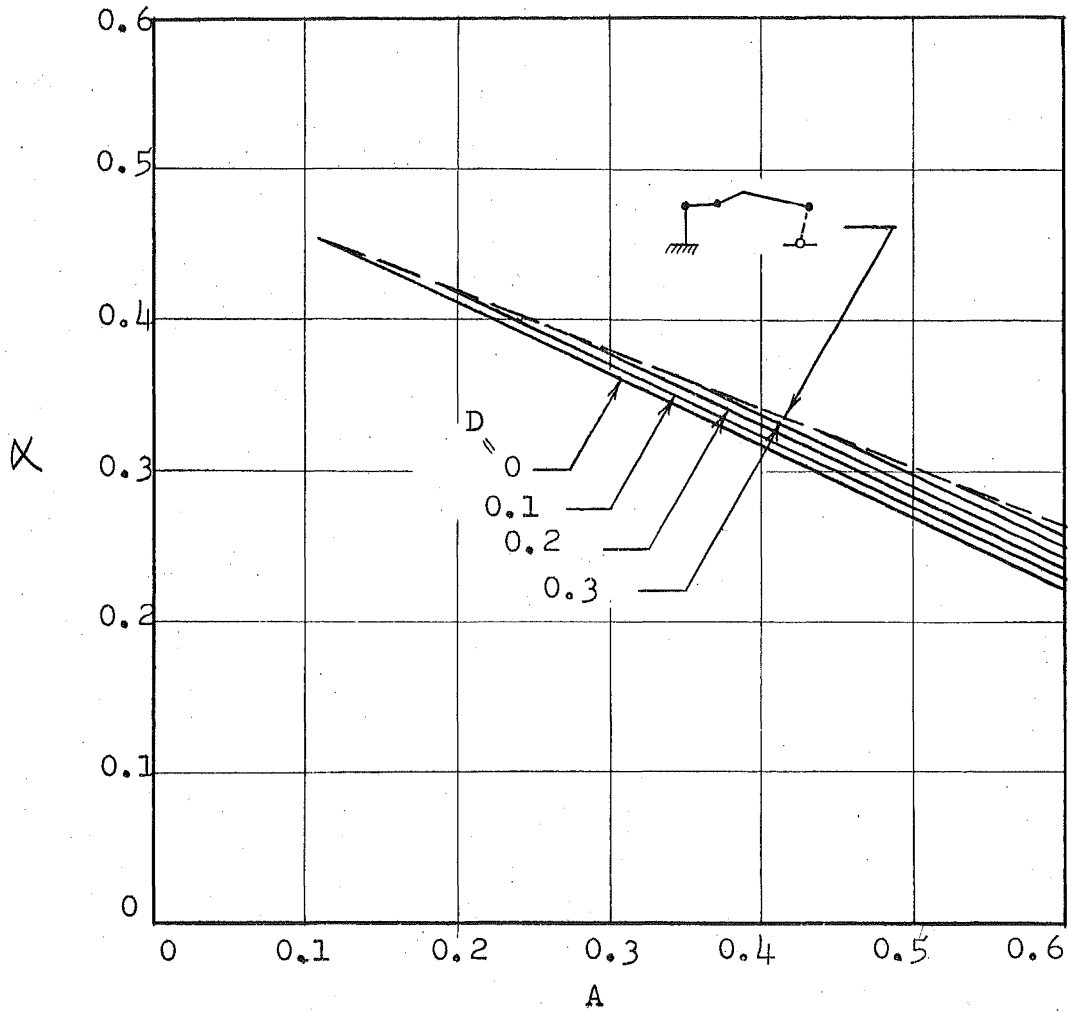
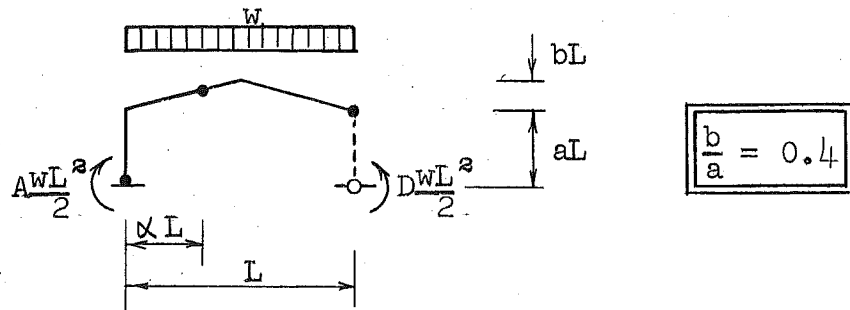


CHART IV-3a

DESIGN CURVES FOR "FIXED-BASE" GABLE FRAMES
LOCATION OF PLASTIC HINGE

DESIGN CHART

IV-4a

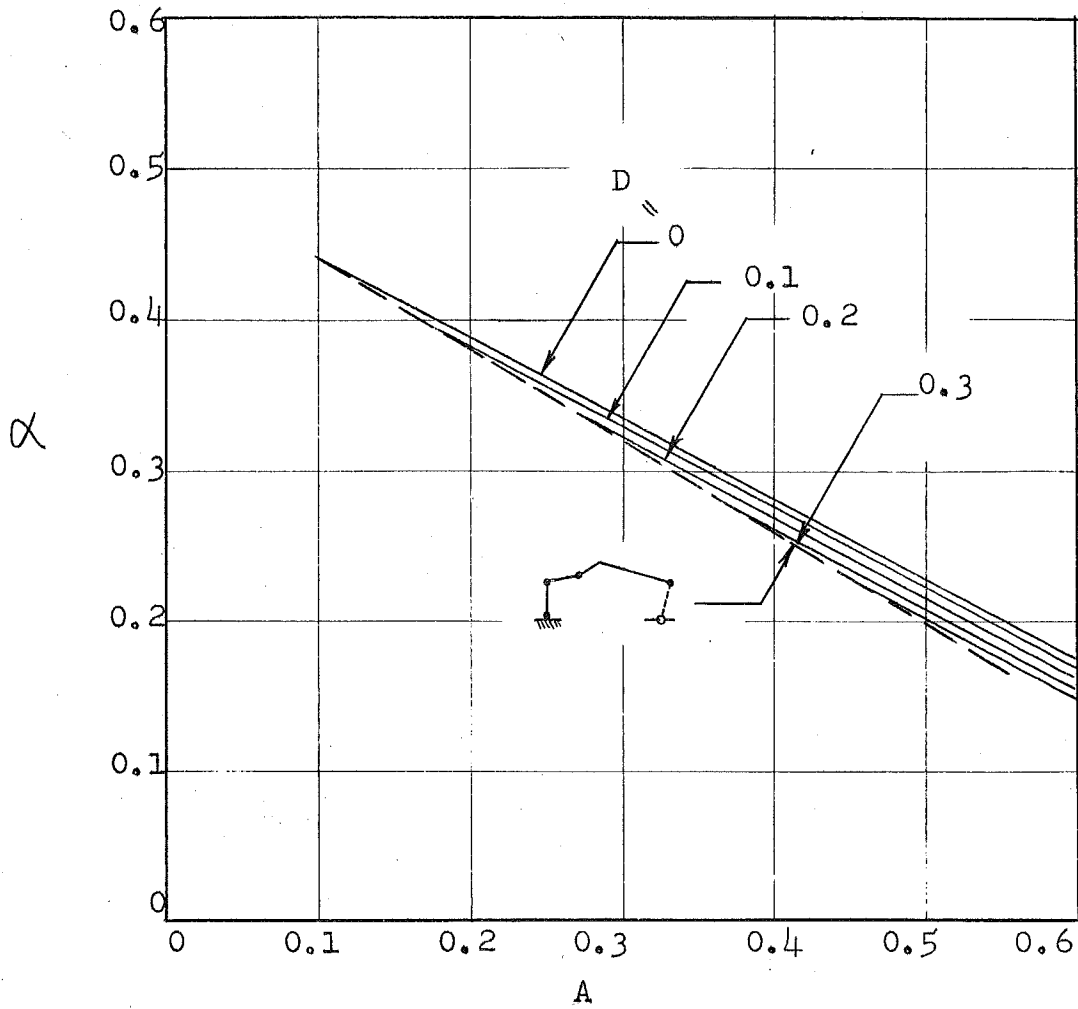
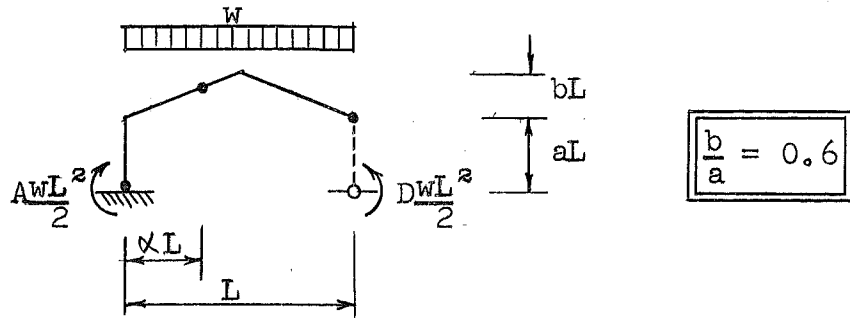
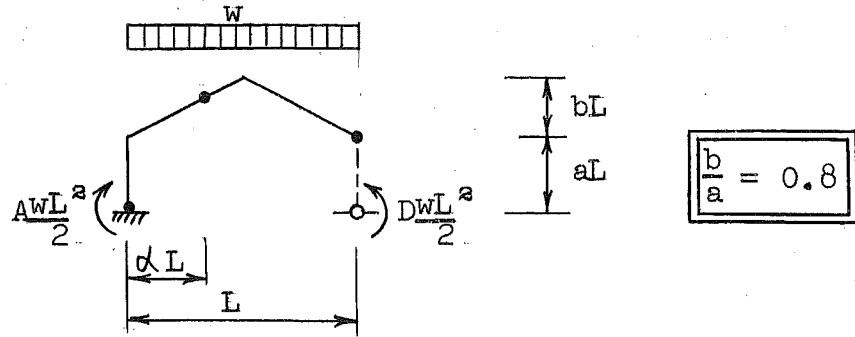


CHART IV-4a

DESIGN CURVES FOR "FIXED-BASE" GABLE FRAMES
LOCATION OF PLASTIC HINGE



$$\frac{b}{a} = 0.8$$

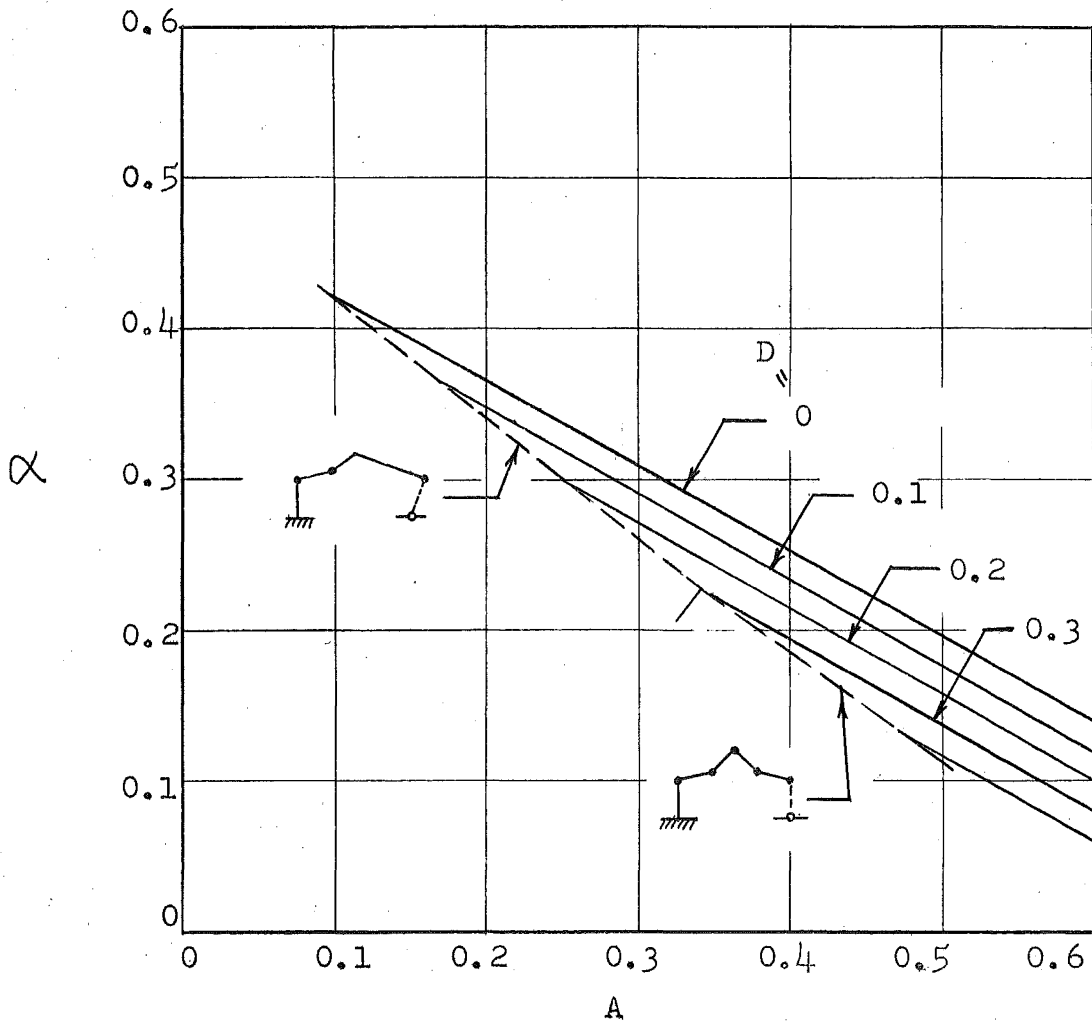


CHART IV-5a

DESIGN CURVES FOR "FIXED-BASE" GABLE FRAMES
LOCATION OF PLASTIC HINGE

DESIGN CHART

IV-6a

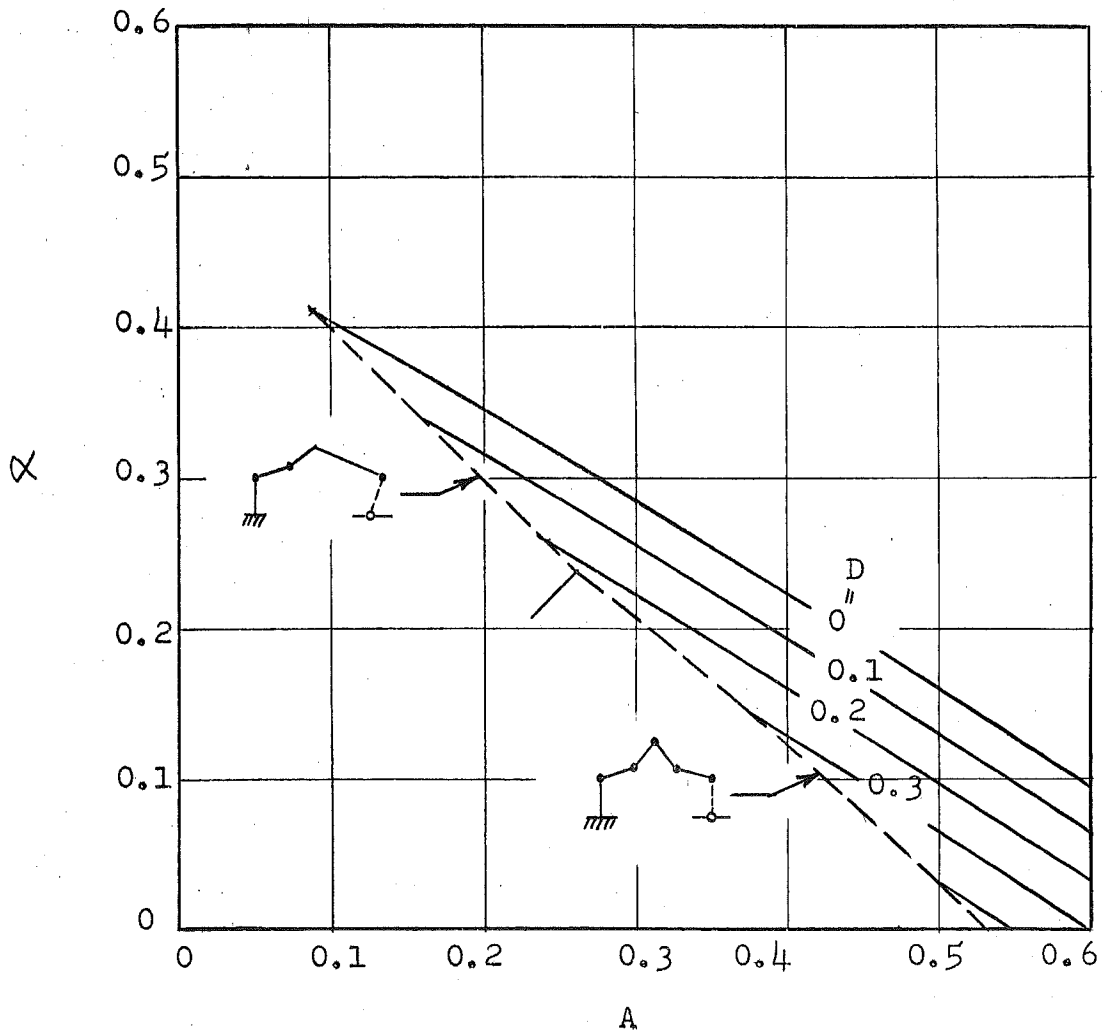
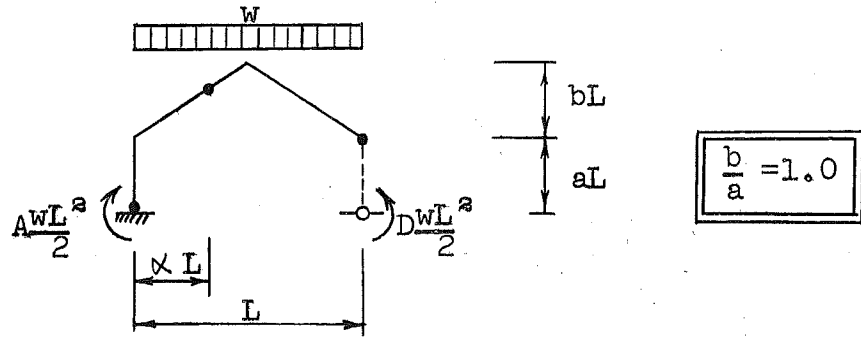


CHART IV-6a

DESIGN CURVES FOR "FIXED-BASE" GABLE FRAMES
LOCATION OF PLASTIC HINGE

DESIGN CHART

V-1a

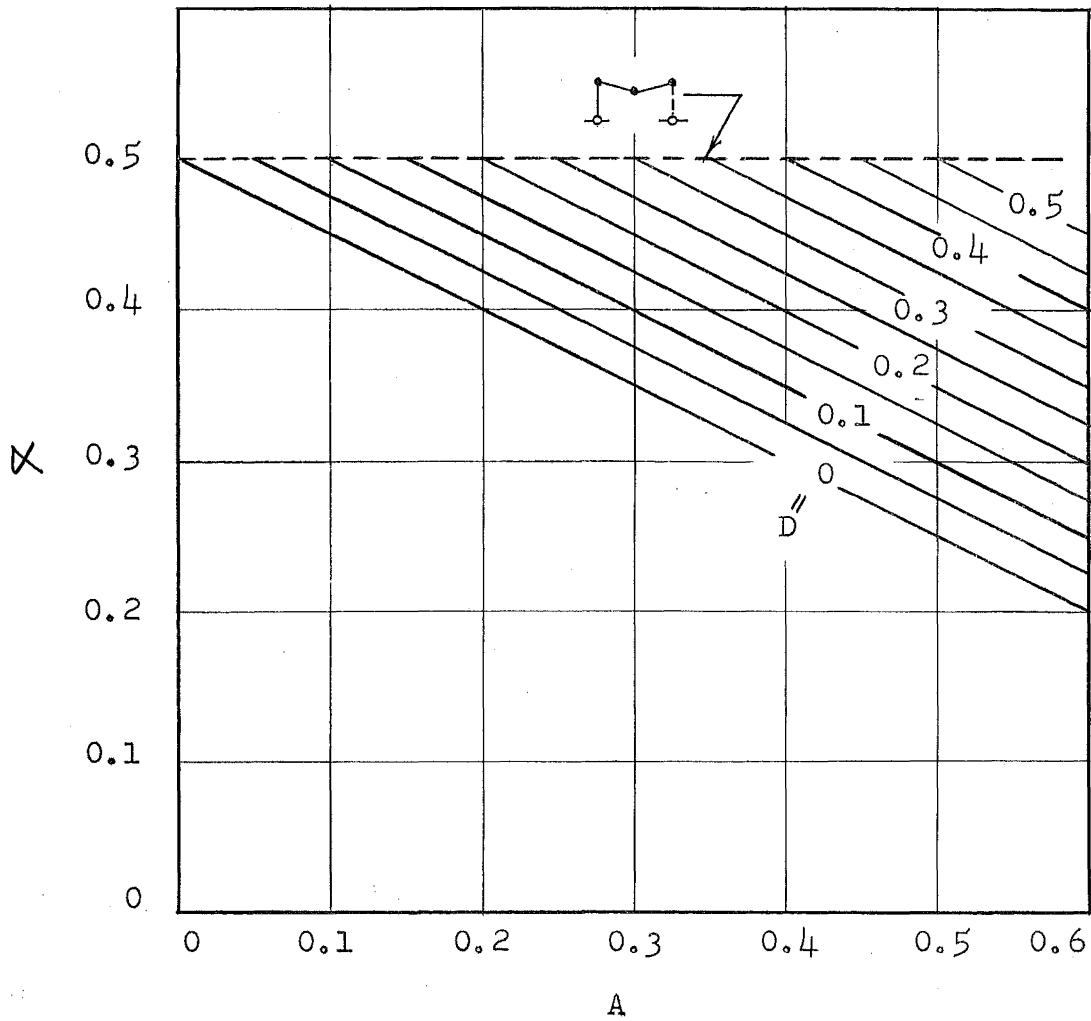
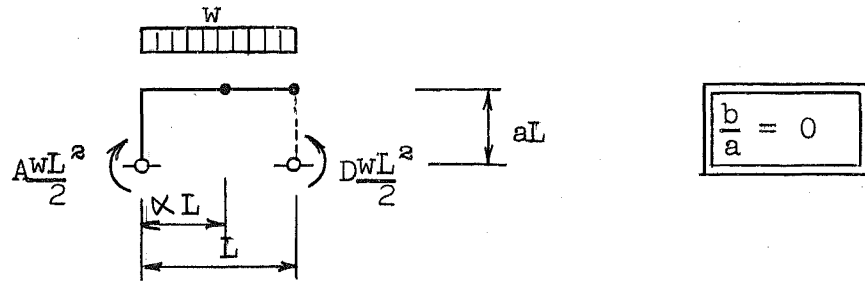


CHART V-1a

DESIGN CURVES FOR "PINNED-BASE", LEAN-TO FRAMES
LOCATION OF PLASTIC HINGE

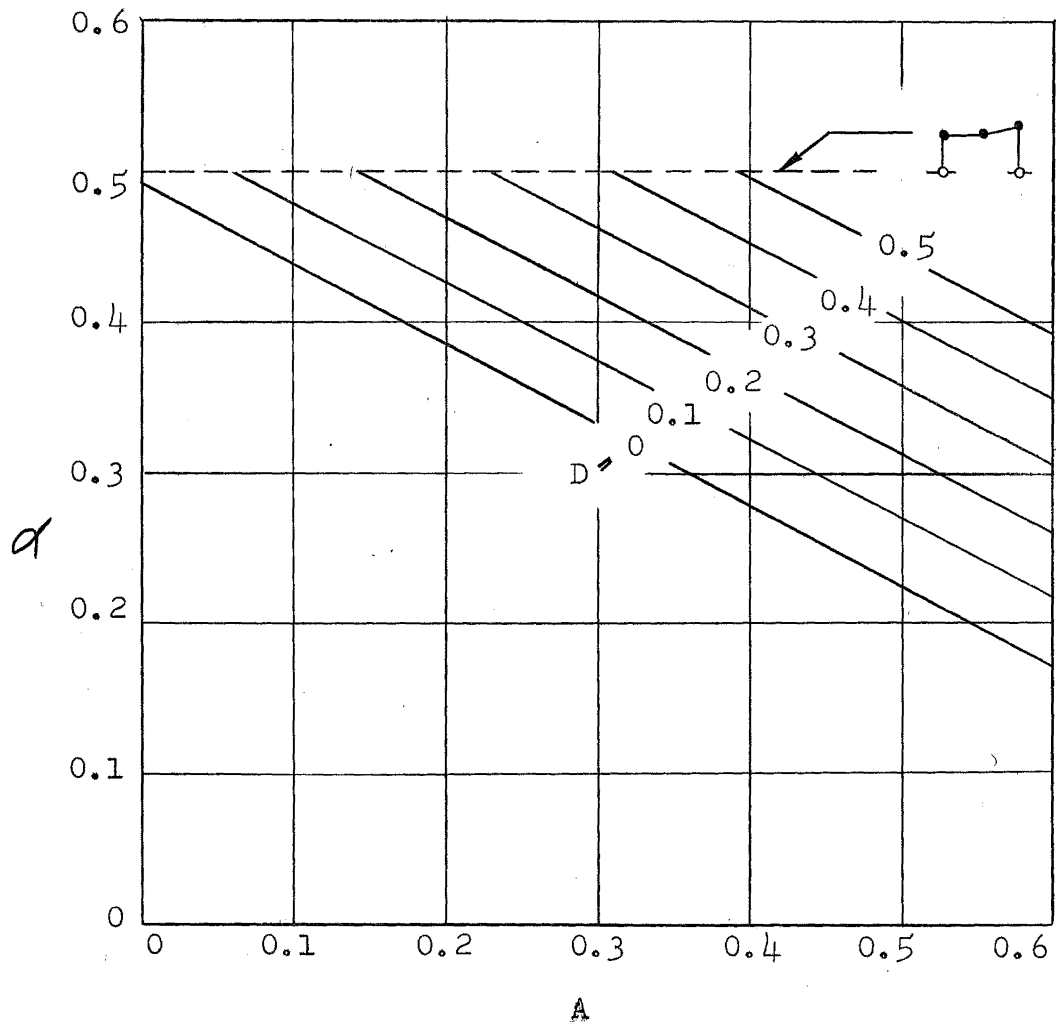
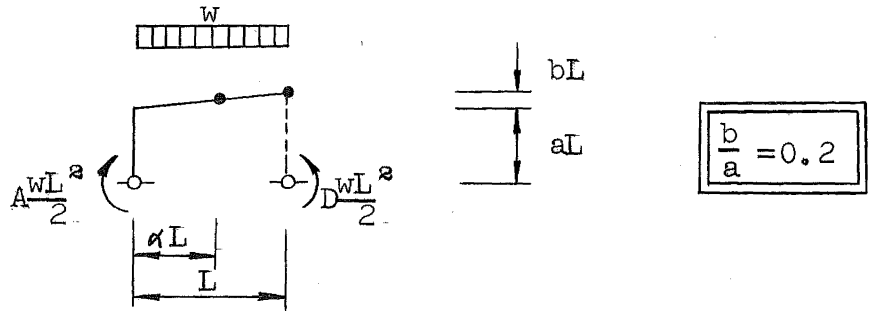


CHART V-2a

DESIGN CURVES FOR "PINNED-BASE", LEAN-TO FRAMES
LOCATION OF PLASTIC HINGE

DESIGN CHART

V-3a

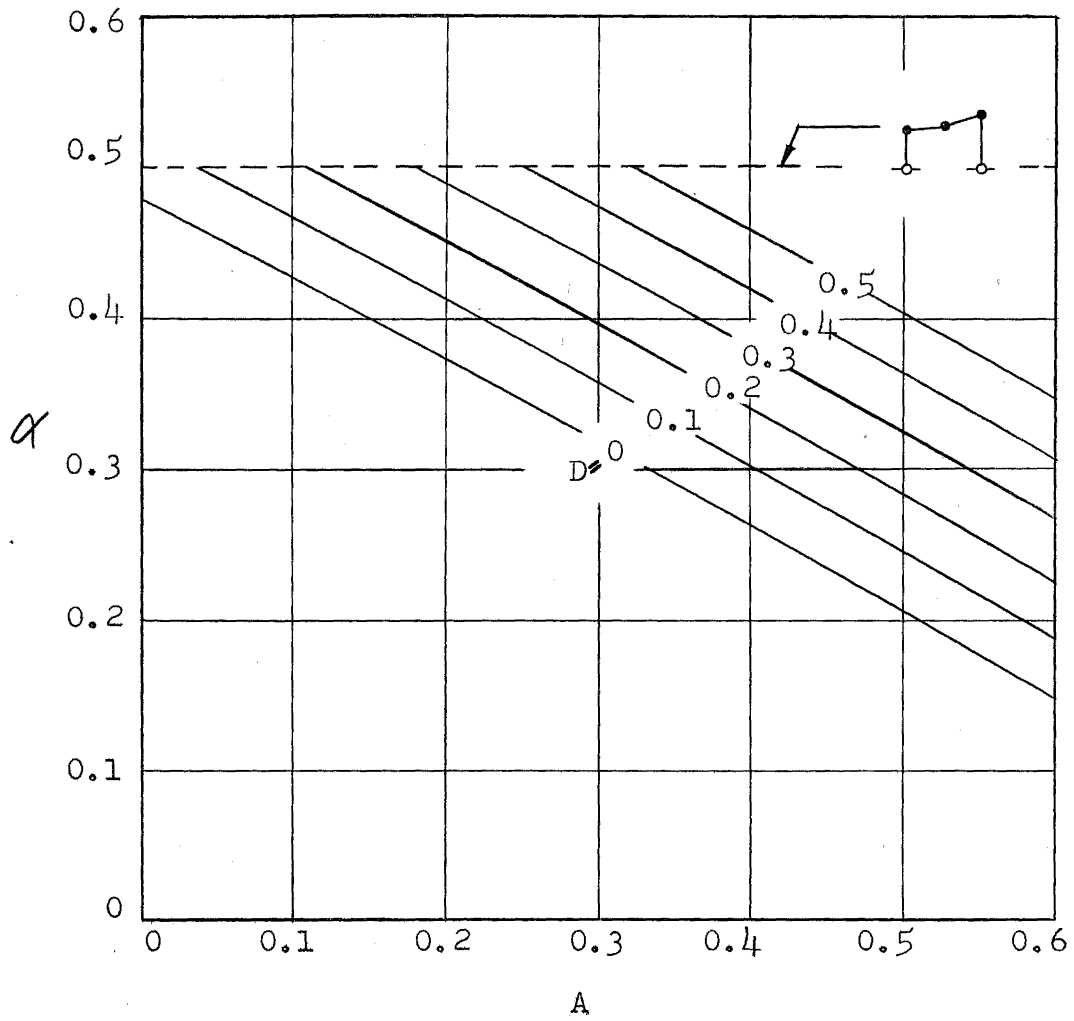
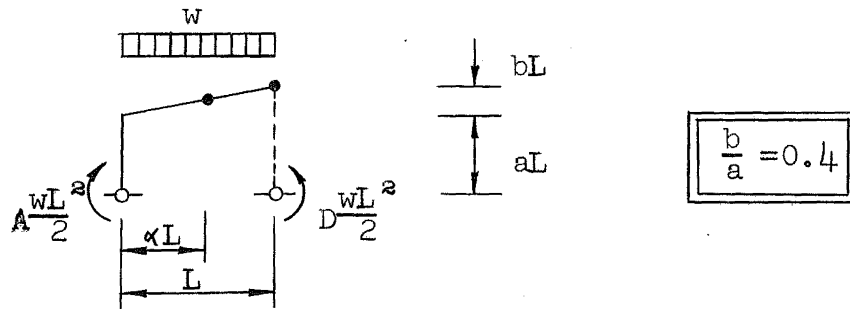


CHART V-3a

DESIGN CURVES FOR "PINNED-BASE", LEAN-TO FRAMES
LOCATION OF PLASTIC HINGE

DESIGN CHART

V-4a

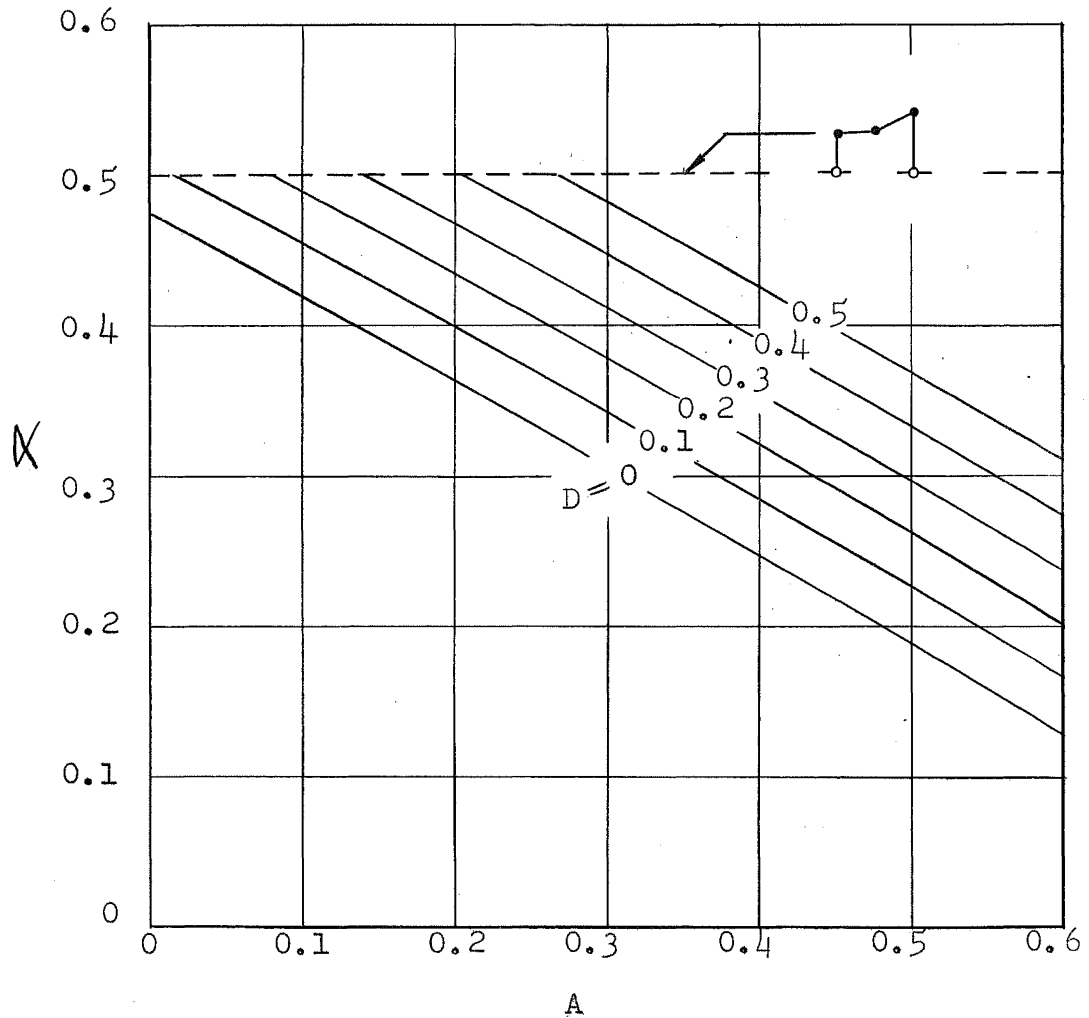
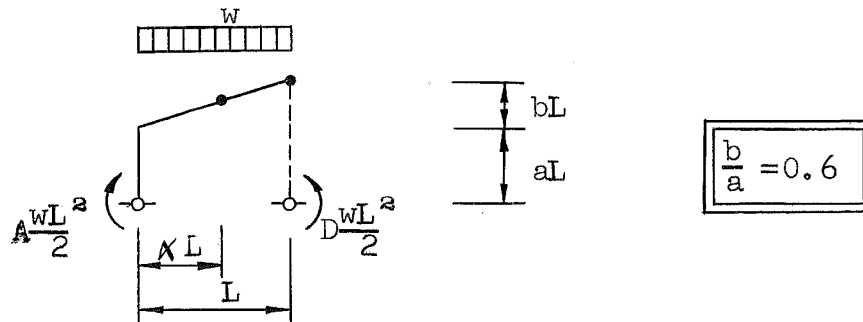


CHART V-4a

DESIGN CURVES FOR "PINNED-BASE", LEAN-TO FRAMES
LOCATION OF PLASTIC HINGE

DESIGN CHART

V-5a

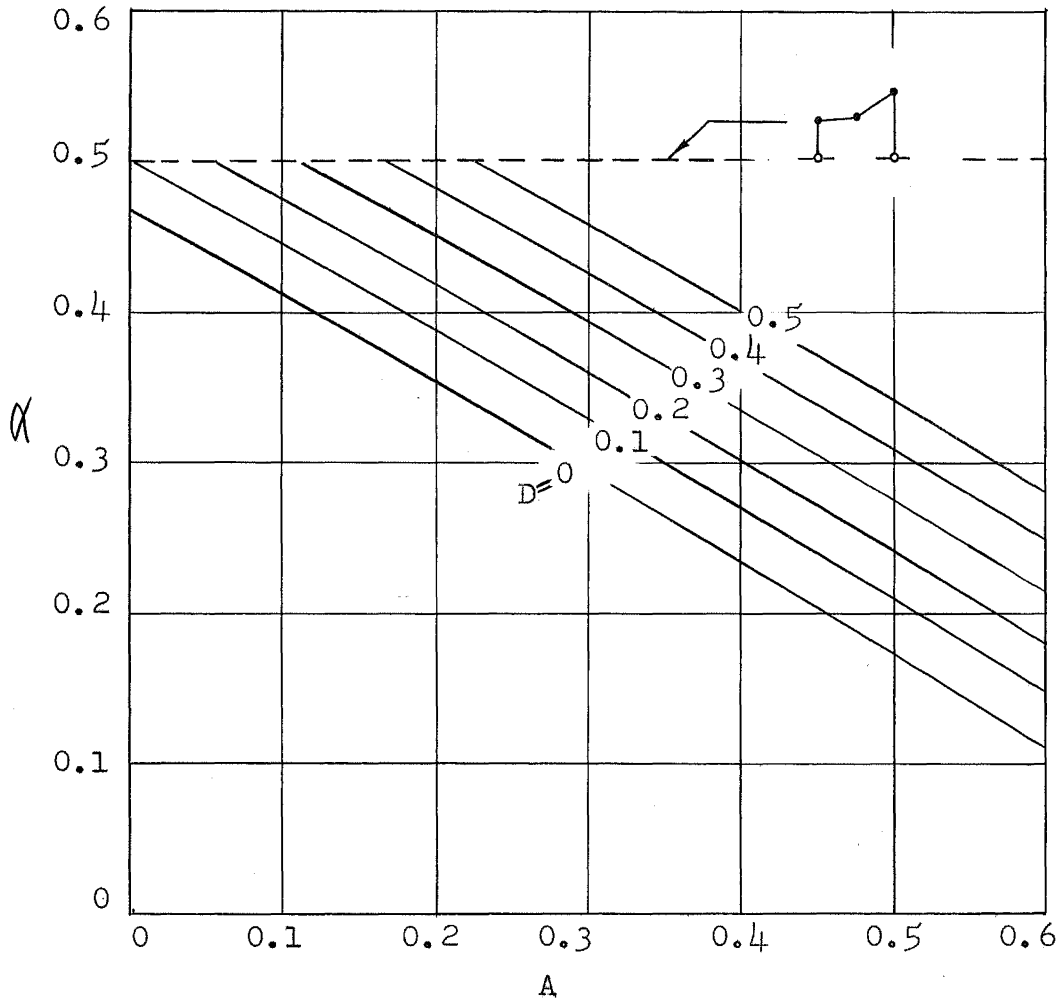
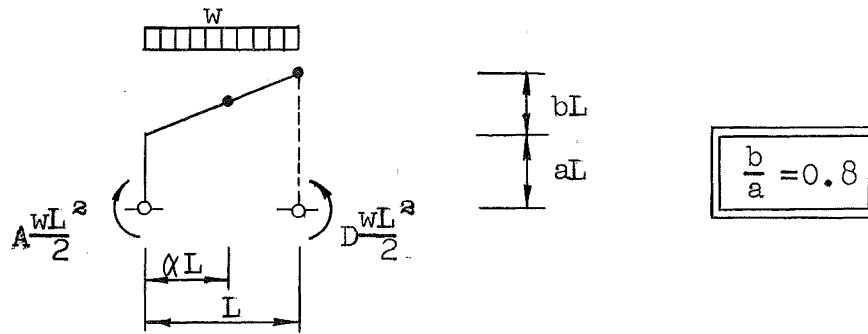


CHART V-5a

DESIGN CURVES FOR "PINNED-BASE", LEAN-TO FRAMES
LOCATION OF PLASTIC HINGE

DESIGN CHART

V-6a

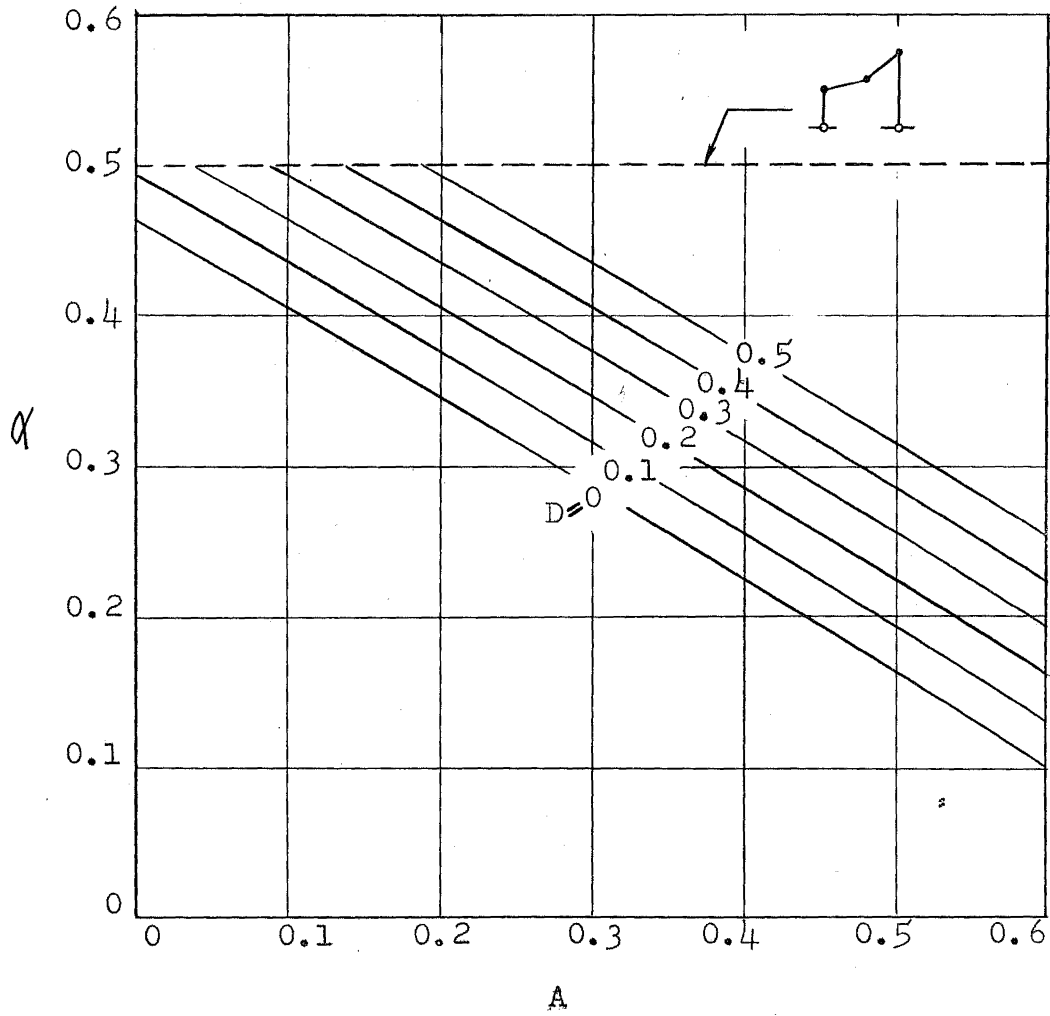
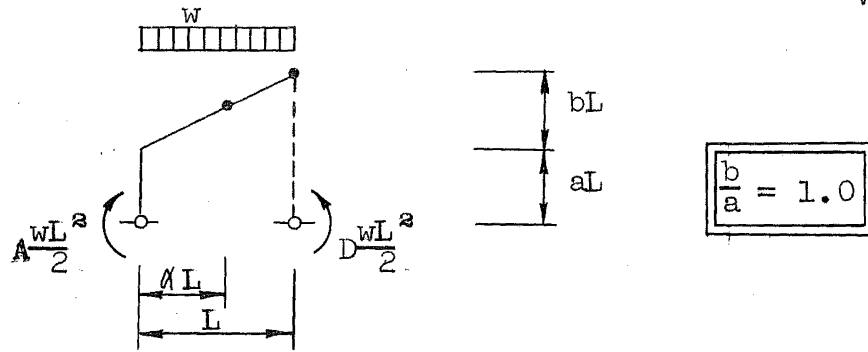


CHART V-6a

DESIGN CURVES FOR "PINNED-BASE", LEAN-TO FRAMES
LOCATION OF PLASTIC HINGE

DESIGN CHART

VI-1a

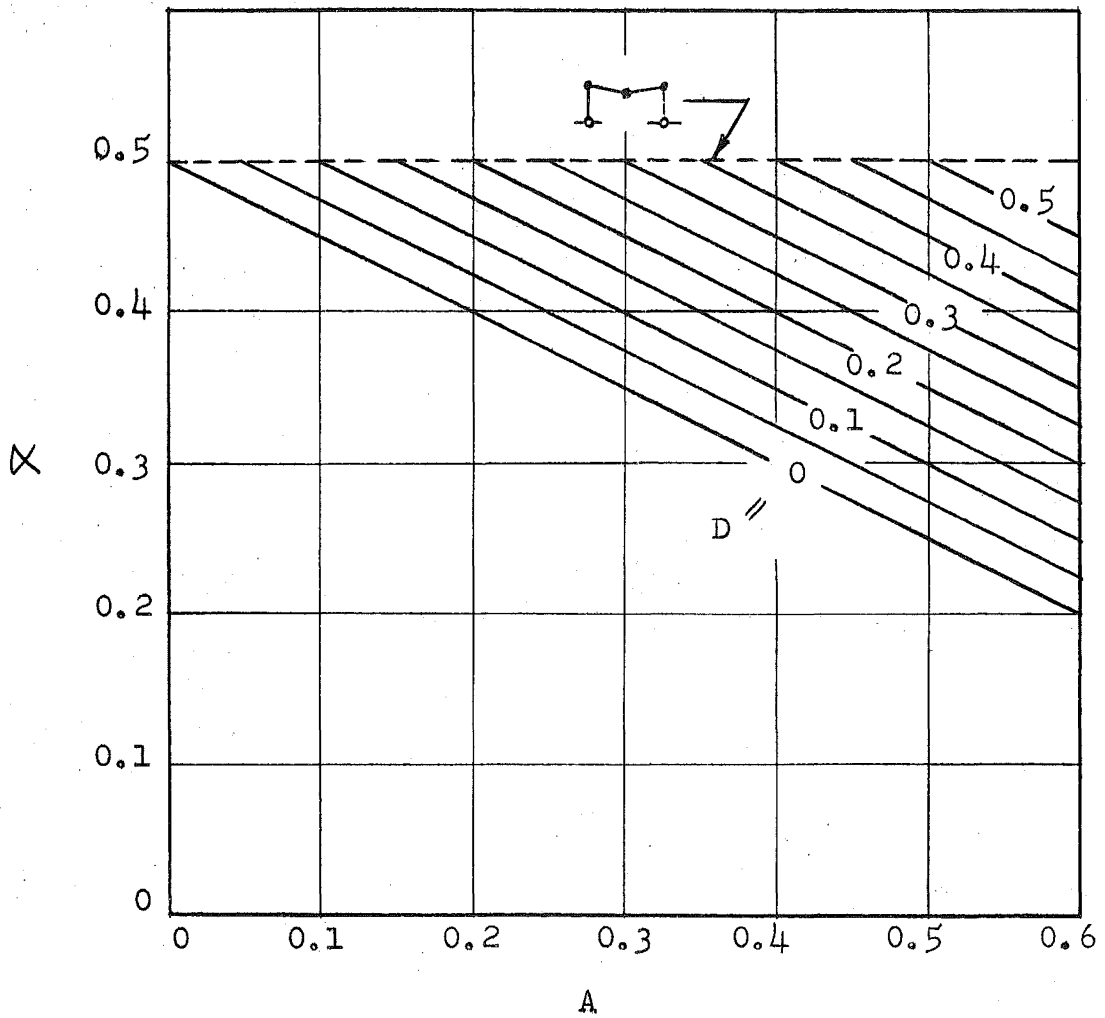
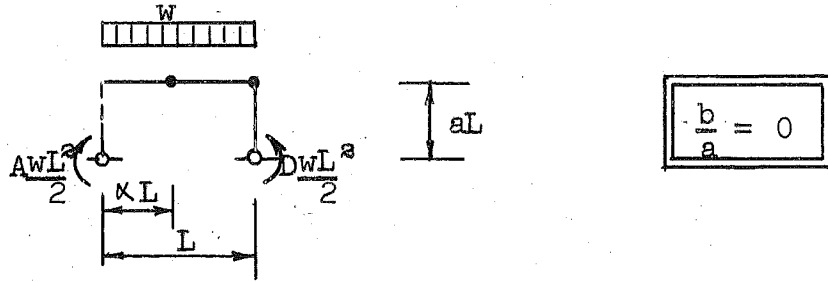


CHART VI-1a

DESIGN CURVES FOR "PINNED-BASE", LEAN-TO FRAMES
LOCATION OF PLASTIC HINGE

DESIGN CHART

VI-2a

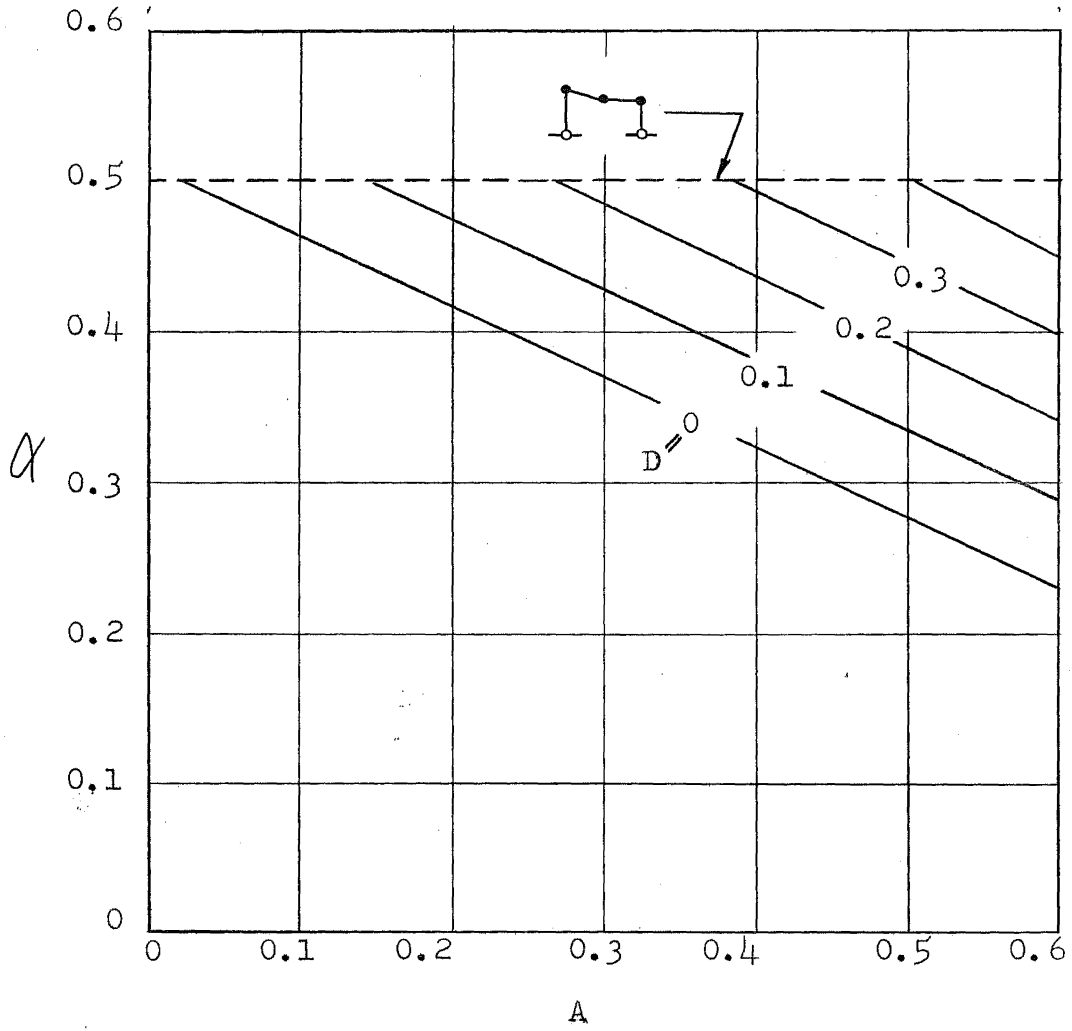
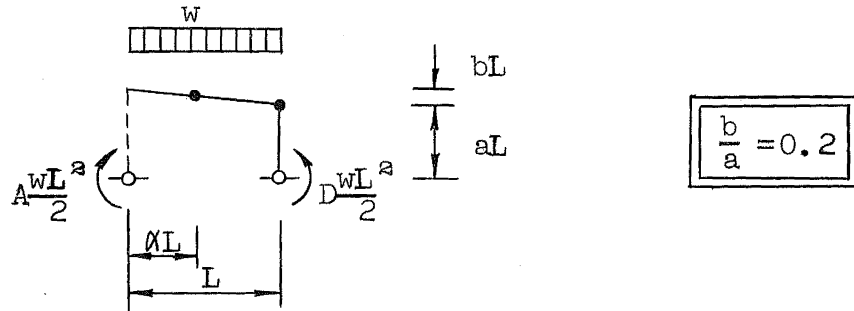


CHART VI-2a

DESIGN CURVES FOR "PINNED-BASE", LEAN-TO FRAMES
LOCATION OF PLASTIC HINGE

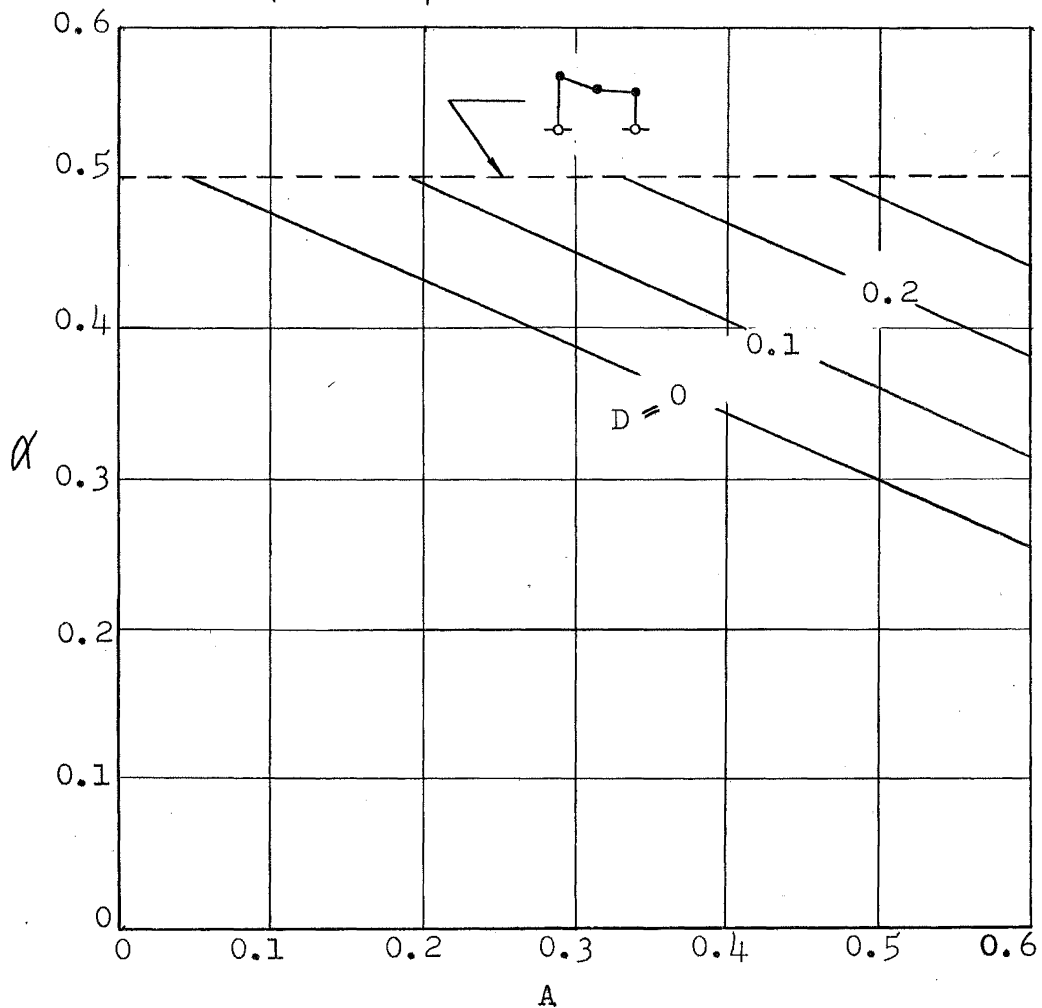
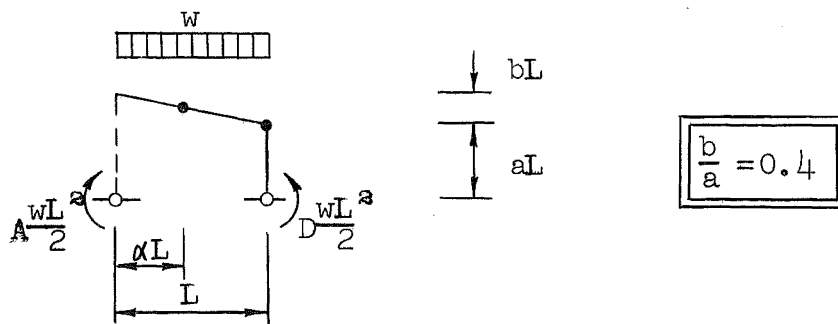


CHART VI-3a

DESIGN CURVES FOR "PINNED-BASE", LEAN-TO FRAMES
LOCATION OF PLASTIC HINGE

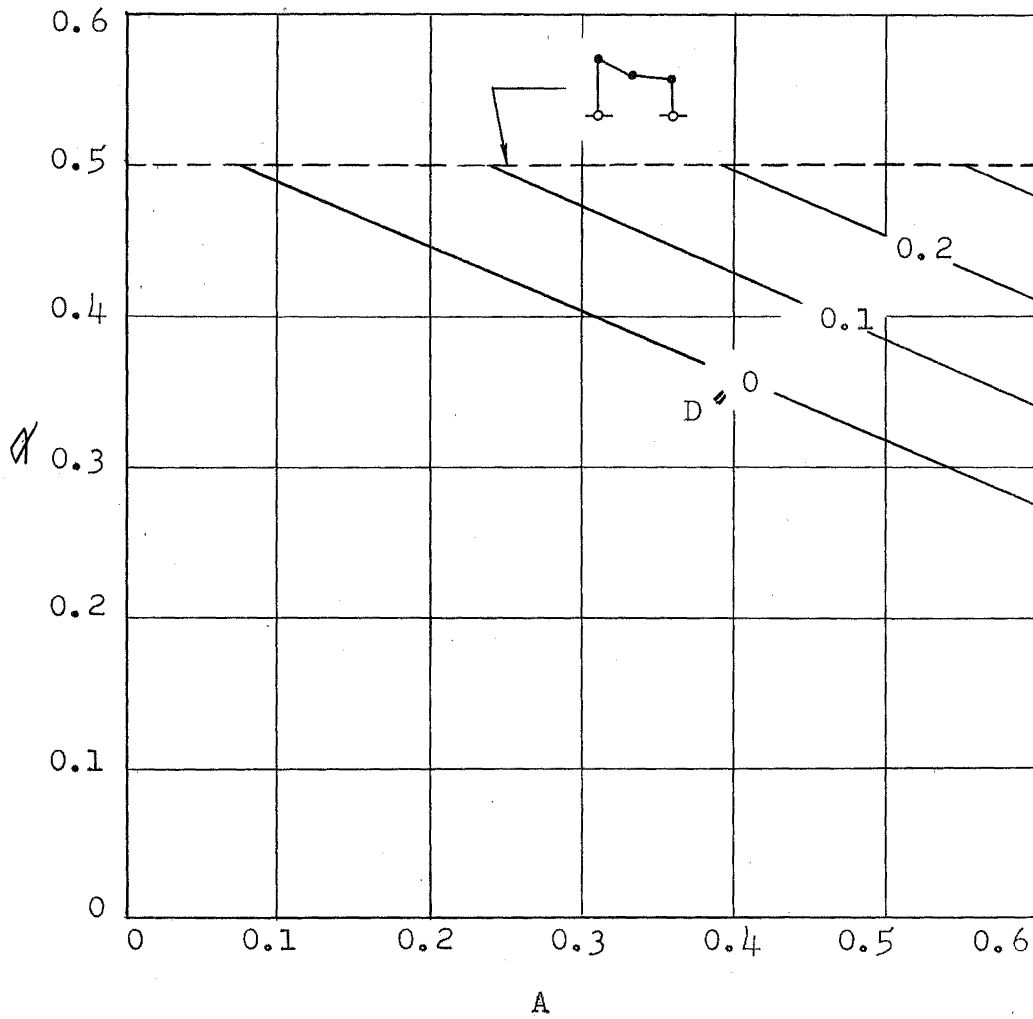
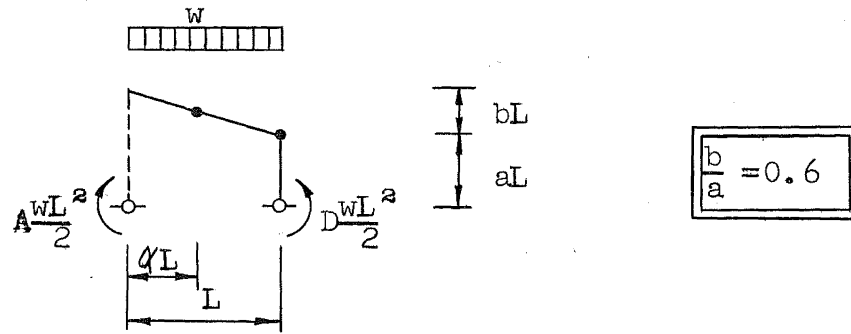


CHART VI-4a

DESIGN CURVES FOR "PINNED-BASE", LEAN-TO FRAMES
LOCATION OF PLASTIC HINGE

DESIGN CHART

VI-5a

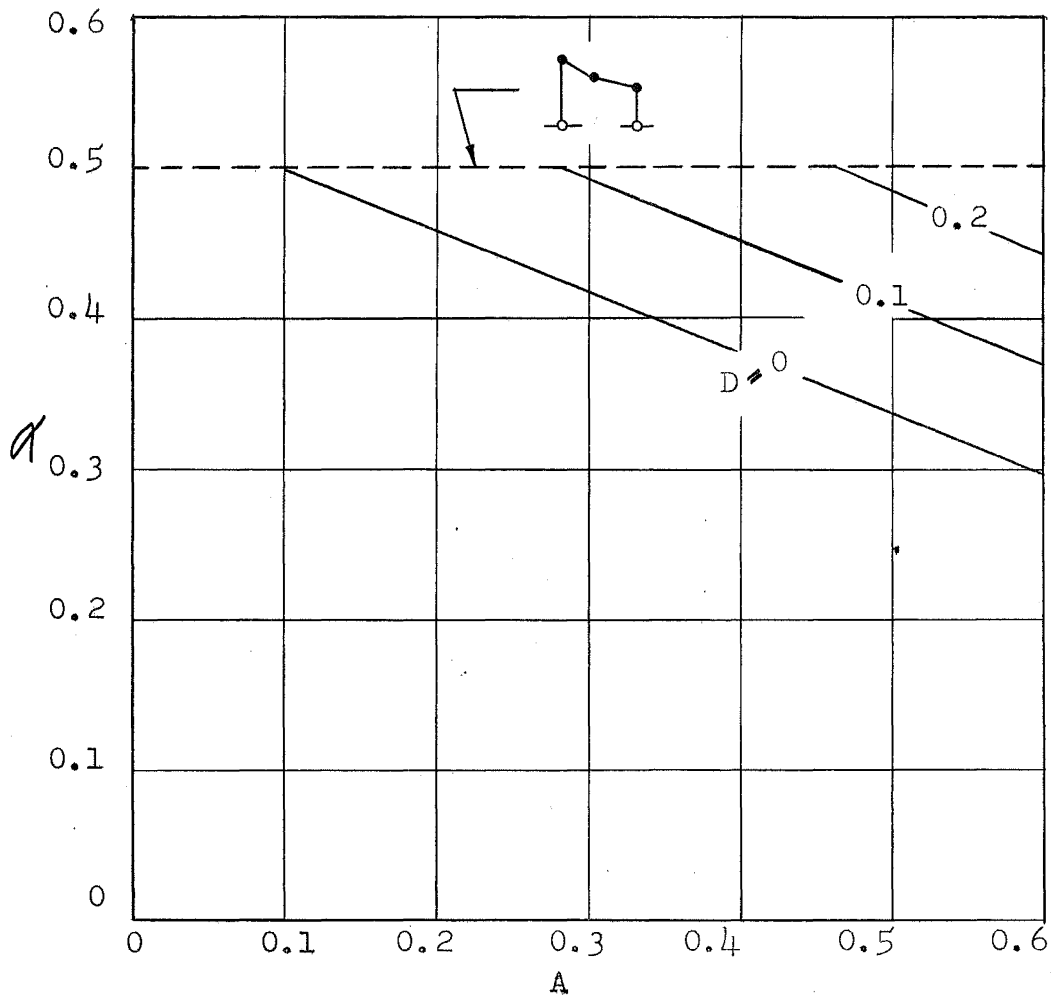
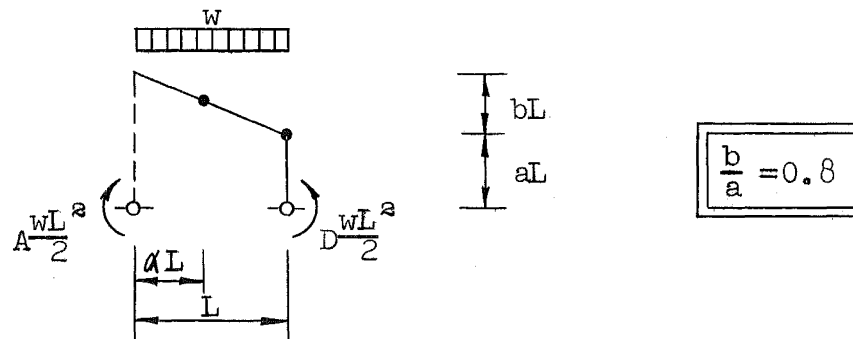


CHART VI-5a

DESIGN CURVES FOR "PINNED BASE", LEAN-TO FRAMES
LOCATION OF PLASTIC HINGE

DESIGN CHART

VI-6a

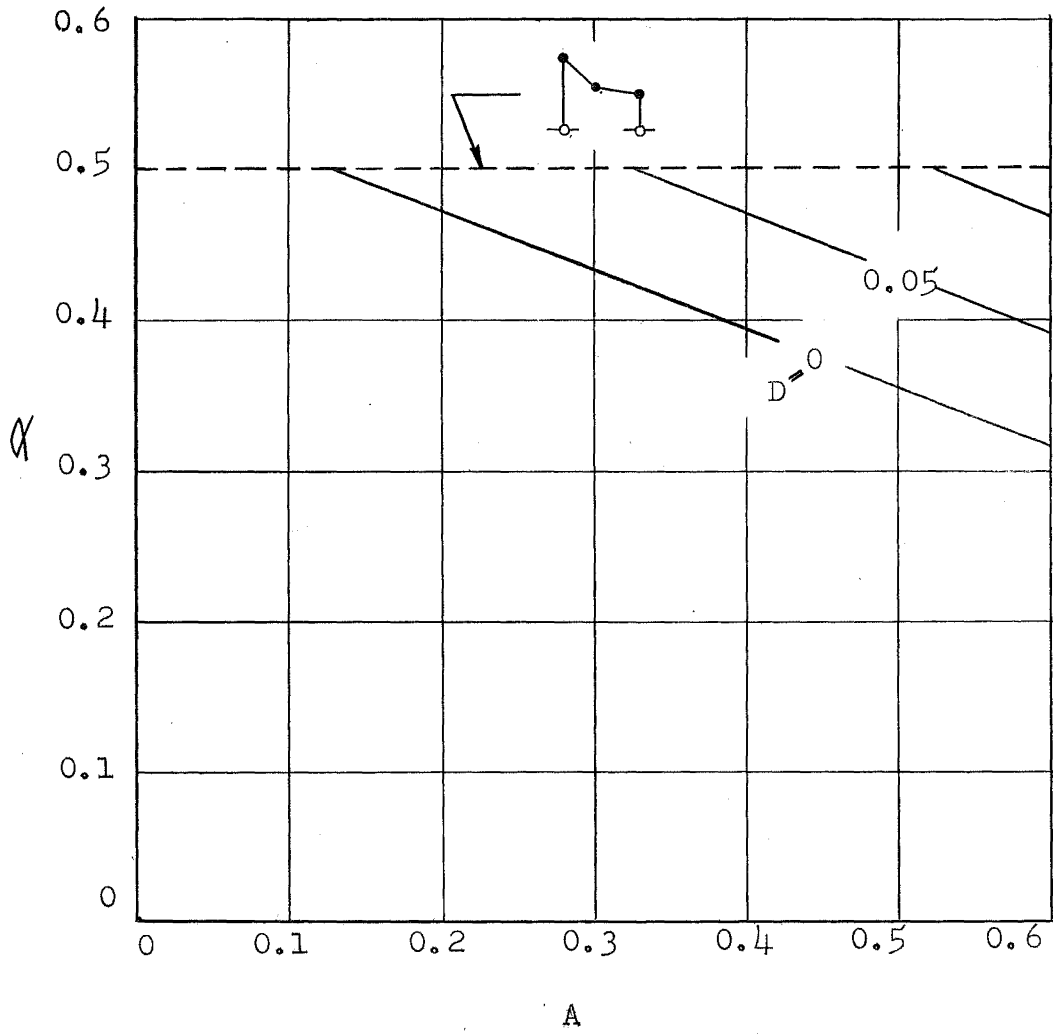
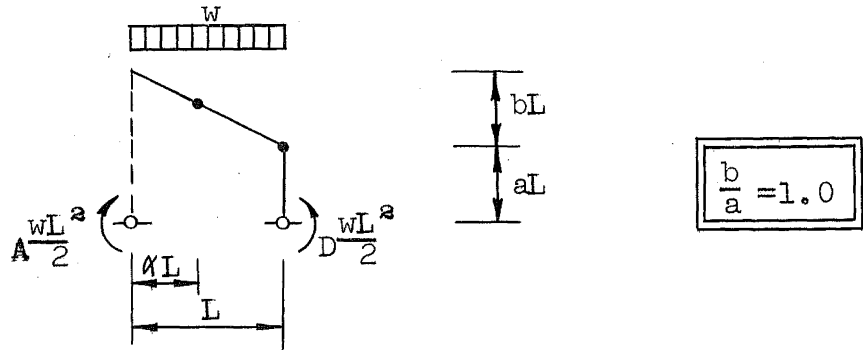


CHART VI-6a

DESIGN CURVES FOR "PINNED-BASE", LEAN-TO FRAMES
LOCATION OF PLASTIC HINGE